UNIVERSITAT DE BARCELONA

Responses of Mediterranean riparian forests to water availability: Insights of present and future conditions. A case study in La Tordera catchment

Respostes dels boscos de ribera mediterranis a la disponibilitat d'aigua: Estudi de les condicions presents i futures a la conca de La Tordera.

Sílvia Poblador Ibáñez

Sílvia Poblador Ibáñez 2018

Responses of Mediterranean riparian forests to water availability: insights of present and future conditions

Responses of Mediterranean riparian forests to water availability:
insights of present and
future conditions

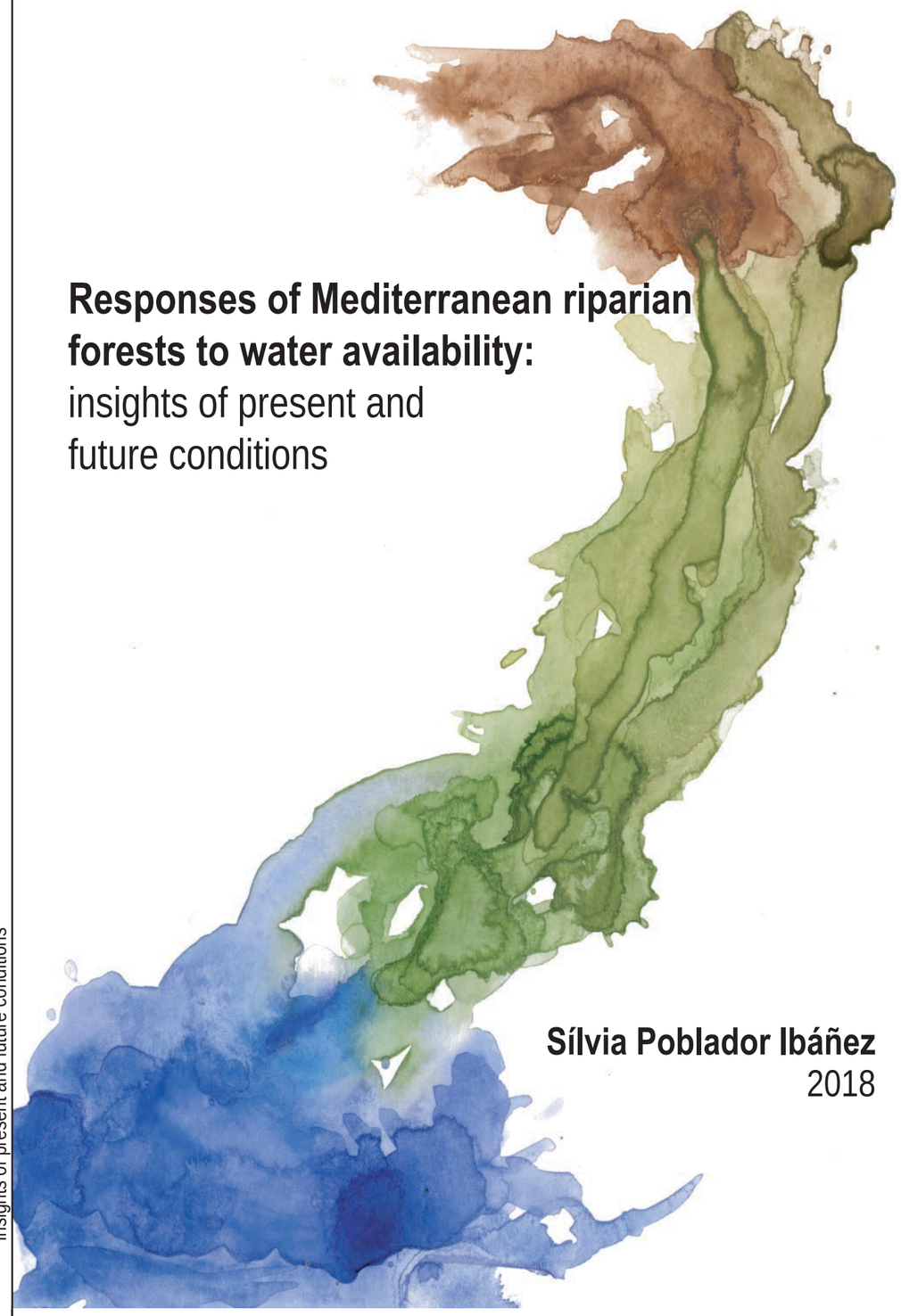

Sílvia Poblador Ibáñez
2018

TESI DOCTORAL

Universitat de Barcelona
Facultat de Biologia
Departament de Biologia Evolutiva, Ecologia i Ciències Ambientals
Programa de Doctorat en Ecologia, Ciències Ambientals i Fisiologia vegetal

RESPONSES OF MEDITERRANEAN RIPARIAN FORESTS TO WATER AVAILABILITY: INSIGHTS OF PRESENT AND FUTURE CONDITIONS. A CASE STUDY IN *LA TORDERA* CATCHMENT.

Respostes dels boscos de ribera mediterranis a la disponibilitat d'aigua: estudi de les condicions presents i futures a la conca de La Tordera.

Memòria presentada per Sílvia Poblador Ibáñez
per optar al grau de doctora per la Universitat de Barcelona

SÍLVIA POBLADOR IBÁÑEZ

Barcelona, Maig de 2018

Vist-i-plau dels directors de la tesi:

Dr. Francesc Sabater i Comas
Professor Titular
Departament Ecologia UB

Dr. Santiago Sabaté i Jorba
Professor Titular
Departament Ecologia UB

Als meus pares,

i a tots els que encara pensem
que podem fer un món millor.

Progrés potser significa deixar de tenir l'aire de conquistador permanent, progrés avui potser significa recuperar aquelles coses que abans teníem a l'abast de la mà, com és l'esperit de convivència, la bona relació amb la naturalesa i no la seva sistemàtica destrucció; la recuperació de la teva identitat, viure la cultura sense complexos ni provincialismes però amb seguretat perquè, al cap i a la fi, cultura és l'aire que respires.

Montserrat Roig

AGRAÏMENTS

Això ha sigut tant llarg que hi ha un munt d'agraïments per fer! Estàs segura de que t'ho vols llegir?

Primer de tot vull agrair al Quico i al Santi la confiança per dur a terme aquesta tesi. Al Quico, per obrir-me les portes del departament quan jo encara no sabia ni què volia fer. Per compartir amb mi una zona tan fantàstica com la *Roureda de Tordera*, i transmetre tan d'interès i estima per l'entorn. Al Santi, per confiar-me la beca, per l'esperit crític que fa que les coses millorin, poc a poc però amb bona lletra.

Per la Susana i l'Eugènia només tinc paraules d'agraïment i admiració, per l'allau d'idees, positivisme i empenta que comparteixen, gràcies! A l'Emilia, que la seva passió pels anells l'empeny a explicar-ho amb un entusiasme que encomana. À Zahra et Pauline, pour essayer de comprendre *Font del Regàs* encore et encore, sans perdre l'espoir d'arriver a la modéliser.

A l'old Quico-team: Lídia, infinites gràcies per tot el que he après de tu al lab, m'has vist passar de la mà tremolosa que agafa la pipeta per primer cop al "Sílvia-l'autosampler". Ada, és fantàstic sentir-te sempre al costat, et trobo a faltar! A l'Anna... podria omplir tantes pàgines com té aquesta tesi amb agraïments i anècdotes! M'encanten tots els riures que hem fet davant les nostres petites desgràcies abans de solucionar-les. No se m'acudeix ningú millor que tu per fer un bon equipo. Moltíssimes gràcies per ser-hi sempre, dins i fora de la ciència, ets una peça clau.

A tots aquells amb els que hem compartit estones de camp, sobretot a l'Eli amb tot el *tingladu* que vam muntar al *Regàs*! I a tots els del CEAB: Edu y Clara :), Marc, Miquel, Steffi i Elliot, sempre era una alegria trobar-vos a la parcel·la. A tots els estudiants que heu tingut una part de les mostres a les vostres mans, avorrint l'olor de les fulles seques o esmerant-vos en tallar els anells, espero que en guardeu un record bonic! I crec que es mereixen un reconeixement també... els treballadors del servei de vehicles per rebre'm cada matí amb un bon somriure davant la meva cara de pànic davant del 4x4; els Guassos per deixar-nos fer totes les manualitats

possibles sense jutjar; i el Miguel i el José Luís per aprendre's el meu nom i fer els matins més agradables.

A toute la famille de PSN pour les cafes autour de la table avec des chuqettes, mmmh! En especial a Zahra pour la confiance et la pacience en m'aider a comprendre l'hydrogeologie, it has been really great to meet you. A Gilles, qui m'a donné l'opportunité de rencontrer des gens et d'enfortir l'interesse pour l'azote. Merci por tous les *after-work* avec vous sur les terrasses de Rennes: Mathilde (*mira a ver si hay mesa en el Gazo*), Maria (*els nostres llargs i fantàstics cafès, trugarez!*), Tamara (*for all those talks with our bottle of wine in the kitchen, there is no better coach than yours!*), Pantelis, Dani, Mariana, Stéph, Inés, les danseurs et danseuses de l'Asso, ... Rennes va être toujours chez moi.

I la tesi no seria el mateix sense les persones fantàstiques que et vas creuant pel departament, un dia hi comparteixes una hora de dinar, i de cop ja ho comparteixes tot. Gràcies, sou indispensables! Espero que ens quedin molts viatges per fer plegats :) Anna (again and again), Núria, Ada, Pol (no et quedis al Tibet!!), Pol2 (You are... wait for it... Iogurin!), Eneko, Aurora, Eli (com se t'ha trobat a faltar en el teu exili a Alemanya!), Pau, Pablo, Núria dC. My girls, Astrid and Myrtaki mou, I'm so glad we have met, you are all kindness and love, I miss you in the row and in Sol. Als que heu anat arribant (Vero, Rebeca (*I'm back*^^), Daniel, Aida, Graci, Dani, Marta, Maria, Alba, Marta) i als que heu retornat (Núria Cid, Tano, Cesc), gràcies per tots els riures provocats aquest darrer any. Com també tots els riures previs amb els que heu marxat (Dani: és un regal parlar amb tu, Lídia, Mari, Jaime, Bet, Isis, Esther...).

A les que els dimecres compren nespres... una abraçada infinita. Txell, no sé que hagués passat si aquell famós dia no t'hagués parlat al metro, però per res del món em voldria haver perdut aquests anys amb tu, la fortalesa i amor que desprèns. Ada, ets capaç d'encomenar-me el teu optimisme, m'encanten els nostres bucles engrescadors amb idees eixelebrades (però factibles, eh!), per molts aniversaris més! Cèlia, els teus dubtes i les teves reflexions encertades m'ajuden a créixer constantment, al teu costat sembla més fàcil. Núria, de tu em quedo l'empenta, des del primer minut compartit a l'oficina Erasmus sabia que funcionaria, encara no tinc clar quina de les dues és "la mala influència" però poc importa ja, que duri. Gràcies a totes per ser-hi.

A la Pitu, que 28 anys compartits se'ns fan curts. Gràcies per recollir-me sempre que ha calgut. A la Manxi, gràcies per aguantar-me el sinusoide, també ens ha portat moments ben graciosos! A la Yepes, que et coneixes Tordera i el Regàs, ara sí!! Als folkis, els xuxiquius i els breizh, perquè seguim ballant valsos, mazurkes, salses i andros, perquè ens cura l'ànima.

A l'Anna i la Catix, les gomets, per dur el "sempre a punt" al top aquests darrers mesos... any i mig? I a tu Pol per recollir-me i cuidar-me tant, ho fas tot molt fàcil, no se m'acudeix ningú millor per dissenyar la portada que conclou aquest període. Gràcies!

Al Gerard, per tot el que ens ha costat. No hauria arribat tan lluny si no fos pel teu suport, moltes gràcies per tots els bons moments compartits.

Finalment, als de casa, als meus pares per ser un suport constant i incondicional sense entendre ben bé els perquès... GRÀCIES! Al Jordi, que vas seguint els passos, ara sí que et passo el relleu de la frase de les sobretaules a casa "i quan acabaràs la tesi?". I a la Mari que sempre estàs allà per fer un cap de setmana diferent (¿quién te quiere?). Sou la meva pinya, i no seria com sóc si nos fos per vosaltres i els iaios, no m'imagino uns referents millors.

Gràcies a tots i totes pel vostre granet de sorra.

Barcelona, 17 de maig del 2018

He tingut el suport econòmic d'una Beca FPI del Ministerio de Competitividad y Ciencia (). La meva recerca ha estat finançada per dos projectes del Plan Nacional del Ministerio de Ciencia e Innovación: MONTESCONSOLIDER i MED_FORESTREAM. He disposat de dues beques de mobilitat de la Facultat de Biologia per assistir a congressos i de dues ajudes per estades breus, associades a la beca FPI.

ABSTRACT

During the last decades, most of the studies based on climate change effects on vegetation physiology have focused on upland forests and species at their border of distribution, since, in both conditions, species are highly affected by water scarcity. Although few studies have focused on water availability effects on riparian vegetation, these species could be extremely affected by water scarcity as they are usually found in wet environments and they may not have enough ecophysiological controls to cope with prolonged drought periods. Moreover, riparian zones are considered hotspots of nitrogen (N) processes. These ecotones can reduce part of the N loads received from adjacent ecosystems before they reach the stream, mainly via denitrification and vegetation uptake. In Mediterranean regions, where shallow organic soil layers are disconnected from groundwater, denitrification process is limited by the weak anoxic conditions on riparian forests soils. There, vegetation uptake becomes the main driver for N removal in Mediterranean riparian zones. Climate change effects on riparian vegetation may cascade down and modify this well-known capacity to remove N from riparian zones.

The findings from two Mediterranean riparian forests in *La Tordera* catchment showed that riparian tree species are already experiencing the effects of drought periods in the Mediterranean region. *Quercus robur* species, typically found in mid-European floodplains, is already experiencing tree growth decline at its southernmost distribution range edge. On the other hand, riparian tree species at Mediterranean forests showed high dependence on soil water availability during summer, obtaining more than 80% of the water transpired from the vadose zone. Phreatophitic species, *Alnus glutinosa* and *Populus nigra*, took up water from the groundwater compartment during spring but soil water was their main water source during summer. *A. glutinosa* did not present ecophysiological controls to avoid drought situations, while *P. nigra* increased its iWUE during dry years. *Fraxinus excelsior* was cohabiting with both species in the riparian forest. This species, located far away from the stream channel, was more depending on soil water availability and did not

present any ecophysiological mechanism to cope with summer drought. Conversely, the N-fixing invasive species *Robinia pseudoacacia*, which was co-occurring all across the riparian forest, showed high plasticity to cope with different water availability conditions.

Additionally, the findings obtained from the effects of riparian vegetation on water and N fluxes highlighted the high spatial heterogeneity of Mediterranean riparian forests within relatively small distances (~25 m). The studied Mediterranean riparian forest showed a remarkable spatial heterogeneity on water availability, with groundwater levels increasing from the near-stream zone (~0.6m deep) to the hillslope edge (~2.2m deep). Shallow groundwater tables enhanced the connectivity between vadose zone and groundwater at the near-stream zone, allowing greater transpiration and N uptake rates compared to the hillslope edge. Conversely, denitrification rates were generally low across all the riparian area due to water limitation and its weak anoxic conditions. Nevertheless, these soil conditions promote respiration rates all across the riparian forest soil, and thus, riparian soils emitted large CO_2 fluxes. Finally, simulation based on climate change projections suggested a future increase in soil N concentrations as well as a reduction of the effective N-removal area of this riparian zones. The feasible substitution of autochthonous species by the already present *R. pseudoacacia* may homogenize soil N availability across the riparian area but would not increase the future soil N availability.

Overall, our findings highlight the spatial heterogeneity of Mediterranean riparian zones and the need to better evaluate spatio-temporal processes to understand their mechanisms. N retention in Mediterranean riparian soils occur mainly by vegetation uptake. Yet, future climate projections may exacerbate water scarcity problems, inhibiting denitrification rates and reducing vegetation uptake. Therefore, these results challenge the well-accepted capacity to reduce N loads reaching the stream, and suggest that Mediterranean riparian soils can become a potential source of N to adjacent aquatic ecosystems in the future.

RESUM

Durant les darreres dècades, la majoria d'estudis sobre els efectes del canvi climàtic en la vegetació s'han centrat en boscos d'alta muntanya amb un gradient latitudinal i espècies en els seus límits de distribució geogràfica, ja que, en ambdues situacions, els individus poden trobar-se afectades per l'escassetat d'aigua. Tot i que pocs estudis s'han centrat en els efectes de disponibilitat d'aigua en la vegetació de ribera, aquestes espècies podrien veure's extremadament afectades per l'escassetat d'aigua, donat que normalment es troben en ambients humits i poden no disposar de controls ecofisiològics suficients per afrontar períodes sequera prolongada. D'altra banda, les zones de ribera es consideren hotspots dels processos del nitrogen (N). Aquests ecotons poden reduir part de les càrregues N que arriben dels ecosistemes adjacents abans d'arribar al riu, principalment a través de la desnitrificació i l'absorció per part de la vegetació. A les regions mediterrànies, on els horitzons orgànics dels sòls orgànics queden desconnectats de l'aigua del freàtic, el procés de desnitrificació està limitat per les baixes condicions anòxiques dels sòls de ribera. Així doncs, l'absorció de N per part de la vegetació es converteix en el principal procés de retenció de N a les zones de ribera mediterrànies. Els efectes del canvi climàtic en la vegetació de ribera poden també modificar aquesta capacitat d'eliminar N de les zones de ribera.

Els resultats obtinguts en dos boscos de ribera mediterranis de la conca de *La Tordera* mostren que les espècies arbòries de ribera estan experimentant els efectes de la sequera a la regió mediterrània. *Quercus robur*, que normalment es troba en planes d'inundació d'Europa central, estan experimentant un declivi en el creixement anual dels individus en el seu límit de distribució geogràfica més meridional. D'altra banda, les espècies arbòries dels boscos de ribera mediterranis una elevada dependència a la disponibilitat d'aigua del sòl durant el període d'estiu, obtenint més del 80% de l'aigua transpirada a la zona de no saturada del sòl. Les espècies freatòfiles, *Alnus glutinosa* i *Populus nigra*, obtenen l'aigua principalment del freàtic durant la primavera, però el sòl no saturat és la principal font d'obtenció d'aigua durant l'estiu. *A. glutinosa* no

presenta controls ecofisiològics per evitar les situacions de sequera, mentre que *P. nigra* augmenta la seva iWUE durant els anys secs. *Fraxinus excelsior* conviu amb ambdues espècies al bosc de ribera. Aquesta espècie, situada a les zones allunyades del llit del riu, presenta una forta dependència a la disponibilitat d'aigua del sòl tot i no tenir mecanismes ecofisiològics per afrontar la sequera estival. Contràriament, l'espècie invasora fixadora de N, *Robinia pseudoacacia*, es troba distribuida al llarg de tot el bosc de ribera i presenta una gran plasticitat per fer front a les diferents condicions de disponibilitat d'aigua.

A més, els resultats obtinguts sobre els efectes de la vegetació de ribera sobre els fluxos d'aigua i N han destacat la gran heterogeneïtat espacial dels boscos de ribera mediterranis en distàncies relativament curtes (~ 25 m). El bosc de ribera mediterrània estudiat mostra una notable heterogeneïtat espacial en la disponibilitat d'aigua, amb nivells freàtics decreixents des de la zona pròxima a la llera del riu (~ 0,6 m de profunditat) fins a les zones més allunyades (~ 2,2 m de profunditat). Els nivells freàtics més superficials faciliten l'intercanvi entre la zona saturada i no saturada del sòl, permetent també una major transpiració de la vegetació i absorció de N per part d'aquesta a les zones més pròximes a la llera del riu. Per contra, les taxes de desnitrificació són baixes a tota la zona de ribera degut a la limitació del sòl de ribera en quant a contingut d'aigua del sòl, i la conseqüent anòxia que afavoreix l'activitat dels bacteris desnitrificadors. No obstant això, aquestes condicions aeròbiques del sòl, amb relativa humitat, promouen altes taxes de respiració a tot el sòl forestal de ribera, i la conseqüent elevada emissió de CO_2. Finalment, la simulació basada en les projeccions del canvi climàtic suggereixen un augment futur de les concentracions del N al sòl, així com una reducció de l'àrea de ribera capaç de retenir N de forma efectiva. La possible substitució de les espècies autòctones per la invasora *R. pseudoacacia* podria homogeneïtzar la disponibilitat de N del sòl al llarg de la zona de ribera, però no augmentaria la futura disponibilitat de N del sòl.

Així doncs, els nostres resultats destaquen l'heterogeneïtat espacial de les zones de ribera mediterrànies i la necessitat d'avaluar els processos a escala espaciotemporal per comprendre'ls millor. La retenció de N en sòls de ribera mediterranis es produeix principalment per l'absorció d'aquest per part de la

vegetació. No obstant, les projeccions climàtiques poden agreujar els problemes d'escassetat d'aigua, inhibint les taxes de desnitrificació i reduint l'absorció de N per part de la vegetació. Per tant, aquests resultats qüestionen la capacitat de les zones de ribera mediterrànies de reduir les càrregues de N que arriben als rius, així com suggereixen que els sòls de ribera mediterranis poden esdevenir una font potencial de N als ecosistemes aquàtics adjacents en el futur.

CONTENTS

LIST OF FIGURES

LIST OF TABLES

CHAPTER 1

General Introduction and Objectives

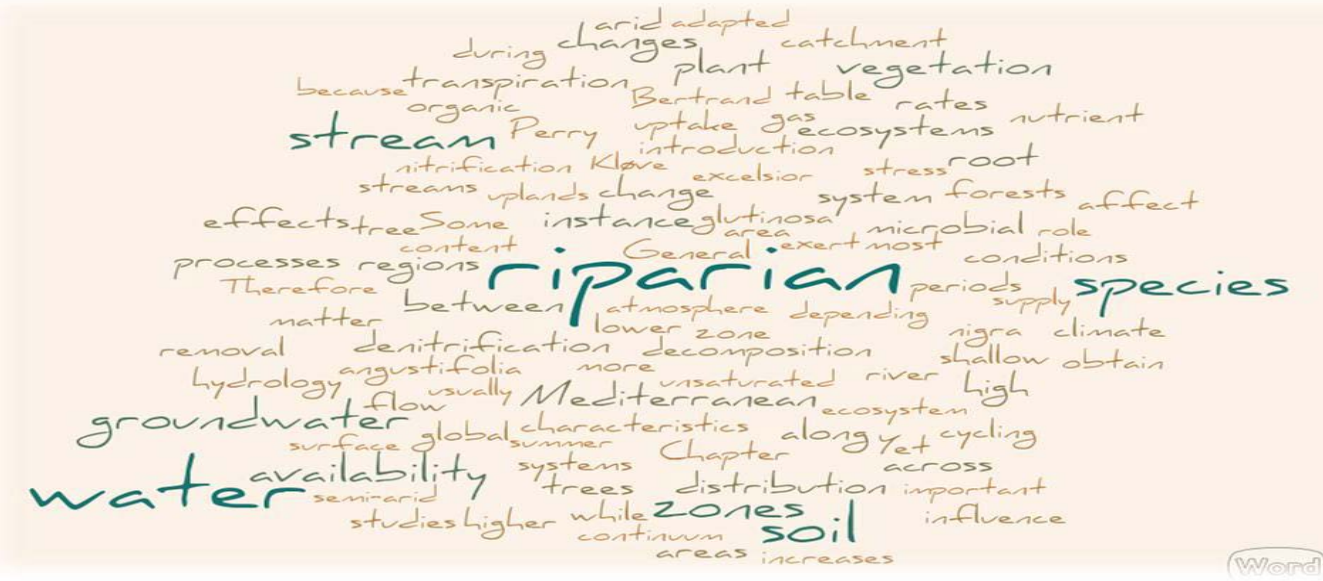

1.1. Riparian zones and hydrological linkages

Riparian zones are those ecosystems lying next to the streams and considered ecotones between uplands and streams. Riparian ecosystems are characterized by having greater water availability than the surrounding uplands given their proximity to streams and the shallow groundwater table. Riparian zones are also characterized by having alluvial soils from the particles transported by the stream flow and deposited at the adjacent zones of the stream channel during flooding events or changes in stream velocity. These characteristics promote that riparian zones become hotspots of biodiversity. For instance, plant communities inhabiting riparian areas have high water requirements and they cannot be found elsewhere in the catchment. Moreover, the high resources at the area support a large number of animal species such as invertebrates, amphibian, reptile, mammals and birds (Naiman et al., 2005; Perry et al., 2012). Despite riparian zones occupy a small proportion (generally <3%) of catchments (Tockner and Stanford, 2002), these systems can provide multiple ecosystem services. Riparian zones can play a key role in regulating water and solute exports from the uplands into the streams because of the presence of riparian vegetation at the stream margins, which constitute a strong influence on geomorphological processes by reducing erosion and minimizing flow effects. Riparian zones also act as a hotspots of biogeochemical processes within catchments (McClain et al., 2003). For instance, high soil moisture from riparian zones also enhance microbial activity accelerating processes such as organic matter decomposition or nitrogen (N) removal via denitrification. Moreover, riparian vegetation supply organic matter to the stream providing food for the in-stream organisms and woody debris that enhance sediment retention and create new habitats (Magdaleno et al., 2014). Finally, riparian forest also influences stream biogeochemistry, by regulating light entrance and water temperature with canopy trees, and processing part of the nutrients arriving from uplands to stream through groundwater fluxes or with stream-spiraling (Lupon et al., 2016b). Therefore, both stream and riparian ecosystem are tightly linked.

Riparian vegetation is representative of these areas not only because of its high water availability requirements, but also because of its capacity to colonize unstructured and alluvial soils from the river margins. The vegetation inhabiting in riparian areas can vary across different spatial scales. At global scale, climatic conditions exert a fundamental influence on riparian zone characteristics. Among climatic variables, the hydrological regime has been reported to be the most important factor influencing riparian species composition across regions (Douda et al., 2016). In the Iberian Peninsula, riparian forests are mainly occupied by species of Atlantic distribution such as *Alnus glutinosa*, *Fraxinus angustifolia* and *F. excelsior*. Nevertheless, in arid and semiarid Mediterranean regions, riparian forests are dominated by species with less water demands, such as *F. angustifolia*, *Populus alba*, *P. nigra* and *Platanus orientalis* (Douda et al., 2016). However, in Mediterranean subhumid riparian zones, species can cohabit with some mid-European species, such as *Quercus petraea* and *Q. robur*, which find in these wet areas of the region the proper conditions to survive. More recently, many invasive species have been detected in Mediterranean riparian zones, as they colonize open spaces caused by human disturbances at these sites such as clearcutting management. *Robinia pseudoacacia* and *Ailanthus altissima* are considered common invasive species across the Iberian Peninsula (Sanz Elorza et al., 2004).

At catchment scale, the riparian community is strongly influenced by hydrology and associated fluvial processes such as base flow, drought periods, and floods magnitude and timing and thus, it can vary along the river continuum dynamics. In mountainous Mediterranean environments, riparian areas differed between the erosion, transfer, and depositional zones. The riparian area increases its width from the headwater to the floodplains downstream, also increases the influence of the stream on the riparian hydrology and the deposition of alluviums (Fig. 1.1). Along the catchment, heavier stream sediments (i.e. cobbles, gravel, and sand) are deposited at the river margins of the headwater and middle reaches, while lighter particles (i.e. silt and clay) settle at the floodplain of the depositional reaches.

Finally, in regions where water availability have strong gradients across the riparian area, such as arid and semi-arid ones, plant species distribute also differently across the area depending on their water requirements or abilities to cope with water stress. For instance, phreatophitic species are located near by the stream edge where their roots can access to the shallow groundwater, while species with less water dependence occupy zones farther from the stream where groundwater table is deeper. In Mediterranean regions this spatial segregation is specially marked. There, the phreatophic species *A. angustifolia* and *P. nigra* are often find near the stream edge. Contrary, *F. excelsior*, *F. angustifolia*, *Ulmus minor*, and *Salix salicaceae*, more tolerant to water availability variability, are located farther away from the stream channel (Magdaleno et al., 2014) (Fig. 1.2).

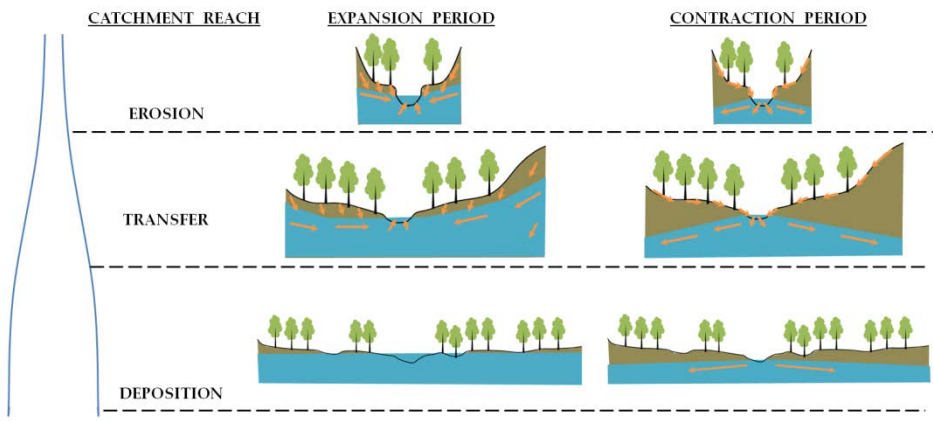

Figure 1.1 Schematic representation of energy and water transfers between the stream and its catchment along the river continuum: erosion-transfer-deposition concept describing alluvial morphological regions. Riparian floodplain width increases along the river continuum (adapted from Church et al 1992 and Tabacchi et al. 1998). Expansion and contraction stream periods are represented along the river continuum. Flow paths are represented with orange arrows.

1.2. Mediterranean riparian trees and water availability

Water exchange between riparian areas and adjacent streams are commonly studied across most of biomes. However, the control that riparian vegetation exert on stream discharge and stream-riparian water exchanges is depending on the hydrological connection between both ecosystems, but also on the climatic regimes and the transpiration rates in the area. Riparian vegetation generally intercepts precipitation before it reaches the soil surface. This mitigates erosion and leaching effects on riparian soils. In temperate systems, groundwater recharges the stream especially during rainfall events. Yet, in arid and semi-arid regions, reversal hydrologic flow paths from streams to riparian zones can occur when water is scarce, like in summer (Butturini et al., 2003a; Martí et al., 2000). These drier periods can switch the characteristics of stream flow from an expansion situation, when the stream is recharged by hyporheic and riparian lateral water fluxes, to a contraction situation, when the stream recharges hyporreic and riparian groundwater compartments (Fig. 1.1). Indeed, in Mediterranean zones stream, riparian forest transpiration can decrease stream discharge during the vegetative period (Lupon et al., 2016c; Medici et al., 2008). For instance, daily transpiration rates can affect groundwater and soil water dynamics (Barnard et al., 2010; Bosch et al., 2014; Ghazavi et al., 2011; Gribovszki et al., 2010). Thus, the high transpiration rates from trees (Huxman et al., 2005; Zhang et al., 2001, 2005) can drive to lower groundwater table and facilitate those reverse patterns from the stream to the riparian zone (Hernandez-Santana et al., 2011; Medici et al., 2008; Sabater and Bernal, 2011; Williams and Scott, 2009) (Fig. 1.1).

Riparian trees can obtain water simultaneously from soil, groundwater, and stream compartments to supply their evapotranspiration demands (Dawson and Ehleringer, 1991a; Sánchez-Pérez et al., 2008). Most of the riparian tree species obtain the hugest amounts of water from the unsaturated soil, but they can switch to other sources depending on its root system distribution and on seasonal and annual conditions. For instance, species with shallow root distribution system would depend more on soil water availability, while those species with deeper root system may obtain water from unsaturated soil and

groundwater depending on the seasonality of water availability (Bertrand et al., 2014). Among the riparian tree species occuring in the Mediterranean region, *F. excelsior* has been reported to develop shallow root system distribution, while *P. nigra* and *A. glutinosa* can develop a deep root system that can reach the groundwater table (Fig. 1.2). Some studies have pinpointed the capacity of these two species to obtain water directly from the stream channel when it is needed (Sargeant and Singer, 2016; Singer et al., 2013). Usually, soil water is the dominant source for tree transpiration whenever soil water content is high (Bertrand et al., 2014). Nevertheless, in arid regions where surface flows are low and annual precipitations do not supply enough water to satisfy the annual potential evapotranspiration rates, groundwater becomes an important source for riparian trees (Liu et al., 2017). This role of groundwater can come by direct water root uptake from the compartment or by capillarity fluxes that recharge soil water content in the unsaturated zone. This particular need of groundwater especially happens during summer drought periods (Bertrand et al., 2014). This may propitiate the above mentioned inverse flow connectivity with the stream.

1.3. Riparian trees and soil nitrogen cycling

Riparian zones are considered hotspots of nitrogen (N) transformations across the landscape, as they provide a filter for nitrate (NO_3^-) transported from surrounding lands via runoff and subsurface path flows (Hill, 1996; Vidon et al., 2010). In most riparian zones, the primary N removal mechanisms is denitrification, an anaerobic process whereby NO_3^- is transformed to N gas or, less frequently, to nitrous oxide (N_2O) (Clément et al., 2002). However, denitrification requires of anoxic conditions to occur, which barely happens in arid or semi-arid regions. Conversely, in these systems, aerobic N transformations, such as mineralization or nitrification dominate the riparian biogeochemistry, suggesting that N removal capacity by denitrification in these riparian zones is really low (Harms and Grimm, 2008) (Fig. 1.3a). Therefore, in arid and semiarid zones plant N uptake can be the main N removal process. Yet, in Mediterranean regions the groundwater table is often lower than 1m, reducing the chance of the emergence of water up to the surface, and

disconnecting the saturated zone from surface soil layers which content the organic matter and N necessary for microbial N removal (Vidon, 2017). Nevertheless, the existence of wetlands can occur in the downstream floodplains due to gentler slopes.

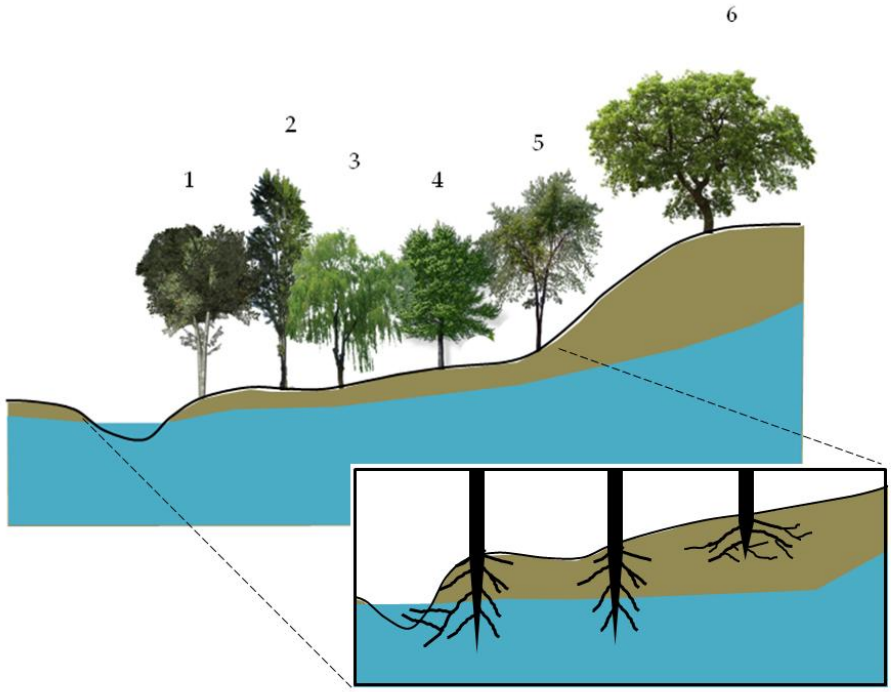

Figure 1.2 Species distribution across a Mediterranean riparian zone: (1) *Alnus glutinosa*, (2) *Populus nigra*, (3) *Salix alba*, (4) *Ulmus minor*, (5) *Fraxinus excelsior* and *F. angustifolia*, and (6) *Quercus pubescens* and *Q. ilex*. A zoom into the riparian tree root system is shown in the inlet. Deep root distribution reached the groundwater table (for *A. glutinosa* and *P. nigra*) or even the stream (*A. glutinosa*), while shallow root distribution remains in the unsaturated soil profile (*S. alba, U. minor, Fraxinus spp.* and *Q. spp.*).

Riparian trees play a key role in riparian biogeochemistry. First, the strong influence that transpiration does on soil water availability influences the seasonality of microbial activity. Decreasing soil water availability along the vegetative period can switch from anaerobic to aerobic soil microbial processes (from denitrification and methanogenesis to mineralitzation, nitrification and respiration), or even stop them when reaching a threshold of low water

availability (Chang et al., 2014). Yet, little is known about how important is transpiration in regulating soil processes. Second, vegetation nutrient uptake partly regulates nutrient cycles in the soil compartment, such as C and N. Plant uptake is usually questioned as an N removal process because of the temporality of this removal, as that C and N removed will return to the ecosystem at the end of the vegetative period or after the death of the individual. Nevertheless, it may have an important role in arid and semi-arid riparian zones due to the negligible denitrification rates. Only few attempts have been carried out to quantify vegetation N uptake, as it is difficult to obtain direct measurements, and it is usually estimated from N concentration in plant tissues (Hefting et al., 2005; Williams and Scott, 2009). Finally, plant species are a source of organic matter and nutrients to the soil compartment that will be mineralized afterwards. These compounds can reach the soil through leaf litter inputs, wood debris or root exudates. The quality of this organic matter is determined by plant species characteristics and it would influence microbial processes characteristics in the soil (e.g. decomposition rates) (Rascher et al., 2012). Some species can fix atmospheric N in symbioses with bacteria. This can induce rapid leaf decomposition rates and end up to an increase of soil N stock. For instance, *A. glutinosa* can fix up to 40-300 kg N ha^{-1} $year^{-1}$ (Silvester, 1976) and its presence is very common in riparian areas.

1.4. Global change implications

Climate change but also human population growth and resources consumption, with all the consequences in land-use practices, energy use and pollution, will impact biological systems across many scales (Green et al., 2011; Perry et al., 2012). For instance, climate change and water management are expected to alter hydrology (Barnett et al., 2008; Kløve et al., 2011), affecting significantly water balances and leading to ecological changes in terms of riparian species distribution and productivity (Bertrand et al., 2014; Magdaleno et al., 2014; Merrit et al., 2010). All these expected changes in ecosystems can induce a loss of their ecosystem services provision (Kløve et al., 2014).

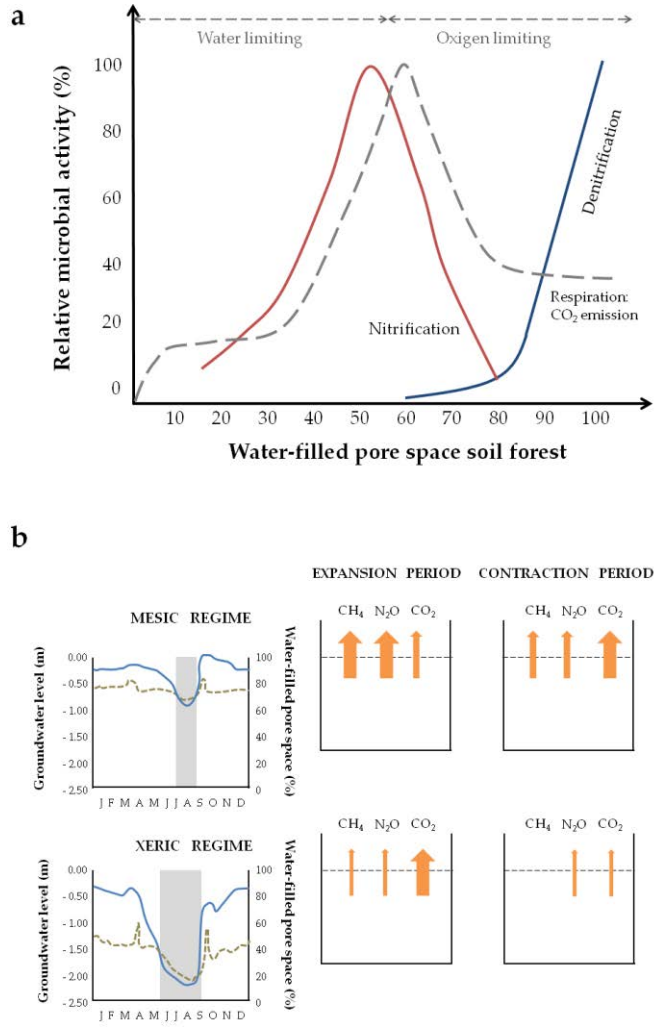

Figure 1.3 (a) Relationship between water-filled soil pore space and relative amount of microbial nitrification, denitrification and respiration (adapted from Linn and Doran 1984). (b) Comparison between riparian zones from mesic and xeric regimes, showing that high groundwater levels and soil water contents promote higher gas emissions, while drier conditions reduce them to punctual rewetting episodes (adapted from Vidon, 2017).

It is challenging to predict the effects that global environmental change can have on riparian forests. First, there are still many uncertainties about the effects that global change can exert on groundwater level (Kløve et al., 2011; Meixner et al., 2016). For instance, ecological changes in small catchments may be more exacerbated than in larger systems, where ecological changes can be

buffered along the catchment (Kløve et al., 2014). Second, it is not fully understood the effects that changing groundwater levels can have on riparian vegetation, since they are adapted to high water availability. Third, riparian ecosystems are already temporally and spatially dynamic systems changing geomorphology and species composition to natural hydrology variations (Webb et al., 2006). However, the study of the effects that natural climate and hydrology variability produce on riparian ecosystems can help to predict the feasible effects that climate change may exert on them.

Climate change forecasts project an increase of temperatures and decrease of precipitation in the Mediterranean region (IPCC, 2013). Higher temperatures may increase the evapotranspiration demand of vegetation, yet lower water resources may difficult to supply this new demand and induce hydrologic stress on vegetation. This hydrologic stress may be particularly troubling for riparian trees, after their high water demand (Huxman et al., 2005), and at present barely encountered with water deficit situations. Therefore, riparian forests species may be exposed to higher water stress conditions and be more vulnerable than species in upland terrestrial forests.

Vegetation can perform different adjustments to cope with water limitations. For instance, trees perform changes in the root system, their hydraulic architecture, transpiration regulation, tree growth or phenology (Jump et al., 2006; Martnez-Vilalta et al., 2014; Perry et al., 2012; Sperry et al., 2002). Yet, severe or long periods of water limitation may lead to the collapse of the plant hydraulic system, especially for riparian tree species. There are already several widespread examples of altered riparian plant composition such as shifts in the dominance of deciduous and coniferous species, increases in drought-tolerant species facilitating the entrance of invasive species, and the increasing global distribution of plantation and crop species (Kominoski et al., 2013). For instance, *R. pseudoacacia* is an invasive N-fixing species that has been already reported to be naturalized in Europe, temperate Asia, Australia, New Zeland northern and southern Africa and temperate South America (Vítková et al., 2015; Weber, 2003). The presence of this species can have a fertilizing effect on N-poor ecosystems (Rascher et al., 2012; Vilà et al., 2011), but their effects on N-

enriched ecosystems are still uncertain (Akamatsu et al., 2011; Castro-Díez et al., 2009).

Therefore, changes on the diversity and distribution of plant functional traits can provoke cascade effects on terrestrial and aquatic food webs, organic matter production and processing, nutrient cycling, water quality, and water availability (Rascher et al., 2012; Reich, 2006). For instance, changes in litter quality and production may also affect decomposition rates and nutrient cycling. On the other hand, species substitution can result in species with a higher performance of plant water use (higher water use efficiency, WUE), preventing drastic soil moisture decreases (Perry et al., 2012). Besides, climate change will affect differently litter decomposition and nutrient cycling in riparian zones. On one side, warmer temperatures may enhance detritivore and microbial activities, enhancing decomposition and nutrient cycle (Briones et al., 2009). Yet, lower water availability may limit microbial activity (Lupon et al., 2015; Rustand et al., 2001). Some authors suggest that in arid and semiarid regions, lower spring and summer water availability under increasing temperatures would lead to slower decomposition rates and nutrient cycling (Perry et al., 2012). However, it is challenging to understand how global change projections can affect the complex interaction between soil, vegetation, and atmosphere at riparian zones (Fig. 1.4)

Microbial soil processes can have gas molecules as a final product of the reaction, which are usually reaching the atmosphere and represent an output/loss of the system. This gas emissions can contribute to greenhouse gas effect, but their magnitudes differ among soil water availability conditions. For instance, riparian zones with shallow groundwater table where soil remains wet during most of the year can be potential sources of methane (CH_4) and N_2O to the atmosphere as they are they are final products of anaerobic processes (methanogenesis and incomplete denitrification and nitrification, respectively). However, during summer drought periods, when soil water availability decreases, aerobic respiration increases emitting higher volumes of CO_2 to the atmosphere (Fig. 1.3b). Contrary, in riparian zones with lower groundwater tables and soil water content, gas emissions remain poor along

the year increasing after rewetting events (Harms and Grimm, 2012; Jacinthe et al., 2015) (Fig. 1.3b).

1.5. Objectives

This thesis aims to contribute to a better understanding on how riparian tree species respond to changes in water availability with changes in both physiological and their relative abundance across the riparian gradient. Besides, it studies how these changes cascade down to C and N cycling in riparian soil, which will ultimately affect stream ecosystems. Although some studies have examined the influence of nutrients and organic matter transfer between riparian and stream ecosystems, very few studies have examined these linkages by explicitly merging perspectives from terrestrial and stream ecology as it is presented in this thesis. Moreover, few studies have paid attention to responses of riparian vegetation to climate and water availability variability, as they occupy small areas in the catchment and they barely encounter water deficit situations.

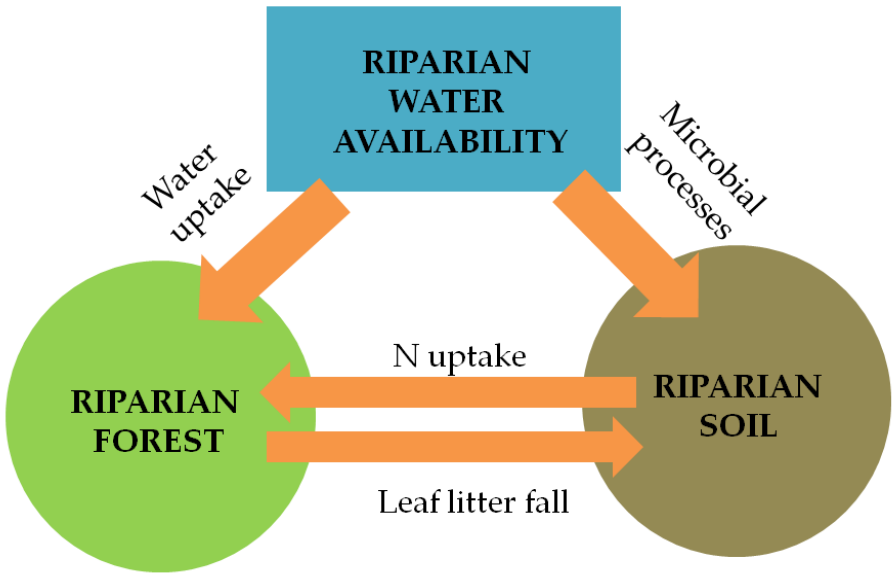

Figure 1.4 Complex interaction between riparian hydrology, and riparian forest and soil compartments. Orange arrows represent the processes studied in this dissertation.

Mediterranean regions provide strong intra- and interannual variability in environmental conditions. This makes Mediterranean riparian forests a suitable natural laboratory to study possible climate change effects on tree species and soil biogeochemistry. For that, we have studied two well developed forest under Mediterranean climate, one at the floodplain of the depositional zone of *La Tordera* river, and the second at the middle reach of the same river. Most of the work included in this thesis have been carried out in the stand at the middle reach. In order to study biogeochemistry at riparian zones, we used N as a proxy due to (i) its high reactivity and (ii) the well-known importance of riparian zones controlling uplands exports to the streams.

The third chapter aimed to study the vulnerability of riparian tree species to warmer and drier conditions from the last decades. For all species, we expected a decline in growth trends and an increase on wood water use efficiency as a consequence of warming over last decades, especially in the zones of the forest where water availability is lower. *Q. robur* species, which founds in the Mediterranean region its southernmost distribution edge, is expected to be the most sensible species

The fourth chapter aimed to evaluate the sensitivity of riparian tree species to water availability limitation and to determine the main water sources to supply their transpiration. For that, we compared tree species between a wet and a dry year. We expected that those species at the stream edge would depend on groundwater availability and would show weak strategies to cope with water stream limitation. Contrary, we expected that those tree species located near the hillslope edge and the invasive *R. pseudoacacia* would present more strategies to cope with environmental conditions of the drier year (i.e. reducing leaf biomass production, producing smaller leaves, increasing iWUE, and increasing leaf litter fall during summer).

In the fifth chapter we aimed to evaluate how the spatiotemporal variability of soil water availability drive soil N processes, and thus soil CO_2 and N2O emissions, in Mediterranean riparian soils. We expected low denitrification

rates due to low water availability. However, aerobic soil conditions would enhance nitrification and microbial respiration, especially during warm conditions. Anoxic processes would take place at the near-stream riparian zone, while aerobic processes would be dominant farther away from the stream channel.

The sixth chapter aimed to estimate the relative contribution of riparian vegetation to influence water and N exports to the stream and simulate climate change effects on this influence. For that, we studied riparian spatial heterogeneity. We expected that transpiration during vegetative periods would promote water and nitrate retention from the soil compartment, especially at the near-stream riparian zone where higher soil water availability would facilitate higher nitrate uptake. Based on climate change projections, we hypothesized that future drier conditions would cause a decrease on soil water content and an increase of soil nitrate concentration due to lower root-uptake rates.

The seventh chapter aimed to estimate the effects of a potential tree species substitution on the riparian forest soil N availability due to changes in leaf litter inputs. We hypothesized that future climate change would difficult native tree species survival and then facilitate their substitution by the already present invasive N-fixing tree species *R. pseudoacacia*. We expected that the expansion of *R. pseudoacacia* would increase soil N inputs, soil N processes and soil N availability.

CHAPTER 2

Study Site and Field Design

2.1. The Tordera basin

The present thesis research has been carried out in *La Tordera* catchment, located in the NE of the Iberian Peninsula. *La Tordera* catchment occupies 869 km^2 and its altitude ranges from 0 m (river mouth) to 1700 m (headwaters). The marked altitudinal gradient that characterizes *La Tordera* basin determines a high variability of local microclimates. At the highest elevations, the local climate is sub-humid Mediterranean (average annual precipitation >900 mm), whereas the surrounding climate in the area is typically semi-arid Mediterranean (average annual precipitation < 500 mm) in the lowland areas close by the river mouth. Given the high variation of local microclimates, a wide range of vegetation characteristic from different climate conditions can be found.. Thus, vegetation types cover from boreo-alpine (*Junipuerus nana*, *Vaccinium myrtillus, Antennaria dioica*), to Atlantic (*Abies alba*, *Quercus petrea*, *Q. obur*, *Fraxinus excelior*, *Castanea Sativa*, *Pinus sylvestris*) and to Mediterranean types (*Quercus ilex, Pinus pinaster, Pinus halepensis*, ...) (Boada et al., 2008). Moreover, *La Tordera* has a wide range of land-uses, from forest (77%) to agricultural (16%) and urban or industrial uses (7%).

The uniqueness of climatic and floristic characteristics of *La Tordera* basin has supported its recognition for protection and conservation. This results in a numerous of protected areas in the catchment, like the Montseny Mountain Natural Park (since 1995) or the *Roureda de Tordera* (since 1993). The ecological importance of the *Roureda de Tordera* has been decisive for its recognition in protecting the area under local (Natural Interesting Place), regional (Natural Interest Spaces Plan (PEIN) and Wetlands Inventory of Catalonia) and European (Nature 2000 network) administrative figures. Moreover, the catchment has been the focus of multiple studies with ecological and biological perspectives (e.g. Àvila and Rodà, 2012; Bernal et al., 2015; Lupon et al., 2015; Pastor et al., 2014; Von Schiller et al., 2008), which are a valuable knowledge background.

We selected two study sites across the catchment with distinct climate and vegetation community: the *Roureda de Tordera*, located at the lowlands of the

catchment, and the *Font del Regàs*, located at the headwaters of the catchment. (Fig. 2.1). Both sites are located in protected areas, thus they are relatively pristine with low anthropic pressure and relatively well preserved riparian forests. These forests are dominated by deciduous trees. Moreover, both sites are characterized for being close to the river and for presenting a strong spatial gradient of water availability. This spatial gradient, together with the seasonality of climatic conditions, typical from Mediterranean regions, make them a perfect natural lab to explore the effects of water availability on tree species distribution and functionality.

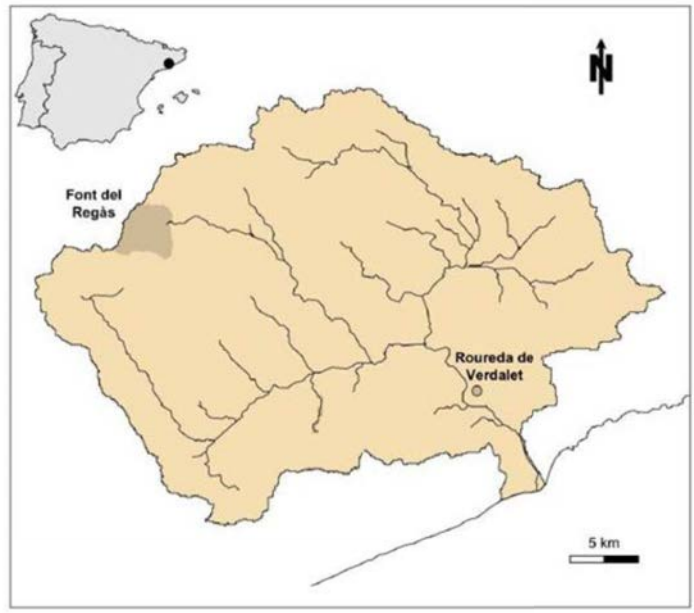

Figure 2.1 *La Tordera* catchment where *Font del Regàs* is at the headwaters and the *Roureda de Tordera* close to the river mouth.

2.2. *Roureda de Tordera*

La *Roureda de Tordera*, also known as *Roureda de Verdalet*, is a flat forested area (35 ha) located at the lowland of *La Tordera* river (Fig. 2.2a). The climate is semi-

arid Mediterranean, with a mean annual temperature of 15.6 ± 0.7 ºC and a mean annual precipitation of 627 ± 185 mm (mean ± SD, period: 1968-2008, Blanes Meteorological Station). The singularity of the *Roureda de Tordera* lies on flooding periods that last from 4-7 months per year, as a result of surface inputs and the emergency of groundwater table level. The flooding is not homogeneous across the area, shows a gradient from dry to flooded zones.

The microclimate and the high water availability in this area facilitates the presence of both Atlantic species such as Pedunculate oak (*Quercus robur*), and riparian species such as Ash (*Fraxinus angustifolia*) and Field elm (*Ulmus minor*). But also Mediterranean species as Algerian oak (*Quercus canariensis*), Holm oak (*Quercus ilex*), Cork oak (*Quercus suber*), and Pubescent oak (*Quercus pubescens*). Among them, *Q. canariensis*, *Q. robur*, and *F. angustifolia* are the most abundant, but their distribution differs across the flooding gradient (Fig. 2.2a). *Q. robur* and *F. angustifolia* cohabit in the flooded areas, while *Q. canariensis* is located in the driest zones. Both *Quercus* species are considered transitional communities between Atlantic and Mediterranean climates, and thus, they only inhabited in singular, restricted areas. *Q. robur* is at its southern distribution edge while *Q. canariensis* at its northern distribution edge.

2.3. *Font del Regàs* catchment

Font del Regàs catchment is relatively small and forested (14.2 km^2), located in the headwaters of *La Tordera* river, within the Natural Park of the Montseny Mountains (UNESCO's Biosphere Reserve). The climate is subhumid Mediterranean and the catchment can be considered as a temperate island surrounded by a semiarid landscape. The mean annual temperature is 12.1 ± 2.5ºC and the mean annual precipitation averages 925 ± 151 mm (mean ± SD, period: 1940-2000, Catalan Meteorological Service). Total inorganic atmospheric N deposition in the Montseny Mountains Range oscillates between 15-30 kg N ha-1 yr-1 (period: 1983-2007, Àvila and Rodà, 2012).

The catchment is dominated by biotitic granite and it has steep slopes (slope ~ 28%). Mediterranean evergreen oak (*Q. ilex*) and temperate European beech (*F.*

sylvatica) forests cover the major part of the catchment, while heathlands and grasslands can be found at higher altitudes (Cartographic and Geological Institute of Catalonia). At the valley bottom of the catchment, the stream channel is flanked by a riparian forest that occupies the 6% of the catchment area. Common riparian tree species are black alder (*Alnus glutinosa*), black poplar (*Populus nigra*) European ash (*Fraxinus excelsior*), black locust (*Robinia pseudoacacia*), and hybrid sycamore (*Platanus hybrid*).

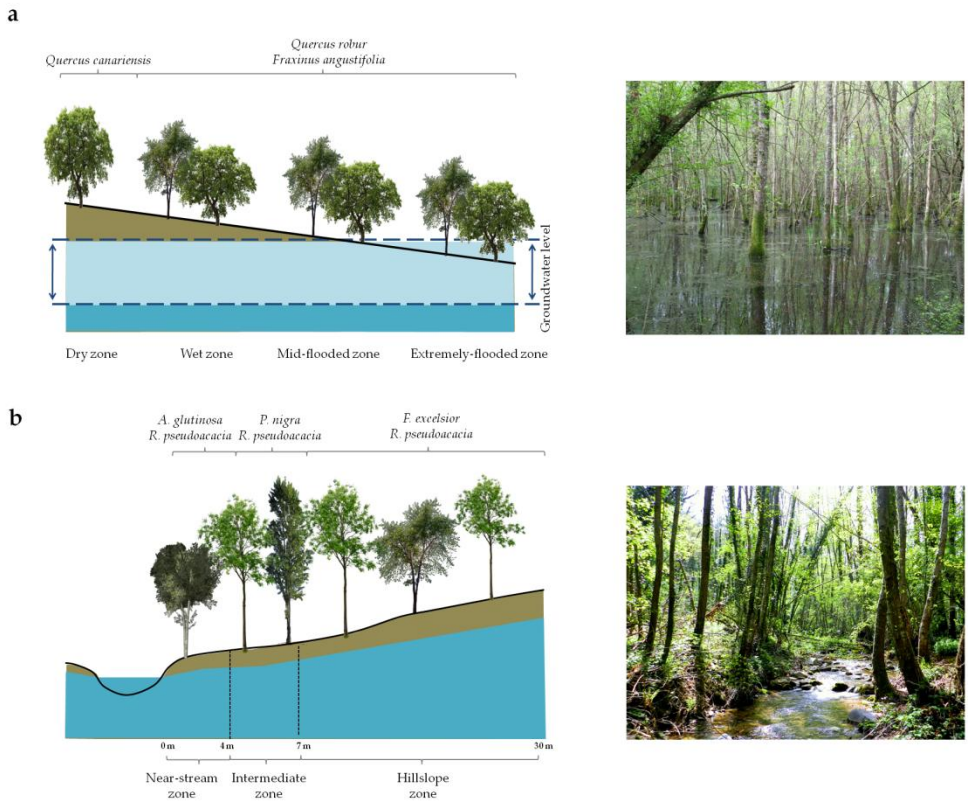

Figure 2.2 Tree species distribution across (a) the flooding gradient of *Roureda de Tordera*, and (b) the riparian area of *Font del Regàs*.

We selected a well-developed riparian stand at the valley bottom of the catchment (surface area = 25 x 30 m). The riparian soil (pH ~ 7) is sandy-loam with a 5 cm deep organic layer followed by a 30 cm deep A-horizon (Lupon et al., 2016a). The riparian stand consisted of *R. pseudoacacia*, *P. nigra*, *A. glutinosa* and *F. excelsior* (74%, 13%, 10%, and 3% of the total basal area (BA),

respectively). As in the *Roudera de Tordera*, riparian trees species were differently located across the water availability gradient, with both phreatophic species (*A. glutinosa* and *P. nigra*) inhabiting the area near by the stream edge, *F. excelsior* inhabiting only by the hillslope edge, and the invasive *R. pseu*doacacia standing across all the riparian area (Fig. 2.2b).

The near-stream section (0-4 m from the stream edge) occupied 16 % of the riparian area and it was composed by *A. glutinosa*, *P. nigra*, and *R. pseudoacacia* (45%, 33%, and 22% of the section's BA). The intermediate section (4-7 m from the stream edge) occupied 12% of the riparian area and it was composed by *P. nigra* and *R. pseudoacacia* (29% and 71% of the section's BA). The hillslope section (7-25 m from the stream edge) was the largest (72% of the riparian area) and it was composed by *F. excelsior* and *R. pseudoacacia* (7% and 93% of the section's BA) (Fig. 2.2b).

2.4. General methods

This spatial gradient of water availability together with the seasonality of climatic conditions typically from Mediterranean regions, make both riparian forests the *Roureda de Tordera* and *Font del Regàs* perfect natural labs to explore the effects of water availability on riparian tree species and soil N dynamics, as well as the effects that riparian trees can have on soil N availability. Table 2.1 presents a summary of all the field methods used in this thesis.

2.4.1.Environmental conditions

A meteorological station was located at ca. 800 m distance from the study site. Air temperature, relative humidity, solar radiation, photosynthetic active radiation (PAR), precipitation, and wind's speed were monitored at a height of 3 m and measured at 30-s intervals. Data were stored as 15-min average in a data-logger (CR1000 Data-logger and AM16/32 Multiplexers, Campbell Scientific, Inc., Logan, UT, USA). Vapor pressure deficit (VPD) was obtained from air temperature and relative humidity. Soil water content (in cm^3 cm^{-3}) and groundwater level (in m below soil surface) fluctuations were monitored across the riparian area during the study period (2010-2013). Soil water content

was measured for the upper 30-cm of soil every 15-min using frequency domain reflectometers (TDR sensors, CS616, Campbell Scientific, Logan, USA) at different distances from the stream channel (1.5, 4, and 14 m).

2.4.2. Riparian forest characterization

In both studied riparian forests we conducted forest inventories to evaluate tree species distribution across the water availability gradients. For each tree we determined the species, DBH, height, and distance to the stream channel.

In *Roureda de Tordera*, we extracted tree cores with a borer to measure tree-ring width and estimate annual tree basal area increment. Moreover, we measured the concentration of the isotope ^{13}C on tree-ring wood to estimate iWUE. See further details in Chapter 3.

In *Font del Regàs* we conducted an exhaustive study of leaf characterization. First, we measured every two weeks the photosynthetic active radiation (PAR) below the canopy forest and outside the forest to estimate temporal changes of leaf area index (LAI) applying Norman and Jarvis equation (1975). PAR measurements were carried out with a Sunfleck Par Ceptometer Model SF-80 (Decagon Devices, USA). Second, we did characterize fully developed sunlit leaves for all riparian tree species. We measured leaf area, leaf wet and dry weight, leaf thickness, leaf C and N concentrations, and 13C to estimate iWUE. Third, we installed 30 baskets of 1 m^2 to collect leaf litterfall. From these samples we measured annual leaf production and leaf litterfall soil inputs by species, in terms of dry weight mass and N (both in g m-2). The study of leaf litterfall seasonality by tree species allows us to evaluate the different species responses to drought. Nutrient reabsorption efficiency (NRE) was also estimated from differences in leaf N concentrations sampled from the canopy and collected from leaf litterfall baskets. Finally, we conducted leaf decomposition experiments to estimate specific decomposition rates. Most of the measurements were conducted along one humid year (2011) and one dry year (2012). For further details see Chapter 4 and Chapter 7.

2.4.3. Soil biogeochemistry characterization

To study the spatio-temporal patterns of soil N processes we evaluated them along one year. We measured soil net mineralization (NNM) and soil net nitrification (NN) using the incubation method (Eno 1960). Soil incubations (Fig. 2.3a) were conducted during 4 days among 5 different environmental conditions, each field day (N=4) we measured soil N_2O emissions with open chambers, soil denitrification using the acetylene method with closed chambers (Fig. 2.3b), and soil CO_2 emissions using and IRGA (PP Systems, Amesbury, MA) (Fig. 2.3c). Soil and gas samples were analyzed afterwards in the laboratory. Further information provided in Chapter 5.

Figure 2.3 (a) Soil incubations to measure soil N processes, (b) soil chambers to measure natural N2O emissions and denitrification, and (c) EGM-4 chamber associated to an IRGA. Source: Anna Lupon, Sílvia Poblador, and Francesc Sabater.

2.4.4. Isotopes analyses

Isotopic techniques have been developed and extensively used in the last decades, conveying some of the most exciting advances in ecological and environmental research (Hobson and Wassenaar, 1999; West et al., 2006). In particular, natural abundance of stable isotopes (i.e. molecules of the same element that differ in neutron number) in organisms are extensively used for ecological research. We measured stable isotopes with two purposes. First, we measured the isotope ^{13}C concentration in tree-ring wood and leaves. This isotope is naturally present in the atmosphere and the proportion ^{12}C:^{13}C is 99:1. Plant species discriminate to preferentially use $^{12}CO_2$ for photosynthesis. However, when plant species control stomatal closure due to drought stress, the isotopic discrimination is reduced and thus ^{13}C concentration in the tissue

(wood, leaf, ...) increases. From this relation ^{12}C:^{13}C an intrinsic water use efficiency (iWUE) can be estimated (Farquhar et al., 1982). Second, the study of ^{18}O and ^{2}H from trees sap and possible water sources (i.e. groundwater, stream water, or soil water) is an extensively used technique to estimate the relative contribution of different water sources to provide water for plant transpiration (Dawson and Ehleringer, 1991a). Water reaching the soil from precipitation has lower proportion of heavy isotopes, as ^{18}O and ^{2}H, while they are enriched in the remaining water after evaporation processes. Therefore, water from different compartments usually differ on their isotopic composition. See Chapter 3 and Chapter 4 in the case of ^{13}C and in Chapter 4 for $^{18}O/^{2}H$ for further details.

2.4.5. Groundwater measurements

A grid of 35 wells were installed at different distances from the stream channel across the study site of *Font del Regàs* (1.5, 2.5, 5, 11, 17, and 25 m distance) to assess groundwater level fluctuations and water quality. Wells were PVC tubes (32 mm Ø) uniformly screened along their length and placed at 1 to 3 m b.s.s. at the near-stream edge and hillslope edge, respectively. At one well of each distance from the stream channel groundwater level was monitored every 15-min using water pressure transducers (HOBO U20-001-04) and measured every two weeks with a water level sensor (Eijelkamp 11.03.30). Moreover, stream water and groundwater were also sampled every two weeks. All water samples were filtered (Whatman GF/F, 0.7 μm pore Ø) and kept cold (< 4ºC) until laboratory analysis (< 24 h after collection). N-NO3- concentration was quantified with cadmium reduction method (Keeney and Nelson, 1982) using a Technicon Autoanalyzer (Technicon, 1976). These results are presented in Chapter 4 and Chapter 6.

2.4.6. Modellization

In order to inferred future scenarios of water and N dynamics in Mediterranean riparian forests we modelled them using HYDRUS 1D model (Simunek et al., 2006). HYDRUS is a well-known software that allow the user to model transfer fluxes and reactions along the unsaturated soil layer

(Simunek et al 2009). We initially applied HYDRUS 1D to determine soil properties of our riparian forest. Afterwards water fluxes were simulated using HYDRUS 1D and 2D. Since similar results were obtained from both approaches we kept the simple 1D approach to study the spatial heterogeneity across the riparian soil (Fig. 2.4). Further details of modeling parameters used for *Font del Regàs* can be found in Chapter 6.

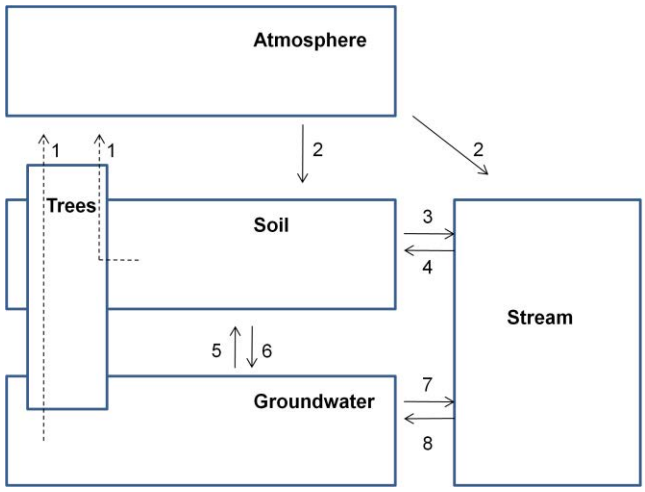

Figure 2.4 Schematic conceptual model showing input/output fluxes from the riparian forest compartments based on riparian trees distribution: evapotranspiration (1), precipitation (2), leaching (3), flooding (4), capillarity (5), infiltration (6), effluent (7) and influent (8) stream situation.

To evaluate the effects of the introduction and complete replacement of native species by *R. pseudoacacia* on soil N availability across the riparian area we developed a conceptual model (Fig. 2.5) and applied it using measured data. More details are found in Chapter 7.

2.4.7. Data analyses

All data analyses were conducted with R statistical software (R Development Core Team, 2016, version 2.15.1). The specific statistical methods are thoroughly explained in each chapter.

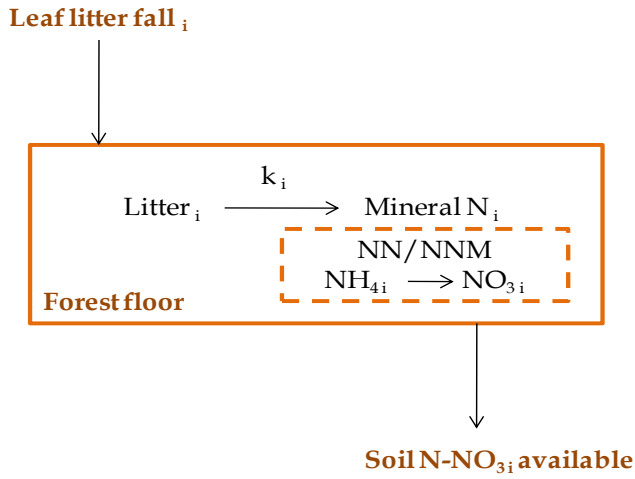

Figure 2.5 Schematic conceptual model showing input/output N fluxes from the riparian forest floor.

Table 2.1 Site, field scale, field data, and frequency and duration of the field work used for each chapter of this dissertation. For field data: GHG (greenhouse gas), GWL (groundwater level), and GW (groundwater).

Chapter	Site	Scale	Field data	Frequency	Duration
3	*Roureda de Tordera*	Forests by flooding zones	Tree-rings	Annual	1 month (80 years)
4	*Font del Regàs*	Forest stand	Fresh leaves and leaf litterfall characterization	2 weeks	24 months
4	*Font del Regàs*	Riparian zones	Sap and water ^{18}O and ^{2}H composition	1 week	2 seasons (spring and summer)
5	*Font del Regàs*	Riparian zones	Soil N processes GHG soil emissions	2 months	12 months
6	*Font del Regàs*	Riparian zones	GW L GW Nconcentration Meteorological data	2 weeks	36 months
7	*Font del Regàs*	Riparian zones	Leaf litterfall Leaf decomposition Soil mineralization Soil nitrification	2 weeks	12 months

CHAPTER 3

Living at the edge of the species distribution: Effects of temperature increase and flooding conditions on growth and iWUE of *Quercus robur* and *Q. canariensis*

The understanding of environmental conditions effects on tree growth performance at species distribution edge is crucial to predict how climate change can modify species distribution. *Roureda de Tordera* is a unique natural lab where *Quercus robur* and *Quercus canariensis* meet, respectively, at their southernmost and northernmost geographic distribution edge, where *Fraxinus angustifolia* is also present. The groundwater table rise produces flooding periods (4-7 months per year) in the forest, providing extra-water to trees. Tree species are distributed over a water availability and flooding gradient in Tordera river floodplain, from non-flooded (*Q. canariensis*) to mid- and extremely-flooded (*Q. robur* and *F. angustifolia*). The aim of this work was to evaluate to what extent, these species out of their core distribution range are already experiencing any effects of last decades climate change, mainly increasing temperatures and flood variability. We analysed species annual wood stem basal area increment (BAI) and intrinsic water use efficiency (iWUE), along a water availability and flooding gradient. Our results show that increasing temperatures from last decades had no effects on *Q. canariensis* growth while increased its iWUE (+21%). In addition, BAI decreased in the wet zone for *Q. robur* (-33%) and in the mid-flooded zone for *F. angustifolia* (-56%). iWUE trends of *Q. robur* increased in wet and mid-flooded zones (+13% and +17%, respecitvely). No effects were found for iWUE of *F. angustifolia*. Since *Q. robur* and *F. angustifolia* are depending on phreatic water availability, on top of rainfall, these species are likely to reduce their presence in the area, facilitating the expansion of *Q. canariensis*. This is likely to happen in these singular areas if human induced dry-out practices of floodplains expands and rainfall at catchment level is reduced as expected by climate change projections.

With permission of: F. Sabater and S. Sabater, who are co-authors of this study.

3.1. Introduction

The inherent microclimatic characteristics of Mediterranean floodplains offer suitable conditions for the occurrence of temperate tree species. In fact, the Mediterranean Basin is considered a hotspot of biodiversity (Myers et al., 2000) due to its large variety of ecosystems and habitats. It is a transitional region where many species from temperate and dry regimes reach their limit of geographic distribution. Pedunculate oak (*Quercus robur*) is a mid-European species that reaches its southern geographic distribution edge in the north of the Iberian Peninsula (Dyderski et al., 2018; Huang et al., 2017). This species, usually found in European floodplains cohabiting with *Fraxinus spp.* (Janík et al., 2016; Kazda et al., 2000), requires high water availability (Breda et al., 1993; Doody and O'Reilly, 2008; Nardini and Tyree, 1999) and soil fertility (Balboa-Murias et al., 2006; Breda et al., 1993; Nardini and Tyree, 1999). Despite *Q. robur* presence in the Mediterranean region is scarce, in some areas with high annual precipitation rates (> 800mm $year^{-1}$) or shallow groundwater level, some stands of this species can be found (Bolós and Vigo, 1984). By contrast, Algerian oak (*Quercus canariensis*) is another deciduous *Quercus spp.* that is usually found in cold and wet areas of the Mediterranean Basin (Urbieta et al., 2008). It reches its northern distribution edge in the north of the Iberian Peninsula (Wazen and Fady, 2015).

Riparian floodplain areas are upon the most severely threatened terrestrial ecosystems, especially downstream, where smooth slopes facilitate the establishment of human activities on them. In particular, downstream floodplains are usually affected by water extraction, habitat fragmentation promoted by agriculture and other land-use practices, forest exploitation or even dry-out to prevent diseases from mosquitoes-vector (Asaeda et al., 2015; Balboa-Murias et al., 2006; Perry et al., 2012; Sala et al., 2000a; Tylianakis et al., 2008). These areas have been pointed to be potentially affected by climate change in the Mediterranean region (IPCC, 2013). Despite rising temperatures can initially promote higher transpiration rates, through increasing evaporation demand and lengthing the growing season, they can also result in vegetation hydrological stress when water availability is scarce. Global change

is expected to reduce flooded areas as a combined result of groundwater recharge reduction, linked to precipitation decrease, the increase in temperatures, and water extraction for human use purposes. Thus, many threats affect the presence of this mid-European species in the Mediterranean region.

The relation between climate and tree-ring width has been widely studied, providing information on tree growth responses to climate variations at ecosystems' past conditions (Becker et al., 1994; Grace et al., 2002; Jump et al., 2006; Linares and Tíscar, 2010; Rozas, 2005; Silva et al., 2010). However, tree-rings widths are also affected by an age-related decline in individual mature stages that can mask environmental conditions effects on growth (Phipps and Whiton, 1988). To avoid that, tree-ring widths can be converted into stem basal area increment (BAI), which shows negative trends when a true decline in tree growth takes place (Pedersen, 1998). Moreover, long-term changes in the gas exchange metabolism of trees are recorded in the variation of carbon isotopic composition (∂13C) in tree-rings wood, and the intrinsic water use efficiency (iWUE) can be indirectly estimated from it (Farquhar et al., 1982; Loader et al., 2003). These measurements indicate how tree individuals have responded to increasing evaporative demands during the last decades. In Mediterranean regions, water availability is the most important factor limiting plant growth and net primary production. Warmer temperatures associated to climate change trends can increase the length of the growing season (Peñuelas and Boada, 2003) and thus enhance tree-ring widths, while the decrease of water availability may counterbalance this positive effect (Pigolt and Hunthy, 1978). Some species in their limit of geographic distribution in the Mediterranean Basin have already shown adverse drought effects, such as growth decline, tree mortality or species distribution shifts (Jump et al., 2006; Martínez-Sancho et al., 2018; Peñuelas and Boada, 2003).

Our study site represents a singular natural lab where two tree species (*Q. robur* and *Q. canariensis*, Fig. 3.1) at their geographic distribution range edge, as wells as another typically riparian species (Narrow-leaf Ash, *Fraxinus angustifolia*), co-occur along a spatial gradient of water availability and flooding

intensity under a Mediterranean climate context. The aim of this study was to investigate the effects of flooding periods' variability, and increasing temperatures reported over the last decades, on these tree species growth and iWUE trends. This should provide valuable information to evaluate their vulnerability to global change. We assessed the annual BAI along the spatial gradient and calculated the iWUE from wood tree-rings for particular water availability extreme years (i.e. dry and wet). In addition we evaluated the effects of environmental conditions on both parameters. We expected to find a tree growth decline over the last decades for all tree species, but especially for *Q. robur*, which is at its southernmost distribution range edge, and it is most likely very dependent on groundwater availability. Similarly, we expected an increase of iWUE over the last years, and a remarkable response of *Q. canariensis*, usually found in drier regions, and likely to better face increasing temperatures. Moreover, these differences in growth and iWUE termporal trends were expected to show up across a spatial gradient of water availability and flooded periods. For *F. angustifolia* we expected a slight decrease in growth and increase in iWUE trends in the wet zone, however, we expected no remarkable differences among forest zones.

3.2. Materials and methods

3.2.1.Study site

This study was conducted in *Roureda de Tordera* (41º 43'N, 2º43'E), a forested area in the floodplain of the Tordera River (35 ha, 25-28 m above sea level), NE of Spain. The area has a humid Mediterranean climate with mean annual temperature of 15.6 ± 0.7 ºC and mean annual precipitation of 627 ± 185 mm. It also shows an arid period during summer months (1968-2008, Blanes Meteorological Station, Fig. A1). Long-term climate data show a positive increase trend of mean annual temperature up to 1.2 ºC (linear regression, $p < 0.001$) along the last forty years, and a slight decrease of precipitation (decrease of 2 mm $year^{-1}$; linear regression, $p = 0.32$) (Fig. 3.2). The forest is located in a floodplain area at 500 m from the river side channel and separated from it by several human infrastructures (i.e. roads, railway, and some industrial parks).

Due to an almost flat topography of the area, the forest remains flooded about 4-7 months per year. However, this area has a gentle slope that results in different flooding levels aligning with the riparian gradient: from flooded zones (>50 cm of surface water column) to non flooded ones. Data of annual flooding level in *Roureda de Tordera* were not available, but it is known to be higher during years with high precipitation and stream discharge. The soil of the forest has a deep organic horizon (15-20 cm) with a significant organic matter content, and a wide clay horizon with iron oxides below it (Borrell, 1989). The microclimate and high water availability of the area allow the presence of typical Atlantic vegetation species such as *Q. robur*; but also riparian species like Ash (*F. angustifolia*), and more Mediterranean deciduous oak such as Algerian oak (*Q. canariensis*). The wetland behavior and the presence of Quercus spp. at their distribution range edge has promoted several local and regional administrative protection figures of the area.

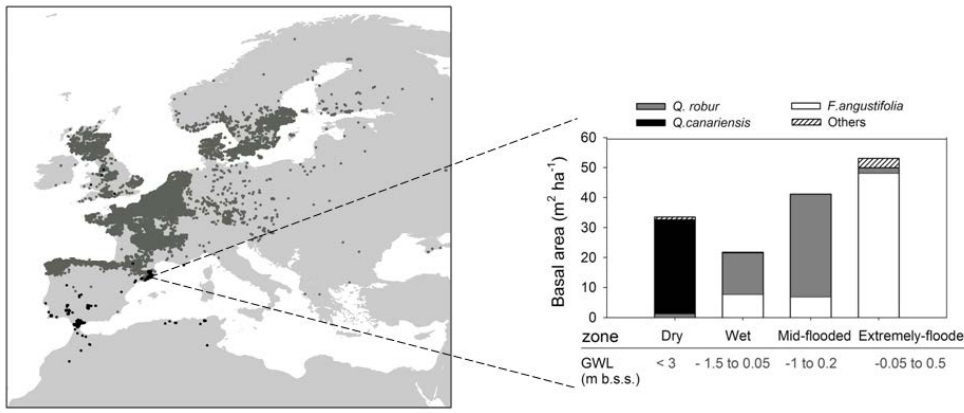

Figure 3.1 Geoprgaphical distribution of *Q. robur* and *Q canariensis* (data source: Global Biodiversity Information Facility). The *Roureda de Tordera* forest location is pointed by dashed lines. Barplot represents tree species basal area (DBH 5>cm) distribution along the zones and groundwater level range at each zone (in m below soil surface (b.s.s.)) in the *Roureda de la Tordera* forest.

3.2.2. Sampling design

We determined four zones within the limits of the protected area of the floodplain, in order to study the effect of increasing temperatures at different flooding levels. Two of them were defined on a non-flooded area: a dry zone

with groundwater level (GWL) at < -3 m from soil surface and wet zone where GWL ranged from -1.5 m to +0.05 m along the year (data from November 2008 to July 2009). The other two zones were settled in the flooded area covering a gradient from the zone where flooding happens during a short period of the year (mid-flooded zone, GWL ranged from -1 m to +0.2 m) to the area flooded for several months (extremely-flooded zone, GWL from -0.5 m to 0.5 m) (Fig. 3.1). Forest inventories (i.e. tree species identification, diameter at breast height and tree height measurements) were conducted at each zone. The three tree species studied (*Q. canariensis, Q. robur,* and *F. angustifolia*) were not evenly distributed across the area. *Q. canariensis* was only present in the dry zone. *Q. robur* was found in all the studied zones, although its presence was scarce in the dry zone, being mainly located in zones with higher water availability together with F. angustifolia. The highest *Q. robur* density was found in the wet zone, where GWL was high but soil barely flooded. In contrast, the highest densities of F. angustifolia were found in the extremely-flooded zone, where the GWL emerged over the soil surface during months (Fig. 3.1, Table 3.1). In each zone, increment wood cores were taken from mature trees of the three species at breast height (1.3 m) in winter 2010 using a 12 mm increment borer.

3.2.3. Tree-ring growth

A total of 78 cores were placed into grooved boards to air-dry them. In order to avoid contamination among rings wood for future isotope analysis, core's surfaces were blade-cut (Gutiérrez et al., 2004). All samples were visually cross-dated. Afterwards, cores were high resolution scanned (1200 d.p.i, Epson Expression 10000 XL Scanner) and tree-ring widths measured using Windendro software (Regent Instrument Inc. 2002). For each species and zone, the resulting tree-ring width series were cross-dated for quality control with the statistical programme COFECHA (Holmes, 1983), showing 99% of correlation among them. Individuals BAI were calculated from ring-width measurements following:

$$BAI = \pi \left(r_n^2 - r_{n-1}^2 \right) \qquad \text{(Eq. 3.1)}$$

where r is the radius of the tree and n is the year of the tree-ring formation. For each zone and species, mean stem BAI chronologies were calculated in order to evaluate stem BAI changes over time from all species. Current mean stem BAI was also analyzed (mean growth per year during last five years) for each specie and zone. The study of wood stem BAI, for the last years is appropriate to evaluate tree's production and reponses in front of environmental conditions (Rubino and McCarthy, 2000).

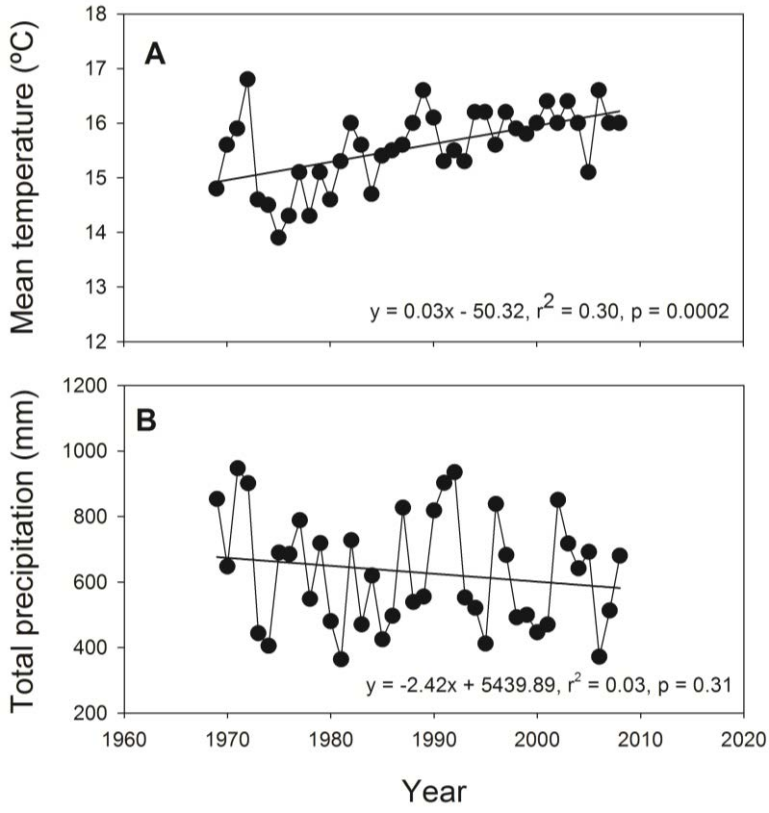

Figure 3.2 A) Mean annual temperature trend and B) total annual precipitation trend at Blanes (1968-2008). Source: Arxiu Municipal de Blanes.

3.2.4. Water use efficiency

We carefully separated tree-rings per year from five individuals of each tree species and zone. Climatic data (1968-2008) from the Meteorological Station located in Blanes (~ 10km from the study site) (Fig. 3.2), was analyzed and we

selected years with extreme precipitation and temperature patterns (i.e. dry and wet years with annual temperature and/or precipitation value > ± 1 SD). The late wood of corresponding tree-rings (n=12 years) were grounded and analyzed for $\partial^{13}C$ wood signature (Loader et al., 2003; Saurer et al., 2004) in an Elemental Analyser Flash 1112 (Carlo Erba, Milano, Italy) coupled to an IRMS Delta C isotope ratio mass spectrometer with a CONFLO III interface (Thermo Finnigan MAT, Bremen, Germany). Analyses were carried out at the Scientific Technical Service of the University of Barcelona. Values are expressed per thousand (‰) on the relative ∂-scale and referred to international standards following the equation:

$$\delta Z = (R_{sample} - R_{standard}) - 1 \quad \text{(Eq. 3.2)}$$

where Z is the heavy isotope of C, and R is the ratio of heavier to lighter isotope for the sample and standard ($^{13}C/^{12}C$). For $\partial^{13}C$, the international standard V-PDB (Vienna Pee Dee Belemnite) was used. From wood $\partial^{13}C$ we calculate intrinsic WUE (iWUE) according to the equations (McCarroll and Loader, 2004):

$$c_i = c_a \left(\frac{\delta\ 13\text{Cplant} - \delta\ 13\text{Cair} + a}{-(b-a)} \right) \quad \text{(Eq.3.3)}$$

$$\text{iWUE} = A/g = ca\ [1 - (Ci/Ca)] \times (0.625) \quad \text{(Eq.3.4)}$$

where a is the discrimination against $^{13}CO_2$ during diffusion through the stomata (±4.4 ‰), b is the net discrimination due to carboxylation (±27 ‰), and ci and ca are intercellular and ambient CO_2 concentrations (Farquhar et al., 1982). A is the rate of CO_2 assimilation and g is the stomatal conductance. Data of ∂^{13}Cair, Ci and Ca were obtained from McCarroll and Loader (2004) who used the high precision records of atmospheric $\partial^{13}C$ from Antarctic ice cores (Francey et al., 1999), and the atmospheric CO_2 concentration (ppm) from Robertson et al. (2001).

3.2.5. Theoretical gas-exchange scenarios

The relationship between carbon uptake and atmospheric carbon (Ci/Ca) was calculated along time for each species and zone. Following Saurer et al. (2004),

we compared the measured temporal trends to the three theoretical scenarios for plant-gas exchange regulation. The three theoretical scenarios differ in how Ci follows changes in Ca. In the scenario 1 (Ci = constant), Ci do not follow Ca variations, remaining constant and reducing Ci/Ca ratio along time. This scenario indicates a strong stomatal closure. In the scenario 2 (Ci/Ca = constant), Ci follows Ca in a proportional way due to a regulation of Ci by both photosynthesis and stomatal conductance. In scenario 3 (Ca-Ci = constant), Ci follows Ca at the same rate, what increase Ci/Ca ratio and suggest a weak stomatal response.

3.2.6. Data statistical analysis

Mean stem BAI for species and zone was smoothed with a 9-running average to reduce interannual variability while highlighting growth trend. Once the smoothed stem BAI was represented, the mature age was clearly identifiable (Becker et al., 1994; Johnson and Abrams, 2009). For *Q. robur* in the wet zone, mean stem BAI was smoothed using a 5-running average, as it fitted better to the BAI trend. All smoothing procedures were conducted using SigmaPlot v11.0.

Statistical analyses were carried out using the package lmer and Hmisc for R 2.15.1 statistical software (R Developement Core Team, 2012). We performed linear-mixed model analysis of variance (ANOVA) to test differences in BAI trends, five last year mean wood stem BAI, and tree-ring WUEi across riparian tree species and zones. We used tree species and zones as fixed effects, and individuals (nested within zones) as random effect. For each model, post hoc Tukey contrasts were used to test which species or zones differed from each other. In all cases, residuals were tested for normality using a Shapiro-Wilk test and homogeneity of variance was visually examined by plotting predicted and residual values. In all analyses, differences were considered significant when $p < 0.05$.

We evaluated the correlation between annual mean mature BAI and annual environmental conditions for each species and zone using Pearson correlations. We considered as environmental conditions annual and monthly average

temperature (T), precipitation (P), and GWL. Climate data (T and P) were obtained from the meteorological station in Blanes (~10 km from the study site) for the period 1968-2008. Annual data was considered for the vegetative year: from October of the previous year tree-ring formation to September of the current year (i.e. assuming all trees growth period ended in September). GWL for the period 2001-08 was recorded nearby the study area (Data obtained from Agència Catalana de l'Aigua: piezometer G-1 Tordera/Maresme, UTMX 476854 UTMY 4617581). Correlation between precipitation and the groundwater level was significant (period 2000-2008; pearson correlation, $p < 0.01$).

3.3. Results

3.3.1. Tree growth and environmental conditions effects

Q. canariensis was the eldest species in *Roureda de Tordera* with an average age of 80 ± 9 years in the dry zone. *Q. robur* was 71 ± 4 years in the wet zone, 71 ± 2 years in the mid-flooded zone and 51 ± 9 years in the extremely-flooded zone. *F. angustifolia's* age ranged from 58 to 76 years (Fig. 3.3, Table 3.1).

Table 3.1 Tree density (individuals ha^{-1}), mean tree age (year $tree^{-1}$), and last 5 years mean BAI (cm^2 yr^{-1} $tree^{-1}$) *for F. angustifolia, Q. robur* and *Q. canariensis* (DBH > 5cm) at the four study zones.

Variable	Species	Dry	Wet	Mid-flooded	Extremely-flooded
Tree density	*Q. canariensis*	1085	-	-	-
	Q. robur	31	604	541	31
	F. angustifolia	-	382	795	1655
Mean tree age	*Q. canariensis*	80 ± 9	-	-	-
	Q. robur	-	71 ± 4^{A}	71 ± 2^{A}	51 ± 9^{B}
	F. angustifolia	-	76 ± 14^{A}	58 ± 15^{A}	61 ± 8^{A}
Mean stem BAI	*Q. canariensis*	5.96 ± 3.49	-	-	-
	Q. robur	-	18.51 ± 6.74^{A}	10.81 ± 2.21^{AB}	9.12 ± 4.85^{B}
	F. angustifolia	-	4.32 ± 3.54^{A}	8.75 ± 5.54^{A}	6.19 ± 3.87^{A}

The average of the last 5 years wood stem BAI (cm^2 $tree^{-1}$ yr^{-1}) was considerably higher in the wet zone, where the wood stem BAI was maximum for *Q. robur* (18.51 ± 6.74 cm^2 $tree^{-1}$ yr^{-1}). In zones where *Q. robur* coexists with *F. angustifolia*, stem BAI values were considerably higher for *Q. robur* although no significant differences were found (Table 3.1). However, in dry areas where *Q. canariensis*

coexists with *Q. robur*, *Q. canariensis* showed the highest wood stem BAI (data not shown as the number of individuals of *Q. robur* where not enough to have a representative sample).

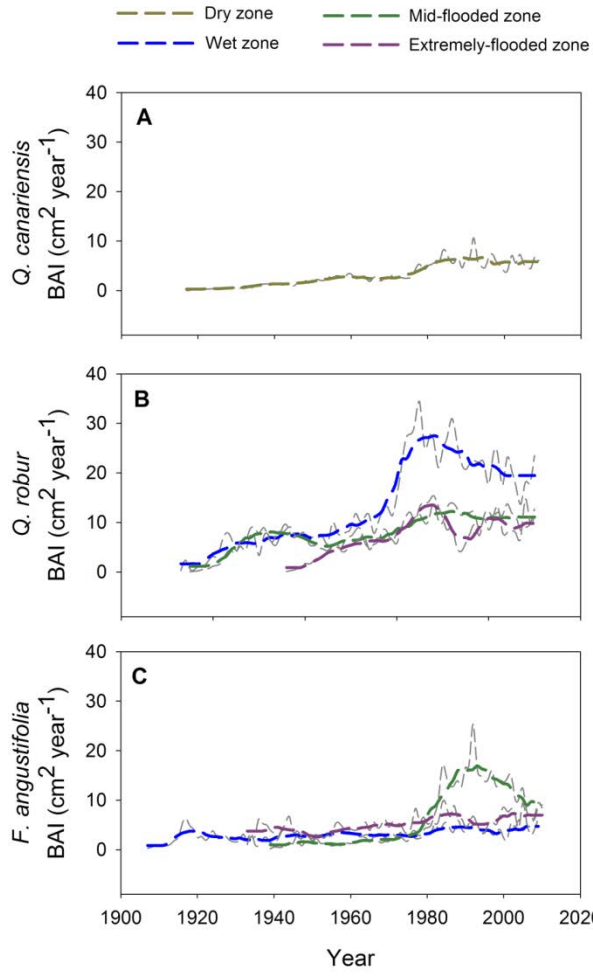

Figure 3.3 Mean stem BAI trends (cm^2 $tree^{-1}$) of *Q.canariensis* (A), *Q. robur* (B), and *F. angustifolia* (C) in floodplain zones where they were present: dry zone (yellow), wet zone (blue), mid-flooded zone (green), and extremely-flooded zone (purple). Dashed coloured lines are the smoothed trends.

The study of mature BAI trend over time showed different trends for different species and zones (Fig. 3.4). *Q. canariensis'* BAI showed no decline since mid-1980s (Fig. 3.4a). Its annual BAI showed a weak correlation with temperatures, being only negatively correlated with July's temperature ($p<0.05$) (Fig. 3.5). On

the contrary, early spring (March), summer (June and July), december and annual precipitation enhanced annual BAI of *Q. canariensis*. Higher summer GWL in the decade of 2000 had also positive effects on its annual BAI (Fig. 3.5).

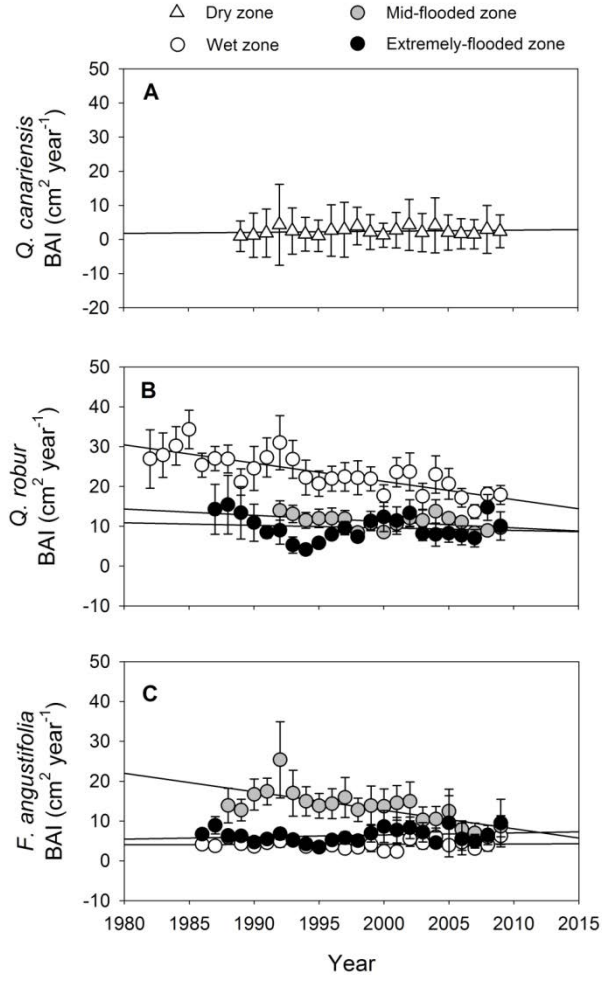

Figure 3.4 Mature mean BAI trends for *Q. canariensis* (A), *Q. robur* (B), and *F. angustifolia* (C) along the riparian zones (means ± standard error). Significant decline trends were found at wet zone for *Q. robur* (y = -0.46x + 937.78, r2 = 0.64, p < 0.0001), and at mid-flooded zone for *Q. robur* (y = -0.16x + 326.88, r2 = 0.23, p = 0.04) and *F. angustifolia* (y = -0.46x + 942.53, r2 = 0.52, p = 0.0001).

BAI trends of *Q.robur* differed among water availability and flooding gradient. In wet and mid-flooded zones, *Q. robur* showed a slight growth decline after mid-1980s (-33% and -36% respectively, Fig. 3.4b). Significant differences ($p < 0.05$) were found between *Q. robur* mean stem BAI trends for the wet zone with

respect to mid-flooded and extremely-flooded zones. Moreover, environmental conditions also showed different effects on *Q. robur* growth depending on the forest zone location. In the wet zone, BAI was negatively correlated with high temperatures during May, June, and annual means (Fig. 3.6). On the contrary, high precipitations during March and July had positive effects on its BAI (Fig. 3.6). In the mid-flooded zones, only annual total precipitation and mean annual temperature influenced *Q. robur* BAI (positive and negative effects on BAI, respectively). Higher GWL during spring (March to May) had also positive effects on BAI in these areas. Nevertheless, the response was completely different in the extremely-flooded zone, where *Q. robur* growth was only negatively affected by high precipitations in September and high GWL in December (Fig. 3.6).

Growth trends of *F. angustifolia* also depended on water availability and flooding gradient, but they differ of those of *Q. robur*. *F. angustifolia* experienced a remarkable decline during the last years in mid-flooded zone (-56%, Fig. 3.4c). A higher stem BAI was found in the mid-flooded zone where it was more productive (+80%) than in the wet (+30%) and the extremely-flooded (+60%) zones (Table 3.1, Fig. 3.3c and 3.4c). In the wet zones of the forest its BAI was enhanced by April, October and annual precipitation, as well as spring and annual high GWL. In the mid-flooded zones, June and July temperatures had a negative effect on *F. angustifolia* growth, while the effect of annual precipitation was positive (Fig. 3.7). In the extremely-flooded zones only temperature from February and November seemed to affect BAI. In mid- and extremely-flooded zones, GWL recharge in October and December had negative effects on BAI of *F. angustifolia*. (Fig. 3.7).

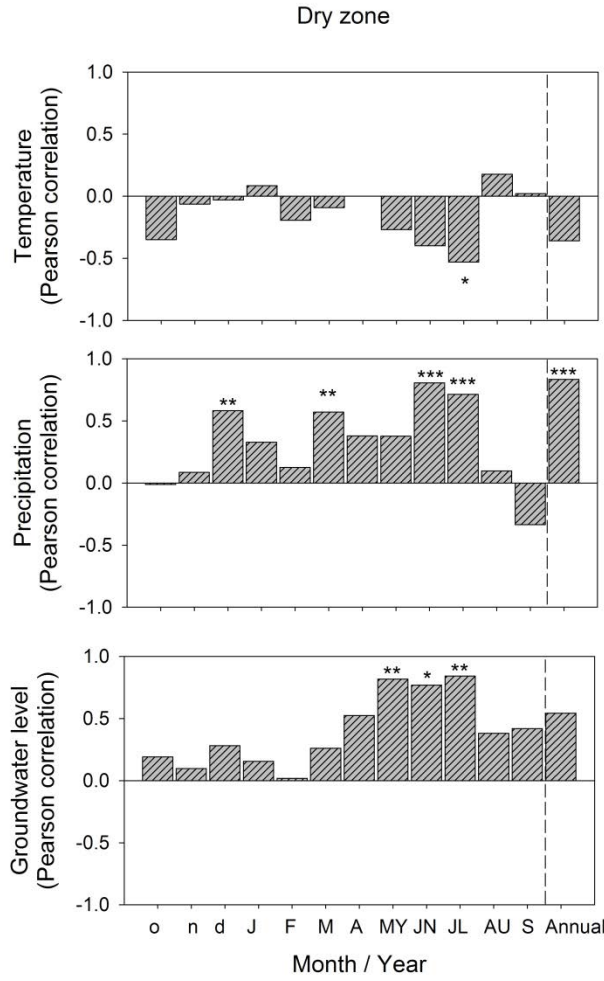

Figure 3.5 Pearson correlation values for mature BAI trends of *Q. canariensis* and monthly and annual environmental conditions (temperature, precipitation, and groundwater level). Data shown from october of previous year to september of current year. Significant correlations are indicated by asterisks: ***, $p < 0.001$; **, $p < 0.01$; *, $p < 0.05$).

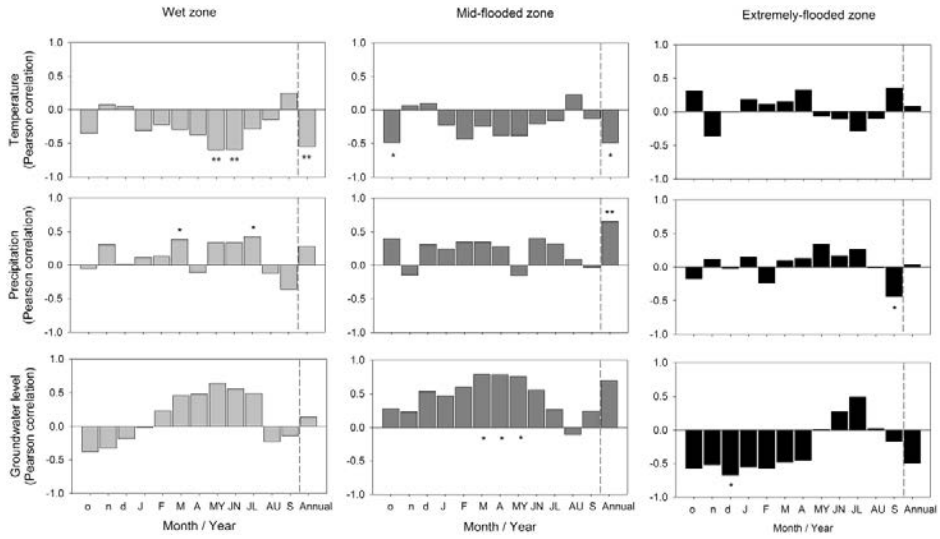

Figure 3.6 Pearson correlation values for mature BAI trends of *Q. robur* and monthly and annual environmental conditions (temperature, precipitation, and groundwater level). Data shown from october of previous year to september of current year. Significant correlations are indicated by asterisks: ***, $p < 0.001$; **, $p < 0.01$; *, $p < 0.05$).

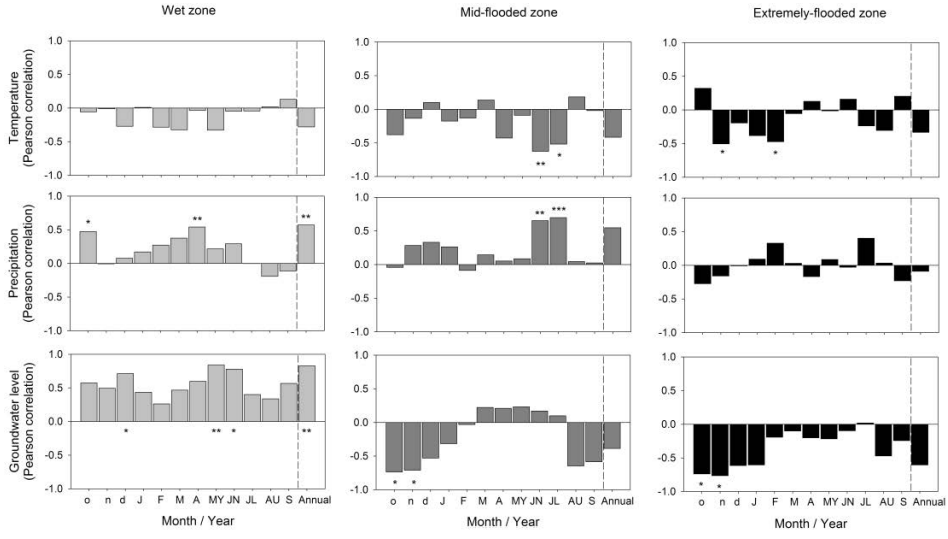

Figure 3.7 Pearson correlation values for mature BAI trends of *F. angustifolia* and monthly and annual environmental conditions (temperature, precipitation, and groundwater level). Data shown from october of previous year to september of current year. Significant correlations are indicated by asterisks: ***, $p < 0.001$; **, $p < 0.01$; *, $p < 0.05$).

3.3.2. Wood iWUE and environmental conditions effects

iWUE trends differed among species and zones. iWUE of *Q. canariensis* increased during the last decades (+21) (Fig. 3.8a). For the same period, *Q. robur* iWUE was lower and only increased in the wet (+13%) and mid-flooded (+17%) zones, while it remained steady in the extremely-flooded zone (+6%) (Fig. 3.8b). *F. angustifolia* showed no trends in iWUE over the last decades but annual iWUE was consistently higher in the extremely-flooded zone (88.28 ± 0.82 $\mu molCO_2\ molH_2O^{-1}$) than in the mid-flooded (81.42 ± 0.99 $\mu molCO_2\ mol\ H_2O^{-1}$) and the wet zones (71.91 ± 0.65 $\mu molCO_2\ molH_2O^{-1}$) (Fig. 3.8c).

Despite these differences among tree species, few correlations between iWUE and environmental conditions were found. *Q. canariensis* iWUE was enhanced by June temperatures and diminished by precipitations in November (Fig. A.2). Precipitation in August decreased *Q. robur* iWUE in the wet zones, while mean temperatures in May and precipitations of November from the previous year decreased iWUE in the mid-flooded one. In the extremely-flooded zone, iWUE was negatively correlated with October temperatures from the previous year (Fig. A.3). High GWL had positive effects on iWUE of *Q. robur* during summer in the wet and mid-flooded zone. iWUE of F. angustifolia was only correlated with water availabiliy: January and June precipitation decreased iWUE in the wet zone, while GWL increased iWUE during spring in the wet zone and winter in the extremely-flooded zone (Fig. A.4).

3.3.3. Ci/Ca theoretical scenarios

The comparision between theoretical gas-exchange scenarios and measured Ci/Ca trends showed differences among tree species and water availiability floodplain zones. *Q. canariensis* showed a significant decrease in Ci/Ca along years (Fig. 3.9). This Ci/Ca trend was close to the Ci = constant (scenario 1). Ci/Ca trends of *Q. robur* were not significant, yet, they were closer to the Ci/Ca = constant scenario (scenario 2) in the wet and the extremely-flooded zones, while closer to the Ci = constant scenario (scenario 1) in mid-flooded zone (Fig. 3.10). More diverse responses were found for *F. angustifolia* among zones (Fig. 3.10). In the extremely-flooded zone Ci/Ca trend was closer to the Ci = constant

scenario (scenario 1) from mid-80s to mid-90s, and closer to the Ci/Ca = constant scenario (scenario 2) from mid-90s to 2008. Ci/Ca trend in the mid-flooded scenario was in between the Ci/Ca = constant and Ca-Ci = constant scenarios (scenario 2 and 3, respectively). Finally, *F. angustifolia* in the wet zone showed a Ci/Ca response close to Ca-Ci = constant scenario (scenario 3).

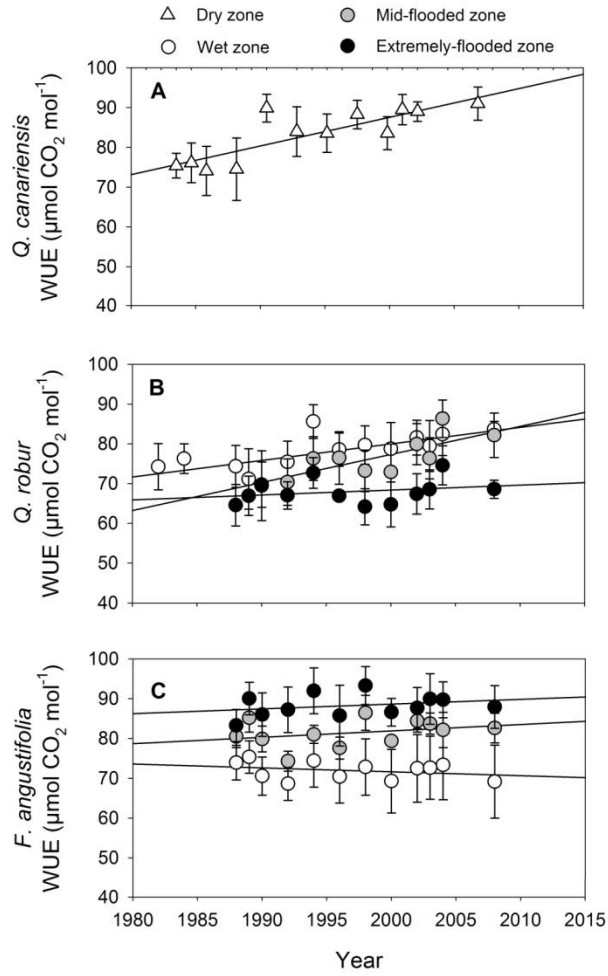

Figure 3.8 iWUE trends for mauture *Q. canariensis* (A), *Q. robur* (B), and *F. angustifolia* (C) along the riparian zones (means ± standard error). Significant trends were found at the dry zone for *Q. canariensis* (y = 0.84x - 1596.29, r2 = 0.67, p = 0.0007), wet zone for *Q. robur* (y = 0.42x + 752.626, r2 = 0.45, p = 0.005), and at mid-flooded zone for *Q. robur* (y = 0.71x - 1333.91, r2 = 0.47, p = 0.03).

3.4. Discussion

3.4.1.Water availability compensation for temperature BAI decline

This study evaluates how individuals of *Q. canariensis* and *Q. robur* perform at the northern and southern edge of their distribution, respectively. Moreover, the flooding gradient in *Roureda de Tordera* allows to distinguish the importance of water availability for *Q. robur* survival in these warm regions, and to enlight the potential future viability of these relict forests. IPCC (2013) climatic change projections for the studied region may difficult tree growth. Hidrologic stress is likely to increase given that increasing temperatures would enhance the evaporative demand, but it would not be compensated by precipitation, since it is projected to decresase. Besides, the expected higher transpiration rates may induce a rapid fall of the GWL in the floodplains, increasing tree competition and reducing growth rates.

The spatial distribution of water availability and flooding intensities of *Roureda de Tordera* affected not only tree species distribution, but also their stem BAI trends across the floodplain promoting different responses to the incresing temperatures over the last decades. Species located at the flooded zones of the forest (*Q. robur* and *F. angustifolia*) presented higher BAI than the one at the adjacent non-flooded zone (*Q. canariensis*). Despite *Q. robur* seemed to better perform in the wet zone and *F. angustifolia* at the mid-flooded one, it is also in these zones were they have experienced their growth decline over the last decades. In this mid-flooding conditions *F. angustifolia's* growth was enhanced by spring GWL and summer precipitation, while constrained by summer temperatures. This might be explained because individuals from this mid-flooded zone are not adapted to lower water availability (as they might be in the wet zone) and, thus, they are more dependend on the annual water availability conditions. Some authors reported the absence of growth trends for *F. angustifolia*, but similar BAI that we found in *Roureda de Tordera* (10 - 20 cm^2 $year^{-1}$; González-Muñoz et al., 2015). Others highlighted the role of precipitation, soil moisture, and GWL on tree growth increases (García-Suárez et al., 2009; Rieger et al., 2017). This species is already in the center of its

distribution area in *Roureda de Tordera* (Douda et al., 2016; Gérard et al., 2013; Rodríguez-González et al., 2017), what can explain why not consistent growth trends are found in the forest.

Contrary to *F. angustifolia*, *Q. robur*'s growth was more affected by environmental conditions. Its BAI showed a strong decline trend in the wet zone over the last decades, yet, this growth decline smoothed down as the species is located at flooded areas. The lack of growth trend in the extremely-flooded zones suggest that *Q. robur* may take advantadge from this extra-water availability that supplies the species water requirements. Moreover, in the wet zone, BAI was constrained by high temperatures during late spring but enhanced by summer precipitation. Similarly, some studies have reported positive interactions with summer precipitations while negative summer temperatures effects for this species growth (Nechita et al., 2017; Rieger et al., 2017; Tessier et al., 1994). These results support that *Q. robur* can cope with increasing temperatures only under high water availability conditions. Therefore, the extra-water availability provided by groundwater on top of rainfall is very likely the explanation of the persistence of this mid-European species within this area.

Although *Q. canariensis* has been reported to show many drought tolerant strategies (Quero et al., 2008), as well as the ability to cope with interannual environmental variability (Messaoudène and Tessier, 1997; Pérez-Ramos et al., 2014), in some areas of its southern distribution it has already been reported a growth decline over the last decades (Ajbilou et al., 2006). However, in *Roureda de Tordera* this species is at its northern distribution range edge and no trend have been detected on its growth. Nevertheless, annual and summer precipitation, and late spring and early summer high GWL enhanced the BAI of this species. These results support the well-known high water requirements of this species despite being at their northern distribution range edge (Marañón and Ojeda, 1998; Tessier et al., 1994; Urbieta et al., 2008; Vila-Viçosa et al., 2015). Therefore, *Q. canariensis* in *Roureda de Tordera* is located in the contiguous dry zones adjacent to wetter zones where *Q. robur* and *F.*

angustifolia coexist. There, they encounter optimal water availability conditions but avoid root hypoxia.

3.4.2. iWUE trends: species adaptability to changing climate conditions

We found different iWUE responses to increasing temperatures and atmospheric CO_2 concentrations during the last decades. *Q. canariensis* showed the highest iWUE increase during its mature period, implying that the ratio between assimilation rates and stomatal conductance has increased. Moreover, its Ci/Ca trend confirm that the increase of iWUE is due to stomatal control. This result concurs with other mediterranean *Quercus spp.* behaviour with the ability to close stomata when environmental conditions are unfavorable for transpiration (Damesin et al., 1997). Contrarily, the changes of carbon isotopic discrimination in tree-rings of the *Q. robur* showed an increase of iWUE over the last decades only in the wet and mid-flooded zones, while no changes were found in the extremely-flooded zone. However, Ci/Ca trends suggested that only individuals in the mid-flooded zone regulate their gas-exchange with the atmosphere by stomatal control. Those in the wet zone regulate simultaneosly stomatal conductance and the rate of CO_2 assimilation. *Quercus spp.* are reported to regulate both photosyntetic activity and stomatal conductance (scenario Ci/Ca = constant) or do not change Ci/Ca ratio along time (scenario Ca-Ci = constant) (Frank et al., 2015; Saurer et al., 2014). Some authors suggest that they might close stomata under drough conditions at their southern distribution limits (Martínez-Sancho et al., 2018). Our results emphasize that global CO_2 concentration rise, but especially the changing climate, are already influencing gas-exchange of *Q. robur* forests at their southernmost distribution range edge. Accordingly, *Q. robur* iWUE was influenced by summer water availability supply (i.e. precipitation and GWL). Some authors have also reported *Q. robur* sensitivity to summer rainfalls (García-Suárez et al., 2009; Santini et al., 1994). The present optimal environmental conditions in the mid-flooded zone supported by iWUE analyses, are likely to shift into the extremely-flooded zone given the scenario projections of temperature and precipitation in the Mediterranean region.

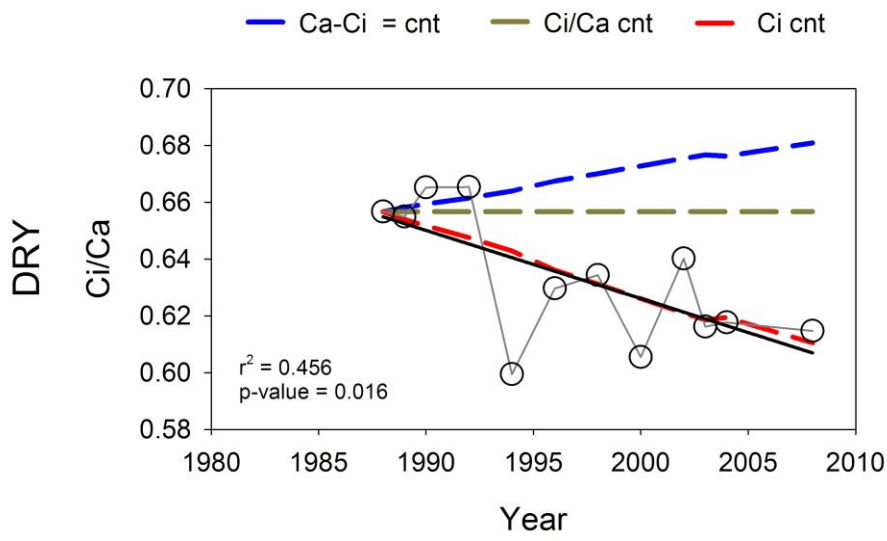

Figure 3.9 Ci/Ca trends for mature *Q. canariensis* (mean values in open circles). Significant trends was found at the dry zone for *Q. canariensis* ($y = -0.002x + 5.42$, $r^2 = 0.46$, $p = 0.016$). Different gas-exchange scenarios are shown in dashed lines (cnt means constant).

Strikingly, *F. angustifolia* showed no iWUE trends along time. Yet, carbon discrimination was correlated with high GWL and higher iWUE was found in the extremely-flooded zone, suggesting some kind of limitation. *F. angustifolia* is typical from riparian areas, hence its presence in areas with high water availability and seasonal floodings is frequent (Jaeger et al., 2009), and supports the absence of differences in iWUE trends across the flooding gradient of the study site. In non-flooded areas from the Iberian Peninsula *F. angustifolia* iWUE has been reported to be > 90 μmol mol^{-1} (González-Muñoz et al., 2015), lower values at *Roureda de Tordera* could be explained by the higher water availability in the area. We hypothesize that higher carbon isotopic discrimination of *F. angustifolia* in the extremely-flooded zone is a consequence of an intrinsic mechanism to face the stress linked to root-hypoxia periods. Ci/Ca trends at study site showed stomatal control on gas-exchange by *F. angustifola* at flooded areas. Gas-exchange in the extremely-flooded zone, seemed to change from a strong stomatal closure to a control of both photosyntetic activity and stomatal conductance during the last years. Then,

flooded periods might have been shortened due to climate change. In this sense, some studies have reported important increases in iWUE during hypoxia for grasslands, although others reported no changes (Pezeshki and Delaune, 1993). Our results offer novelty on *F. angustifolia* growth constraints in these flooded areas, and therefore more research is needed to better enlight it.

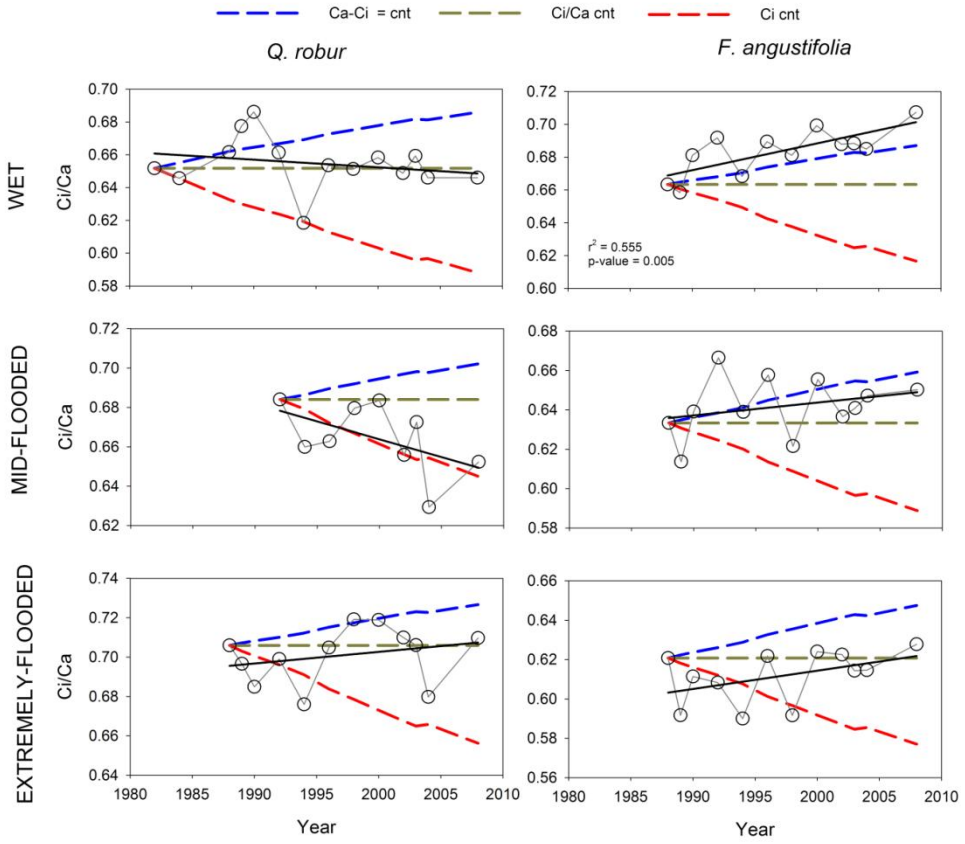

Figure 3.10 Ci/Ca trends for mature *Q. robur* and *F. angustifolia* (mean values in open circles). Significant trends was found at the wet zone for *F. angustifolia* ($y = 0.002x - 2.57$, $r^2 = 0.56$, $p = 0.005$). Different gas-exchange scenarios are shown in dashed lines (cnt means constant).

Flooding can be beneficial or detrimental to forest seeding survival and individuals growth depending on its frequency and duration. It can supply soil nutrients and water but also create a physiological stress due to soil hypoxia over large flooding periods (Anderson and Mitsch 2008, Urbieta et al 2008).

Most of the studies about soil hypoxia effects on plants are conducted in seedlings germination during shorter flooding periods than those found in *Roureda de Tordera*. In our study area, shorter flooding periods (i.e. mid-flooded zone) were positive for *Q. robur* growth and thus, this groundwater supplied the transpiration demands of the species over the last decades. In this zone *Q. robur* showed tolerance to short periods of root hypoxia as it has been reported for some authores (Alaoui-Sossé et al., 2005; Colin-Belgrand et al., 1991; Dreyer, 1994, Rémy et al., 2003; Schmull and Thomas, 2000; Bourgeade et al 2017, Copini et al 2016). Nevertheless, negative correlation between *Q. robur* growth and groundwater recharge during the dormant period in the extremely-flooded zone, together with its low BAI trend, and the only presence of few individuals there, suggest constrictions root-hypoxia for *Q. robur*, but some advantage for *F. angustifolia* recruitment (Becker et al., 1996; Tessier et al 1997). In other areas where *Q. robur* cohabits with *F. angustifolia*, long exposition to hypoxia stress gave advantadge to *F. angustifila* germination seeds (Janik et al 2016). *F. angustifolia* has high tolerance to flooding hypoxia (Jaeger et al 2009) and its seeds do not tolerate dry conditions (Drvodelic et al 2016). Despite higher GWL constrained growth rates of *F. angustifolia* in the extremely-flooded zones, the high presence of this species in the flooded areas of *Roureda de Tordera* suggest its better mechanisms to overcome the stress induced by waterlogging (for example enhancing iWUE). Altogether, long flooding periods can be detrimental for *Q. robur*, decreasing the probability of seed germination and/or hampering root developpment. Nevertheless, the acess to groundwater may facilitate the survival of this species at its southern distribution range edge. Little is known about hypoxia effects on *Q. canariensis* but, since is one of the Meditterranean oaks with more water requirements, there are some studies confirming that this species is able to tolerate short periods of hypoxia stress in seeds survival and root growth (~30days, Perez-Ramos et al 2009, Urbieta et al 2008). However, the low probability of floodings in the zones of the floodplain habited by *Q. canariensis* may not compromise this species survival at its northern range edge.

3.4.3. Future viability of range edge forests

The presence of European species such as *Q. robur* in our region is already constrained by the Mediterranean climate conditions. *Roureda de Tordera* constitutes a microrefugia of this species where it finds favourable habitat conditions (Dobrowski 2010). Our results suggest that global change might have been already modifying tree growth rates over the last decades and this may change the distribution of these species along the water availability gradient in the future. A new climate scenario, with lower water availability and flooding periods at *Roureda de Tordera*, is likely to promote the expansion of *Q. canariensis* to the current wet zones, while *Q. robur* and *F. angustifolia* could become restricted to the zones where flooding would still occur. From a wider perspective, our results show that *Q. robur* populations at their southernmost distribution range edge are already affected by increasing temperatures. Their survival may be endangered if water availabilty is reduced in the future. In agreement, some models of future species distribution have already suggested a shift of *Q. robur* distribution to higher latitudes (Dyderski et al 2017), where tree growth might be promoted by increasing temperatures (Huang et al 2017). This, may also imply a shift of its southern distribution edge to higher latitudes, while other species more adapted to water scarcity, such as *Q. canariensis*, may be stabilshed in the area. Furthermore, *Q. canariensis* at the mid-southern limit of distribution has been already reported to reduce seed production, arising regeneration problems due to drought (Perez-Ramos et al 2015, Urbieta et al 2011). Some studies also highlighted future dificulties for F. angustifolia habitat in our region (Temunovic et al 2013). The study and conservation of these areas where current and future distribution of species overlap is of crucial importance to understand climate change damages on species distribution (Temunivic et al 2013, Huang et al 2017). In the Mediterranean Basin, many studies have already reported how species and biomes have shifted towards the poles or higher altitudes as a result of past climate warming events (Peñuelas et al., 2002, Jump et al 2006, Mariotti 2010, Collins et al. 2013), restricting the climatic niche of the temperate species growing in the region (Gazol et al. 2015). The intensity and length of future climate change-induced droughts will be decisive for the performance and

survival of these species at their distribution range edge in such singular forests.

Aknowledgements
We are thankful to Emilia Gutierrez for her invaluable encouraging help in the lab. We also thank Sergi Fontseca to provide meteorological data of Tordera. Financial support was provided by the Spanish Government through the projects MONTES-Consolider (CSD2008-00040-MONTES), MEDFORESTREAM (CGL2011-30590), and MEDSOUL (CGL2014-59977-C3-2). Sílvia Poblador was supported by a FPI PhD fellowship from the Spanish Ministry of Economy and Competitiveness (BES-2012-054572). We also thank site cooperators, including Tordera City Governement for permission to sample at the *Roureda de Tordera*. Sílvia Poblador, Santiago Sabaté, and Francesc Sabater are members of the research group FORESTREAM (AGAUR, Catalonia 2017SGR976).

CHAPTER 4

Linking foliar traits and foliar dynamics to water availability. The idiosincratic tree species responses in a Mediterranean riparian forest.

Climate change is already affecting tree species performance all around the world. However, little is known abou the effects that climate change can have on riparian vegetation. Riparian trees are inhabiting the wettest areas of the catchment, and thus they may not present ecophysiological mechanisms to cope with future drier conditions. In this work we aimed to evaluate tree species in a mixed Mediterranean riparian forest during two years with different environmental conditions (one wet and one dry). For that, we evaluated tree canopy dynamics (i.e. temporal leaf litterfall) and foliar chemical and morphological traits (i.e. iWUE, CN ratios, leaf area, etc). Moreover, we conducted oxygen and deuterium isotopic analyses to determine water sources (soil or groundwater) of riparian trees transpiration. Our results showed that all riparian trees obtained more than 80% of the water transpired from the soil compartement, being specially remarkable during summer. Autochthonous species reduced their leaf biomass production during the dry year. Yet, only *P. nigra* was able to increase its iWUE during drought conditions. The invasive N-fixing species *R. pseudoacacia*, distributed all across the riparian forest, showed high plasticity to adapt to environmental conditions. This species modified its water sources depending on the environmental conditions and its location on the riparian area. Moreover, *R. pseudoacacia* was able to produce more leaf biomass during the dry year, as well as increase its iWUE. Overall, our results highlight the extreme sensitivity of riparian tree species to water availability, and arise the risk of these autouchthonous species to be substitute by invasive species more adapted to drought periods.

With permission of: D. Nadal-Sala, D. Sperlich, F. Sabater and S. Sabater, who are co-authors of this study.

4.1. Introduction

Riparian areas are considered hot spots in terms of exchange dynamics of carbon (C), nitrogen (N), and water due to the connection of the stream with the entire catchment (Hill, 1996; Hoover et al., 2011; Pert et al., 2010; Qualls and Haines, 1992). Thus, riparian areas are intermediate ecosystems between streams and uplands ones, where shallow groundwater levels facilitate the establishment of species with high water availability demand (Huxman et al., 2005; Pielech et al., 2015; Zhang et al., 2005). These species may benefit of high soil water contents, reachable shallow groundwater or even stream water depending on its water requirements, root system or location at the riparian site (Dawson and Ehleringer, 1991a; Sánchez-Pérez et al., 2008; Singer et al., 2013).

In arid and semi-arid regions, such us the Mediterranean Basin, riparian areas are characterized by particularly steep gradients in water availability decreasing from the near stream edge to the hillslope (Chang et al., 2014; Poblador et al., 2017). This results in a highly diverse tree species distribution with different water requirements along this gradient. In turn, the species occupying the different riparian zones will determine the timing, quantity and quality of organic matter (i.e. leaf litter fall) to the forest floor and the adjacent stream, determining their biogeochemical processes and foodwebs (Hoover et al., 2011; Sanpera-Calbet et al., 2016; Vitousek, 1984).

Mediterranean regions are characterized by mild winters and dry and warm summers. Climate change projections at these regions suggest an increase of temperatures and decrease of summer precipitation (IPCC, 2013), also exacerbating seasonal and inter-annual variability of both variables. In up-land Mediterranean forests, climate change effects have been widely studied, and drought has reported to induce tree mortalities and forest decline (Jump et al., 2006; O'Neill et al., 2008; Peñuelas and Boada, 2003). However, little is still known about how these changes in water availability can affect species that are not well adapted to water scarcity, such as riparian tree species. The consequent decrease of water availability in an environment with high

evaporative demand is likely to affect riparian vegetation reducing its compositional heterogeneity and motivating cascade effects for the ecosystem functioning (Hoover et al., 2011). Climate change may induce species shifts, increasing drought-tolerant species abundance, and promoting the establishment of allocthonous and/or invasive species (Follstad Shah and Dahm, 2008; Kominoski et al., 2013; Lite and Stromberg, 2005). For instance, the replacement of native riparian vegetation by Eucalyptus in Portugal has decreased the heterogeneity of litter inputs to the soil and stream, shifted the fall period to summer and lowered groundwater levels (Graça et al., 2002). The intrinsic heterogeneity of water availability in Mediterranean riparian areas, together with differences in physiology and rooting systems among co-occurring riparian tree species makes it difficult to predict the response of riparian forest communities to (local and regional) changes in water resources arising from meteorological drought or alterations in groundwater levels (Perry et al., 2012).

Traits associated with plant morphology, production, and physiology can show adaptations to environmental stressors such as drought. Leaves, together with fine roots, are one of the most dynamic part of the plants, especially for deciduous trees (Menzel, 2002). Accordingly, plant phenology period is one of the most sensitive indicator of how plant species respond to favorable or stress conditions (Fernandes et al., 2014; Traiser et al., 2005), phenologic leaf fall is directly related to air temperature and photoperiod (Menzel, 2002). Thus, changes on environmental conditions have the capacity to modulate leaf litter quantity and quality, altering also nutrient (C and N) cycle dynamics. For instance, annual riparian inputs are related to precipitation (Benfield, 1997), and summer drought or physical perturbations (i.e. windstorms) can cause an incomplete nutrient remobilization and an increase in quality of litter inputs (Sanpera-Calbet et al., 2016). Moreover, environmental conditions are identified to determine morphological leaf traits of different species across biomes (Poorter et al., 2009; Wright et al., 2004). In regions where water is not limiting tree species exhibit higher leaf area and less succulent leaf structures, as strategies to reduce evaporative loses are less critical (Ogaya and Peñuelas,

2007; Wright et al., 2017). Nevertheless, changes on environmental conditions at local scales can have effects on species morphological leaf traits, indicating its plasticity to overcome adverse conditions (Quero et al., 2006). For instance, species with plasticity to drought situation can produce leaves with higher specific leaf mass area (LMA), leaf thickness and leaf density, and thus, more resistant to water scarcity (Coble and Cavaleri, 2015; Niinemets, 2001; Ogaya and Peñuelas, 2006). Leaves stomatal closure is another plant mechanism to avoid water losses and overcome drought periods. The consequent decrease in ^{13}C discrimination during transpiration, recorded in leaves and wood, is used as a proxy to estimate species water use efficiency (iWUE) of plants in drier sites or during drier years (Ogaya and Peñuelas, 2006; Peñuelas et al., 2008). Tree species responses to dry periods in up-lands forests are widely studied, but still little is known about the capacity of riparian tree species adaptability where, to our best knowledge, most of the morphological studies have focused on shade tolerance responses to light exposition (Legner et al., 2013). Comparing all these physiological parameters among co-occurring native and invasive species in riparian areas is much-needed information about their different responses and resilience under potential water stressful conditions, a relevant issue in Mediterranean regions (González-Muñoz et al., 2015; Perry et al., 2012).

The aim of this study was to evaluate the sensitivity of four co-occurring tree species to water availability variability in a riparian mixed forest in the NE Iberian Peninsula. The forest is composed by one native N-fixing species (*Alnus glutinosa*), two natives non-fixing species (*Populus nigra* and *Fraxinus excelsior*), and the invasive N-fixing species (*Robinia pseudoacacia*). Specifically, we aimed (i) to evaluate riparian tree species responses to changes on water availability, and (ii) to identify the main water sources of these species. Therefore, we investigated how canopy structure and dynamics changed with changing water availability by monitoring and quantifying leaf litter inputs to the forest soil of the four tree species during two vegetative years (one with wet and another with dry conditions), and identifying the environmental drivers of peak falls (i.e. physic perturbations, drought stress responses or phenologic

fall). We also measured leaves morphological traits for both years and calculated iWUE from leaves and wood. In addition, we analyzed water sources contribution to xylem water for all tree species through isotopic composition. We hypothesized that those species typically located at the stream edge zones (i.e. *A. glutinosa* and *P. nigra*) would have higher water demands and, thus, would be more sensible to changes in water availability, than those located at the hillslope edge (*F. excelsior*) or adapted to drier conditions (*R. pseudoacacia*). We expected *A. glutinosa* and *P. nigra* to be more sensible to water scarcity contributing with higher relative leaf litterfall amounts during drier periods of the year (i.e. summer) and during drier years (i.e. the year 2012). Accordingly, we expected higher leaf traits plasticity to drier annual conditions for *F. excelsior* and *R. pseudoacacia* (i.e. lower LMA, and higher leaf density, iWUE, and nutrient reabsorption efficiency before senescence). Finally, we expected that those species at the near-stream edge (*A. glutinosa, P. nigra* and some individuals of *R. pseudoacacia*) would use soil water but even more groundwater, while those farer from the stream edge (*F. excelsior* and *R. pseudoacacia*) would feed mainly from soil water.

4.2. Materials and methods

4.2.1. Study site

Font del Regàs is a subhumid Mediterranean catchment located in the Montseny Natural Park, NE Spain (41º50'N, 2º30'E). The catchment area is 14.2 km2 and its altitude ranges from 475 m to 1500 m above the sea level (a.s.l.). Evergreen oak (*Quercus ilex*) and European beech (*Fagus sylvatica*) forests cover the 54% and the 38% of the catchment, respectively (ICC, 2010). The riparian zone covers 6% of the catchment area and it consists mainly of two non-fixing species, european ash (*F. excelsior*) and black poplar (*P. nigra*), and two N-fixing species alder (*A. glutinosa*) and black locust (*R. pseudoacacia*). The latter one is a non-native invasive species that has widely spread in the NE and NW of the Iberian Peninsula (Sanz-Elorza 2004). Long-term annual precipitation averages 925 ± 151 mm and mean annual temperature is 12.1 ± 2.5 ºC (mean ± SD, period 1940-2000, Catalan Metereologic Service). During the study period, mean

annual precipitation and mean annual temperature were 1078 mm and 13.3± 5.9ºC, and, 872 mm and 13.1± 6.9ºC, for the wet and the dry year respectively. Total inorganic N deposition oscillates between 15-30 kg N ha^{-1} yr^{-1} (period 1983-2007; Àvila et al. 2010).

We selected a well-developed riparian stand (30x20 m) that flanked the stream at the valley bottom of the catchment (475 m a.s.l.). The riparian stand consisted of *R. pseudoacacia*, *P. nigra*, *A. glutinosa* and *F. excelsior* (74%, 13%, 10%, and 3% of the plot total basal area, respectively). The riparian soil (pH ~ 7) was sandy-loam and had a 5-cm deep organic layer followed by a 30-cm deep A-horizon. Groundwater table at the near-stream edge (<2 m from the stream) oscillated from 0.5 to 0.8 m below the soil surface (b.s.s.), while groundwater table at the hillslope edge (~25 m from the stream channel) oscillated from 2 to 4 m b.s.s..

4.2.2. Environmental conditions and water availability monitoring

Meteorological data were monitored in a meteorological station, located at ca. 800 m distance from the study site. Air temperature, relative humidity, solar radiation, photosynthetic active radiation (PAR), precipitation, and wind's speed sensors were installed at a height of 3 m and measured at 30-s intervals. Data were stored as 15-min average in a data-logger (CR1000 Data-logger and AM16/32 Multiplexers, Campbell Scientific, Inc., Logan, UT, USA). Vapour pressure deficit (VPD) was obtained from air temperature and relative humidity. Every two weeks, leaf area index (LAI) across the riparian plot was inferred from field PAR measurements carried out with a Sunfleck Par Ceptometer Model SF-80 (Decagon Devices, USA) using Norman and Jarvis equation (1975).

Soil water content (in cm^3 cm^{-3}) and groundwater level (in m b.s.s.) fluctuations were monitored across the riparian area during the study period. Soil water content was measured for the upper 30-cm of soil every 15-min using frequency domain reflectometers (TDR sensors, CS616, Campbell Scientific, Logan, USA) at different distances from the stream channel (1.5, 4, and 14 m). Wells were installed at different distances from the stream channel across the

study plot (1.5, 2.5, 5, 17, and 25 m distance) to assess groundwater level fluctuations. Wells were PVC tubes (32 mm Ø) uniformly perforated along their length and placed at 1 to 3 m b.s.s. at the near-stream edge and hillslope edge, respectively. At each location, groundwater level was monitored every 15-min using water pressure transducers (HOBO U20-001-04) and measured every two weeks with a water level sensor (Eijelkamp 11.03.30).

4.2.3. Leaf litter production

The temporal patterns of leaf litter inputs were measured throughout the vegetative years 2011 and 2012 by using collector baskets of 1-mm mesh, which allow rapid drainage of rainwater and reduce weight loss by leaching. We placed 30 baskets (1 m^2 each) covering 5% of the riparian plot. Baskets were placed 1 m above soil and water surface at different distances from the stream edge (0, 4, 7, 10, 16 and 18m). Twice a month, leaf litter was collected and separated by tree species. At the laboratory, leaf litter was oven-dried (60º, 48-72h) until constant mass and weighted (González, 2012). For each species and sampling date, we determined the dry weight of leaf litter (DW, in g m^{-2}).

4.2.4. Leaf morphological traits and chemical analyses

In summer 2011 and 2012 fully developed sunlit leaves of all species were sampled from the top canopy. Branches from individuals of each species (N=6) were sampled using a pruning pole and a tree climber. After sampling 30 leaves per tree we measured immediately after the field work in the laboratory leaf area (LA, in cm^2), leaf fresh weight (FW, in g), and leaf thickness (LT, in μm). LA was measured by scanning fresh sampled leaves (EPSON EXPRESSION 10000 XL) and analyzing the images afterwards by using ImageJ program (National Institutes of Health, Image processing in analysis in Java), pixel data obtained was converted to cm^2. LT was measured using a penatometre. Leaf dry weight (DW, in g) was measured after being oven-dried for 48-72h at 60º C. LMA (mg cm^{-2}) was obtained from the quotient DW/LA. Leaf density (LD, in mg cm^{-3}) was obtained from the quotient between LMA/LT. Succulence (S) is the % of water in leaves and was obtained from the difference between FW/DW.

Leaf N concentrations (in % dry weight and mg cm^{-2}) and foliar $\partial^{15}N$ and $\partial^{13}C$ were analyzed for each tree species. Therefore, a composite of leaves sampled per each individual was ground and analyzed in an Elemental Analyser Flash 1112 (Carlo Erba, Milano, Italy) coupled to an IRMS Delta C isotope ratio mass spectrometer with a CONFLO III interface (Thermo Finnigan MAT, Bremen, Germany). Analyses were carried out at the Scientific Technical Service of the University of Barcelona. Values are expressed per thousand (‰) on the relative ∂-scale and referred to international standards following the equation:

$$\delta Z = (R_{sample} - R_{standard}) - 1 \quad \text{(Eq. 4.1)}$$

where Z is the heavy isotope of either N or C, and R is the ratio of heavier to lighter isotope for the sample and standard ($^{13}C/^{12}C$ or $^{15}N/^{14}N$). For $\delta\ ^{13}C$ the international standard V-PDB (Vienna Pee Dee Belemnite) was used. For $\delta^{15}N$ the international secondary standards of known $^{15}N/^{14}N$ ratios (IAEA N1 and IAEA N_2 ammonium sulphate and IAEA NO_3 potassium nitrate) relative to N_2 in air were used.

From these analyzes we used C and N concentrations to calculate CN ratios and N leaf concentrations. Moreover, we used foliar $\delta\ ^{13}C$ to calculate intrinsic WUE (iWUE) according to the equations (McCarroll and Loader, 2004):

$$c_i = c_a \left(\frac{\delta\ 13\text{Cplant} - \delta\ 13\text{Cair} + a}{-(b-a)}\right) \quad \text{(Eq.4.2)}$$

$$\text{iWUE} = A/g = ca\ [1 - (Ci/Ca)] \times (0.625) \quad \text{(Eq.4.3)}$$

where a is the discrimination against $^{13}CO_2$ during diffusion through the stomata (±4.4 ‰), b is the net discrimination due to carboxylation (±27 ‰), and ci and ca are intercellular and ambient CO_2 concentrations (Farquhar et al., 1982). A is the rate of CO_2 assimilation and g is the stomatal conductance. Data of ∂^{13}Cair, Ci and Ca were obtained from McCarroll and Loader (2004) which used the high precision records of atmospheric $\partial^{13}C$ from Antarctic ice cores (Francey et al., 1999), and the atmospheric CO_2 concentration (ppm) from Robertson et al. (2001).

4.2.5. Long-term WUE changes recorded in wood

For each species, increment wood cores were taken from trees at breast height (~1.3 m) in winter 2011/12 using a 12-mm increment borer. Two cores were taken from each sampled individual and tree-rings were dated following standard procedures (Gutiérrez et al., 2004). We analyzed climatic data from Viladrau meteorological station (~15 km from the studied area) and identified dry and wet years within the period. We carefully sepeared tree-rings per year from five individuals of each species. We ground late wood of tree-rings created during typical dry and wet years (13 and 12 years respectfully). Ground rings were analyzed for $\delta\ ^{13}C$ and calculated iWUE from the results following the same procedures than for leaves analyzes (Loader et al. 2003).

4.2.6. Determining the source of plant water uptake

During root water uptake and sap transfer there is no fractionation of oxygen (^{18}O) nor deuterium (^{2}H) and thus it is widely used to determine water sources by vegetation (Dawson and Ehringer, 1991; Wang et al 2010). In spring (end of May) and summer (begging of August) of 2013 samples of xylem, soil and groundwater were collected and analyzed for isotopic compositions ($\partial^{18}O$ and $\partial^{2}H$) in order to determine water sources of the riparian trees. All samples were collected between 12 and 3 pm. For that, 5 individuals of *A. glutinosa*, *P. nigra*, and *F. excelsior* were sampled. In the case of *R. pseudoacacia*, that is established across the riparian plot, 15 individuals were sampled (5 at each riparian area: near-stream edge, intermediate zone, and hillslope edge). For each individual, one twig was cut and the bark and phloem were removed to prevent interference from the isotopes in the water of the leaves. The twigs were transferred to borosilicate glass vials with PTFE/silicone septa tops (National Scientific Company, Rockwood, USA) and sealed with parafilm. The samples of soil were extracted with a soil corer layer across the riparian plot (N=9) and stored in glass vials divided into two categories: shallow soil water (0-30 cm) and deep soil water (30-60 cm). Groundwater samples were obtained by pumping from wells across the riparian plot (N=9). All water samples were immediately filtered (Whatman GF/F, 0.7 μm pore Ø), and sealed in glass vials without air to avoid exchange with the atmosphere. All samples were kept

cold until processing and analyses. Water from xylem and soil samples was extracted by cryogenic vacuum distillation following West et al. (2006) and Barbeta et al (2015). The isotopic compositions ($\partial^{18}O$ and $\partial^{2}H$) of the distilled water and groundwater samples were determined using isotope ratio infrared spectroscopy (IRIS) with a Picarro L2120-i Analyzer (Picarro Inc., Santa Clara, USA). The isotope ratios in this study are expressed as:

$$\partial^{18}O \text{ and } \partial^{2}H = [(R_{sample} - R_{standard}) - 1] \quad \text{(Eq. 4.4)}$$

where Rsample and Rstandard are the heavy/light isotope ratios ($^{2}H/H$ and $^{18}O/^{16}O$) of the sample and the standard (VSMOW, Vienna Standard Mean Ocean Water), respectively. The water extractions and isotopic analyses were conducted at the Department of Crop and Forest Sciences (University of Lleida, Catalonia, Spain) and the Scientific Technical Service of the University of Lleida, respectively.

We determined the relative contribution of the three different water sources in our riparian trees' water supplies by analyzing our data with the siar (stable-isotope analysis in R) package in R (Parnell et al., 2010). The package allowed us to estimate the most likely proportion of plant water taken up simultaneously from each source through Bayesian mixing models. We applied these models to our data to infer the relative contribution of each water source (i.e. shallow soil water, deep soil water, and groundwater) to the xylem water, producing simulations of plausible contributing values from each source using Markov chain Monte Carlo (MCMC) methods. Our model inputs were the isotopic composition ($\partial^{18}O$ and $\partial^{2}H$) and their standard errors for each potential source and the isotopic compositions of the xylem water, which were assigned as the target values. We set the TEF (trophic enrichment factor) to 0, because of the absence of fractionation during water uptake from soil by roots (Dawson and Ehleringer, 1991), and set concentration dependence to 0. We ran 500 000 iterations and discarded the first 50 000. We ran a model for the isotopic values from each sampled tree in each season with the isotopic values from the soil water of the corresponding season.

Afterwards, mean relative contribution per species and season was used to estimate water volume extracted from each source per species during the study period. From the sap flow density values reported in Nadal-Sala et al. (2017), two daily transpiration values were calculated for each tree species: spring and summer daily tree transpiration values. Daily transpiration was corrected by the height of the sampled twigs (~12m) and the day of the year when the sampling was performed. We calculated mean daily sap flow from a 10-days mobile mean centered in the day in which water was uptaken for each tree species to take into consideration daily variability in sap flow values. Based on the allometric equations described in Nadal-Sala et al. (2017) between sapwood area and DBH, we obtained actual specific tree sapwood area for each tree species in each riparian zone. Then, we multiplied specific mean daily sap flow for actual tree sapwood area to obtain specific tree daily transpiration both spring and summer.

4.2.7. Leaf litter fall C and N analyses

For each year and species, a composite of samples collected during the three different peak of leaf litter fall (i.e. physical perturbation, drought stress, and end of the phenologic period) was analyzed for C and N content with a gas chromatograph coupled to a TCD detector after a 1000 ºC combustion at the Scientific Technical Service of the University of Barcelona. Afterwards we calculated N resorption efficiency (NRE) for each species as the difference in N concentration between the green and the abscised leaves expressed as percentage of the N concentration in green leaves. We calculate NRE for the three different types of abscised leaves: physic perturbation, drought stress and phenologic fall.

4.2.8. Data analysis

All the statistical analyses were carried out with the R statistical software (R Development Core Team, 2016, version 2.15.1; packages lme, ggplot2, and siar). We used a metric Euclidean multidimensional scaling (MDS) analysis to identify differences in environmental conditions driving leaf litter-fall. Afterwards, we run a cluster analysis to assign two categories of the main

drivers of leaf dropping (phenology or physiology) to each leaf litterfall campaign, based on the environmental variables and the day of the year. By using only the campaigns outside the senescent period, we calculated the Spearman's correlation coefficient between each tree species, leaf litterfall and the different environmental conditions .

Differences between years and among riparian species for leaves morphological traits, leaves N concentrations, and leaves WUE were assessed by using a linear model ANOVA test. For each model, differences were tested with post-hoc Tukey contrasts. In all cases, residuals were tested for normality using a Shapiro-Wilk test and homogeneity of variance was examined visually by plotting the predicted and residual values. When necessary, we normalized data using log or square-root transformations to meet model assumptions. In all analyses, results were considered significant when p-value was < 0.05. The same procedure was used to confirm differences between $\partial^{18}O$ and $\partial^{2}H$ from the three water sources and, after siar results, the mean distribution of the MCMC simulation of each source for each individual sampled was also compared between seasons and among riparian tree species.

We modeled differences in water use efficiency recorded in tree rings wood by using mixed models as follows: as we searched to model differences in water use efficiency among tree species, we selected tree species as fixed factor for our model. In addition, as we wanted to compare the differences in WUE between dry and wet years, we also selected year as a fixed factor in our model. We potentially had two autocorrelation structures within our data. A spatial autocorrelation structure inside the individual factor, which we included in the random part of the mixed model, and a temporal autocorrelation structure inside the tree ring year factor, which was included initially as a random factor nested in the individual factor. Based in the AIC criteria (Fuentes et al., 2018; Paredes et al., 2015), we selected the most parsimonious model from all the possible models including all the factors noted before and their interactions. We then calculated the R2 for the most parsimonious model according to Nakagawa and Schielzeth (2013) to have an

estimate of the variability of the data supported by both fixed and random parts of our most parsimonious model.

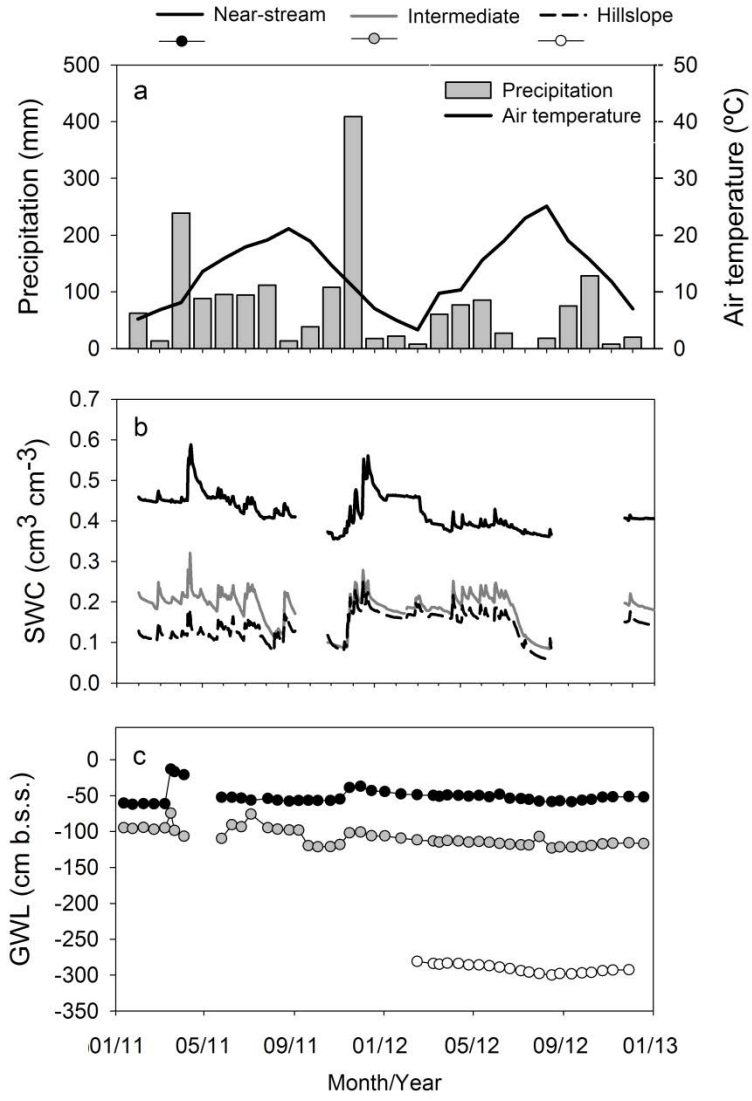

Figure 4.1 (a) Mensual precipitation (in mm) and mean temperature (in ºC) in *Font del Regàs*, (b) Soil Water Content (%) and (c) groundwater table elevations (cm b.s.s.) at different near-stream., intermediate and hillslope zones in 2011 and 2012.

4.3. Results

4.3.1. Environmental conditions

Our measurements were conducted during a year with wet conditions (2011) and a year with dry conditions (2012). Annual precipitation was 20% higher during wet year than during dry one (annual precipitation of 1078 mm and 872 mm, respectively). Moreover, seasonal variation between both years was remarkable (Fig. 4.1a). Summer precipitation in 2011 was 4-fold the precipitation in 2012 (220 and 46 mm, respectively) and summer temperatures were lower during 2011 than during 2012 (21.1ºC and 23.3ºC, respectively) (Fig. 4.1a). Soil water content presented a fast response to precipitation events and differed significantly between near-stream, and intermediate and hillslope riparian zones. The soil water contents in summer 2012 were more than 0.10 cm^3 cm^{-3} lower than in 2011 (Fig. 4.1b). Groundwater levels showed no high seasonal variation. However, summer groundwater level during summer 2012 were 20 cm higher than during the wet 2011 (Fig. 4.1c).

Table 4.1 Leaf litter fall (g DW m^{-2}) of four riparian tree species in the years 2011 and 2012. *R. pseudoacacia* is shown by riparian zones.

	A. glutinosa	*P. nigra*	*F. excelsior*	*R. pseudoacacia*		
				Near-stream	Intermediate	Hillslope
2011						
Physiology	31.70	40.12	17.79	38.92	63.19	64.05
Phenology	21.03	53.68	9.07	77.60	100.57	124.30
Annual	**52.73**	**93.80**	**26.87**	**116.52**	**163.76**	**188.35**
2012						
Physiology	14.49	15.97	2.62	60.98	61.11	82.75
Phenology	24.21	49.20	18.69	95.18	101.49	108.18
Annual	**38.71**	**65.17**	**21.31**	**156.16**	**162.61**	**190.93**

4.3.2. Leaf and wood riparian tree species production

R. pseudoacacia was the main species contributing to leaf litter fall in our study site (~40%). The native riparian species *A. glutinosa*, *P. nigra*, and *F. excelsior* contributed to ~20, 15 and 8% respectively (Table 4.1). In terms of stem BAI P. nigra species was the most productive species one (> 38 cm^2 $year^{-1}$) while *F. excelsior* was the lowest (< 6 cm^2 $year^{-1}$). *A. glutinosa* and *R. pseudoacacia* had

similar wood production (10 and 13 cm^2 $year^{-1}$, respectively) (Table 4.2). Due to the young age of the individuals, correlations between tree-rings width and climatic data were not performed.

Table 4.2 Wood production and WUE for wet and dry years registered in tree rings of four riparian tree species (*A. glutinosa*, *P. nigra*, *F. excelsior*, and *R. pseudoacacia*). Values are mean ± standard error from sampled trees. Capital letters indicate significant differences among species growth (P-value < 0.05).

	A. glutinosa	*P. nigra*	*F. excelsior*	*R. pseudoacacia*
Wood production				
cm^2 $year^{-1}$	9.72 ± 2.00^{AB}	37.98 ± 8.55^{C}	5.81 ± 1.39^{B}	12.65 ± 1.63^{A}
WUE				
Wet years	63.06 ± 1.92^{A}	71.00 ± 1.40^{B}	78.63 ± 2.73^{C}	86.64 ± 2.47^{D}
Dry years	62.90 ± 1.00^{A}	71.40 ± 1.86^{B}	76.53 ± 2.24^{C}	83.37 ± 2.99^{D}

During the dry year, native species reduced their leaf litter production in a 20 - 30%, while *R. pseudoacacia* maintained its leaf litter production at the hillslope edge and increased it + 30% at the near-stream edge. Nevertheless, the relative amount of physiological leaf litter fall (i.e. drought stress) to annual one was not higher during the dry year with respect to the wet one (Table 4.1). *R. pseudoacacia* was the only species that had higher contribution of leaf litter fall during drought stress period of 2012 (~40% of annual leaf litter fall) than the one of 2011 (~30% of annual leaf litter fall) (Fig. 4.2a). LAI in the study plot had a maximum of 4.2 and 4.7 m^2 m^{-2} during 2011 and 2012, respectively (Fig. 4.2b).

We did not find clear patterns relating environmental conditions with leaf litter fall during the physiological fall (i.e. drought stress) for the dry and the wet year (Table 4.3). Nevertheless, accounting for both vegetative years, the leaf litter of all species that was shed before the phenologic fall (i.e. before the end of the growing season) were mainly positively influenced by air temperature and VPD. Water availability was negatively correlated with leaf fall of *A. glutinosa* only when groundwater level was at its minimum. Contrary, for *P. nigra* and *F. excelsior* water availability had a bigger influence. Windspeed was

correlating positively with *P. nigra* litter fall, which is also the tallest of all species with the most exposed crow, and negatively with *F. excelsior*. Leaf fall of *R. pseudoacacia* was mainly influenced positively by air temperature and negatively by soil water content. Correlations of soil water content with *R. pseudoacacia* leaf fall were stronger at the hillslope than at the intermediate or near-stream riparian zones, where also minimum groundwater level was important.

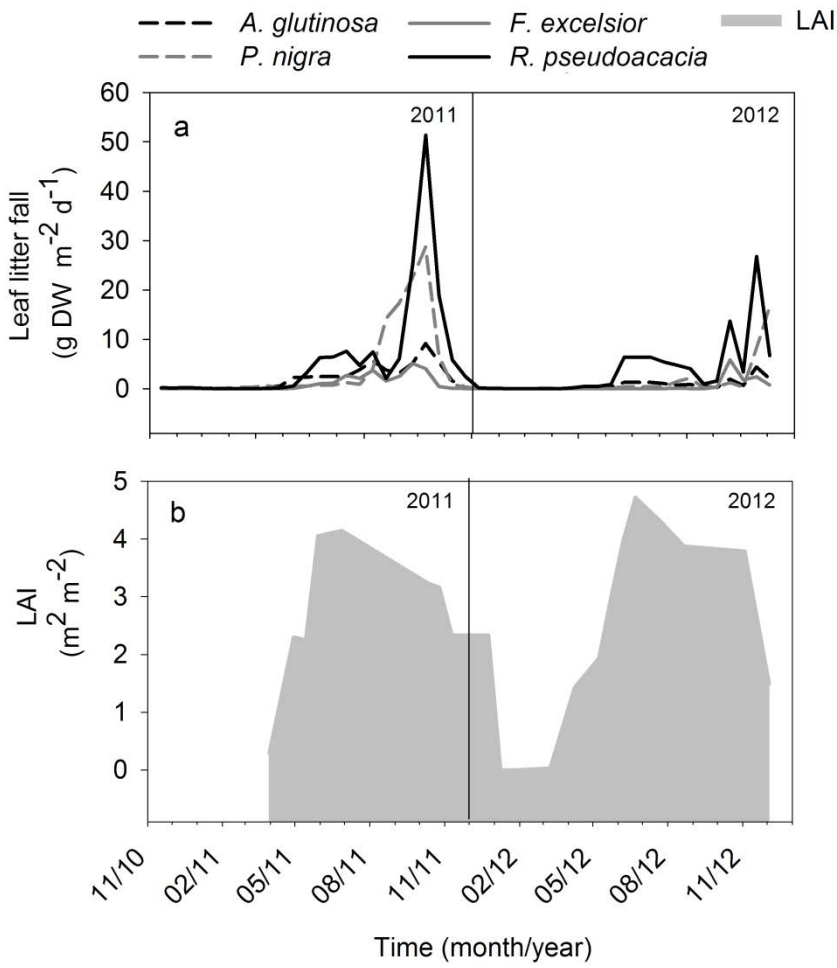

Figure 4.2 For years 2011 and 2012, (a) Leaf litter fall (in g DW m^{-2} d^{-1}) from of *A. glutinosa* (dashed black), *P. nigra* (dashed grey), *F. excelsior* (grey line), and *R. pseudoacacia* (black line) for the years 2011 and 2012, and (b) Leaf area index (LAI, in m^2 m^{-2}) of the entire riparian study site.

Leaf N content differed among litter fall types and species (Fig. 4.3). Fresh and senesced leaves from the two N-fixing species, *A. glutinosa* and *R. pseudoacacia*, had significantly higher N content than the ones of *P. nigra* and *F. excelsior*. *F. excelsior* presented the lowest capacity to N-reabsorption before drought fall (~5%) but increased it during phenologic fall (~26%). *A. glutinosa* and *P. nigra* reabsorpted ~30% of N during physiologic fall, but it differed between both species before phenologic fall (<20% and ~40% for *A. glutinosa* and *P. nigra*, respectively). *R. pseudoacacia* reabsorpted ~40% of N before both types of fall.

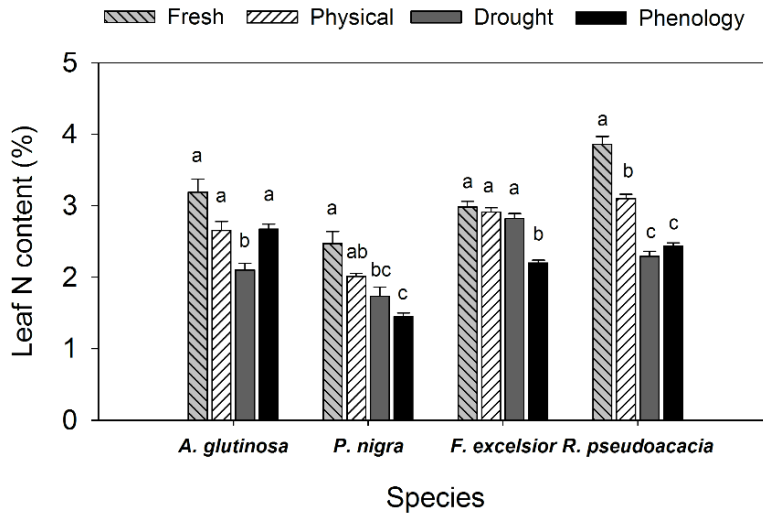

Figure 4.3 Nitrogen content of leaves of four riparian tree species (A. glutinosa, P. nigra, F. excelsior, and R. pseudoacacia). For each species nitrogen is measured for fresh and different litter fall (i.e. physical perturbation, drought, and phenology). Values are mean ± standard error. Small letters indicate differences among leaf type within species.

Table 4.3 Spearman correlations of environmental variables influencing leaf litterfall from riparian tree species during non phenological fall period. Leaf litterfall is considered as relative annual contribution. Meteorological data is calculated as mean value between sampling dates. All correlations (r2) are shown for all sampling dates, year 2011, and year 2012 ($p<0.05$; n = 19, 11, and 8, respectfully).

Species	Varible	r2 leaf litter	2011	2012
A. glutinosa	Air T°	0.472	-	-
	VP	0.511	-	-
	AirSatP	0.505	0.721	-
	Soil T°	0.685	-	-
	MinGWL	-0.708	-	-0.708
P. nigra	Air T°	-	-	0.714
	AirSatP	-	-	0.714
	WindMax	-	-	0.786
	SWC	-	-0.714	-
	GWL	-	-0.770	-
	MinGWL	-	-0.770	-
	T° ac	-	-0.721	-
F.excelsior	Air T°	0.477	-	-
	VP	0.713	-	-
	AirSatP	0.508	0.705	-
	WindSeep	-0.632	-	-0.810
	WindMax	-0.512	-	-
	Precip	-	-	-0.874
	SWC	-0.577	-	-1.000
	Soil T°	-	-	-1.000
	GWL	-	-0.689	-
	MinSWC	-	-	-1.000
	MinGWL	-	-0.689	-
	T° ac	-0.601	-	-0.810
R. pseudoacacia				
Near-stream	Air T°	0.610	0.661	-
	VP	0.583	-	-
	AirSatP	0.643	0.745	-
	VPD	0.515	0.721	-
	SWC	-0.657	-0.714	-
Intermediate	Air T°	0.631	0.721	-
	VP	0.678	-	-
	AirSatP	0.649	0.770	-
	SWC	-0.615	-	-
	Soil T°	0.608	-	-
Hillslope	Air T°	0.660	0.717	-
	VP	0.611	0.650	-
	AirSatP	0.686	0.766	-
	VPD	0.541	-	-
	SWC	-0.680	-	-
	GWL	-0.529	-	-
	MinGWL	-0.535	-	-

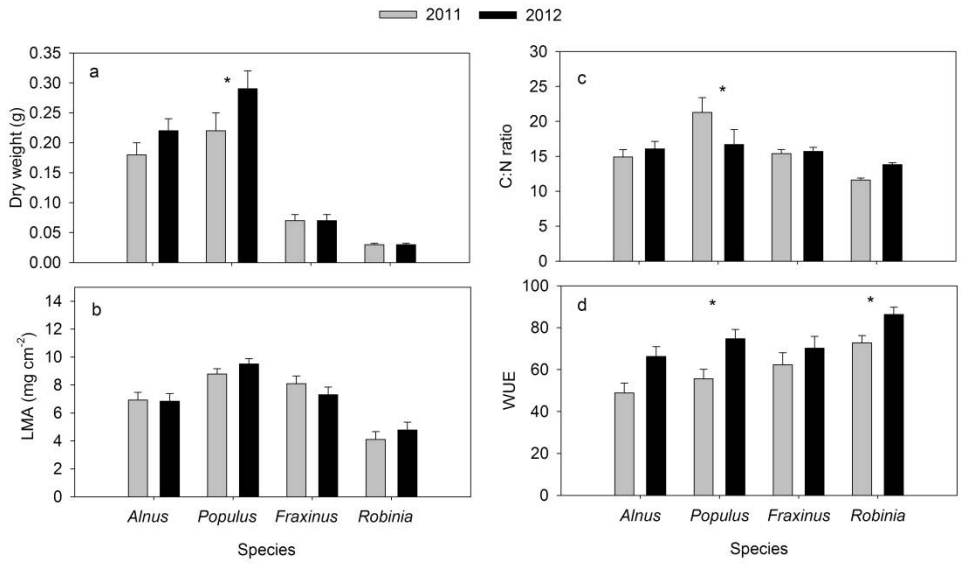

Figure 4.4 For each riparian tree species (a) leaf dry weight (in g), (b) leaf mass area (in mg cm^{-2}), (c) leaf CN ratio, and (d) water use efficiency. Data are means and standard errors for years 2011 (in grey) and 2012 (in black). Asterisks indicate significant differences among zones (ANOVA, $p < 0.05$).

4.3.3. Foliar morphological traits and iWUE

Despite significant differences of foliar morphological traits were found among species, few differences were found between years for each species (Table B.3, Table B.4). All riparian trees had similar leaf water content, but it tended to be lower in the dry year. Nevertheless, fresh and dry leaf weight differed among species and only for *P. nigra* leaves had significantly higher dry weight during the dry year (Fig. 4.4a). Although morphological traits did not differ significantly between years, leaves of *A. glutinosa*, *P. nigra*, and *F. excelsior* tended to have a higher leaf area during the dry year. Nevertheless, *A. glutinosa* and *F. excelsior* had a lower leaf thickness and *P. nigra* and *R. pseudoacacia* had a higher leaf density (Fig. 4.3b). The lowest CN ratios were found in leaves of *R. pseudoacacia* and the highest in *P. nigra*, which had significantly lower CN ratios during the dry year (Fig. 4.3c).

Foliar iWUE differed among species, being the from the less efficient to the latest one: *A. glutinosa*, *P. nigra*, *F. excelsior*, and *R. pseudoacacia*. Despite all isotopic leaf composition indicated higher iWUE for the dry year that for the

wet one, differences were only significant for *P. nigra* and *R. pseudoacacia* (Fig. 4d).

4.3.4. Water use sources

Isotopic signal of ^{18}O and ^{2}H differed ($p < 0.001$) between the three water sources compartments (i.e. shallow soil water, deep soil water, and groundwater), but they did not present differences between seasons within each compartment (i.e. spring and summer). The isotopic signature of our water sources is similar to that reported for Mediterranean areas (for $\partial^{2}H$: soil water = -43 ‰, stream = -46 ‰, and groundwater = -31 ‰ for soil; Evaristo et al., 2015). Similarities between the groundwater signature in our riparian plot ($\partial^{18}O$ = -7.55 ± 0.25‰, $\partial^{2}H$ = -43.41 ± 1.43‰) and the adjacent stream one ($\partial^{18}O$ = -7.45 ± 0.05‰, $\partial^{2}H$ = -42.87 ± 0.03‰), indicated high connectivity between both compartments. However, groundwater signature was different from that in the shallow soil compartment ($\partial^{18}O$ = -5.18 ± 1.05‰, $\partial^{2}H$ = -34.03 ± 3.68‰ for the shallow soil; $\partial^{18}O$ = -5.89 ± 1.06‰, $\partial^{2}H$ = -37.32 ± 4.61‰ for the deep soil), which was similar to precipitation ($\partial^{18}O$ = -4.04 ± 1.62‰, $\partial^{2}H$ = -23.80 ± 10.82‰) and soil lixiviates ($\partial^{18}O$ = -4.39 ± 1.65‰, $\partial^{2}H$ = -23.20 ± 13.38‰), suggesting that soil water may come from precipitation water enriched by evaporation (Oshun et al., 2016; Sargeant and Singer, 2016) or groundwater by capillarity. The mixing model suggested that the four riparian tree species take up water from the three water sources simultaneously (Fig. 4.5, Table B.5). Deep soil water was the main contributor in % to total water transpired. During spring season the phreatophitic species, *A. glutinosa* and *P. nigra*, together with *R. pseudoacacia* at the near-stream zone, took up significantly higher proportion of water from the groundwater table (73 ± 5, 69 ± 6 and 43 ± 13 % of the water uptake per species, respectively). Contrary, the contribution of this compartment during summer was reduced and no significant differences among species were found. *F. excelsior* was mainly depending on deep soil water during spring, and despite increasing dependence of shallow ground water during summer these seasonal differences were not significant. *R. pseudoacacia*'s water uptake behavior was different depending on the riparian zone where it was present. For all riparian zones the contribution of shallow soil water during summer

was significantly reduced from that of spring season. In general, the contribution of groundwater-uptake by *R. pseudoacacia* decreased from the near-stream zone (43 ± 13 %) to the hillslope (19 ± 5%) during spring, but increased from 14 ± 3 % to 35 ± 5% during summer. During summer, the contribution of deep soil water increased for all species, being statistically different between seasons for *A. glutinosa*, *P. nigra* and *R. pseudoacacia* at near-stream zone.

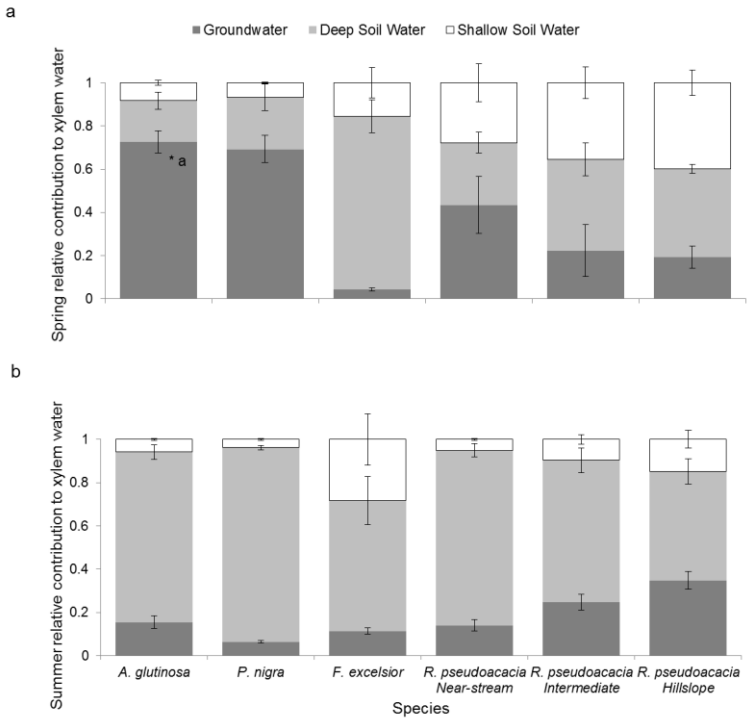

Figure 4.5 Percentage of water obtained from shallow soil water (white), deep soil water (light grey) and groundwater (dark grey) by four riparian tree species (*A. glutinosa*, *P. nigra*, *F. excelsior*, and *R. pseudoacacia*) during (a) spring and (b) summer. Values are mean from SIAR results and error bars are standard errors of the means.

In terms of volume, the lowest quantities of water were extracted from shallow soil water for spring and summer, while major volumes were extracted from groundwater during spring and deep soil water during summer (Table 4.4). *P.*

nigra was the species the highest and *F. excelsior* the lowest volumes of water uptake.

Table 4.4 Volume of water transpired (L d^{-1} $tree^{-1}$) from three water sources (shallow soil water, deep soil water and groundwater). Values are calculated for each riparian tree species during spring and summer season.

	A. glutinosa	*P. nigra*	*F. excelsior*	*R. pseudoacaia*		
				Near-stream	Intermediate	Hillslope
Spring						
Shallow Soil Water	0.36	1.89	0.47	0.81	1.76	2.13
Deep Soil Water	0.82	8.04	2.41	0.85	2.10	2.20
Groundwater	3.13	17.32	0.13	1.27	1.11	1.04
Summer						
Shallow Soil Water	0.41	1.44	0.75	0.20	0.65	1.06
Deep Soil Water	5.54	34.27	1.61	3.19	4.38	3.64
Groundwater	1.08	2.45	0.30	0.56	1.65	2.51

4.4. Discussion

4.4.1. Riparian tree species dependence on water availability

Tree species were distributed differently across the riparian site of *Font del Regàs*. The two phreatophitic species, *A. glutinosa* and *P. nigra*, were mostly found near the stream, likely due their higher water requirements (Singer et al., 2014; McVean 1956) while *F. excelsior* was found at the hillslope zone. The spatial distribution of the invasive N-fixing *R. pseudoacacia* contrasted with that of the three natives ones. *R. pseudoacacia* was distributed all across the riparian plot but higher densities were found at the hillslope edge. This species spatial distribution is supported by our results of water sources. The significant differences among the three water sources identified (i.e. shallow soil water, deep soil water and groundwater) allowed us to estimate water sources that supply trees transpiration in our plot. On annual trends, deep soil water is the main water source used by riparian tree species in *Font del Regàs*, as it has been found in other riparian studies (Bertrand et al., 2014). Nevertheless, species change the main sources between seasons. Both phreatophic species, *A. glutinosa* and *P. nigra*, used water mostly from groundwater during spring while in summer deep soil was the main source for both of them. Some studies already suggested that riparian tree species in *Font del Regàs* might use high

quantities of groundwater to explain stream discharge decreases during the vegetative period (Bernal et al., 2015)and to support tree transpiration rates (Nadal-Sala et al., 2017). Despite *A. glutinosa* has been reported to be able to uptake water directly from the stream (Dawson and Ehleringer, 1991b), under anoxic environments in the roots *A. glutinosa* can present lower growth rates and individuals density (Rodríguez-González et al., 2010). This may explain a more shallow root system that uses higher volumes of soil water than from groundwater during summer. *P. nigra* has been reported to take up water from both soil and groundwater sources in other riparian areas when groundwater table was reachable (Sargeant and Singer, 2016; Singer et al., 2013; Snyder and Williams, 2000). Despite the fact that the main water source for *F. excelsior* was deep soil water, the higher importance of water-uptake from groundwater and shallow soil water during summer and a higher variability among individuals, suggest that *F. excelsior* is sensible to summer drought. In concordance, some authors have reported that root system from *F. excelsior* is located at the first soil layers and that water in vadose zone is its main source (Sánchez-Pérez et al., 2008; Sargeant and Singer, 2016; Singer et al., 2013). Contrary to native species, *R. pseudoacacia* present more equitative dependance on water sources across all riparian zones during summer, even deep soil water was also the main water source during summer. The switched pattern on groundwater uptake is particularily noteworthy: While higher dependence is found in individuals at the near-stream edge during spring, it is higher in individuals at the hillslope edge during summer. This is explained by the capacity of this species to develop a deep root system (> 8m) to reach groundwater (Bunger and Thomson, 1938; Mórics et al,2016) and can explain the capacity to maintain transpiration rates across the riparian plot despite reductions in water availability (Nadal-Sala et al.,2017).

In accordance with our analyses of the trees' water sources, the correlations between leaf litter falls during summer and environmental conditions confirms that phreatophitic species at our riparian plot were more dependent on air temperature and minimum groundwater level - except for *P. nigra* which also induced leaf litter fall at lower soil water contents. For both, *F. excelsior* and *R.*

pseudoacacia, low soil water contents and groundwater levels increased their leaf litter falls, showing these species dependence on water availability. Moreover, minimum groundwater level was also an important factor for *R. pseudoacacia* at the hillslope edge, so this species may be also sensible at this riparian zone.

4.4.2. Riparian tree species responses to changes in water availability

Environmental conditions differed between summer 2011 and 2012. Summer 2012 was drier than 2011 being reflected in the responses on riparian tree species. For instance, leaf litter production of native species during the dry year were reduced in > 20% in terms of biomass (g DW m^{-2}). This reduction was especially high for phreatophitic species (~30%), which are mainly situated at the near-stream edge. However, *R. pseudoacacia* at the near-stream edge increased its leaf production by more than 30% during the dry year, while no differences were detected in the other individuals (differences < 2%). These changes in leaf productivity showed a clear dependence on water availability for native riparian tree species, underlining the low tolerance of *R. pseudoacacia* to low water availability (Vítková et al., 2015) and its shade intolerance behavior (Motta et al., 2009). Thus, the lower leaf litter production of native species situated at the near-stream edge might have allowed the arrival of enough radiation to stimulate leaf production of *R. pseudoacacia* individuals located at this riparian zone. This pattern is not repeated at other riparian zones as *F. excelsior* individuals density is low.

Contrasting with native species strategy of reduction of leaf litter production, the temporal patterns of leaf litter fall suggested that *R. pseudoaciacia* is able to lose higher quantities of leaves when drought stress conditions increase. (Medina-Villar et al., 2015b) already reported peaks of leaf litter fall for *R. pseudoacacia* with respect to native species during summer droughts in central Spain, but lower leaf production for both coexisting species *Fraxinus angustifolia* and *R. pseudoacacia* between 2012 and 2011 (decrease of 33 and 24% respectively). Nevertheless, *F. excelsior* have been also reported to be sensible to

decreases in water availability across biomes (Tsai et al., 2016; Vitasse et al., 2009).

Contrary to our expectations, morphological traits from riparian species did not differ between years except for *P. nigra* which had a significantly higher leaf density and thus also LMA and leaf density in the drier year 2012. This can be attributed to (i) low differences among climatic years or (ii) low adaptation to drought situations for riparian tree species... This results confirms the sensitivity of this species to drought environmental conditions (De La Riva et al., 2016; Lang et al., 2016; Niinemets, 2001; Ogaya and Peñuelas, 2007). Although not significantly different, all native species presented higher leaf area during the dry year 2012. Higher leaf area may respond to the decrease in leaf productivity, and confirm that transpiration of riparian tree species in our study plot were limited by radiation rather than by lower water availability situations (Nadal-Sala et al., 2017). Moreover, most of the studies found in the bibliography about morphological leaf traits changes in riparian species were focused on light limitation and reporting higher leaf area in sun exposed leaves (Legner et al., 2013).

iWUE seemed to respond to species water availability demand, being higher as less dependence on it. Thus, lower iWUE were found for *A. glutinosa* and *P. nigra*, while the highest were found for the invasive *R. pseudoacacia*. Moreover, leaves from *P. nigra* and *R. pseudoacacia* during the dry year were found to have higher iWUE than during the wet one, but no significant differences in wood, probably due to the young age or the higher variability among years than among. The increase in iWUE of *P. nigra* showed its high sensitivity to groundwater decrease and confirms the capacity to acclimate to water limitation to supply evaporative demand shown by some *Populus spp.* (Lang et al., 2016; Scott et al., 2008). Despite we found no significant differences in leaf iWUE for *A. glutinosa* and *F. excelsior*, dry years tended to increase iWUE. *F.excelsior* has been reported to present stronger stomatal control than co-ocurring species when soil water availability is difficult (Lemoine et al., 2001).

Changes on species litter production and litter fall dynamics can alter the composition of the organic matter (i.e. leaves) that reach the forest soil and stream, affecting the functioning of both terrestrial and aquatic ecosystems (Medina-Villar et al., 2015a). For instance, higher leaf N content was found for N-fixing species while lower for *P. nigra*, and thus, an increase in *R. pseudoacacia* leaf litter production may increase leaf N inputs to stream and forest floor. Higher leaf litter falls during summer may have a contrasting effect as both N-fixing species have higher NRE during drought stress fall than during senescent fall. Differences in NRE can be explained as a strategy to keep N for the rest of the phenologic period, while they can fix N atmospheric for the following vegetative period. Similarly, N-fixing species as *R. pseudoacacia* has been already reported to reabsorb higher N than native species (Sürmen et al., 2014) and be more effective during summer drought fall than phenologic fall (González-Muñoz et al., 2011).

4.4.3. *R. pseudoacacia* future perspectives

Species coexisting in the same area usually present a combination of strategies for the resource use to achieve the optimum plant functioning (de la Riva et al., 2017; Peñuelas et al., 2008). In our study plot, the different water availability dependence determine species tree distribution across the riparian area. For instance, *A. glutinosa*, *P. nigra* and riparian mixed forests are found in areas with well developed soils, precipitation rates ~1000 mm year^{-1}, and mean annual temperatures ~13ºC (Aguiar et al., 2013). Yet, *F. excelsior* has been reported to be more sensible to water availability than temperature variations (Tsai et al., 2016; Vitasse et al., 2009; Walentowski et al., 2017), having its niche in areas with precipitation rates of 650-1500 mm year^{-1} (Aguiar et al., 2013). Thus, bibliography suggests these native species are already at their limit environmental conditions in *Font del Regàs* (precitpitation rates 925 ± 151 mm), and *R. pseudoacacia* may be favored. In contrast to native species, *R. pseudoacacia* has been reported to be a highly drought tolerant, by using strategies such as reducing transpiration rates, decrease leaf size, or increase iWUE (González-Muñoz et al., 2015; Mantovani et al., 2014; Vítková et al., 2015).

In *Font del Regàs*, *R. pseudoacacia* presented different mechanisms to avoid drought stress (higher rates of leaf litter fall during summer, production of leaves with slightly lower area or higher WUE than natives ones, and also during the dry year than the wet one) at the same time that took advantage from the decrease in native species leaf productivity. These different mechanisms among co-occurring species highlight *R. pseudoacacia* advantages respect to native species, especially at areas with less groundwater level such as hillslope, and thus in contrast to *F. excelsior*. Concordantly, Nadal-Sala et al. (2017) found a soil water content threshold at which *F. excelsior* drastically reduced its transpiration. Some studies have indicated that although the *R. pseudoacacia* may have marked drought sensitivity, the higher efficiency drought adaptations of native species did not suppose any advantages for them (Werner et al., 2010; Gonzalez-Muñoz et al., 2015). Moreover, *R. pseudoacacia* is often considered an intermediate species during a successional process that may end with the establishment of autochthons species able to tolerate the perturbation. Thus, despite having already been to be naturalized across the globe, a complete invasion is difficult to predict (Vítková et al., 2015; Weber, 2003).

All in all, our study highlights the necessity to compare different physiological parameters to better understand consequences of water availability variability among co-occurring riparian species. In *Font del Regàs*, native riparian tree species seems to be highly water availability dependant and *R. pseudoacacia* seems to better performed in drier conditions. Thus, future drier climate conditions projected in the Mediterranean area (IPCC, 2013) may strengthen the establishment of this species and its substitution of native species.

Aknowledgements

We are thankful to Anna Lupon, Alfons Casalé, Abdellah Bougmar, and Laia Torres for their invaluable assistance in the field. Financial support was provided by the Spanish Government through the projects MONTES-Consolider (CSD2008-00040-MONTES), MEDFORESTREAM (CGL2011-30590), and MEDSOUL (CGL2014-59977-C3-2). Sílvia Poblador was supported by a FPI PhD fellowship from the Spanish Ministry of Economy and Competitiveness (BES-2012-054572). Daniel Nadal-Sala was supported by a FPI PhD fellowship from the Spanish Ministry of Economy and Competitiveness (BES-2012-054572). We also thank site cooperators, including Vichy Catalan and the Catalan Water Agency (ACA) for permission to sample at the *Font del Regàs* catchment. Sílvia Poblador, Daniel Sala-Nadal, Santiago Sabaté, and Francesc Sabater are members of the research group FORESTREAM (AGAUR, Catalonia 2014SGR949).

CHAPTER 5

Soil water content drives spatiotemporal patterns of CO_2 and N_2O emissions from a Mediterranean riparian forest soil

Riparian zones play a fundamental role in regulating the amount of carbon (C) and nitrogen (N) that is exported from catchments. However, C and N removal via soil gaseous pathways can influence local budgets of greenhouse gases (GHG) emissions and contribute to climate change. Over a year, we quantified soil effluxes of carbon dioxide (CO_2) and nitrous oxide (N_2O) from a Mediterranean riparian forest in order to understand the role of these ecosystems on catchment GHG emissions. In addition, we evaluated the main soil microbial processes that produce GHG (mineralization, nitrification, and denitrification) and how changes in soil properties can modify the GHG production over time and space. Mediterranean riparian soils emitted larger amounts of CO_2 (1.2 – 10 g C m^{-2} d^{-1}) than N_2O (0.001 – 0.2 mg N m^{-2} d^{-1}) to the atmosphere attributed to high respiration and low denitrification rates. Both CO_2 and N_2O emissions showed a marked (but antagonistic) spatial gradient as a result of variations in soil water content across the riparian zone. Deep groundwater tables fueled large soil CO_2 effluxes near the hillslope, while N_2O emissions were higher in the wet zones adjacent to the stream channel. However, both CO_2 and N_2O emissions peaked after spring rewetting events, when optimal conditions of soil water content, temperature, and N availability favor microbial respiration, nitrification, and denitrification. Overall, our results highlight the role of water availability on riparian soil biogeochemistry and GHG emissions and suggest that climate change alterations in hydrologic regimes can affect the microbial processes that produce GHG as well as the contribution of these systems to regional and global biogeochemical cycles.

Original Work: Poblador, S., A. Lupon, S. Sabaté and F. Sabater. 2017. Soil water content drives spatiotemporal patterns of CO_2 and N_2O emissions from a Mediterranean riparian forest soil. Biogeosciences 14:4195–4208.

5.1. Introduction

Riparian zones are hotspots of nitrogen (N) transformations across the landscape, providing a natural filter for nitrate (NO_3^-) transported from surrounding lands via runoff and subsurface flow paths (Hill, 1996; Vidon et al., 2010). Although interest in riparian zones has primarily been motivated by the benefits of these ecotones as effective N sinks, enhanced microbial activity in riparian landscapes can play a key role on atmospheric pollution. For instance, riparian zones can account by 70% of global (natural processes and human activities) terrestrial emissions of nitrous oxide (N_2O) to the atmosphere, a powerful greenhouse gas (GHG) with 298 times the global warning potential of carbon dioxide (CO_2) (Audet et al., 2014; Groffman et al., 2000; Hefting et al., 2003). Moreover, riparian soils can significantly contribute to global CO_2 emissions because they can hold high rates of heterotrophic and autotrophic respiration (Chang et al., 2014). Soil respiration is the main natural carbon (C) efflux to the atmosphere, contributing to 20% of the global emission of CO_2 (Kim and Verma, 1990; Raich et al., 2002; Rastogi et al., 2002). Finally, riparian zones can support large methane (CH_4) fluxes that account for the 15 – 40 % of global emissions (Audet et al., 2014; Segers, 1998). However, there are still many uncertainties regarding the magnitude and spatio-temporal variability of soils GHG emissions in riparian zones, reaching contradictory results concerning the potential role of riparian zones as sinks or sources of C and N (Bruland et al., 2006; Groffman et al., 1992; Harms et al., 2009; Walker et al., 2002).

Understanding the processes regulating GHG emissions from riparian soils is essential to quantify the role of riparian zones in the global C and N cycles. Multiple environmental variables, such as soil temperature, soil water content, and both C and N availability have been identified as key factors influencing the rate and variability of soil microbial activities that produce GHG (Chang et al., 2014; Hefting et al., 2003; Mander et al., 2008; McGlynn and Seibert, 2003). Among them, riparian hydrology seems to play a fundamental role on GHG production because it controls the substrate subsides and, most importantly, the redox conditions of riparian soils (Jacinthe et al., 2015; Vidon, 2017b).

Under saturated conditions, anaerobic processes such as methanogenesis (i.e. the transformation of CO_2 to CH_4) and denitrification (i.e. the transformation of NO_3^- to N gas (N_2) or N_2O) are the primary processes involved in the C and N cycles (Clément et al., 2002). Conversely, in dry soils, aerobic transformations involved in the oxidation of the organic matter (i.e. respiration, mineralization, nitrification, methane oxidation) dominate the riparian biogeochemistry (Harms and Grimm, 2008). From such observations, some one would expect that there is a strong correlation between soil wetness and the relative importance of CO_2, N_2O and CH_4 riparian soil emissions to the total GHG fluxes. However, there are still relatively few studies that analyze the direct influence of soil water content on several GHG effluxes simultaneously (but see Harms and Grimm, 2008; Jacinthe et al., 2015), and even less that combine such analyses with other environmental factors and soil processes. Thus, it is still unclear under which circumstances soil water content (rather than temperature or substrate availability) is the primary control factor of the riparian functionality.

Mediterranean systems are a unique natural laboratory to understand the close link between spatio-temporal variations in hydrology and riparian biogeochemistry because they are characterized by a marked spatial gradient of soil water content, that can range from <10% in the hillslope edge to > 80% close to the stream (Chang et al., 2014; Lupon et al., 2016a). Moreover, Mediterranean regions are subjected to seasonal alterations of precipitation and temperature regimes that might affect riparian hydrology as well as microbial activity in the riparian soils (Bernal et al., 2007; Bruland et al., 2006; Harms and Grimm, 2008; Harms et al., 2009). Increments in GHG emissions in riparian zones might occur following storms or flood events because sharp increments in soil water content enhance nitrification, denitrification, respiration, and methanogenesis rates (Casals et al., 2011; Jacinthe et al., 2015; Werner et al., 2014). However, because recent studies have shown that high temperatures and relatively moist soils can sustain large rates of C respiration and N mineralization in summer in the near-stream zone (Chang et al., 2014; Lupon et al., 2016a), the contribution of such microbial pulses to annual CO_2

and N_2O production in Mediterranean riparian soils is still under debate. Moreover, improved understanding of interactions among hydrology, microbial processes, and gas emissions within Mediterranean riparian zones is not only fundamental to understand the temporal pattern of riparian biogeochemistry, buy also necessary to estimate the contribution of these ecosystems to atmospheric GHG budgets at local and global scale.

In this study, soil properties, soil N processes, and CO_2 and N_2O soil emissions were measured over a year across a Mediterranean riparian forest that exhibited a strong gradient in soil water content (Fig. 5.1a). We did not measure CH_4 emissions because previous studies reported extremely low values in dry systems (-0.06 – 0.42 mg C m^{-2} d^{-1}; Batson et al., 2015; Gómez-Gener et al., 2015). Specifically, we aimed (i) to evaluate the spatio-temporal patterns of CO_2 and N_2O emissions in Mediterranean riparian soils, (ii) to analyze under which conditions soil water content rules microbial processes and GHG over other physicochemical variables, and (iii) to provide some reliable estimates of GHG emissions from Mediterranean riparian soils. We hypothesized that the magnitude and the relative contribution of N_2O and CO_2 to total GHG emission strongly depend on soil water content and redox conditions rather than other variables during all year long (see conceptual approach in Fig. 5.1b). In the near-stream zone, we expected that saturated anoxic soils would enhance denitrification but constrain both respiration and nitrification. Thus, we predicted higher N_2O than CO_2 emissions in this zone. In the intermediate zone, we expected that wet (but not saturated) soils would enhance aerobic processes such as respiration, N mineralization or nitrification, and thus, we predicted high CO_2 emissions compared to N_2O. Finally, we expect that dry soils would deplete (or even inhibit) the soil microbial activity near the hillslope edge, and therefore, we predicted low GHG emissions in this zone. Because Mediterranean regions are subjected to strong intra-annual variations in soil water content, we expected that this general behavior would be maximized in summer, when only near-stream soils would keep wet. Conversely, we expected that all microbial processes would be enhanced short-

after rainfall events, and thus, simultaneous pulses of CO_2 and N_2O emissions would occur in spring and fall.

5.2. Materials and methods

5.2.1. Study site

The research was conducted in a riparian forest of *Font del Regàs*, a forested headwater catchment (14.2 km^2, 500 – 1500 m above the sea level (a.s.l.)) located in the Montseny Natural Park, NE Spain (41º50'N, 2º30'E) (Fig. 5.1a). The climate is sub-humid Mediterranean; with mean temperature ranging from 5ºC in February to 25ºC in August. In 2013, annual precipitation (1020 mm) was higher than long-term average (925 ± 151 mm), with most of rain falling in spring (500 mm) (Fig. 5.2a). Total inorganic N deposition oscillates between 15 – 30 kg N ha^{-1} yr^{-1} (period 1983 – 2007; Àvila and Rodà, 2012).

We selected a riparian site (~600 m^2, ~30 m wide) that flanked a 3rd order stream close to the catchment outlet (536 m a.s.l., 5.3 km from headwaters). The riparian site was divided into three zones characterized by different species compositions (Fig. 5.1a). The near-stream zone was located adjacent to the stream (0 – 4 m from the stream edge) and was composed of *Alnus glutinosa* (45% of basal area) and *Populus nigra* (33% of basal area). The intermediate zone (4 – 7 m from the stream edge) was composed by *P. nigra* and *Robinia pseudoacacia* (29% and 71% of basal area respectively). Finally, the hillslope zone (7 – 30 m from the stream edge) bordered upland forests and was composed by *R. pseudoacacia* (93% of basal area) and *Fraxinus excelsior* (7% of basal area). The three riparian zones had sandy-loam soils (bulk density = 0.9 – 1.1 g cm^{-3}), with a 5-cm deep organic layer followed by a 30-cm deep A-horizon. The top soil layer (0 – 10 cm depth) was mainly composed by sands (~90%) and silts (~7%) at the near-stream zone, whereas gravels (~16%) and sands (~80%) were the dominant particle sizes at the intermediate and hillslope zones. During the study period, groundwater level averaged -54 ± 14 cm below the soil surface (b.s.s.) at the near-stream zone, and decreased to -125 ± 4 and -358 ± 26 cm b.s.s. at the intermediate and hillslope zones, respectively (Fig. 5.1a and Fig. 5.2b).

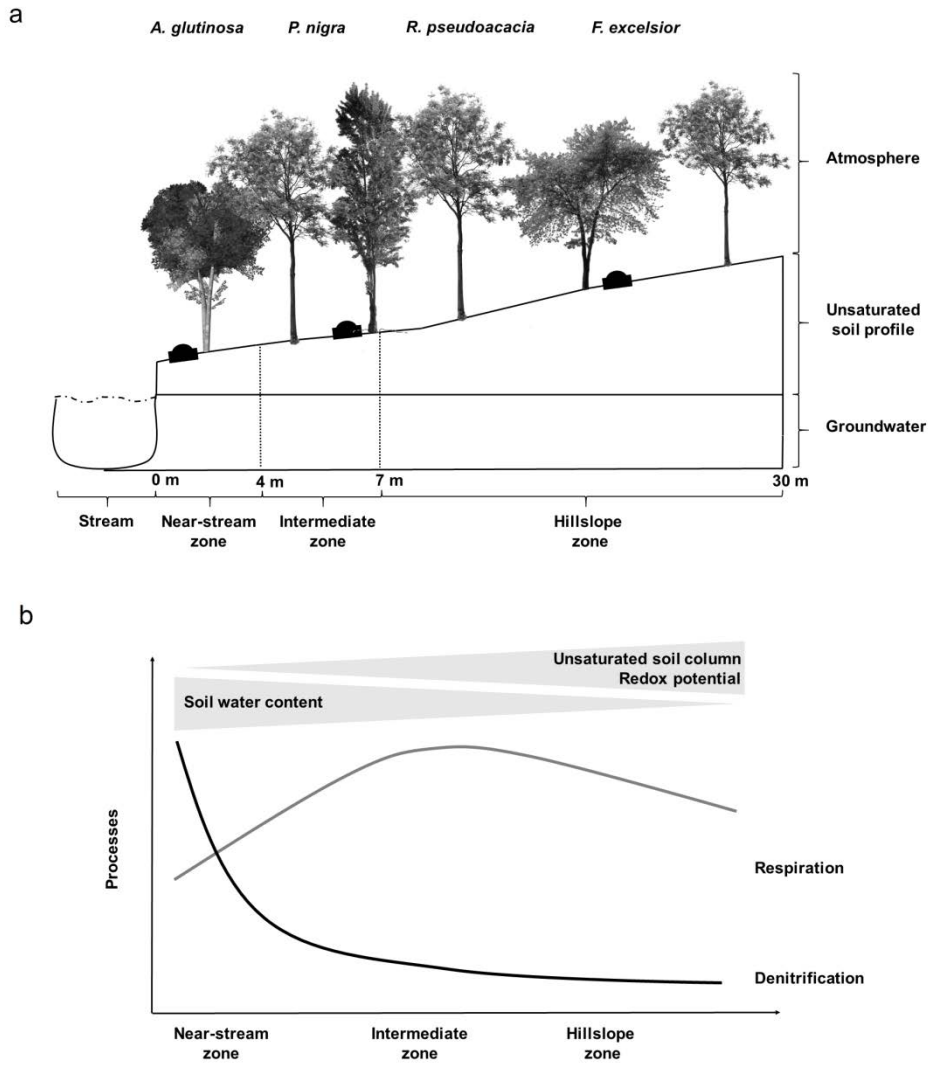

Figure 5.1 (a) Plot layout for the studied Mediterranean riparian forest showing the three riparian zones and the location of the chambers (n=5 for each riparian zone) (b) Conceptual approach of the influence of riparian hydrology on soil microbial processes across a Mediterranean riparian zone. Soil water content decreases from the near-stream to the hillslope zones due to changes in groundwater table, increasing unsaturated soil column and oxic conditions. Anaerobic processes (denitrification) occur under anoxic conditions while aerobic processes (respiration) are optimized under a moderate range of soil water content.

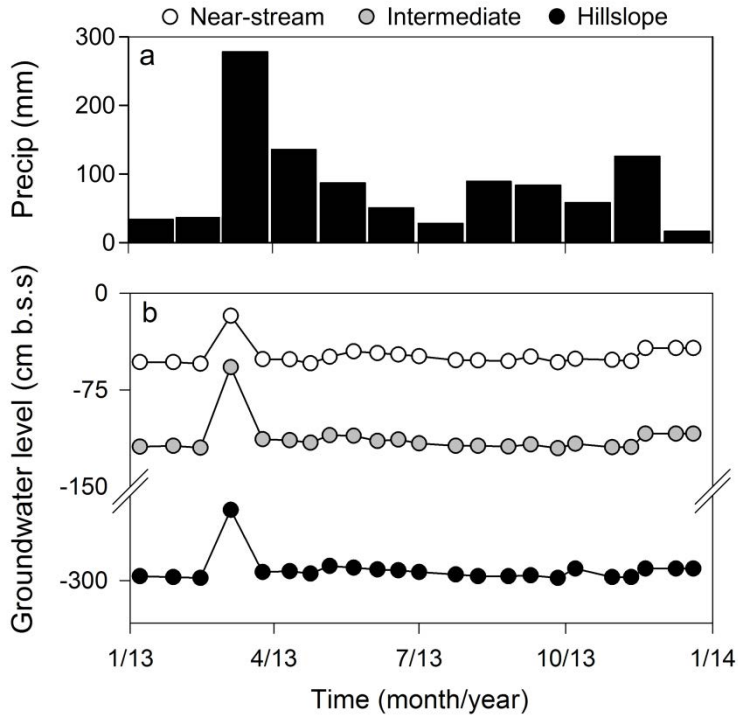

Figure 5.2 Temporal pattern of (a) mean monthly precipitation and (b) biweekly groundwater level at the studied riparian site during the year 2013. Circles are mean values of groundwater level at the near-stream (white), intermediate (grey), and hillslope (black) zones. Precipitation data was obtained from a meteorological station located at ca. 300 m from the studied riparian site. At each riparian zone, groundwater level was measured in 3 PVC piezometers (32-mm diameter, 1–3 m long) with a water level sensor (Eijkelkamp 11.03.30).

5.2.2. Field sampling

We delimited five plots (1 x 1 m) within each riparian zone (near-stream, intermediate and hillslope) (Fig. 5.1a). During the year 2013, soil physicochemical properties, soil N processes, and gas emissions were measured in each plot every 2 – 3 months in order to cover a wide range of soil water content and temperature conditions. On each sampling month, one soil sample (0 – 10 cm depth, including O- and A- horizons) was collected randomly from each plot to analyze soil physicochemical properties. Soil samples were taken with a 5-cm diameter core sampler and placed gently into plastic bags after carefully removing the litter layer. Close to each soil sample, we performed *in situ* soil incubations to measure soil net N mineralization and

net nitrification rates (Eno, 1960a). For this purpose, a second soil core (0 – 10 cm depth) was taken, placed in a polyethylene bag, and buried at the same depth. Soil incubations were buried 4 days and then removed from the soil.

Gas emissions and denitrification rates were measured simultaneously and during four consecutive days (i.e. during the entire soil incubation period) in order to facilitate the direct comparison between microbial rates and gas fluxes. Soil CO_2 effluxes were measured with a SRC-1 soil chamber attached to an EGM-4 portable infrared gas analyzer (IRGA) (PP Systems, Amesbury, MA). The EGM-4 has a measurement range of 0 – 2000 ppm (μmol mol^{-1}), with an accuracy of 1% and a linearity of 1% throughout the range. Every field day, CO_2 measurements started at 12 p.m. and were conducted consecutively at the 15 plots starting for the near stream zone. At each plot, the SCR-1 soil chamber was placed over the top soil for a 120 s incubation. Before each measurement, we carefully removed the litter layer to ensure no leaks. Furthermore, we aerated the SCR-1 between samples to ensure the accuracy of the instrument as well as to avoid contamination between samples. For each plot, CO_2 emissions rates were calculated from the best fit linear regression of the CO_2 accumulated in the head-space with incubation time (Fig. C.1). CO_2 fluxes on an areal basis (F_{CO2}, in μmol m^{-2} h^{-1}) were calculated following Healy et al. (1996):

$$F_g = \frac{dg}{dt} \times \frac{V P_0}{S R T_0} \qquad \text{(Eq.5.1)}$$

where dg/dt is the rate of change in gas concentration (in μmol mol^{-1} h^{-1}) in the chamber, V is chamber volume (in m^3), P_0 is initial pressure (in Pa), S is the soil surface area (in m^2), R is the gas constant (8.314 Pa m^3 K^{-1} mol^{-1}), and T_0 is the initial chamber temperature (in °K). For budgeting, moles of CO_2 and N_2O were converted to grams of C and N, respectively.

In situ denitrification rates and N_2O emissions were measured using closed cylinder (0.37 L) and open cylinder (0.314 m^2) chambers, respectively. For denitrification analyses, an intact soil core (0 – 10 cm depth) was introduced in the chamber, closed with a rubber serum stopper, amended with acetone-free acetylene to inhibit the transformation of N_2O to N_2 (10% v/v atmosphere), and

placed at the same depth. For N_2O analysis, chambers were placed directly on the soil and no special treatment was carried out. Gas samples for both denitrification and N_2O chambers were taken at the same time (0h, 1h, 2h, and 4h of incubation) with a 20-mL syringe and stored in evacuated tubes. All soil and gas samples were kept at < 4ºC until laboratory analysis (< 24 h after collection).

Soil physical properties were measured within each plot simultaneously to gas emissions. Volumetric soil water content (%) (5 replicates per plot) and soil temperature (ºC) (1 replicate per plot) were measured at 10-cm depth by using a time-domain reflectometer sensor (HH2 Delta-T Devices Moisture Meter) and a temperature sensor (CRISON 25), respectively. Soil pH and reduction potential (Eh, mV) (1 replicate per plot) were measured at 0 – 10 cm depth by water extraction (1:2.5 v/v) using a Thermo-Scientific ORION sensor (STAR 9107BNMD). Although Eh measures performed by water extraction may not be as accurate as other field techniques, these values have been previously used as a good proxy of the soil redox potential (Yu and Rinklebe, 2013).

5.2.3. Laboratory analyses

Pre-incubation soil samples were oven dried at 60ºC, sieved, and the fraction < 2 mm was used for measuring soil chemical properties. The relative soil organic matter content (%) was measured by loss on ignition (450ºC, 4 h). Total soil C and N contents were determined on a gas chromatograph coupled to a TCD detector after combustion at 1000ºC at the Scientific Technical Service of the University of Barcelona.

To estimate microbial N processes, we extracted 5 g of pre- and post-incubation field-moist soil samples with 50 ml of 2 M KCl (1g : 10ml, ww : v; 1 h shacking at 110 r.p.m. and 20ºC). The supernatant was filtered (Whatman GF/F 0.7 μm pore diameter) and analyzed for ammonium (NH_4^+) and nitrate (NO_3^-). NH_4^+ was analyzed by the salicilate-nitropruside method (Baethgen and Alley, 1989) using a spectrophotometer (PharmaSpec UV-1700, SHIMADZU). NO_3^- was analyzed by the cadmium reduction method (Keeney and Nelson, 1982) using a Technicon Autoanalyzer (Technicon, 1987). For each pair of

samples, net N mineralization and net nitrification were calculated as the differences between pre- and post-incubations values of inorganic N (NH_4^+ and NO_3^-) and NO_3^-, respectively (Eno, 1960a). Pre-incubation NH_4^+ and NO_3^- concentrations were further used to calculate the availability of dissolved inorganic nitrogen in riparian soils.

To estimate denitrification and natural N_2O emissions, we analyzed the N_2O of all gas samples using a gas chromatograph (Agilent Technologies, 7820A GC System) that was calibrated using certified standards (4.66 ppm N_2O; , AirLiquide). Both denitrification and N_2O emissions rates were calculated similarly to CO_2 fluxes (Fig. S1). In addition, we measured the denitrification enzyme activity (DEA) for 3 soil cores of each riparian zone to determine the factors limiting denitrification. For each soil core, four sub-samples (20 g of fresh soil) were placed into 125-ml glass jars containing different treatments. The first jar (DEA_{MQ}) contained Milli-Q water (20 ml) to test anaerobiosis limitation. The second jar (DEA_C) was amended with glucose solution (4 g glucose kg $soil^{-1}$) to test C limitation. The third jar (DEA_{NO3}) was amended with nitrate solution (72.22mg KNO_3 kg $soil^{-1}$) to test N limitation. Finally, the fourth jar (DEA_{C+NO3}) was amended with both nitrate and glucose solutions (4 g glucose kg $soil^{-1}$ and 72.22mg KNO_3 kg $soil^{-1}$) to test simultaneously C and N limitation. All jars were capped with rubber serum stoppers, made anaerobic by flushing N_2, and amended with acetone-free acetylene (10% v/v) (Smith and Tiedje, 1979). Gas samples were collected after 4 h and 8 h of incubation and analyzed following the same procedure of field DNT samples. DEA rates were calculated similarly to denitrification rates.

5.2.4. Statistical analysis

Statistical analyses were carried out using the package *lmer* and *pls* of R 2.15.1 statistical software (R Core Team, 2012). We performed linear mixed-model analysis of variance (ANOVA) to test differences in soil properties, microbial N processes, and gas emissions across riparian zones and seasons. We used riparian zone and season as fixed effects, and plot (nested within riparian zones) as a random effect. When multiple samples were taken within a plot (soil physical properties, denitrification, and gas emissions), the ANOVA was

performed on plot means, with n = 75 (5 plots x 3 zones x 5 dates). For each model, post-hoc Tukey contrasts were used to test which zones or seasons differed from each other. In all cases, residuals were tested for normality using a Shapiro-Wilk test, and homogeneity of variance was examined visually by plotting the predicted and residual values. In those cases that the normality assumption was unmet, data was log transformed. In all analyses, differences were considered significant when $p < 0.05$.

We used partial least squares regression (PLS) to explore how soil properties, C and N availability, groundwater level, and soil N processes predict variation in CO_2 and N_2O emissions. PLS identifies the relationship between independent (X) and dependent (Y) data matrices through a linear, multivariate model; and produces latent variables (PLS components) representing the combination of X variables that best describe the distribution of observations in 'Y space' (Eriksson et al., 2006). We determined the goodness of fit (R^2Y) and the predictive ability (Q^2Y) of the model by comparing modeled and actual Y observations through a cross-validation process. Each model was refined by iteratively removing variables that had non-significant coefficients in order to minimize the model overfitting (i.e. low Q^2Y values) as well as the multicollinearity of the explanatory variables (i.e. variance inflation factor (VIF) < 5). Furthermore, we identified the importance of each X variable by using variable importance on the projection (VIP) scores, calculated as the sum of square of the PLS weights across all components. VIP values > 1 indicate variables that are most important to the overall model (Eriksson et al., 2006). In all PLS models, data was ranked and centered prior analysis.

5.3. Results

5.3.1. Spatial pattern of soil properties, microbial rates, and gas emissions

During the study period, all riparian zones had similar mean soil temperature (11 – 12ºC), pH (6 – 7) and redox potential (170 – 185 mV) (Table 5.1). However, soil water content exhibited strong differences across riparian zones (Table 5.2), with the near-stream zone holding wetter soils than the intermediate and the hillslope zones (Table 5.1). There were significant differences in most of soil

chemical properties (Table 5.1, Table 5.2). Both organic matter and soil C and N content were 2-fold lower in the near-stream zone than in the intermediate and hillslope zones, though all zones exhibited similar C:N ratios (CN = 14). Moreover, inorganic N concentrations (NH_4^+ and NO_3^-) were from 2- to 5-fold lower for the near-stream zone than for the other two zones.

Table 5.1 Mean annual values (± standard deviation) of soil water content (volumetric), soil temperature, soil pH, soil redox capacity (Eh), soil organic matter, soil molar C:N ratio, soil carbon (C) and nitrogen (N) content, and soil ammonium (NH_4^+) and nitrate (NO_3^-) concentrations for the three riparian zones. For each variable, different letters indicate statistical significant differences between riparian zones (*post-hoc* Tukey HSD test, $p < 0.05$).

	Near-stream	Intermediate	Hillslope
Soil water content (%)	29.58 ± 7.55 ^{A}	19.36 ± 6.00 ^{B}	19.81 ± 6.24 ^{B}
Temperature (ºC)	11.37 ± 5.39 ^{A}	11.82 ± 5.90 ^{A}	12.01 ± 6.34 ^{A}
Eh	170 ± 111 ^{A}	184 ± 103 ^{B}	184 ± 95 ^{C}
pH	6.66 ± 0.42 ^{A}	6.31 ± 0.50 ^{A}	6.68 ± 0.53 ^{A}
Organic matter (%)	4.41 ± 0.71 ^{A}	7.98 ± 2.88 ^{B}	9.53 ± 1.99 ^{C}
C:N ratio	14.25 ± 3.64 ^{A}	14.09 ± 1.78 ^{A}	13.63 ± 1.18 ^{A}
C (mg kg^{-1})	2004 ± 1038 ^{A}	4007 ± 1785 ^{B}	4923 ± 1428 ^{B}
N (mg kg^{-1})	160 ± 44 ^{A}	330 ± 135 ^{B}	418 ± 107 ^{C}
NH_4^+ (mg N kg^{-1})	1.88 ± 1.21 ^{A}	5.58 ± 3.48 ^{B}	3.90 ± 2.07 ^{B}
NO_3^- (mg N kg^{-1})	0.75 ± 0.58 ^{A}	4.66 ± 4.25 ^{B}	5.30 ± 4.20 ^{B}

On annual basis, net N mineralization averaged 0.14 ± 0.40, 0.39 ± 1.23, and 0.22 ± 1.03 mg N kg^{-1} d^{-1} at the near-stream, intermediate, and hillslope zones, respectively. Mean annual net nitrification rates were close to net N mineralization, averaging 0.17 ± 0.38, 0.25 ± 0.69, and 0.28 ± 0.73 mg N kg^{-1} d^{-1} at the near-stream, intermediate, and hillslope zones, respectively. There were no significant differences in mean annual net N mineralization and net nitrification rates among riparian zones (in both cases: mixed-model ANOVA test, $F > F_{0.05}$, $p > 0.05$). Mean annual denitrification was higher at the near-stream zone (2.69 ± 5.30 mg N kg^{-1} d^{-1}) than at the intermediate (0.72 ± 1.85 mg N kg^{-1} d^{-1}) and hillslope (0.76 ± 1.59 mg N kg^{-1} d^{-1}) zones (mixed-model ANOVA test, $F = 4.33$, $p = 0.038$). However, potential denitrification rates were lower in the near-stream zone (0.3 – 0.6 mg N kg^{-1} d^{-1}) compared to

intermediate (1.0 – 2.4 mg N kg^{-1} d^{-1}) and hillslope (1.3 – 3.8 mg N kg^{-1} d^{-1}) zones (Table 5.3).

Table 5.2 Results from the mixed-model analysis of variance (ANOVA) showing the effects of riparian zones and seasons on soil water content, soil temperature, soil pH, soil redox capacity (Eh), soil organic matter, soil molar C:N ratio, soil carbon (C) and nitrogen (N) content, and soil ammonium (NH_4^+) and nitrate (NO_3^-) concentrations. Plot was treated as a random effect in the model whereas riparian zones, seasons and their interactions were considered fixed effects. Values are *F*-values and the p-values are shown in brackets. P-values < 0.05 are shown in bold.

	Riparian Zone	Seasons	Zone × Seasons
Soil water content	**18.6 [< 0.001]**	**100 [< 0.001]**	**13.6 [< 0.001]**
Temperature	0.33 [0.721]	**2117 [< 0.001]**	0.42 [0.906]
pH	1.97 [0.182]	2.43 [0.060]	2.73 [0.052]
Eh	1.34 [0.247]	3.53 [0.062]	1.88 [0.084]
Organic matter	**27.8 [< 0.001]**	2.77 [0.053]	1.62 [0.144]
C:N ratio	0.99 [0.400]	**10.9 [< 0.001]**	1.72 [1.118]
C	**27.1 [< 0.001]**	1.86 [0.132]	0.77 [0.630]
N	**39.7 [< 0.001]**	1.22 [0.311]	0.63 [0.746]
NH_4^+	**12.4 [0.001]**	2.71 [0.051]	1.52 [0.176]
NO_3^-	**22.4 [< 0.001]**	**5.63 [< 0.001]**	**4.09 [< 0.001]**

Zone = near-stream, intermediate, hillslope.
Season = February, April, June, August and November.

Table 5.3 Mean values (± standard deviation) of potential denitrification rates (in mg N kg^{-1} d^{-1}) after anoxia (DEA_{MQ}), carbon addition (DEA_C), nitrogen addition (DEA_{NO3}) and carbon and nitrogen addition (DEA_{C+NO3}) treatments for the three riparian zones during the study period. For each zone, different letters indicate statistical significant differences between treatments (*post-hoc* Tukey HSD test, n = 15, p < 0.01).

Potential Denitrification Rates (mg N kg^{-1} d^{-1})				
	DEA_{MQ}	**DEA_C**	**DEA_{NO3}**	**DEA_{C+NO3}**
Near-stream	0.31 ± 0.41^{A}	0.26 ± 0.27^{A}	0.42 ± 0.42^{A}	0.63 ± 0.85^{A}
Intermediate	1.01 ± 1.12^{A}	1.88 ± 1.59^{A}	2.28 ± 3.57^{A}	2.40 ± 2.45^{A}
Hillslope	1.34 ± 1.33^{A}	2.35 ± 1.97^{AB}	1.73 ± 1.43^{AB}	3.82 ± 2.78^{B}

Natural CO_2 and N_2O emissions differed among riparian zones, yet they showed opposite spatial patterns. Near-stream zone exhibited lower CO_2 emissions (318 ± 195 mg C m^{-2} h^{-1}) compared to the intermediate (472 ± 298 mg C m^{-2} h^{-1}) and hillslope (458 ± 308 mg C m^{-2} h^{-1}) zones (mixed-model ANOVA test, F = 7.08, p = 0.009). Conversely, near-stream zone showed higher N_2O emissions (0.035 ± 0.022 mg N m^{-2} h^{-1}) than the other two zones (intermediate = 0.032 ± 0.025 mg N m^{-2} h^{-1}; hillslope = 0.022 ± 0.012 mg N m^{-2} h^{-1}) (mixed-model ANOVA test, F = 7.31, p = 0.008).

5.3.2. Temporal pattern of soil properties, microbial rates, and gas emissions

During the study period, there was a marked seasonality in most of soil physical properties, except for pH and Eh, which did not show any temporal pattern (Table 5.2). Soil water content exhibited a marked seasonality, though it differed among riparian zones (Table 5.2, "zone x season"). In the intermediate and hillslope zones, soil water content was maxima in November and minima in August, while the near-stream soils were wetter during both spring (April-June) and autumn (November) (Fig. 5.3a). Conversely, soil temperature showed similar seasonality but opposite values in all riparian zones (Table 5.2), with a maxima in summer (August) and minima in winter (February) (Fig. 5.3b). Soil chemical properties (soil organic matter and both soil C and N content) did not show any seasonal trend, but all riparian zones exhibited lower C:N ratios in February compared to the other seasons (Fig. 5.3c). There was no seasonality in soil NH_4^+ concentrations at any riparian zone (Table 5.2). However, soil NO_3^- concentrations showed a marked temporal pattern, yet it differed among riparian zones (Table 5.2, "zone x season"). The highest soil NO_3^- concentrations occurred in February at both the near-stream and hillslope zones, but in June-August at the intermediate zone (Fig. 5.3d).

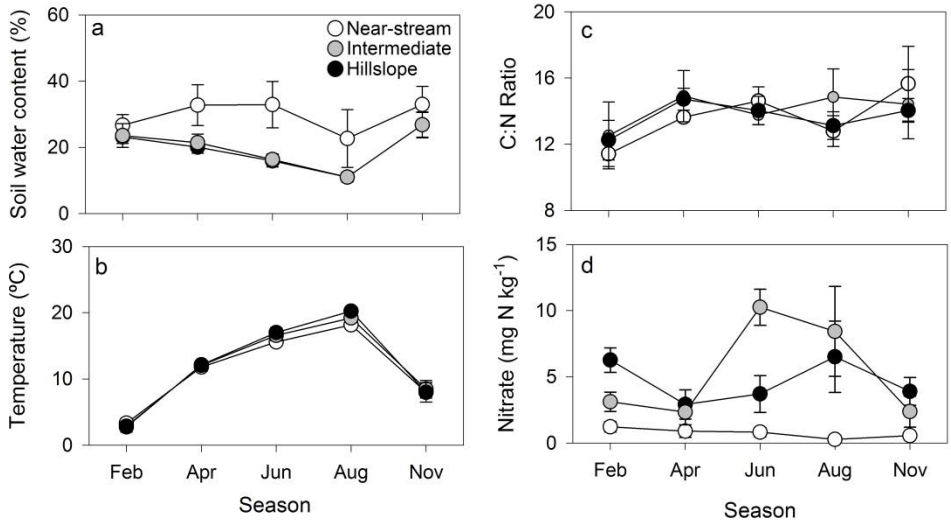

Figure 5.3 Temporal pattern of (a) soil water content, (b) soil temperature, (c) soil C:N molar ratio, and (d) soil nitrate concentration at 10-cm depth. Data is shown for the near-stream (white), intermediate (grey), and hillslope (black) zones during the study period. Circles are mean values and error bars are standard deviations.

Soil N processes showed similar seasonal patterns in all riparian zones (in all cases: $F_{date} < F_{0.05}$, $F_{interaction} > F_{0.05}$). Both net N mineralization and net nitrification rates were higher in April than February, June, and November (Fig. 5.4a and 5.4b), while denitrification rates were higher in April and June compared to the rest of the year (Fig. 5.4c). In April, both net N mineralization and net nitrification rates differed across riparian zone, with higher rates in the intermediate zone than in the near-stream one. Net N mineralization rates also differed in August, when the intermediate zone exhibited 2-fold higher rates than the other two zones. Finally, denitrification was higher at the near-stream than at the other two zones in both June and August.

Natural gas emissions showed a clear seasonal pattern (in both cases: mixed-model ANOVA test, $F_{date} < F_{0.05}$, $p < 0.001$), yet it differed between CO_2 and N_2O emissions. In all zones, CO_2 emissions were maxima in June and minima in February (Fig. 5.5a), while highest N_2O emission rates occurred in April and lowest in both February and August (Fig. 5.5b). In spring (April and June), CO_2 emissions were higher at the intermediate and hillslope zones compared to the

near-stream one (Fig. 5.5a). Moreover, the near-stream zone showed higher N_2O emissions than the hillslope zone in February, April, and June (Fig. 5.5b).

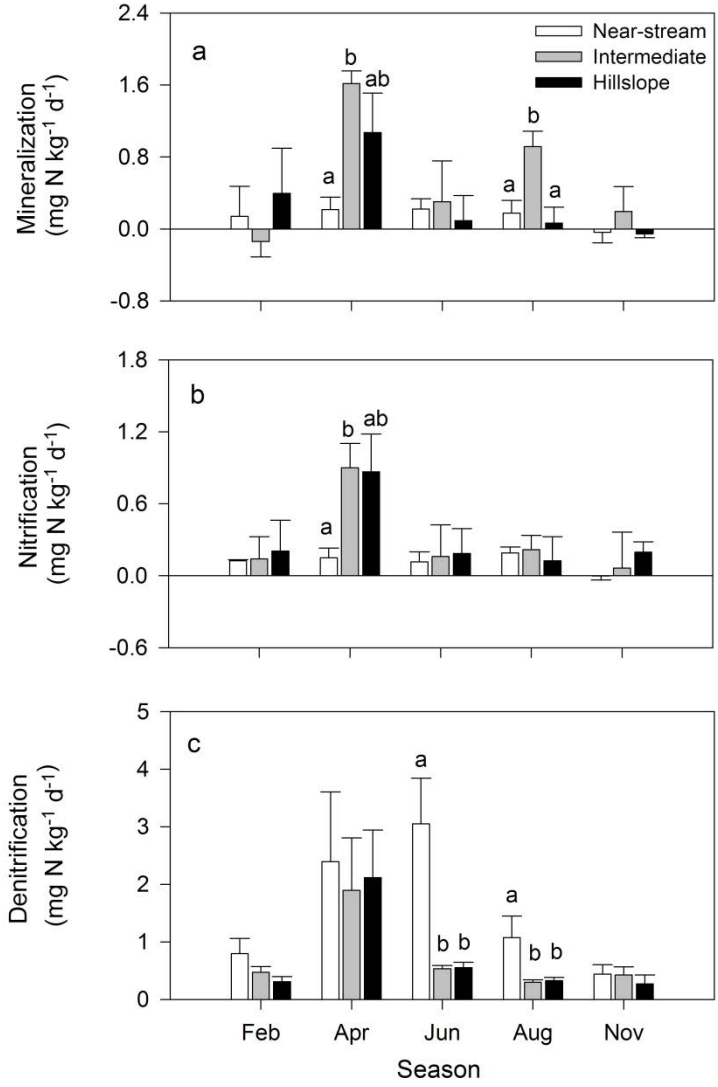

Figure 5.4 Temporal pattern of (a) soil net N mineralization, (b) net nitrification and (c) denitrification rates at the near-stream (white), intermediate (grey), and hillslope (black) zones during the study period. Bars are mean values for each section and error bars are standard errors. For each season, different letters indicate significant differences among sections (mixed-model ANOVA, $p < 0.05$).

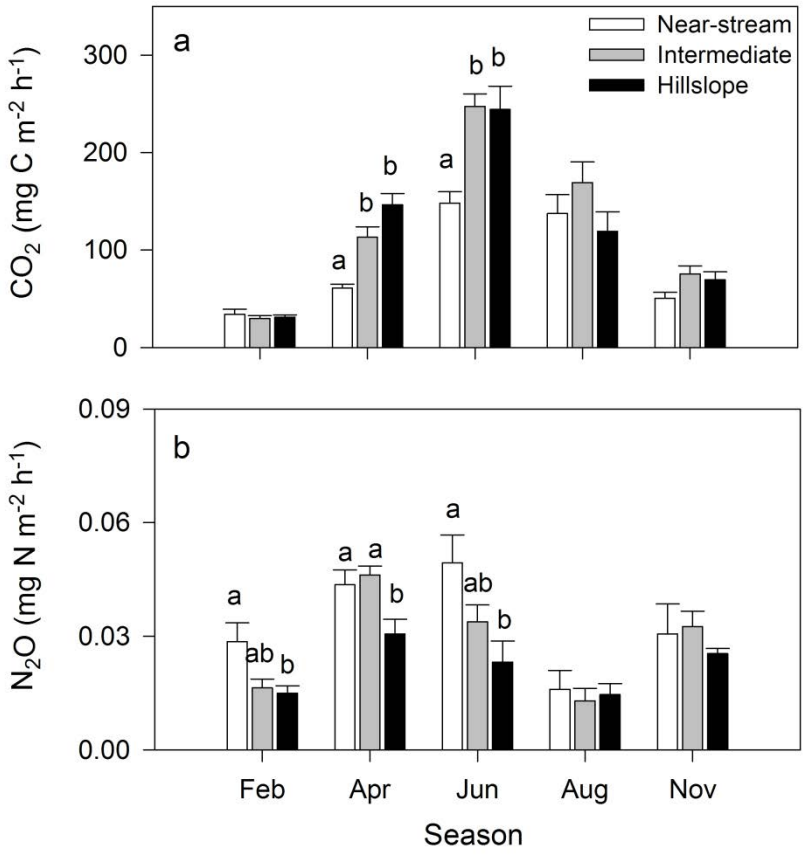

Figure 5.5 Temporal pattern of soil (a) CO_2 and (b) N_2O emissions at the near-stream (white), intermediate (grey), and hillslope (black) zones during the study period. Bars are mean values for each section and error bars are standard errors. For each season, different letters indicate significant differences among sections (mixed-model ANOVA, $p < 0.05$).

5.3.3. Relationship between soil properties, microbial processes, and gas emissions

PLS models extracted two components that explained the 71% and the 40% of the variance in CO_2 and N_2O emissions, respectively (Table 5.4). The model predictability was high for CO_2 ($Q^2Y = 0.66$), but weak for N_2O ($Q^2Y = 0.34$). Moreover, PLS models identified few variables as key predictors of GHG emissions (VIF < 2, VIP > 0.8), yet these variables differed between CO_2 and N_2O emissions (Table 4). Soil temperature (PLS coefficient [coef] = +0.60), and soil water content (coef = -0.24) explained most of the variation in CO_2

emissions (Table 5.4, Fig. C.2a). Conversely, variations in N_2O emissions were primarily related to changes in denitrification rates (coef = +0.45), soil water content (coef = +0.21) and, to less extent, groundwater level (coef = -0.16) (Table 5.4, Fig. C.2b).

Table 5.4 Summary of the partial least squares (PLS) models produced for CO_2 and N_2O emissions at the riparian site (n = 75). Values are the coefficients from PLS models which describe the relationship (direction and relative strength) between explanatory variables and gas emissions. The variance inflation factor (VIF) of each explanatory variable, indicative of collinearity, are shown in brackets. Bold values indicate the most influencing variables (variable importance in the projection (VIP) >1.0).

	X-variable	Acronym	CO_2	N_2O
Soil Properties	Soil water content (%)	SWC	**-0.235 [1.72]**	**0.205 [1.32]**
	Groundwater level (cm b.s.s.)	GWL	**---**	-0.157 [1.24]
	Temperature (C)	Tsoil	**0.599 [1.45]**	**---**
	pH	pH	---	---
	Redox potential (mV)	Eh	**---**	**---**
	Bulk density (g cm^{-1})	BD	---	**---**
	Coarse texture (%)	% Sand	---	**---**
	Organic matter (%)	SOM	---	---
	Total Carbon	C	---	---
	Total Nitrogen	N	---	---
	Molar C:N ratio	C:N ratio	---	---
	Ammonium	NH_4^+	0.167 [1.61]	---
	Nitrate	NO_3^-	0.066 [1.80]	-0.060 [1.47]
Soil N processes	Net N Mineralization	NNM	---	---
	Net Nitrification	NN	---	---
	Denitrification	DNT	---	**0.449 [1.09]**
R^2Y			**0.71**	**0.40**
Q^2Y			**0.66**	**0.34**

Acronym is used in Figure C.2 for PLS loading plots.

5.4. Discussion

This study emphasized the role of soil water content as a main driver of riparian biogeochemistry and GHG emissions. By analyzing soil microbial processes and GHG emissions over a year in a Mediterranean riparian forest, we clearly demonstrate that soil water content has a major role in driving soil microbial processes, the spatio-temporal patters of CO_2 and N_2O emissions and the overall role of Mediterranean riparian soils in the global C and N cycles.

5.4.1. Microbial processes regulating GHG emissions

Mean daily emissions of CO_2 found in the present study (1.2 – 10 g C m^{-2} d^{-1}) were generally high, especially during spring and summer months. These soil CO_2 emissions were higher than those reported for temperate riparian regions (0.2 – 4.8 g C m^{-2} d^{-1}(Batson et al., 2015; Bond-Lamberty and Thomson, 2010; Mander et al., 2008), although similar values have been reported in some dry forested wetlands of Europe and North America (Harms and Grimm, 2008; Oertel et al., 2016). These substantially high CO_2 emissions observed in *Font del Regàs* may be attributed to high microbial respiration rates associated with relatively moist and organic matter enriched soils (Mitsch and Gosselink, 2007; Pacific et al., 2008; Stern, 2006). In agreement, previous studies have reported that microbial heterotrophic respiration can be an important contributor (> 60%) to CO_2 soil effluxes in water-limited riparian zones (Harms and Grimm, 2012; McLain and Martens, 2006). However, the absence of a relationship between soil N processes and CO_2 emissions suggests that soil C and N cycles are decoupled in Mediterranean riparian forests, and thus, soil N mineralization may be not a good descriptor of bulk organic matter mineralization. Moreover, plant roots respiration and methane oxidation can increase the CO_2 emissions in riparian soils with deep groundwater tables such as in *Font del Regàs* (Chang et al., 2014).

Conversely, N_2O emissions of our riparian site (0.001 – 0.2 mg N m^{-2} d^{-1}) were relatively low during the whole year. Similar N_2O emissions were reported in other water-limited riparian forests that are rarely flooded (-0.9 – 0.39 mg m^{-2} d^{-1}; Bernal et al., 2003; Harms and Grimm, 2012; Vidon et al., 2016), yet these

values were, on average, much lower than those found in temperate riparian regions (0 – 54 mg N m^{-2} d^{-1}; Burgin and Groffman, 2012; Hefting et al., 2003; Mander et al., 2008). In *Font del Regàs*, most N_2O was produced by denitrification, as we found an intimate link between this microbial process and N_2O emissions. Additionally, other processes such as nitrification or nitrate ammonification can contribute to N_2O emissions (Baggs, 2008; Hefting et al., 2003). However, it seems unlikely that nitrification could account for the observed N_2O emissions because no relationship was found between net nitrification rates and N_2O emissions. Likewise relatively oxic conditions (Eh > 100) and low C:N ratios (C:N < 20) in Font del Regàs suggest low nitrate ammonification in riparian soils (Schmidt et al., 2011). Currently, the influence of soil denitrification on N_2O emissions in riparian zones is still under debate (Giles et al., 2012). Nonetheless, our results suggest that performing simultaneous measurements of different soil N can contribute to disentangling the mechanisms underlying net N_2O emissions in riparian areas.

5.4.2. Effects of soil water content on soil CO_2 effluxes

As expected, we found higher soil CO_2 effluxes at the intermediate and hillslope zones than at the near-stream zone. This spatial pattern was negative and strongly related to soil water content (Table 4), suggesting that, as soils become less moist and more aerated, oxidizing aerobic respiration increases, ultimately stimulating CO_2 production in the top soil layer (Muller et al., 2015). In agreement, other aerobic processes, such as N mineralization were also higher in the intermediate and hillslope zones. Moreover, deep groundwater tables in the hillslope zone can increase the volume of aerated soil, which can increase the area-specific soil CO_2 emissions near the hillslope edge (Chang et al., 2014). Increasing CO_2 emissions from wet to dry zones has been reported in other wetlands and riparian forests (Batson et al., 2015; Morse et al., 2012; Welti et al., 2012), pinpointing a close linkage between riparian hydrology and spatial variations in microbial respiration rates..

Nonetheless, the intra-annual variations of soil CO_2 emissions were strongly dependent on soil temperature (Table 4). Probably, cold temperatures (< 4ºC) limited soil respiration during winter, while warmer conditions (> 15ºC)

stimulated this process in June and August (Emmett et al., 2004; Suseela et al., 2012; Teiter and Mander, 2005). However, lower CO_2 emissions than expected for temperature dynamics were reported in summer at the intermediate and hillslope zones, likely because extreme soil dryness (soil water content < 20%) limited respiration rates during such period (Chang et al., 2014; Goulden et al., 2004; Wickland et al., 2010). Although the mechanisms by which soil dryness may affect microbial C demand are still poorly understood, suppressed microbial respiration in summer can be attributed to a disconnection between microbes and resources (Belnap et al., 2005; Davidson et al., 2006), decreases in photosynthetic and exo-enzimatic activities (Stark and Firestone, 1995; Williams et al., 2000), or a relocation of the invested energy on growth (Allison et al., 2010). Altogether, these results suggest that soil water content may be as important as soil temperature to understand soil CO_2 effluxes, and therefore, future warmer conditions may not fuel higher CO_2 emissions, at least in those regions experiencing severe water limitation.

5.4.3. Effects of soil water content on soil N_2O effluxes

As occurred for CO_2 emissions, N_2O fluxes showed a clear spatial pattern associated with changes in soil water content across the riparian zone. In the near-stream zone, relatively wet conditions (SWC = 30 – 40%) likely promoted denitrification rates, while dry soils (SWC = 10 – 25%) could limit both nitrification and denitrification in the intermediate and hillslope zones (Linn and Doran, 1984; Pinay et al., 2007a). Such spatial pattern differed from those found in non-water limited riparian forests, where higher N_2O emissions occurred in the hillslope edge as a result of high resource supply (DeSimone et al., 2010; Dhondt et al., 2004; Hedin et al., 1998). These results suggest that riparian hydrology is the primary mechanisms controlling denitrification but, once water is unlimited, substrate availability controls the magnitude of denitrification rates. This former idea is supported by our potential denitrification results, which showed that, after adding water, denitrification rates were similar to those observed in the field for the near-stream zone, but increase by 3-4 fold in the other two zones. Moreover, N_2:N_2O ratios estimated from acetylene method suggest that there was a spatial pattern in

denitrification efficiency as well. During the study period, N_2:N_2O ratios were always higher at the near-stream (21.50 ± 40.32) than at the intermediate and hillslope zones (5.90 ± 16.02 and 4.23 ± 8.31, respectively), yet all values were much lower than those reported for temperate riparian forests (184 – 844; Mander et al., 2014). All together, these results support the idea that saturated soils favored the complete denitrification process to N_2 and can potentially emit less N_2O compared to less saturated soils (Giles et al., 2012).

Intra-annual variation in N_2O emission was also related to riparian hydrology because high rates of N_2O effluxes occurred in April, when large precipitation events (400 mm) raised the groundwater level and increased soil water content at the whole riparian plot. Such pulses of N_2O emissions short-after rewetting events can reflect the microbial use of the NO_3^- that has been accumulated during dry antecedent periods (Chang et al., 2014; Hefting et al., 2004; Pinay et al., 2007a). In agreement, the PLS model showed a negative relation between soil water content and NO_3^- concentrations. Moreover, our results further suggest that rewetting events promote a fast N cycle because all microbial N processes were maxima in April. Nevertheless, we also expected a fast N cycle as well as large N_2O emissions following rains in November because, similarly to spring, environmental conditions (i.e. high soil water content and increments in soil NO_3^- concentrations during the antecedent dry summer) should enhance microbial activity. Likely, low rates of N transformations during fall may be attributed to an increase in microbial N demand following large C inputs from litterfall (Guckland et al., 2010). Moreover, leaf litter from *R. pseudoacacia*, the main tree species in our study site, holds a high lignin content (Castro-Díez et al., 2009; Yavitt et al., 1997), which might enrich the riparian soil with phenolic compounds and ultimately limit the use of N by microbes (Bardon et al., 2014). These results suggest that the response of N cycling to changes in water availability is more complex and less predictable than C cycling, likely because N processes depend on the interplay of additional ecosystem factors not included in this study.

5.4.4. Riparian soils as hot spots of GHG effluxes

There are several studies that attempt to upscale riparian GHG emissions at catchment scale, yet there are still fundamental uncertainties regarding the magnitude and sources of GHG emissions (Hagedorn, 2010; Pinay et al., 2015; Vidon and Hill, 2006). When accounting for all GHG (CO_2 + N_2O), our study suggest that our riparian soils can emit between 438 – 3650 g C m^{-2} yr^{-1}. Assuming that GHG emissions (CO_2 + N_2O) from upland evergreen oak and beech soils (54% and 38% of the catchment, respectively) are similar to other Mediterranean regions (oak: 19 – 1240 g C m^{-2} yr^{-1}; Asensio et al., 2007; Barba et al., 2016; Inclán et al., 2014); beech: 214 – 1182 g C m^{-2} yr^{-1}; Guidolotti et al., 2013; Kesik et al., 2005), then riparian soils (6% of the catchment area) can contribute between 16 – 22% to the total catchment soil GHG emissions. Although these estimates are rough (i.e. we assumed that riparian soils emit the same rate of GHG that our study site), our results clearly pinpoint that riparian soils can be potential hot spots of GHG emissions within Mediterranean catchments. These findings contrast with the common knowledge that water limited soils are powerless GHG sources to the atmosphere (Bernal et al., 2007; Vidon et al., 2016) and stress the importance of simultaneously consider several GHG emissions (i.e. CO_2, N_2O, CH_4) to get a whole picture of the role of riparian soils in climate change.

5.5. Conclusions

Mediterranean riparian zones are dynamic systems that undergo spatial and temporal shifts in biogeochemical processes due to changes in both soil water content and substrate availability. In a first attempt to simultaneously quantify CO_2 and N_2O emissions from Mediterranean riparian soils, we showed that most of GHG emissions occur in form of CO_2, even in the wet soils located near the stream. In addition, our results clearly illustrate a strong linkage between riparian hydrology and the microbial processes that produce GHG. Deep groundwater tables fueled large respiration rates in the relatively dry soils near the hillslope, while denitrification mostly occurred in the wet zones located near the stream channel. As occurred at spatial scale, riparian soil water

content was a primarily control of the temporal patterns of CO_2 and N_2O emissions. Soil dryness diminished respiration rates during summer, while a fast soil N cycling promoted high N_2O emissions after a rewetting event in spring. Overall, our study highlights that future variations in catchment hydrology due to climate change can potentially affect the riparian functionality in Mediterranean zones, as well as their contribution to regional and global C and N cycles.

Aknowledgements

We are thankful to Ada Pastor and Lídia Cañas for their invaluable assistance in the field. Special thanks are extended to Núria Catalán for helpful comments on an earlier version of the manuscript. Financial support was provided by the Spanish Government through the projects MONTES-Consolider (CSD2008-00040-MONTES), MEDFORESTREAM (CGL2011-30590), and MEDSOUL (CGL2014-59977-C3-2). Sílvia Poblador was supported by a FPI PhD fellowship from the Spanish Ministry of Economy and Competitiveness (BES-2012-054572). Anna Lupon was supported by a Kempe Foundation post-doctoral grant (Sweden) and the MEDSOUL project. We also thank site cooperators, including Vichy Catalan and the Catalan Water Agency (ACA) for permission to sample at the *Font del Regàs* catchment. Sílvia Poblador, Anna Lupon, Santiago Sabaté, and Francesc Sabater are members of the research group FORESTREAM (AGAUR, Catalonia 2014SGR949).

CHAPTER 6

Riparian forest transpiration under the current and projected Mediterranean climate: effects on soil water and nitrate uptake

Riparian vegetation plays a key role in riparian area functioning by controlling water and nitrate ($N\text{-}NO_3^-$) transfers to streams. We investigated how spatial heterogeneity modifies the influence of vegetation transpiration on soil water and $N\text{-}NO_3^-$ balances in the vadose soil of a Mediterranean riparian forest. Based on field data, we used the HYDRUS-1D model to simulate water flow and $N\text{-}NO_3^-$ transport in three riparian zones (i.e. near-stream, intermediate, and hillslope). We investigated spatio-temporal water and $N\text{-}NO_3^-$ patterns across the riparian area over a 3-year period and for future years using an IPCC/CMIP5 2015-2100 climate projection for the Mediterranean region. Potential evapotranspiration was partitioned between evaporation and transpiration, and several scenarios were created to test model sensitivity to the transpiration rate. $N\text{-}NO_3^-$ removal was considered to come only from plant uptake (i.e. denitrification was not considered). For the three riparian zones, the model successfully predicted field soil moisture (θ). The near-stream zone exchanged larger volumes of water and supported higher θ (0.38 ± 0.01 cm^3cm^{-3}) and transpiration rates (666 ± 75 mm) than the other two riparian zones. Total water fluxes, θ, and transpiration rates decreased near the intermediate (θ=0.25 ± 0.04 cm^3cm^{-3}, 536 ± 46 mm transpired) and hillslope zones (θ=0.17 ± 0.04 cm^3cm^{-3}, 406 ± 26 mm transpired), suggesting that water availability was restricted due to deeper groundwater. Transpiration strongly decreased θ and soil $N\text{-}NO_3^-$ in the hillslope and intermediate zones. Our climate projections highlight the importance of groundwater availability and indicate that soil $N\text{-}NO_3^-$ concentrations increased due to changes in plant-root uptake. Lower water availability in the hillslope zone may reduce the effectiveness of $N\text{-}NO_3^-$ removal in the riparian area, increasing the risk of excess $N\text{-}NO_3^-$ leaching into the stream.

Original Work: Poblador, S., Z. Thomas, P. Guentin-Rousseau, S. Sabaté and F. Sabater. 2018. Riparian forest transpiration under the current and projected Mediterranean climate: effects on soil water and nitrate uptake. Ecohydrology (under review)

6.1. Introduction

Riparian areas are considered key ecosystems because of their great ability to regulate stream discharge and reduce nitrogen (N) loads from uplands to streams via vegetation N uptake and microbial denitrification in saturated soils (Clément et al., 2002, 2003; Hill, 1996). Among riparian forms of plant life, trees have the highest transpiration rates (Huxman et al., 2005; Zhang et al., 2001, 2005), which have strong effects on soil moisture (θ) and daily groundwater fluctuations (Barnard et al., 2010; Bosch et al., 2014; Ghazavi et al., 2011; Gribovszki et al., 2010). These transpiration rates ultimately influence annual water balances in riparian areas and exchanges with adjacent streams (Hernandez-Santana et al., 2011; Medici et al., 2008). Consequently, forested riparian areas can remove more nitrate ($N\text{-}NO_3^-$) via root uptake from unsaturated and saturated zones than grasslands (Connor et al., 2013; Hefting et al., 2005; Mayer et al., 2005; Osborne and Kovacic, 1993). Vegetation has especially strong effects on hydrological and biogeochemical processes in arid and semiarid regions, where water availability is lower and groundwater tends to be deeper (Butturini et al., 2003b; Lupon et al., 2016c; Sabater and Bernal, 2011; Williams and Scott, 2009). Because of lower water availability in these regions, soil is rarely anoxic, and thus denitrification is negligible (Bernal et al., 2007; Poblador et al., 2017). Hence, root uptake can influence N retention under these climate conditions.

Climate change and human activities (e.g. water extraction, riparian forest exploitation, land use changes) impact riparian areas and related ecosystem services, affecting not only water budgets but the ability of riparian areas to act as N filters (Radtke et al., 2013; Sala et al., 2000a; Tylianakis et al., 2008). Climate-change scenarios project an increase in mean annual temperature and a decrease in summer rainfall in the Mediterranean region (IPCC, 2013). An increase in temperature might initially stimulate transpiration rates in riparian areas by increasing atmospheric evaporative demand, but transpiration can also be restricted when θ decreases and groundwater falls below the rooting zone (Jung et al., 2010; Oliveira et al., 2011; Williams and Scott, 2009). Shifts in plant species due to changes in water availability have already occurred in the

Mediterranean region and can be exacerbated by aridification. The most vulnerable species are those adapted to a relatively narrow range of environmental conditions (O'Neill et al., 2008; Peñuelas and Boada, 2003), such as those present in riparian areas (Grady et al., 2011; Hultine et al., 2013). Some studies have reported higher tree N-NO_3^- uptake from soils when soil temperatures increase (Rennenberg et al., 2009). However, changes in transpiration rates due to changes in climate or shifts in tree species can decrease N uptake capacity in riparian areas, increasing N losses from soils into streams and influencing downstream water quality (Gerber and Brookshire, 2014; Lupon et al., 2016a).

Because seasonal and inter-annual variability in climate conditions can affect riparian ecosystems and their water and N budgets, an increasing amount of research focuses on modeling fluxes in these areas to better understand their functioning and predict cascade effects. Combining modeling and field experiments can provide essential information to investigate interactions between climate and both the water and N cycles (Chen et al., 2016; Weiler and McDonnell, 2004). Models that predict N transport and transformation rely on a good understanding of hydrology (Connor et al., 2013; Ranalli and Macalady, 2010), of which θ is one of the most widely studied variables. Soil water is the main component of the hydrological cycle available to plants, and its dynamics depend on interactions between the soil, vegetation, and the atmosphere.

Catchment modeling typically considers riparian areas as homogeneous, even though this is not always the case (Ford et al., 2008; Tromp-van Meerveld and McDonnell, 2006). Little is known about how spatial patterns of soil characteristics (such as θ, soil texture, soil thickness, and groundwater level (GWL)) can regulate the influence of vegetation on water and N fluxes (Angstmann et al., 2013; Meixner et al., 2016; Ocampo et al., 2006). For instance, θ in riparian areas in the Mediterranean region has high spatial variability due to shallow groundwater in the near-stream zone and deeper groundwater in the hillslope zone. In areas where groundwater lies more than 1 m deep, the biogeochemistry of the unsaturated zone is clearly disconnected from that of the saturated zone (Jacinthe and Dick, 1997; Vidon, 2017). Understanding this

spatial heterogeneity is crucial to conceptualize the functioning of riparian areas and to evaluate potential effects of climate change on them (Hassler et al., 2017; Schume et al., 2004; Tromp-van Meerveld and McDonnell, 2006).

This study investigates how spatial heterogeneity modifies the influence of tree transpiration on soil water and N-NO_3^- balances in the soil profile of a Mediterranean forest. Water flow and N-NO_3^- transport were simulated based on field data at the riparian zone scale. Root uptake of water and N-NO_3^- was predicted over a 3-year period (2012-2014), and then over a projected climatic period (2015-2100) following the Intergovernmental Panel on Climate Change projection for the Mediterranean region (IPCC 2013). Since transpiration has been identified as the main component of water balances (Thomas et al., 2012), we hypothesized that it and N-NO_3^- uptake would drive water and N-NO_3^- balances in the riparian area studied. We expected that shallow groundwater in the near-stream zone would have high transpiration rates and large water fluxes, while deeper groundwater in the hillslope zone would restrict all water fluxes. Nevertheless, we expected stronger effects of transpiration on θ dynamics and annual water balances in the hillslope zone, due to lower soil water availability for plants. Based on expected differences in spatial transpiration rates, higher root uptake of N-NO_3^-, and thus higher N retention, was expected in the near-stream zone than in the hillslope zone. Finally, we predicted the influence of projected climate change on water and N-NO_3^- balances in riparian zones. We hypothesized that future drier conditions would cause θ to decrease and N-NO_3^- concentration to increase in the soil profile due to lower root-uptake rates.

6.2. Materials and Methods

6.2.1. Study site

Font del Regàs is a subhumid Mediterranean forested catchment in the Montseny Natural Park, NE Spain (41º50'N, 2º30'E). The catchment is dominated by biotitic granite (ICC, 2010). The catchment covers 14.2 km^2 and ranges in elevation from 475-1500 m above sea level. The riparian area covers 6% of the catchment.

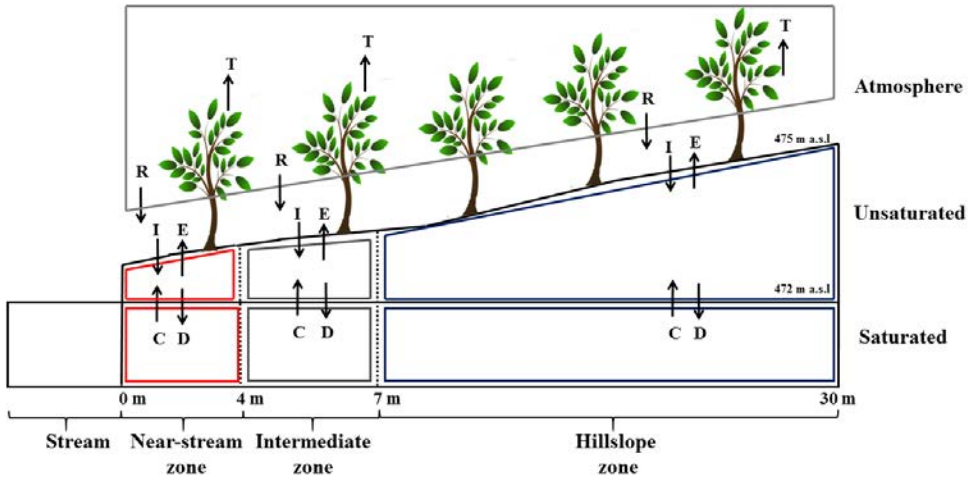

Figure 6.1 Diagram of riparian zones at the study site. Arrows represent water and nitrogen fluxes in the HYDRUS-1D model: (R) rainfall, (I) infiltration, (E) evaporation, (T) transpiration, (D) drainage, and (C) capillarity. For nitrate fluxes, evaporation does not exist, while transpiration represents uptake by vegetation.

We selected a well-developed riparian stand (~600 m^2, ~25 m wide) that flanked the stream at the valley bottom of the catchment. The riparian soil (pH ~7) was sandy and had a 5 cm organic layer followed by a 30 cm A-horizon. We established three riparian zones based on the observed spatial segregation of riparian tree species and GWL (Fig. 6.1). The near-stream zone (0-4 m from the stream edge), where GWL laid 0.41-0.60 m below the soil surface (b.s.s.), occupied 16% of the riparian plot and was composed of *Alnus glutinosa*, *Populus nigra* and *Robinia pseudoacacia* (45%, 33%, and 22% of the zone's basal area (BA), respectively). The intermediate zone (4-7 m from the stream edge), where GWL ranged from 1.20-1.35 m b.s.s., occupied 12% of the riparian plot and was composed of *P. nigra* and *R. pseudoacacia* (29% and 71% of the zone's BA, respectively). The hillslope zone (7-25 m from the stream edge), with GWL > 2.20 m b.s.s., was the largest (72% of the riparian plot) and was composed of *Fraxinus excelsior* and *R. pseudoacacia* (7% and 93% of the zone's BA, respectively). Mean (± 1standard deviation) of porosity in the near-stream soil profile was 0.56 ± 0.05%, and that of its bulk density was 1.17 ± 0.14 g cm^{-3}. Intermediate and hillslope zone soil profiles had similar porosities (0.50 ±

0.07% and 0.50 ± 0.05%, respectively) and bulk densities (1.31 ± 0.19 g cm^{-3} and 1.32 ± 0.18 g cm^{-3}, respectively) (Boumghar, 2012).

During the study, which encompassed three vegetative periods (2012, 2013, and 2014), mean annual rainfall (572 ± 134 mm) and mean annual temperature (13.3 ± 0.9 ºC) fell within their long-term annual means for this region (period 1940-2000; Catalan Meteorological Service). Total inorganic N deposition ranges from 15-30 kg N ha^{-1} yr^{-1} (period 1983-2007; Àvila and Rodà, 2012).

6.2.2. Soil and groundwater field measurements

We monitored θ (i.e. volumetric soil water content (cm^3 cm^{-3})), GWL fluctuations and groundwater N-NO_3^- across the riparian area from March 2012 to October 2014. θ in the topsoil (upper 30 cm) was measured every 15 min using frequency domain reflectometers (CS616, Campbell Scientific, Logan, USA) at 1.5, 4, and 14 m from the stream edge.

A grid of wells was installed at multiple locations inside the plot (1.5, 5, and 17 m from the stream edge) to monitor GWL fluctuations and groundwater dynamics and quality. Wells were PVC tubes (32 mm Ø) uniformly screened along their length and sunk 1, 1.5 and 3 m b.s.s. deep in near-stream, intermediate, and hillslope zones, respectively. At each riparian zone, GWL was measured every 15 min by water pressure transducers (HOBO U20-001-04, Onset, Bourne, Mass., USA). Stream water and groundwater were sampled every two weeks and stored in pre-acid-washed polyethylene bottles previously rinsed with sampled water. Sampling also included water from a rainfall collector from the nearby meteorological station. All water samples were filtered (Whatman GF/F, 0.7 μm pore Ø) and kept cold (< 4ºC) until laboratory analysis (< 24 h after collection). N-NO_3^- concentration was quantified with the cadmium reduction method (Keeney and Nelson, 1982) using a Technicon Autoanalyzer (Technicon, 1976).

6.2.3. Modeling method

To analyze the complex interaction among soil, vegetation, and the atmosphere (Fig. 6.1), we developed a modeling approach based on a vertical 1D flow

domain representing each riparian zone. Preliminary hydraulic head results from the study plot revealed parallel groundwater fluxes to the stream most of the year, while lateral fluxes occurred only during drier summer periods, when stream water entered the near-stream zone. We used the HYDRUS-1D model (Simunek et al., 2006; Šimůnek et al., 2008) to simulate water flow and $N\text{-}NO_3^-$ transport in variably unsaturated media. The model simulates water flux by adapting Richards equation (Eq. 6.1), assuming that air and thermal gradients can be ignored in the liquid flow process. A sink term represented in Richards equation was used to represent root uptake by trees (Richards, 1934):

$$\frac{\partial \theta}{\partial t} = \frac{\partial}{\partial z}\left[K(h)\left(\frac{\partial h}{\partial z} + cos\,\alpha\right)\right] - S \qquad \text{(Eq. 6.1)}$$

where θ is volumetric soil moisture [$L^3\ L^{-3}$], K(h) is unsaturated hydraulic conductivity [$L\ T^{-1}$], h is the soil water pressure head, z is the vertical coordinate, α is the angle between the direction and the vertical axis ($\alpha = 0^o$ for vertical flow, $\alpha = 90^o$ for horizontal flow), and S is the sink term for root water uptake [$L^3\ L^{-3}\ T^{-1}$]. The Feddes model was applied to capture the relationship between the pressure head and water uptake limitation (Feddes et al., 1974). Soil hydraulic properties and retention curve parameters were assessed using the Van Genunchten empirical model (Van Genunchten, 1980).

6.2.4. Modeling set-up and boundary conditions

According to our study site configuration, a 1D model with a flow domain thickness of 2.5 m was defined for each riparian zone (i.e. near-stream, intermediate, and hillslope). The thickness of unsaturated soil depended on the GWL in each riparian zone. Each application of the model to a riparian zone included (i) inverse modeling to define soil parameters, (ii) model validation using field data, and (iii) simulation of the studied period (2012-2014). First, the model's soil hydraulic properties – residual θ (θr), saturation θ (θs), and hydraulic conductivity (Ks) – for each riparian zone were predicted using inverse modeling. Initial values of these parameters were defined from previous field data on particle size distribution and bulk density profiles (Boumghar, 2012) using the Rosetta module (Schaap et al., 2002), which is included in the HYDRUS-1D software package. In the inverse modeling, our

observations of topsoil θ in spring 2012 were defined as the objective function. An inverse solution was obtained after 2, 4, and 5 iterations of the near-stream, intermediate, and hillslope models, respectively. Field θ data for 2012 and 2013 were used to evaluate prediction accuracy, excluding data from summers to avoid incorporating plant transpiration effects, which strongly influence θ (Table 6.1).

Table 6.1 Soil hydraulic properties for the near-stream, intermediate and hillslope riparian zones. Residual soil moisture (θ_r), saturation soil moisture (θ_s), α and n (parameters describing the shape of the soil water retention curve and hydraulic conductivity, respectively), the tortuosity parameter (l), and saturated hydraulic conductivity (K_s) estimated from inverse modeling. The table also shows goodness of fit (root mean squared error (RMSE) and Nash-Sutcliffe model efficiency (Nash)) between observed and predicted θ.

	Near-stream	Intermediate	Hillslope
Soil hydraulic properties			
θr ($cm^3\ cm^{-3}$)	0.01	0.16	0.10
θs ($cm^3\ cm^{-3}$)	0.565	0.560	0.480
α ($1\ cm^{-1}$)	0.043	0.048	0.048
n (-)	1.493	1.694	1.713
l ($cm\ cm^{-1}$)	0.5	0.5	0.5
Ks ($cm\ day^{-1}$)	800	200	200
Model goodness of fit			
RMSE	0.007	0.018	0.025
Nash	0.739	0.879	0.765

Subsurface and surface boundary conditions were specified for each riparian zone. Subsurface boundary conditions were pressure head measurements calculated from GWL field data for each riparian zone. During the study period, mean GWL (± 1 SD) measured in the field was 0.61 ± 0.03 m b.s.s. in the near-stream zone and decreased to 1.29 ± 0.05 and 2.23 ± 0.07 m b.s.s. in the intermediate and hillslope zones, respectively (Fig. 6.2a). Daily meteorological data were recorded at a meteorological station located ca. 800 m from the study site. Daily potential evapotranspiration (PET) ($mm\ d^{-1}$) was calculated using the Penman-Monteith equation following Allen et al. (1998). Surface boundary conditions (i.e. rainfall and PET) were the same in all riparian zones. Rainfall was used in HYDRUS-1D to estimate infiltration rates.

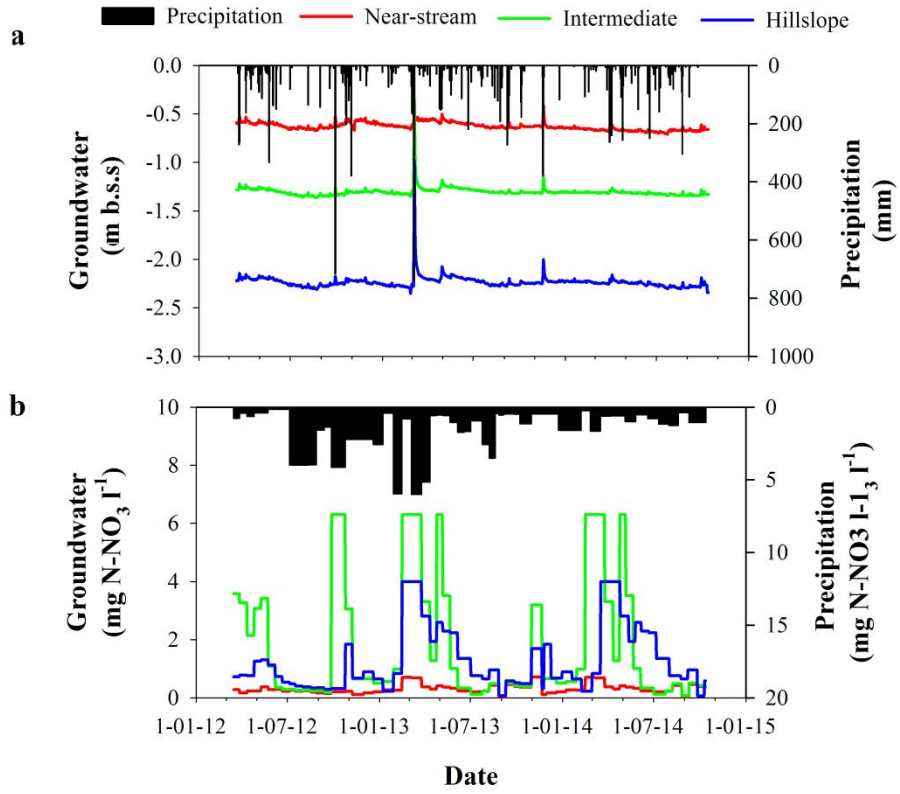

Figure 6.2 Boundary conditions used for simulations. (a) Precipitation (mm) as a surface water flow boundary condition and groundwater level (m below the soil surface, b.s.s.) as subsurface water flow boundary conditions. (b) Nitrate concentrations (mg $N\text{-}NO_3^-$ l^{-1}) in precipitation and groundwater used for solute transport surface and subsurface boundary conditions, respectively. Nitrate concentrations where measured every two weeks and were applied to each day of the associated two-week period. Groundwater data are shown for near-stream, intermediate, and hillslope riparian zones.

For $N\text{-}NO_3^-$ boundary conditions, discontinuously measured field data of rainfall were the same for all three zones, while groundwater $N\text{-}NO_3^-$ concentration differed among zones. Field data for $N\text{-}NO_3^-$ concentration in rainfall and groundwater collected every two weeks were applied to each day of the associated two-week period and used as boundary conditions (Fig. 6.2b). Predicted $N\text{-}NO_3^-$ transport was neither calibrated nor validated, since $N\text{-}NO_3^-$ uptake is a function of water uptake.

6.2.5. Transpiration rates: water and N-NO_3^- flux simulations

After estimating and validating the soil hydraulic parameters, we introduced tree water uptake, with root distribution concentrated in each unsaturated soil column. All root systems reached the groundwater table and had maximum root depth density in the middle of the unsaturated soil profile. The partition between evaporation and transpiration was estimated for each riparian zone. We evaluated the influence of transpiration on θ by testing transpiration partitioning rates equal to 20%, 50%, 60%, 70% and 80% of PET. For each riparian zone and transpiration rate, we simulated water flow to determine the adjusted transpiration rate by comparing observed and predicted θ in the topsoil.

For the best-fit model of transpiration partitioning in each riparian zone, N-NO_3^- transport and N uptake by tree roots was simulated assuming that N-NO_3^- concentrations in the fluxes equaled those in soil water. All uptake was considered passive (i.e. no discrimination in uptake and not a dissimilatory N process) and that the proportional decrease in soil N-NO_3^- concentration equaled the proportional increase in root water uptake (Šimůnek and Hopmans, 2009).

6.2.6. Goodness of fit

For each riparian zone, we evaluated the goodness of fit between observed and predicted θ data using the root mean squared error (RMSE) and Nash-Sutcliffe model efficiency coefficient (Nash).

$$RMSE = \sqrt{\frac{\sum_{i=1}^{N}(\theta_i pred - \theta_i pred)^2}{N}} \quad \text{(Eq. 6.2)}$$

$$Nash = 1 - \frac{\sum_{i=1}^{N}(\theta_i pred - \theta_i obs)^2}{\sum_{i=1}^{N}(\theta_i pred - \bar{\theta}_i obs)^2} \quad \text{(Eq. 6.3)}$$

where θpred is predicted θ, θobs is observed field θ, θobs is mean observed θ over the simulation period, and N is the number of observations in the period (time series). RMSE values closer to 0 indicate higher correlation between observed and predicted values. The Nash-Sutcliffe coefficient is used to

evaluate the predictive power of the model. A Nash=1 indicates a perfect match between observed and predicted data, whereas a Nash=0 indicates that the mean of observed data has the same predictive power as the model.

6.2.7. Water and N-NO3- mass balances

Water and N-NO_3^- balances in the soil profile of each riparian zone were calculated from model predictions of daily fluxes. Each year was divided in two periods: (i) the vegetative period (April-October) and (ii) the dormant period (November-March). Water balances were calculated as:

$$\Delta Ws = I - E - T + C - D \quad \text{(Eq. 6.4)}$$

where ΔWs is water storage, I is infiltration, E is evaporation, T is transpiration, C is capillarity from groundwater, and D is drainage into the groundwater. All fluxes in the model are expressed in mm. Soil N-NO_3^- mass balances (ΔNO_3^-) were calculated like water balances (Eq. 6.4), but evaporation (E) was excluded, and transpiration (T) was considered as plant root uptake (U). All other water fluxes from Eq. 6.4 were multiplied by predicted soil N-NO_3^- concentrations (mg l^{-1}) to obtain the N-NO_3^- mass balance for each riparian zone.

6.2.8. Evaluation of the influence of climate change on soil water-vegetation interactions

To explore how climate change may influence soil water-vegetation interactions in our study site, we ran the HYDRUS-1D model under projected climate change conditions for each riparian zone. IPCC scenarios for the Mediterranean zone predict a 2ºC increase in air temperature and a 5% decrease in precipitation by 2100 (IPCC, 2013). We based our climate projections on Representative Concentration Pathways 2.6, 4.5, and 8.5. Data were downloaded from the Earth System Grid Federation website (https://esgf-node.llnl.gov/projects/esgf-llnl/). We extracted 4-pixel data around our study area from CMPI5 long-term simulations (Fig. D.1). Daily data obtained for precipitation (PR in the database) and latent heat fluxes (HFLS) were summed annually (2015-2100) to run our projections.

For the climate projection simulations, for each model application, we used projected rainfall and PET (with specific transpiration partitioning) as surface boundary conditions and specific GWL as subsurface boundary conditions. For all riparian zones, we simulated both (i) keeping this transpiration partitioning constant and (ii) using a transpiration partitioning 20 percentage points lower throughout the projected period, as described for models simulating climate change scenarios for vegetation (Luo et al., 2008). Little is known about the influence of climate change on GWL and ecosystems that depend on GWL across biomes (Klove et al, 2014). Therefore, to test the sensitivity of model projections to GWL, we examined two possible scenarios: (i) steady GWL during the period and (ii) GWL depletion due to climate change. For the steady GWL scenarios, the GWL predicted at the end of the current period (October 2014) was kept constant through to 2100. Pascual et al. (2015) predicted a 30% decrease in summer stream discharge in the headwaters of our catchment by 2100. Since groundwater recharges the stream in summer, we assumed that GWL would decrease by the same rate. We thus simulated a decrease in GWL of 3 mm $year^{-1}$ to reach a GWL 30% lower by 2100. For $N\text{-}NO_3^-$ boundary conditions, surface inputs and subsurface concentrations were calculated as a function of projected rainfall using field-data correlations from the period studied. We used model predictions to evaluate the influence of this projected climate on θ and soil $N\text{-}NO_3^-$ in the riparian zones.

6.3. Results

6.3.1. Soil properties and transpiration rates in the riparian zones

Predicted saturated hydraulic conductivity (K_s) from the inverse solution was four times as high in the near-stream zone as in the intermediate and hillslope zones (Table 6.1). The near-stream zone also had higher water storage capacity ($\theta_s - \theta_r$) than the intermediate and hillslope zones: 0.56, 0.40 and 0.38 $cm^3\ cm^{-3}$, respectively. Soil hydraulic properties were predicted accurately for all riparian zones (RMSE < 0.03 and Nash > 0.74).

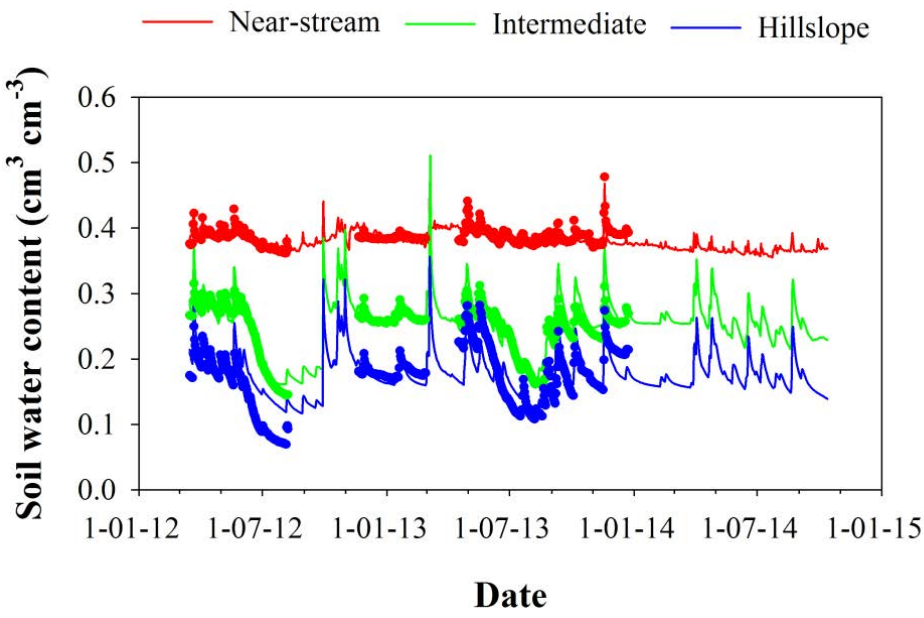

Figure 6.3 Observed (dots) and predicted (lines) soil moisture (in $cm^3\ cm^{-3}$) in the near-stream, intermediate, and hillslope riparian zones.

Predicted θ had low sensitivity (i.e. variability in Nash and RMSE) to transpiration rates (i.e. 20%, 50%, 60%, 70%, and 80% of PET) in the near-stream and hillslope zones but high sensitivity in the intermediate zone (Table D.1). Nevertheless, the transpiration rate yielding the most accurate prediction of observed θ differed among riparian zones. The most accurate transpiration rate was highest in the near-stream zone (80% of PET; Nash=0.52, RMSE=0.01) and lower in the intermediate (70% of PET; Nash=0.82, RMSE=0.02) and hillslope (60% of PET; Nash = 0.57, RMSE = 0.03) zones (Fig. 6.3, Table D.1). Actual transpiration is the effective transpiration simulated by the model from potential value. For all zones, differences between annual potential and actual transpiration increased as transpiration rate increased (i.e. from 20-80% of PET) and were larger in the hillslope than in the intermediate and near-stream zones. In the near-stream zone, annual potential transpiration lay within 1 mm of actual transpiration. In the intermediate and hillslope zones, differences ranged from 0-74 and 0-210 mm, respectively (Table D.1).

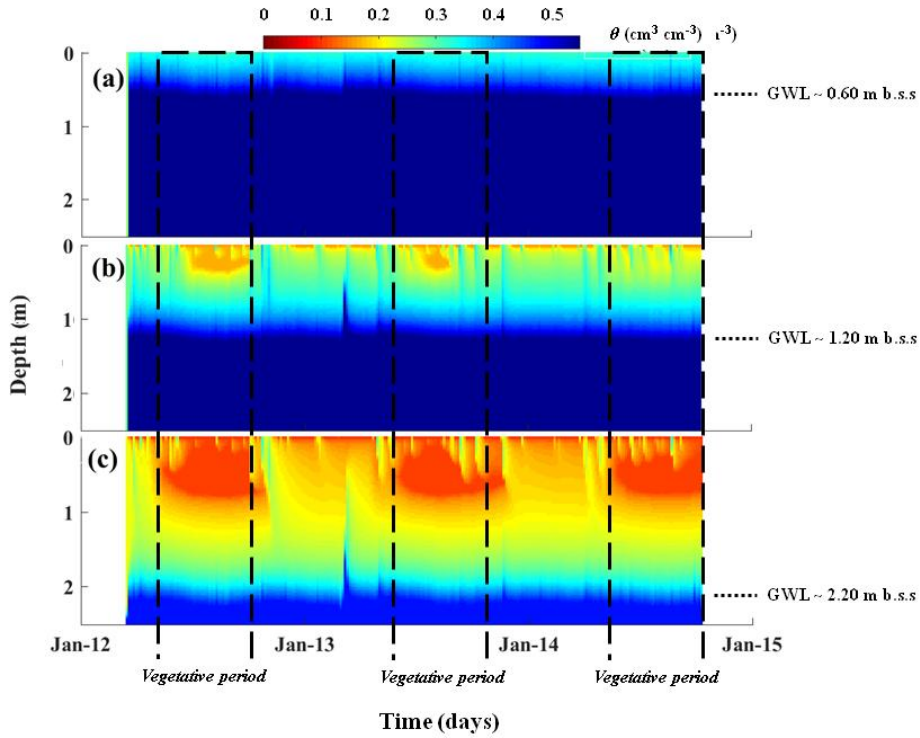

Figure 6.4 Dynamics of predicted soil moisture (θ, in %) in (a) near-stream, (b) intermediate, and (c) hillslope riparian zones from March 2012 to October 2014. Dashed blocks represent vegetative periods. Mean groundwater level (GWL) was approximately 0.6, 1.20, and 2.20 m below the soil surface (b.s.s.) of the near-stream, intermediate, and hillslope zones, respectively.

6.3.4. Spatial and temporal patterns of θ and soil $N\text{-}NO_3^-$ concentration

In each riparian zone, the variability in predicted θ in the soil profile throughout the year depended on the GWL used in the boundary conditions (Fig. 6.4). θ varied least in the near-stream riparian zone (0.38 ± 0.01 $cm^3\ cm^{-3}$) (Fig. 6.3), which had the highest θ and annual transpiration rates (589-729 mm) (Fig. 6.4a, Table D.1). In contrast, θ varied more (0.25 ± 0.04 $cm^3\ cm^{-3}$) in the intermediate zone, where annual transpiration ranged from 515-591 mm (Fig. 6.4b, Table D.1). In the hillslope zone, annual transpiration rates (380-416 mm) and θ (0.18 ± 0.03 $cm^3\ cm^{-3}$) were the lowest (Fig. 6.4c, Table D.1). The intermediate and hillslope zones had distinct vertical θ profiles, with the highest θ near GWL and the lowest θ near areas with the highest root density. In all riparian zones, θ responded quickly to rainfall events, which occurred

mainly in autumn and early spring. During heavy rainfall events, such as that in early March 2013, θ briefly (< 1 day) reached saturation throughout the entire soil profile.

Groundwater $N\text{-}NO_3^-$ data used as boundary conditions had higher mean concentrations in the intermediate zone (2.67 ± 0.18 mg $N\text{-}NO_3^-$ l^{-1}) than in the near-stream and hillslope zones (0.48 ± 0.13 and 1.42 ± 0.39 mg $N\text{-}NO_3^-$ l^{-1}, respectively) throughout the period studied (Fig. 6.2b). In saturated soil profiles, soil $N\text{-}NO_3^-$ concentrations were defined by groundwater $N\text{-}NO_3^-$ concentrations in each riparian zone (Fig. 6.5). Mean predicted soil $N\text{-}NO_3^-$ concentrations in the topsoil were highest in the hillslope zone (1.82 ± 1.24 mg $N\text{-}NO_3^-$ l^{-1}) and lower but similar in the near-stream and intermediate zones (0.85 ± 0.62 and 0.69 ± 0.60 mg $N\text{-}NO_3^-$ l^{-1}, respectively). In the intermediate and hillslope zones, soil $N\text{-}NO_3^-$ decreased during the vegetative period (spring and beginning of summer) in unsaturated soil profiles, resulting in lower soil $N\text{-}NO_3^-$ concentrations (< 1 mg $N\text{-}NO_3^-$ l^{-1}) as root density increased. Conversely, mid-summer soil $N\text{-}NO_3^-$ concentrations in both zones increased until the end of the vegetative period (Fig. 6.5b, 6.5c). Large inputs of $N\text{-}NO_3^-$ through infiltration and higher $N\text{-}NO_3^-$ concentrations in the groundwater occurred during rainfall events, especially in the intermediate zone.

6.3.5. Predicted water and $N\text{-}NO_3^-$ fluxes: mass balance

The near-stream zone had the largest predicted water fluxes (i.e. infiltration, evaporation, transpiration, capillarity, and drainage) (Table 6.2). Nevertheless, all surface fluxes (i.e. infiltration, evaporation, and transpiration) represented a relatively larger percentage of predicted water fluxes in the hillslope zone than in the near-stream and intermediate zones (Fig. 6.6). Transpiration was the main water outflow flux in all zones. Mean transpiration was lowest in the hillslope zone (406 ± 26 mm) and highest in the near-stream zone (666 ± 75 mm). Nevertheless, it represented 35% and 25% of predicted water fluxes in the hillslope and near-stream zones, respectively. Evaporation represented a similar percentage (13-16%) of predicted water fluxes in the zones.

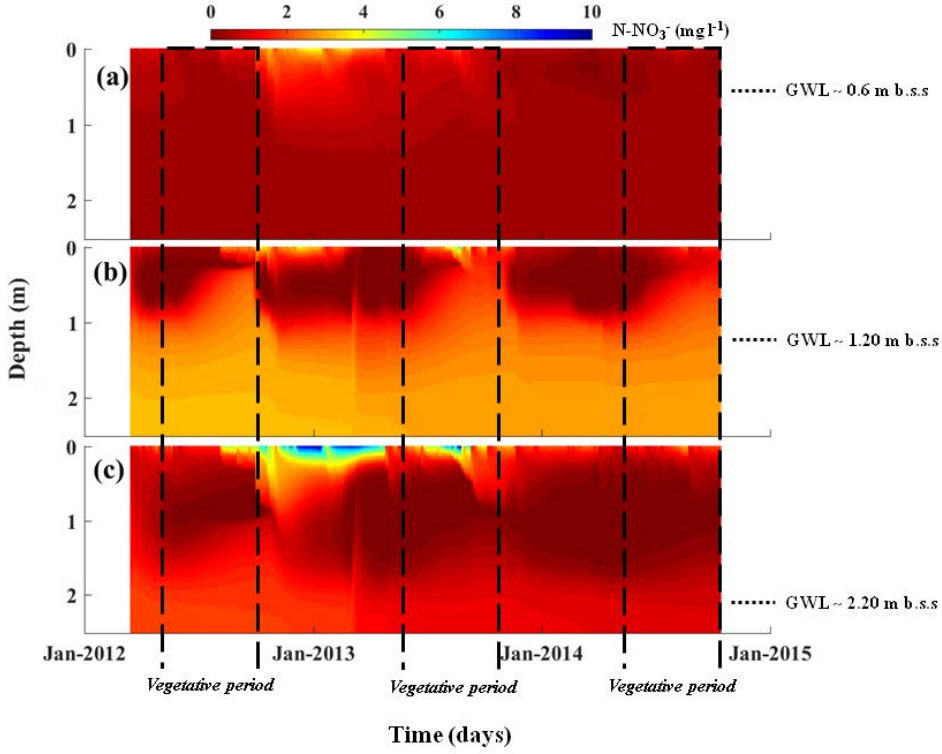

Figure 6.5 Dynamics of predicted nitrate concentration (mg $N\text{-}NO_3^-$ l^{-1}) in (a) near-stream, (b) intermediate, and (c) hillslope riparian zones from March 2012 to October 2014. Dashed blocks represent vegetative periods. Mean groundwater level (GWL) was approximately 0.6, 1.20, and 2.20 m below the soil surface (b.s.s.) of the near-stream, intermediate, and hillslope zones, respectively.

Groundwater recharge due to drainage represented 14% and 13% of predicted water fluxes in the near-stream and hillslope zones, respectively, but only 6% of those in the intermediate zone. When considering input fluxes, infiltration and capillarity had similar percentages (23% and 27% of all fluxes, respectively) in the intermediate zone. Conversely, capillarity and infiltration were the largest water inputs (33% and 28% of all fluxes, respectively) in the near-stream and hillslope zones, respectively. Vegetative periods had higher evaporation and infiltration fluxes than dormant periods. Capillarity was generally higher, and drainage lower, during vegetative periods than dormant periods. Annual water balances were negative for all riparian zones, being larger in the hillslope zone (ΔWs = -317 mm $year^{-1}$) than in the near-stream (-55 mm $year^{-1}$) and intermediate (-23 mm $year^{-1}$) zones.

Table 6.2 Mean (± 1 standard deviation) water fluxes (all in mm) predicted by the HYDRUS-1D model for near-stream, intermediate, and hillslope riparian zones for the three years studied. Results are presented separately for the dormant period, the vegetative period, and the entire year. Infiltration and capillarity are input fluxes, while evaporation, transpiration, and drainage are output fluxes.

Riparian zone	Infiltration	Evaporation	Transpiration	Capillarity	Drainage
Near-stream					
Dormant	*136 ± 48*	*209 ± 113*	*0*	*204 ± 105*	*143 ± 51*
Vegetative	*286 ± 54*	*139 ± 22*	*666 ± 75*	*699 ± 97*	*223 ± 59*
Annual	422 ± 47	348 ± 93	666 ± 75	903 ± 51	366 ± 41
Intermediate					
Dormant	*136 ± 48*	*129 ± 61*	*0*	*66 ± 17*	*87 ± 66*
Vegetative	*286 ± 55*	*116 ± 17*	*563 ± 46*	*417 ± 32*	*22 ± 23*
Annual	412 ± 45	245 ± 77	563 ± 46	483 ± 14	109 ± 58
Hillslope					
Dormant	*88 ± 55*	*75 ± 18*	*0*	*45 ± 20*	*103 ± 97*
Vegetative	*238 ± 59*	*115 ± 4*	*406 ± 26*	*55 ± 12*	*46 ± 4*
Annual	326 ± 61	190 ± 17	406 ± 26	100 ± 13	149 ± 94

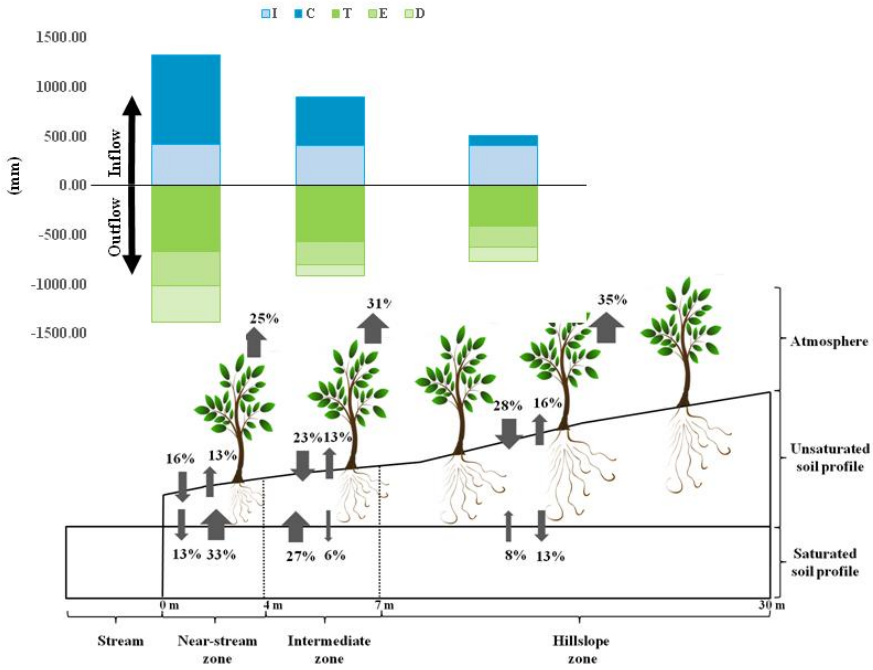

Figure 6.6 Predicted annual water balances in near-stream, intermediate, and hillslope riparian zones. Histograms represent volumes (mm), and arrows represent fluxes. The latter are expressed as percentage of total mass in each riparian zone. Infiltration (I) and capillarity (C) are input fluxes; evaporation (E), transpiration (T), and drainage (D) are output fluxes.

$N\text{-}NO_3^-$ fluxes were largest in the intermediate zone and smallest in the hillslope zone (Table 6.3). The largest flux of $N\text{-}NO_3^-$ in all zones (56-78% of all fluxes) was infiltration, which was also the main input of $N\text{-}NO_3^-$ (Fig. 6.7). Capillarity represented low percentages (8-9%) of $N\text{-}NO_3^-$ fluxes but was largest in the intermediate zone (21%). Relative $N\text{-}NO_3^-$ losses due to drainage into groundwater decreased from the near-stream to the hillslope zone. Conversely, transpiration uptake was a larger outflow in the hillslope than in the near-stream zone. Nevertheless, the intermediate zone had the highest $N\text{-}NO_3^-$ removal, due to root uptake. The annual mass balances indicated that all riparian zones accumulated $N\text{-}NO_3^-$ in the soil profile. The intermediate zone accumulated more $N\text{-}NO_3^-$ in the unsaturated soil column (ΔNO_3^- = 1.22 g $N\text{-}NO_3^-$ m^{-2}) than the near-stream (1.02 g $N\text{-}NO_3^-$ m^{-2}) and hillslope (1.16 g $N\text{-}NO_3^-$ m^{-2}) zones. Since $N\text{-}NO_3^-$ uptake is associated with water uptake, water fluxes during vegetative periods mobilized more $N\text{-}NO_3^-$ than those during dormant periods. Still, $N\text{-}NO_3^-$ outputs during dormant periods due to drainage in the intermediate and hillslope zones were 90% smaller than those during vegetative periods.

Table 6.3 Mean (± 1 standard deviation) nitrate ($N\text{-}NO_3^-$) fluxes (mg $N\text{-}NO_3^-$ m^{-2}) predicted by the HYDRUS-1D model for near-stream, intermediate and hillslope riparian zones for the three years studied. Results are presented separately for the dormant period, the vegetative period, and the entire year. Infiltration and capillarity are input fluxes, while plant-root uptake and drainage are output fluxes.

Riparian zone	Infiltration	Uptake	Capillarity	Drainage
Near-stream				
Dormant	*105 ± 76*	*0.00*	*24 ± 5*	*58 ± 51*
Vegetative	*1180 ± 1556*	*188 ± 72*	*114 ± 19*	*159 ± 113*
Annual	1285 ± 1572	188 ± 72	138 ± 17	217 ± 116
Intermediate				
Dormant	*105 ± 76*	*0*	*133 ± 173*	*205 ± 231*
Vegetative	*1172 ± 1556*	*297 ± 128*	*339 ± 63*	*23 ± 32*
Annual	1277 ± 1572	297 ± 128	472 ± 220	228 ± 216
Hillslope				
Dormant	*105 ± 76*	*0*	*121 ± 157*	*102 ± 158*
Vegetative	*1134 ± 1554*	*116 ± 42*	*19 ± 11*	*1 ± 0*
Annual	1239 ± 1570	116 ± 42	140 ± 153	103 ± 158

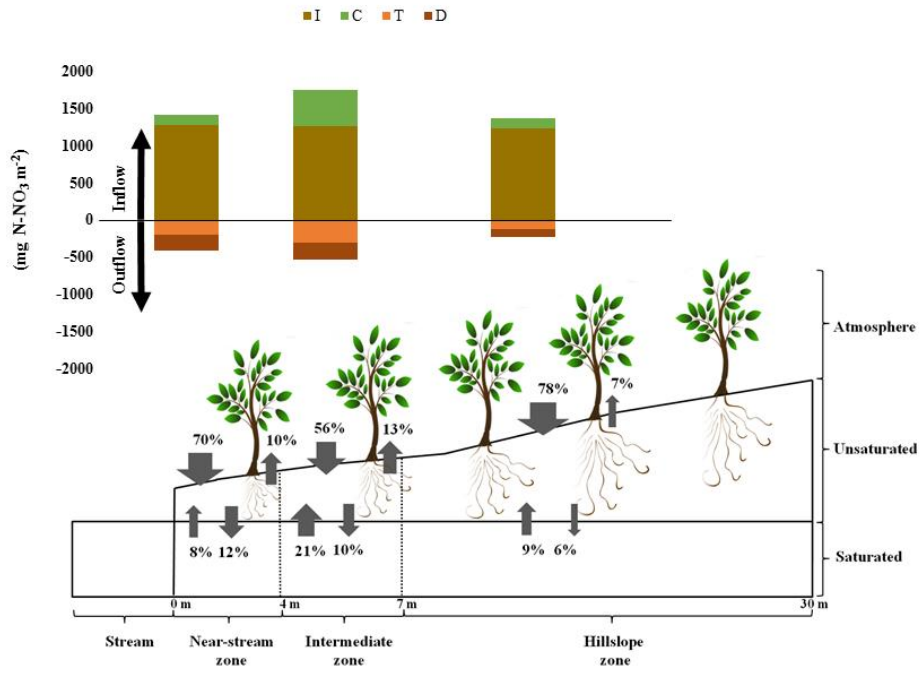

Figure 6.7 Predicted annual nitrate (N-NO3-) mass balances in near-stream, intermediate, and hillslope riparian zones. Histograms represent mass (mg N-NO3- m-2), and arrows represent fluxes. The latter are expressed as percentage of total mass in each riparian zone. Infiltration (I) and capillarity (C) are input fluxes; plant-root uptake (T) and drainage (D) are output fluxes.

6.3.6. Influence of climate change scenarios on soil-water-vegetation interactions

According to our projections, the main changes in θ and soil $N\text{-}NO_3^-$ were driven by long-term transpiration rates and GWL assumptions across the riparian area. No trends in θ or soil $N\text{-}NO_3^-$ in the topsoil were predicted when transpiration partitioning was kept constant (data not shown). In contrast, the 20 percentage points decrease in transpiration percentage yielded a ~1 mg l^{-1} increase in soil $N\text{-}NO_3^-$ concentration (Fig. 6.8). Steady GWL scenarios yielded no differences in θ of the soil profile over time, while GWL depletion scenarios yielded drier soil conditions throughout the soil profile by 2100, almost disconnecting the rooting zone from the groundwater table in the hillslope zone (Fig. 6.9). In the near-stream zone, θ was similar throughout the soil

profile from the beginning (2015) to the end (2100) of the period. In the intermediate and hillslope zones, θ decreased by a smaller amount in the topsoil (< 0.05 cm^3 cm^{-3}) and by a larger amount in the deeper profile (~ 0.2 cm^3 cm^{-3}) from the beginning to the end of the period. No notable differences in predicted θ were observed among the IPCC scenarios.

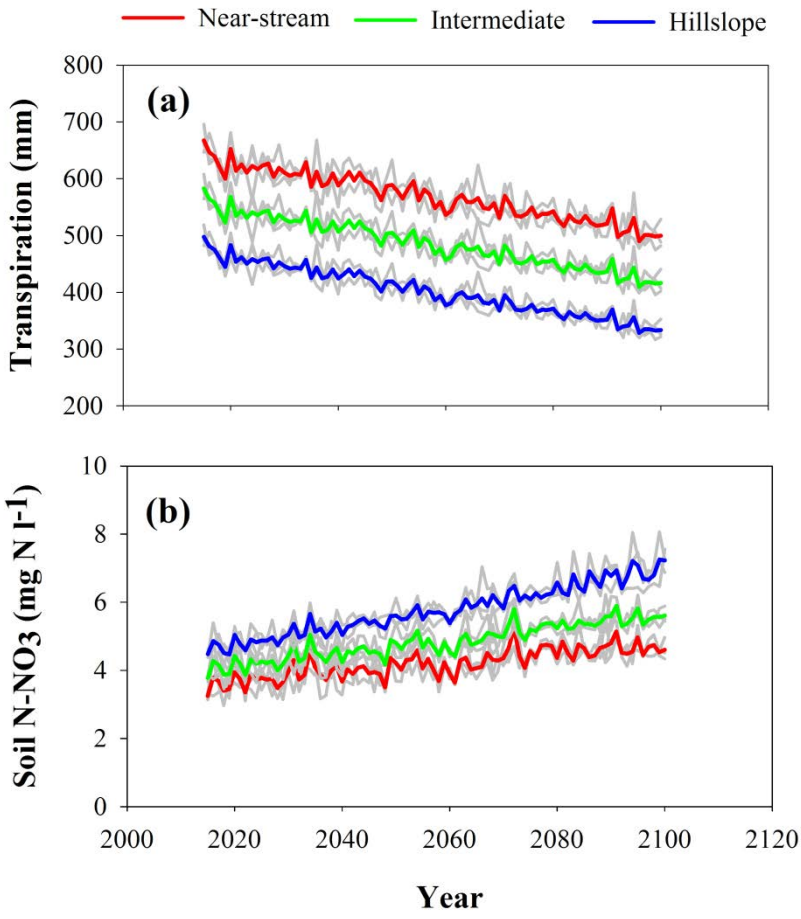

Figure 6.8 (a) Transpiration (mm), (b) topsoil (upper 30 cm) nitrate (mg N-NO3- l-1) predicted using a HYDRUS-1D model climate change projection. Predictions shown are based on IPCC Representative Concentration Pathway 4.5 projections for the Mediterranean region including all steady and depleted groundwater scenarios. Results are shown for near-stream, intermediate, and hillslope riparian zones in *Font del Regàs*, Spain.

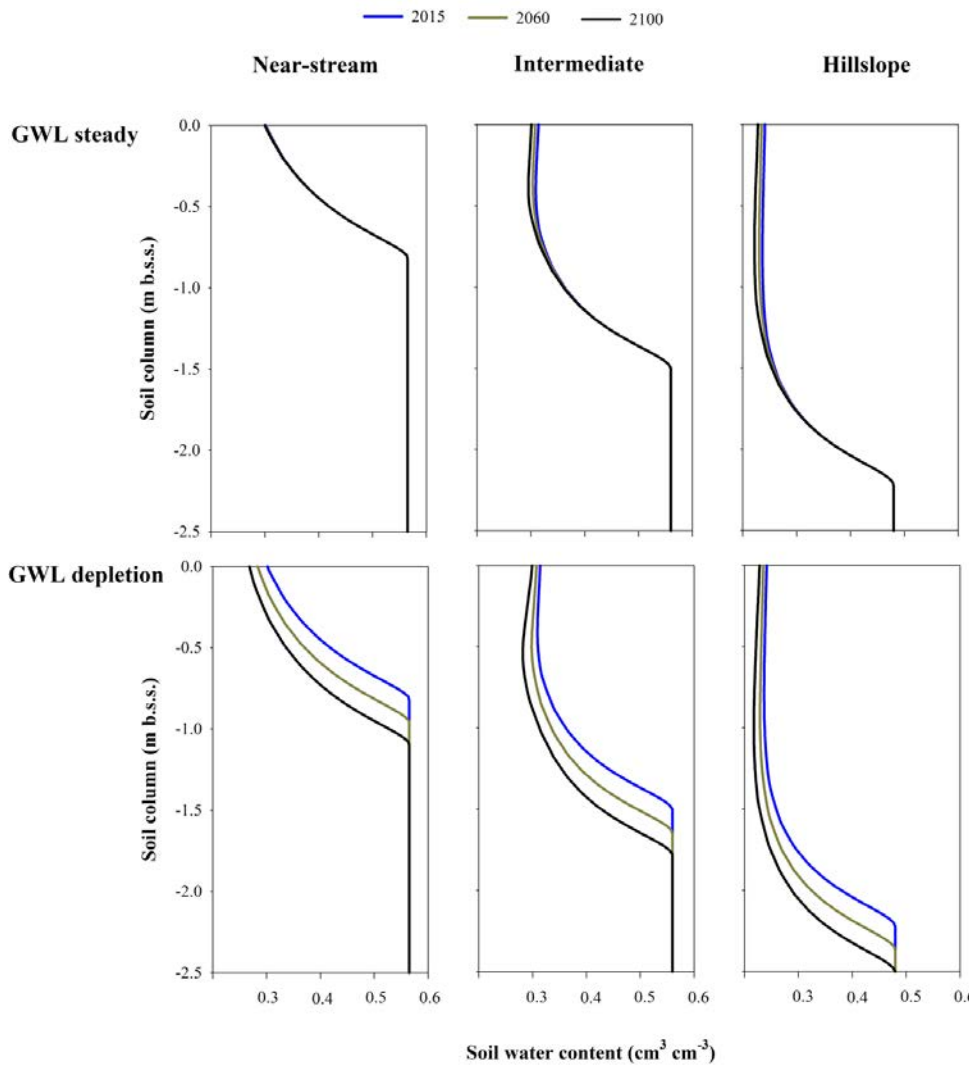

Figure 6.9 Predicted soil water content (cm3 cm-3) throughout the soil profile of the near-stream, intermediate, and hillslope riparian zones in *Font del Regàs*, Spain. Predictions shown are based on IPCC Representative Concentration Pathway 4.5 projections for the Mediterranean region and two groundwater level (GWL) scenarios (steady or depleted). Results are shown for 2015, 2060, and 2100.

6.4. Discussion

Dividing the riparian area into three zones (i.e. near-stream, intermediate, and hillslope) allowed us to identify its spatial heterogeneity. Although HYDRUS-1D models do not quantify lateral fluxes between riparian zones, and thus

water fluxes between the riparian area and the stream, they are a powerful tool to evaluate interactions among saturated and unsaturated soil profiles, vegetation, and the atmosphere (Doble and Crosbie, 2017; Simunek et al., 2006). Water fluxes in riparian areas depend strongly on soil properties, water availability, and the thickness of unsaturated soil (i.e. distance from the GWL) (Soylu et al., 2011). At our site, the near-stream zone had higher soil porosity, water storage capacity, and hydraulic conductivity than the other two zones, which had similar soil properties. Soil properties usually differ over short distances in riparian areas, where zones near the stream bed have higher hydraulic conductivities than those near the hillslope (Butturini et al., 2003).

6.4.1. Water balances and vegetation regulation

Predictions obtained by combining our dataset of field measurements with HYDRUS-1D simulation suggest that transpiration of riparian vegetation represents 60-80% of PET in the forested site. Predicted transpiration (432-666 mm $year^{-1}$) was higher than the one estimated from sap-flow measurements by Nadal-Sala et al. (2017) (211 mm, ~20% of PET). Nevertheless, in that study, field transpiration measurements accounted for the main tree species, but not the understory (i.e. grass, bushes, and small trees) species, whose collective transpiration may have a large influence on total ecosystem fluxes, contributing up to 30% of transpiration in riparian ecosystems (Roberts, 1983; Scott et al., 2008; Yepez et al., 2003). For instance, Hedera helix is attached to most of the trees in our study site, and its transpiration can reach 100 mm $year^{-1}$ (Hoelscher et al., 2015). The transpiration predicted in the present study is similar to those reported for arid and semiarid areas (400-600 mm $year^{-1}$; Sabater and Bernal 2011; Scott et al., 2008) and those estimated by mass-balance calculations at the catchment scale in the same study area (350-450 mm $year^{-1}$; Lupon et al., 2016a).

Partitioning between evaporation and transpiration depends on the regional climate and vegetation, due to the incoming solar radiation that drives evaporative demand, but also on soil water availability (Calder, 1998). The spatial heterogeneity of θ in the Mediterranean riparian forest studied allowed us to evaluate interactions between transpiration and θ. As expected, predicted

transpiration rates decreased from the near-stream to the hillslope zone along the gradient of soil water availability. Similar spatial differences in transpiration rates are described for semiarid riparian areas (Ford et al., 2008, Baird and Maddock 2005) and non-riparian hillslope zones (Tromp-van Meervel and McDonnel, 2006), with differences in soil water availability across the area. However, temperate riparian areas with permanent shallow groundwater usually have homogeneous transpiration rates (Bosch et al., 2014; Cermák and Prax, 2001). Thus, soil hydraulic properties (i.e. higher water storage capacity and hydraulic conductivity) and shallower GWL (~0.6 m b.s.s.) in the near-stream zone in *Font del Regàs* resulted in the highest water fluxes in the unsaturated soil column, with large water fluxes from the groundwater that ultimately promoted higher transpiration rates. Actual and potential transpiration rates did not differ in this zone, suggesting that the vegetation could supply all vapor pressure deficit, and thus transpiration there is not water-limited (Bosch et al., 2014; Clausnitzer et al., 2011; Schume et al., 2004). This strong connection with the groundwater is also supported by the small variations observed in θ, which remained high throughout the year.

Soil hydraulic properties were similar in the intermediate and hillslope riparian zones, but the thickness of the unsaturated zone differed (~1.3 and 2.2 m, respectively). Larger differences between actual and potential transpiration suggested restricted water supply in response to evaporative demand due to lower water availability in the hillslope zone (Bosch et al., 2014; Ford et al., 2005). Despite the lower transpiration in the hillslope, it had more relative importance due to the zone's lower soil water availability and low inflow through capillarity, which was restricted by lower GWL (supplying only 25% of transpired water). Surface fluxes represented a larger percentage of the total water balance, indicating disconnection from the groundwater. The intermediate zone is a transitional zone whose connectivity with the groundwater varies throughout the year. The larger percentage of capillarity fluxes (supplying 53% of the transpired water) and lower drainage in this zone than in the hillslope zone suggests that transpiration is not as restricted as in the hillslope zone due to greater groundwater availability. In both of these

zones, however, transpiration had a large influence on θ throughout the vegetative period and in the unsaturated soil profile (mainly where root density was higher). This has been observed in other riparian zones (Bosch et al., 2014; Schume et al., 2004). The influence of transpiration on the decrease in θ was larger under extreme conditions, such as in summer, when transpiration is higher (Nadal-Sala et al., 2017), in drier years, and in the hillslope zone. This is consistent with isotopic analyses in the field. Isotopic analysis of sap from our study site revealed that during summer up to 80% of water transpired by trees can come from the soil (Chapter 4). Other studies have observed trees obtaining 30-90% of their water requirements from the soil (Brooks et al., 2010; Sánchez-Pérez et al., 2008; Snyder and Williams, 2000).

In all riparian zones, exchanges between groundwater and surface water (i.e. larger infiltration and drainage fluxes) increased during dormant periods. During vegetative periods, however, transpiration was the main flux, and capillarity was necessary to supply the water demand. All riparian zones had negative water balances, which increased from the near-stream to the hillslope zone (-55 to -317 mm). These vegetative-period effects on unsaturated soil profiles can decrease GWL, decreasing inputs from groundwater to streams and thus decreasing stream discharge (Barnard et al., 2010; Connor et al., 2013; Lupon et al., 2016c; Moore and Heilman, 2011).

6.4.2. Vegetation N-NO_3^- uptake

We evaluated the influence of plant-root uptake on N-NO_3^- removal in a riparian forest in a Mediterranean climate. We did not consider the denitrification and microbial processes that can occur in riparian soils. Although microbial denitrification is considered the main N-NO_3^- removal process in riparian areas (Hill, 1996; Pinay et al., 2007), it contributes little in Mediterranean areas due to drier conditions and non-anoxic soil limitations (Bernal et al., 2007, Poblador et al., 2017). Denitrification measured in *Font del Regàs* was low (< 4 μg N kg $soil^{-1}$ d^{-1}; Poblador et al., 2017) compared to that measured in temperate regions (up to 2 mg N kg $soil^{-1}$ d^{-1}; Clément et al., 2002). As a riparian area with low human impact, our study site did not have high groundwater N-NO_3^- concentrations (0.39-2.67 mg N-NO_3^- l^{-1}). Concentrations

were similar to those in Mediterranean forested catchments (0.15-3.20 mg N-NO_3^- l^{-1}; Butturini et al., 2003, 2005) and far lower than those in catchments with > 70% of land in agriculture, whose concentrations can reach 15-35 mg N-NO_3^- l^{-1} (Clément et al., 2003; Hefting et al., 2005). Although the model was not calibrated for N-NO_3^- mass balances, its predicted soil N-NO_3^- concentrations were similar to field measurements from other studies at the site (0.09-2.34 mg N-NO_3^- l^{-1}; Lupon et al., 2016b, Poblador et al., 2017).

In all riparian zones, infiltration was the main (> 90%) N-NO_3^- input by mass. This inflow occurred mainly through high infiltration during rainfall events and was evident among temporal patterns and when comparing wet and dry years. Large inputs during rainfall events influenced soil concentrations not only due to infiltration, but also through higher groundwater concentrations due to inputs from the catchment. Other studies of forested Mediterranean catchments also reported higher N-NO_3^- concentrations in streams and groundwater after rainfall events (Bernal et al., 2002; Butturini et al., 2003, 2005). Rainfall events can enhance soil nitrification processes (Lupon et al., 2016b) and can also leach N-NO_3^- that accumulated in the topsoil into groundwater and streams as a result of high net nitrification in riparian areas (Bernal et al., 2003; Hefting et al., 2005; Lupon et al., 2016b). For instance, Bernal et al. (2002) reported concentrations of 14-115 mg N-NO_3^- l^{-1} in soil leaches after rainfall events and that one heavy storm provided 80% of the N-NO_3^- that reached the stream. In the intermediate zone, infiltration had less influence on N-NO_3^- inflow due to higher groundwater N-NO_3^- concentrations, which facilitated higher inflow of N-NO_3^- through capillarity. Differences in groundwater N-NO_3^- concentrations among riparian zones result from a flow path configuration that is parallel with stream flow (unpublished data). Flow path analysis is a relevant measure of catchment vulnerability to pollutant transport or removal for different degrees of human disturbance. Differences observed among sites are strongly influenced by topography and geomorphology, highlighting the need for worldwide analysis to address catchment behavior (Meixner et al., 2016). At the local scale, near-stream groundwater may be influenced more by an exchange with stream water that

is regulated by groundwater-stream interactions and surface inputs, while the hillslope may receive N-NO_3^- fluxes from the upland-connected groundwater and surface inputs. This indicates the importance of hydrological and biogeochemical connectivity between streams and adjacent forested riparian zones (Laudon et al., 2016; Lupon et al., 2016a; Petrone et al., 2007; Pittroff et al., 2017).

Accordingly to distinctly higher N-NO_3^- inflow in the unsaturated soil profile, the intermediate zone mobilized more N-NO_3^- than the near-stream and hillslope zones. Although transpiration was higher in the near-stream zone, it had greater influence on the water balance in the hillslope zone. More N-NO_3^- was removed from unsaturated soil in the intermediate zone via plant-root uptake due to high concentrations in the groundwater. In the near-stream zone, where the GWL is shallower, drainage has slightly more influence on N-NO_3^- removal from unsaturated soil than vegetation uptake. Plant-root uptake was the main sink for N-NO_3^- from the intermediate and hillslope zones. High correlation between plant-root N-NO_3^- uptake and N-NO_3^- concentrations leached into the stream has been reported (Schade et al., 2005), highlighting the influence of vegetation on N retention. Riparian areas similar to *Font del Regàs* (~25 m wide) can remove > 75% of N-NO_3^- via plant uptake before it is exported to the stream (Mayer et al., 2005). Although some authors have reported ~30% reductions via plant N-NO_3^- uptake when groundwater is deep (Hefting et al., 2004; Mayer et al., 2005), based mainly on groundwater concentrations, others have highlighted the considerable ability of plant uptake to reduce N-NO_3^- in unsaturated soils in a variety of conditions (Gerber and Brookshire, 2014).

Temporal patterns of soil N-NO_3^- concentration depended on vegetative periods in the intermediate and hillslope zones, decreasing soil N-NO_3^- concentrations when transpiration peaked. In contrast, the near-stream zone had low N-NO_3^- concentrations throughout the year due to a stronger connection between saturated and unsaturated soil. Denitrification, four times as high in the near-stream zone as in the other riparian zones (Poblador et al., 2017), could also have removed N. Despite plant uptake, annual mass balances

suggest a ~ 1 g $N\text{-}NO_3^-$ m^{-2} increase in all riparian soils. This might lead to N-enrichment of riparian soil, because soil denitrification rates at the site ranged from 0.41-4.93 mg N m^{-2} (Poblador et al., 2017). Ranalli and Macalady (2010) observed an increase in $N\text{-}NO_3^-$ removal during the vegetative period, decreasing $N\text{-}NO_3^-$ concentrations to nearly zero. However, some authors do not consider N uptake by deciduous vegetation as N removal, since N returns to the soil at the end of the vegetative period in the form of leaf litter that can be mineralized and leached into the groundwater and the stream (Hefting et al., 2005).

6.4.3. Influence of climate change

The modeled climate projection predictions are based on assumptions of transpiration rates and GWL, and no differences were observed among IPCC scenarios. No differences in θ or soil $N\text{-}NO_3^-$ were predicted when we assumed constant transpiration partitioning over time (i.e. 80%, 70%, and 60% of PET in the near-stream, intermediate, and hillslope zones, respectively). Several factors can influence future transpiration rates. For certain species, higher temperatures can increase their transpiration rates when water availability is not limiting, and other species may have highly adaptive strategies (i.e. increase in water use efficiency or rooting depth) or they can be replaced by other species with lower water requirements (Moore and Heillman, 2011; Schenk, 2008). For instance, Nadal-Sala et al. (2017) observed high transpiration for most tree species at the study site when water availability was not limiting. However, F. excelsior individuals in the hillslope zone already showed transpiration restrictions due to a decrease in soil water availability during summer. Consequently, we also ran the model assuming that climate change decreased transpiration rates by 20% (Luo et al., 2008). In this case, θ decreased in all riparian zones, and the resulting increase in soil $N\text{-}NO_3^-$ was caused by lower plant-root uptake. In this assumption of decreased transpiration, the final soil $N\text{-}NO_3^-$ was higher in the hillslope zone due to lower transpiration.

A potential decrease in GWL may also decrease θ throughout the entire soil profile. The GWL depletion projected may strongly decrease transpiration rates, especially in the hillslope zone, where disconnection between

groundwater and root systems can severely decrease the ability of vegetation to regulate soil N-NO_3^- removal and increase soil N-NO_3^- concentrations. Similar to our results, some authors have reported lower plant-root N-NO_3^- uptake under drier conditions due to lower transpiration rates and reduced N-NO_3^- mobility in drier soil (Rennenberg et al., 2009). This increase in soil N-NO_3^- can be exacerbated by acceleration of soil N processes due to higher temperatures (Brookshire et al., 2011). Climate projections in the same area, however, suggested that nitrification would not be enhanced by higher temperatures, since limited water availability would prevent it (Lupon et al., 2015). Nonetheless, more sporadic rainfall events predicted in the climate change scenarios may promote the inflow of N at regular intervals (Lupon et al., 2016b).

Spatial variation in the influence of climate change was also evident at our study site, decreasing vegetation regulation of soil N-NO_3^- removal as water availability decreased. This indicates possible reduction in the effectiveness of riparian zones at removing N, due not only to lower rates of vegetation uptake, but also because of a decrease in their effective areas (i.e. near-stream and intermediate zones in our riparian plot). For N-NO_3^- balances, our results suggest that lower plant-root uptake can increase soil N-NO_3^- concentrations. This decrease in uptake can cause N saturation, which can leach into the stream (Brookshire et al., 2011), especially in semiarid areas where microbial denitrification is low, changing the riparian area from an N sink to an N source.

6.5. Conclusions

Mediterranean riparian areas are systems with high spatial heterogeneity in water availability and soil properties over short distances (~25 m wide), mainly due to large differences in soil and bedrock materials and the GWL from near-stream to hillslope edges. This spatial heterogeneity helps to better understand transpiration as a key process for water fluxes in these areas. Vegetation transpiration is a main driver of riparian water fluxes, which have a large influence on θ. However, transpiration is strongly limited by soil water

availability, which is lower at the hillslope edge in riparian areas. Even though $N\text{-}NO_3^-$ mass balances depend strongly on $N\text{-}NO_3^-$ inputs (i.e. groundwater $N\text{-}NO_3^-$ concentration), plant-root uptake plays a key role in N retention and turnover in Mediterranean riparian areas, especially in zones where the GWL is deeper and dry conditions lead to almost zero denitrification. Preliminary climate change projections suggest that drier future conditions may decrease riparian plant transpiration and N uptake. This may be detected, especially at hillslope edge, and reduce N removal area. Therefore, future $N\text{-}NO_3^-$ plant uptake in Mediterranean riparian areas might not be sufficient to prevent an increase in soil $N\text{-}NO_3^-$ concentrations, which increases the risk of N leaching from riparian areas into streams. These spatial differences highlight the importance of considering spatial heterogeneity of riparian hillslopes when modeling Mediterranean catchments. More research is needed to understand the extent to which GWLs, and thus the species that depend on them, will change due to climate change.

Acknowledgments

We thank Anna Lupon, Ada Pastor and Lídia Cañas for their invaluable assistance in the field. Financial support was provided by the Spanish Government through the projects MONTES-Consolider (CSD2008-00040-MONTES), MEDFORESTREAM (CGL2011-30590), and MEDSOUL (CGL2014-59977-C3-2). Sílvia Poblador was supported by a FPI Ph.D. fellowship from the Spanish Ministry of Economy and Competitiveness (BES-2012-054572). We also thank site collaborators, including Vichy Catalan and the Catalan Water Agency (ACA) for permission to sample at the *Font del Regàs* catchment. Sílvia Poblador, Santiago Sabaté, and Francesc Sabater are members of the research group FORESTREAM (AGAUR, Catalonia 2014SGR949).

CHAPTER 7

The influence of the invasive nitrogen-fixing *Robinia pseudoacacia* on soil nitrogen availability in a mixed Mediterranean riparian forest

This study investigates the influence of the invasive nitrogen (N)-fixing *R. pseudoacacia* on leaf litter N inputs and soil N availability in a mixed riparian forest plot in NE Spain. We measured annual leaf litter N inputs, decomposition rates, soil N processes, and soil N concentrations at three sections (near-stream, intermediate, and hillslope) across a riparian plot. Moreover, we explored changes in soil N availability associated with the arrival of *R. pseudoacacia* by means of an empirical forest floor model. Leaf litter N content was higher for *R. pseudoacacia* than for non-fixing species. The contribution of *R. pseudoacacia* to annual leaf litter N inputs increased from the near-stream to the hillslope section. However, soil N processing rates and soil N availability were similar among sections. Simulations suggest that soil N availability was higher at the near-stream than at the hillslope section before the arrival of *R. pseudoacacia*. This pattern smoothed down as *R. pseudoacacia* spread across the riparian plot over time. The spreading of *R. pseudoacacia* across the riparian plot contributed to homogenize soil N availability over time. An integrated spatio-temporal view of the invasive process is needed to assess its impact on soil N biogeochemistry.

With permission of: A.Lupon, E. Marti, F. Sabater, S. Sabater and S. Bernal, who are co-authors of this study.

7.1. Introduction

Riparian ecosystems are biogeochemical hot spots, with a high potential to reduce nitrogen (N) loads arriving from adjacent terrestrial lands via biological N assimilation and denitrification (Follstad Shah and Dahm, 2008; Hill, 1996). Nonetheless, the buffer capacity of riparian ecosystems can be altered by human activities that affect riparian hydrology and biogeochemistry such as water extraction, changes in land uses, forest exploitation, and intentionally or unintentionally introduction of exotic species (Asaeda et al., 2015; Castro-Díez et al., 2009; Radtke et al., 2013; Sala et al., 2000b; Tylianakis et al., 2008). In the Iberian Peninsula, riparian zones are upon the most severely threatened terrestrial ecosystems and, in most cases, native vegetation has been either substituted by tree plantations or altered by the establishment of invasive species (Sanz Elorza et al., 2004). However, the extent to which these changes in vegetation can affect the N cycle in riparian zones, and ultimately modify forest N retention, is still poorly understood.

Black locust (*Robinia pseudoacacia*) is one of the most widespread invasive species in the Iberian Peninsula, occupying extensive riparian areas in the northern and eastern part of the Mediterranean region (Sanz Elorza et al., 2004). This N-fixing species is the second most abundant deciduous tree in the world (Boring and Swank, 1984) and an extremely successful invader given its ability to grow in a broad range of soils types and climatic conditions (De Marco et al., 2012). Similar to other N-fixing species, *R. pseudoacacia* produces large quantities of leaf litter with high N content, which can accelerate leaf litter decomposition and increase soil N availability (Malcolm et al., 2008; Rice et al., 2004). Riparian zones have traditionally been considered effective N sinks, despite being already N enriched ecosystems. Therefore, the presence of *R. pseudoacacia* in riparian zones could decrease the ability of these ecosystems to reduce N loads or even enhance the export of N to adjacent aquatic ecosystems (Aber et al., 1998; Buzhdygan et al., 2016; Follstad Shah and Dahm, 2008).

The influence of invasive tree species on soil N cycling does not exclusively depend on the characteristics of the invasive species itself, but also on the intrinsic properties of the ecosystem that colonizes (Castro-Díez et al., 2009; Wolfe and Klironomos, 2005). For instance, leaf litter from *R. pseudoacacia* can increase soil N availability in N limited forests by enhancing soil N mineralization and nitrification (Rascher et al., 2012; Rice et al., 2004). However, its potential to influence soil N cycling in more N enriched ecosystems such as riparian zones remains elusive. Some studies reported increases in soil N availability in riparian zones invaded by *R. pseudoacacia* (Akamatsu et al., 2011; Buzhdygan et al., 2016; Medina-Villar et al., 2015b; Staska et al., 2014), while others suggested that changes are minimal (Castro-Díez et al., 2009; González-Muñoz et al., 2013). Moreover, the influence of invasive species on ecosystem functioning depends on the time elapsed since its establishment. During the first stages of invasion, litter of endogenous species still dominated soil organic matter, and thus, changes on soil nutrient availability may be small. Conversely, long time after the invasion starts, increases in nutrient availability can be reflected both in soils and in the biomass content (Castro-Díez et al., 2009; Vilà et al., 2011). Yet, it is still under debate how much time is needed to observe a noticeable impact of invasive N-fixing species on nutrient cycling in riparian forests, what is ultimately crucial for sound and integrated forest management strategies.

The aim of this study was to investigate the influence of *R. pseudoacacia* on soil N availability in a riparian forest plot in the NE Iberian Peninsula. The native forest was initially composed by one N-fixing (*Alnus glutinosa*) and two non-fixing (*Populus nigra* and *Fraxinus excelsior)* species. *R. pseudoacacia* appeared at least 25 years before our study was conducted. We quantified leaf litter N inputs and decomposition rates for the four tree species, as well as soil N concentrations and cycling (net N mineralization and net nitrification) across the riparian plot. We expected higher leaf litter quality (lower C:N ratios) and faster decomposition rates for *R. pseudoacacia* than for the non-fixing species. Further, we expected differences in soil N processing rates and N availability associated with the spatial distribution of individuals of *R. pseudoacacia* within

the plot. Finally, we developed a simple forest floor model to test weather differences in the density of *R. pseudoacacia* over the invasion process could influence soil N availability, from a pre-invasion stage with only native species to a final stage with a complete replacement of native species by *R. pseudoacacia*.

7.2. Materials and methods

7.2.1. Study site

Font del Regàs is a subhumid Mediterranean catchment located in the Montseny Natural Park, NE Spain (41º50'N, 2º30'E). During the study period, mean annual precipitation (975 ± 146 mm; mean ± SD) and mean annual temperature (14.6 ± 6.7 ºC) fall within the long-term annual average for this region (period 1940-2000; Catalan Metereologic Service). Total inorganic N deposition oscillates between 15-30 kg N ha^{-1} yr^{-1} (period 1983-2007; Àvila and Rodà 2012).

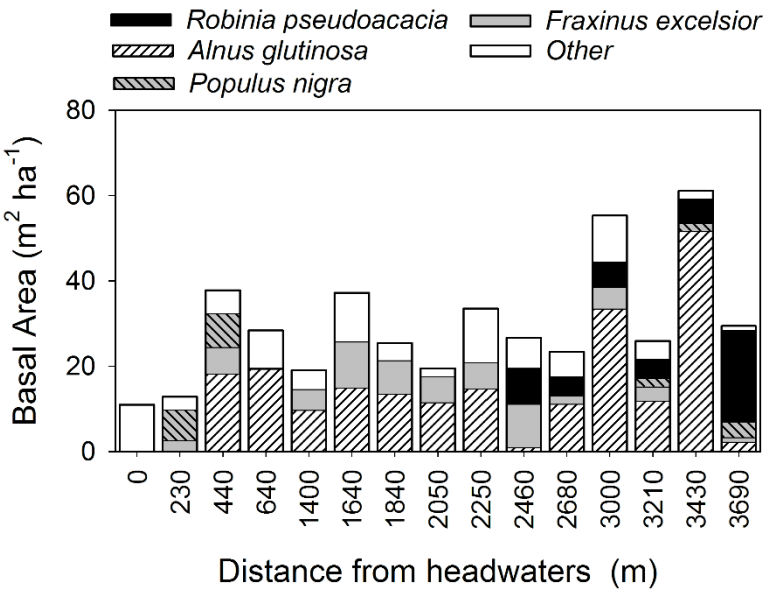

Figure 7.1 Basal area of riparian trees (in m^2 ha^{-1}) from the headwaters to the valley bottom of the *Font del Regàs* catchment. The study plot was the downstream most site. Leaf litter of native species from riparian plots free of *R. pseudoacacia* were collected at 1840 to 2250 m downstream of headwaters. Adapted from Bernal et al. 2015.

The catchment area is 14.2 km^2 and its altitude ranges from ~ 475 m to 1500 m above the sea level (a.s.l.). The riparian zone covers 6% of the catchment area and it consists mainly of three non-fixing species (*F. excelsior*, *P. nigra* and *Platanus x hispanica*) and two N-fixing species (*A. glutinosa* and *R. pseudoacacia*). The relative contribution of *R. pseudoacacia* to the total basal area of riparian trees increases from headwaters (0%) to the valley bottom of the catchment (74%; 820 ind ha^{-1}) (Fig. 7.1). At the valley bottom, the riparian soil (pH ~ 7) is sandy-loam with a 5 cm deep organic layer followed by a 30 cm deep A-horizon (Lupon et al., 2016a).

We selected a well-developed riparian stand (delimiting a sampling plot of 30 m x 25 m) invaded by *R. pseudoacacia* that flanked the stream at the valley bottom of the catchment (475 m a.s.l.). The riparian plot consisted of *R. pseudoacacia*, *P. nigra*, *A. glutinosa* and *F. excelsior* (74%, 13%, 10%, and 3% of the plot total basal area (BA), respectively). Individuals of *F. excelsior* were ca. 45 years old, while individuals of *R. pseudoacacia, A. glutinosa*, and *P. nigra* were younger (ca. 25 years old). *R. pseudoacacia* was present across the riparian plot, yet its density increased from the stream to the hillslope edge. The three native tree species followed a clear spatial segregation depending on their water requirements (Singer et al., 2013). Based on this spatial segregation, we established three sections across the riparian plot. The near-stream section (0-4 m from the stream edge) occupied 16 % of the riparian plot and it was composed by *A. glutinosa, P. nigra,* and *R. pseudoacacia* (45%, 33%, and 22% of the section's BA). The intermediate section (4-7 m from the stream edge) occupied 12% of the riparian plot and it was composed by *P. nigra* and *R. pseudoacacia* (29% and 71% of the section's BA). The hillslope section (7-25 m from the stream edge) was the largest (72% of the riparian plot) and it was composed by *F. excelsior* and *R. pseudoacacia* (7% and 93% of the section's BA) (Fig. 7.2a).

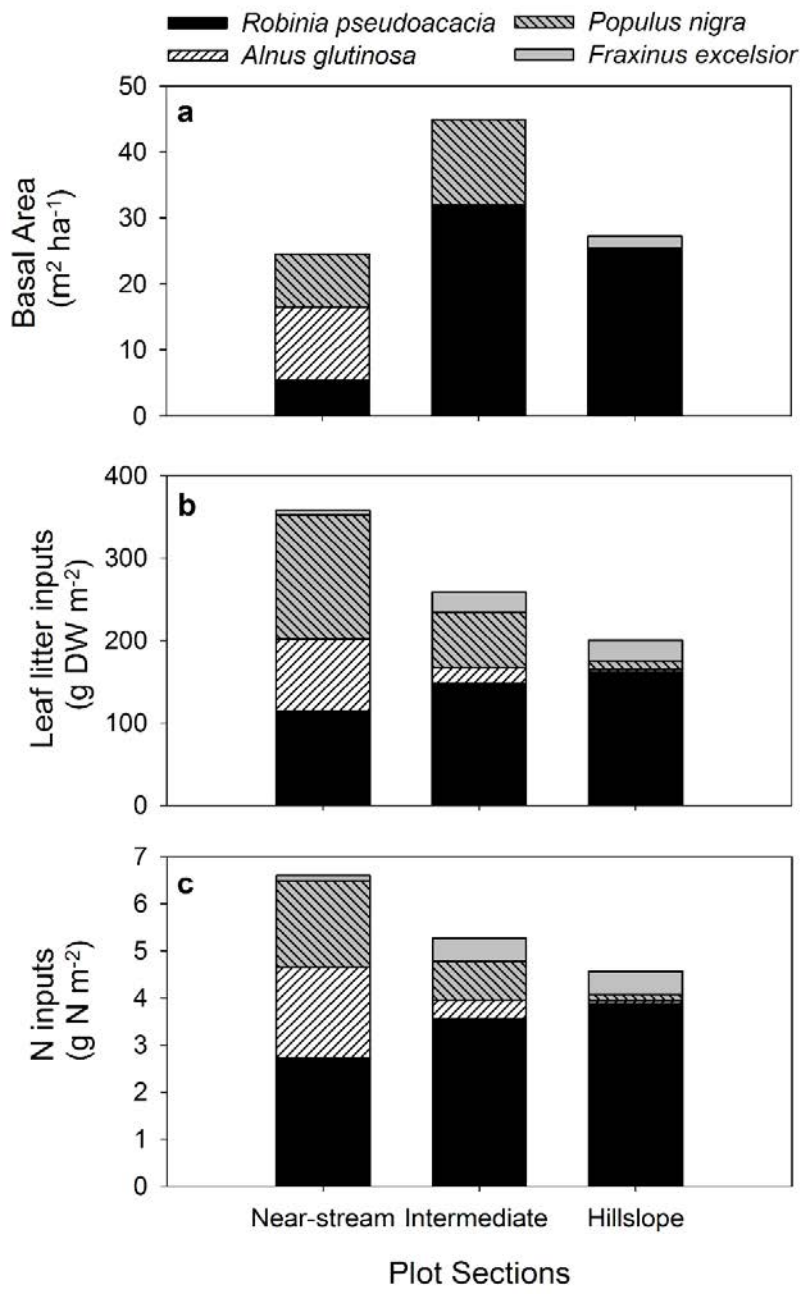

Figure 7.2. Contribution of *R. pseudoacacia* (black), *A. glutinosa* (hatched white), *P. nigra* (hatched grey), and *F. excelsior* (grey) to (a) the total basal areal of riparian trees (in m2 ha-1), (b) leaf litter inputs to the forest floor (in g dw m-2), and (c) annual leaf N inputs to the forest floor (in g N m-2) for each section.

7.2.2. Soil physicochemical properties and N cycling rates

From March 2010 to February 2011 (18 sampling dates), 4 soil samples (0-10 cm depth, including O- and A- horizons) were collected randomly from each section every 2-4 weeks to analyze soil physicochemical properties. Soil samples were taken with a 5-cm diameter core sampler and placed gently into plastic bags after carefully removing the litter layer. Before laboratory analyses, soil samples were carefully homogenized. Close to each soil sample, we performed *in situ* soil incubations to measure net N mineralization and net nitrification rates (NNM and NN, respectively; both in mg N kg $soil^{-1}$ day^{-1}). For this purpose, a second soil core (0-10 cm depth) was taken, placed in a polyethylene bag, and buried at the same depth for 12-15 days (Eno 1960). Finally, volumetric soil moisture (in %) and soil temperature (in ºC) at 10-cm depth were measured at each location by using a TDR sensor (HH2 Delta-T Devices Moisture Meter) and a temperature sensor (CRISON 25), respectively.

Pre-incubation soil samples were sieved and the fraction < 2 mm was used for measuring the relative content of organic matter (SOM), carbon (C) and N (all in %) following standard procedures (Page et al. 1982). In addition, we extracted 5 g of field-moist soil for both pre- and post-soil incubation samples with 50 ml of 2 M KCl (1 h shacking at 110 r.p.m. and 20ºC). The supernatant was filtered (Whatman GF/F 0.7 μm pore diameter) and analyzed for ammonium (NH_4^+) and nitrate (NO_3^-) following standard procedures (Page et al., 1982). At each sampling point, NNM and NN rates were calculated by subtracting pre-incubation mineral N (NH_4^+ + NO_3^-) and NO_3^- from post-incubation values (Eno 1960). Then, we calculated the nitrification fraction (i.e., NN/NNM) as a proxy of the fraction of NH_4^+ that was used by nitrifiers (Pardo et al. 2006). More details about field and laboratory analyses can be found in Lupon et al. (2016).

7.2.3. Annual leaf litter production and decomposition rates

From 2011 to 2012 (i.e. two vegetative years), we quantified the temporal and spatial pattern of leaf litter inputs to the forest floor by using collector baskets of 1-mm mesh, which allow rapid drainage of rainwater and reduce weight

loss by leaching. We placed 10 baskets (1 m^2 each) along each section (n = 30 in total), covering 5% of the plot area. Twice a month, leaf litter was collected from each basket and separated by tree species. At the laboratory, dry weight of leaf litter (DW, in g m^{-2}) was measured after oven-drying leaf samples (60ºC, 48-72 h) until constant mass. For each tree species, a composite of samples collected during the peak of leaf litter fall in autumn 2012 was analyzed for C and N content following the same procedure than soil samples. We calculated mean annual leaf litter inputs (in g DW m^{-2} $year^{-1}$) to the riparian forest floor by summing up the leaf litter trapped in the collectors over the whole year. The N inputs to the forest floor were calculated by multiplying mean leaf litter DW by the mean relative N content for each tree species separately. Values were referred to the total surface covered by the collector baskets, both for each section separately and for the whole riparian area.

For each tree species, leaf litter decomposition rates (k, in $year^{-1}$) were measured from January to December 2011 by using the *in situ* litterbag technique. Five litter bags per species were collected at day 7, 14, 28, 56, 143, and 368. After collection, litter content was dried and weighted. For each tree species, the loss of weight was adjusted to an exponential decay model to calculate the decomposition rate (Olson, 1963).

7.2.4. Description of the forest floor model and lead litter fall scenarios

To evaluate the potential contribution of *R. pseudoacacia* to soil N availability, we used a simple empirical model based on first order kinetics (Olson 1963). The model was tree species specific, and thus, allowed to calculate the contribution of each tree species to N availability in the forest floor on an annual basis. We approximated the input/output fluxes to and from the forest floor with a single pool model for each riparian section and tree species similar to Bernal et al. (2012). For each riparian section, changes in leaf litter in the forest floor pool over time (dL_i/dt) were described by:

$$dL_i/dt = f_i\,(t) - k_i\,L_i, \qquad \text{(Eq. 7.1)}$$

where L is the amount of leaf litter in the forest floor (in g DW m^{-2}), k is the decomposition rate (in $year^{-1}$), and $f(t)$ is the input of leaf litter to the forest floor at each time step (t) (in g DW m^{-2} $year^{-1}$) for each species (i). We assumed that the forest floor was at steady state, so that the stock of leaf litter (L) was constant over time and the input of leaf litter equaled the outputs:

$$k_i L_{i,} = f_i (t) \quad \text{(Eq. 7.2)}$$

Then, we calculated the annual input of NO_3^- to the soil based on stoichiometric principles. For each species (i), the potential input of N to the mineral soil was calculated by multiplying its leaf litter N content by its f_i. Finally, for each tree species and section, we partitioned the mineralized N pool into NH_4^+ and NO_3^- by using the average NN/NNM measured at each section during the study period.

We evaluated the potential influence of *R. pseudoacacia* on soil N availability by considering three different scenarios. In the Pre-invasion scenario, *R. pseudoacacia* was absent and only native species (*A. glutinosa*, *P. nigra*, *F. excelsior*) were present. The Mid-invasion scenario was referred to the present situation, as a process of establishment and spread of *R. pseudoacacia.* The Replacement scenario simulated the total substitution of native species by *R. pseudoacacia.* For the Mid-invasion scenario, f_i was measured from the leaf litter collected during the study period. To infer f_i for the Pre-invasion and Replacement scenarios, we calculated the Leaf Area Index (LAI, in m^2 m^{-2}) for each species at each riparian section with:

$$LAI_i = f_i(t) / LMA_i \quad \text{(Eq. 7.3)}$$

where LMA_i is the area specific leaf dry weight (in mg cm^{-2}) (Poorter et al 2009, Gutschick and Wiegel 1988) (Table 7.1, E.1). We assumed no changes in total stand *LAI* between scenarios because the forest had already a closed crown (Michelot et al., 2011). For the Pre-invasion scenario, we considered that each native species contributed to total stand *LAI* in the same proportion than in the Mid-invasion scenario. The Replacement scenario was monospecific (only *R. pseudoacacia*) and thus *LAI* for this species equaled the total *LAI* (Table E.1). For

each scenario, we used Eq.3 to calculate $f_i(t)$ at each riparian section. The potential NO_3^- available was calculated using the N content in leaf litter and the nitrification factor, as described above. Note that for the Mid-invasion and Replacement scenarios, leaf litter N contents were those measured in the study riparian plot. For the Pre-invasion scenario, we used the N content in leaf litter collected from riparian plots free of *R. pseudoacacia* (Fig. 7.1, Table E.1). In order to calculate the model uncertainties, we considered standard deviation of f_i, specific leaf litter N content, and soil N processes to estimate variability in leaf N inputs and soil N available for all scenarios and sections.

Table 7.1 Leaf and soil parameters used in the forest soil model and invasion scenarios: acronym, units and description.

Acronym	Units	Description
L	g DW m^{-2}	Stock of leaf litter in the forest floor
k	$year^{-1}$	Leaf litter decomposition rate
f	g DW m^{-2} $year^{-1}$	Leaf litter input to the forest floor
N	%	Leaf nitrogen content per dry weight
NN/NNM	---	Nitrification fraction: proxy of NH_4^+ used by nitrifiers
LAI	m^2 m^{-2}	Leaf area index: m^2 leafs in the crown per m^2 soil
LMA	mg cm^{-2}	Leaf mass area: specific leaf dry weight per specific leaf area

7.2.5. Statistical data analysis

All the statistical analyses were carried out with the R 2.15.1 statistical software (packages *lme* and *multcomp*) (R-project 2012). We analyzed differences in leaf litter properties (N content, C:N ratio, and *k*) among the tree species using one-way ANOVA tests followed by Tukey HSD *post-hoc* tests (Zar 2010). Moreover, we explore differences in soil physicochemical properties (moisture, temperature, SOM, and C:N ratio) and microbial N processing rates (NNM, NN, and NN/NNM) among riparian sections by using a linear mixed-model ANOVA test. We used sections as fixed effect and time as random effect. For each model, differences between sections were tested with *post-hoc* Tukey contrasts. Finally, differences in simulated leaf litter N inputs and soil N availability among scenarios were also analyzed for each riparian section separately by using one-way ANOVA tests followed by Tukey HSD *post-hoc* tests (Zar, 2010). In all cases, residuals were tested for normality using a

Shapiro-Wilk test and homogeneity of variance was examined visually by plotting the predicted and residual values. When necessary, we normalized data using log or square-root transformations to meet parametric assumptions. In all analyses, results were considered significant when p-value was < 0.05.

7.3. Results

7.3.1. Annual leaf litter production and decomposition

During the study period, total annual leaf litter input was 313 ± 21 g DW m^{-2}. *R. pseudoacacia* was the major contributor to annual leaf litter production (52%), followed by *P. nigra* (25%), *A. glutinosa* (15%), and *F. excelsior* (7%) (Table 2). Leaf litter inputs provided 6.4 g N m^{-2} to the forest floor, being *R. pseudoacacia* and *F. excelsior* the highest (61%) and lowest (8%) contributors to leaf litter N, respectively (Table 2).

Leaf litter N content was higher for N-fixing species (2.39% and 2.20% for *R. pseudoacacia* and *A. glutinosa*, respectively) than for *P. nigra* (1.22%). Leaf litter C and N contents differed between species (Table 2): *P. nigra* showed the highest C:N ratio and the lowest N content, while *R. pseudoacacia* exhibited the highest N content. Leaf litter k differed among species: *F. excelsior* decomposed the fastest (0.69 $years^{-1}$), while *P. nigra* was the slowest (0.25 $years^{-1}$). Leaf litter k was 0.29 and 0.56 $years^{-1}$, for *R. pseudoacacia* and *A. glutinosa* respectively (Table 2).

7.3.2. Spatial patterns of leaf litter inputs and soil N availability

Leaf litter inputs were heterogeneously distributed across the riparian plot. Most of the leaf litter entered to the forest floor at the near-stream section (44%), while the intermediate and hillslope sections received 32% and 24% of total leaf litter, respectively. The contribution of each species to leaf litter inputs varied among riparian sections following the spatial distribution of tree species (Fig. 7.2b). At the near-stream section, *P. nigra* and *A. glutinosa* contributed 42% and 24% to leaf litter inputs, respectively. At the intermediate section, the contribution of these two species decreased to 26% and 7%, respectively. *F. excelsior* contributed by 12% to leaf litter inputs at the hillslope

sections, while its contribution was < 10% at the near-stream and intermediate sections. The contribution of *R. pseudoacacia* to leaf litter inputs was the highest at the hillslope section (81%), where it was the dominant tree species (Fig. 7.2a, b). The relative contribution of each tree species to the forest floor N inputs was similar to those observed for specific leaf litter inputs. Yet, N-fixing species contributed to N input to a major extend than to leaf litter inputs, especially *R. pseudoacacia* (Fig. 7.2c).

Table 7.2 C:N molar ratio, N content, decomposition rate (k), and annual inputs of leaf litter and N contained in leaf litter for the four studied riparian tree species. The annual inputs of leaf litter (DW) and N in leaf litter are shown by soil surface area. For leaf litter characteristics, values are mean ± standard deviations. For the amount of N in leaf litter, the variance represents the standard deviation of N content in leaves. For each leaf litter characteristic, different letters indicate statistical significant differences between species (Tukey HSD, p-value < 0.05). For each variable, n = 17, 13, 17 and 19 for R. pseudoacacia, A. glutinosa, P. nigra and F. excelsior, respectively.

	R. pseudoacacia	*A. glutinosa*	*P. nigra*	*F. excelsior*
Leaf litter characteristics				
C:N	23.21 ± 0.24 ^{A}	26.20 ± 8.47 ^{A}	45.49 ± 12.48 ^{B}	25.51 ± 2.00 ^{A}
N (%)	2.39 ± 0.24 ^{A}	2.20 ± 0.39 ^{AB}	1.22 ± 0.33 ^{C}	2.04 ± 0.17 ^{B}
k (year $^{-1}$)	0.29 ± 0.03 ^{A}	0.56 ± 0.21 ^{AB}	0.25 ± 0.17 ^{A}	0.69 ± 0.18 ^{B}
Annual leaf litter input				
g DW m^{-2} year^{-1}	163.01 ± 12.71	45.72 ± 9.91	79.49 ± 20.25	24.09 ± 3.93
g N m^{-2} year^{-1}	3.90 ± 0.03	1.01 ± 0.04	0.97 ± 0.07	0.49 ± 0.01

During the study period, there were no differences in soil temperature, SOM, and mineral N content among the three riparian sections. Both intermediate and hillslope sections presented low soil moisture (intermediate = 21.74 ± 7.63%, hillslope = 20.57 ± 6.57%) and low C:N ratios (intermediate = 11.95 ± 0.36, hillslope = 11.93 ± 0.37) compared to the near-stream section (water content = 26.38 ± 8.71%, C:N ratio= 15.58 ± 2.00). Soil N processes (NNM and NN) as well as the nitrification factor (NN/NNM) were similar among the three riparian sections (Table 7.3).

Table 7.3 Soil volumetric moisture, soil temperature, soil organic matter (SOM), soil C:N molar ratio, soil N content (total N, NH_4^+ and NO_3^-), net N mineralization (NNM), net nitrification (NN) and nitrification fraction (NN/NNM) for the three riparian sections during the study period. Values are mean ± standard deviations. Different letters indicate significant differences between sections (Tukey HSD, General Linear Hypothesis Testing, p-value < 0.05). For each variable, n = 67, 68, and 64 for the near-stream, intermediate, and hillslope sections, respectively.

	Near-stream	Intermediate	Hillslope
Soil Properties			
Moisture (%)	26.38 ± 8.71^A	21.74 ± 7.63^B	20.57 ± 6.57^B
Temperature (ºC)	12.9 ± 6.9 ^{A}	13.1 ± 6.8 ^{A}	13.1 ± 6.9 ^{A}
SOM (%)	11.17 ± 3.75^A	11.62 ± 3.39^A	10.67 ± 3.31^A
C:N	15.58 ± 2.00^A	11.95 ± 0.36^B	11.93 ± 0.37^B
Total N (%)	0.37 ± 0.04 ^{A}	0.36 ± 0.09 ^{A}	0.35 ± 0.06 ^{A}
NH_4^+ (mg N kg^{-1})	10.6 ± 7.5 ^{A}	10.3 ± 6.7 ^{A}	8.9 ± 6.9 ^{A}
NO_3^- (mg N kg^{-1})	6.8 ± 4.3 ^{A}	8.6 ± 5.1 ^{A}	7.5 ± 3.9 ^{A}
Microbial Processes			
NNM (mg N kg^{-1} d^{-1})	1.30 ± 0.75^A	1.23 ± 0.70^A	1.08 ± 0.50^A
NN (mg N kg^{-1} d^{-1})	1.04 ± 0.47^A	0.94 ± 0.37^A	1.08 ± 0.40^A
NN/NNM	1.07 ± 0.76^A	0.89 ± 0.41^A	1.16 ± 0.58^A

7.3.3. Changes in leaf litter inputs and soil N availability under different forest scenarios

According to our simulations, total leaf litter inputs to the forest floor differed among the scenarios considered. At plot scale, leaf litter N inputs decreased from Pre-invasion to Mid-invasion (-11%) and to Replacement scenarios (-13%) (Table E.2). Similarly, the three riparian sections showed higher leaf litter N inputs at the Pre-invasion scenario than at both the Mid-invasion and Replacement scenarios (ANOVA; $p < 0.05$) (Fig. 7.3, Table E.2).

Yet, simulated declines in leaf litter N inputs from the Pre-invasion to the Replacement scenarios were more pronounced for the near-stream section (from 8 to 6.8 g N m^{-2} $year^{-1}$, respectively) than for the intermediate (from 6.6 to 5.8 g N m^{-2} $year^{-1}$) and hillslope (from 5.6 to 4.9 g N m^{-2} $year^{-1}$) sections. Regarding soil N availability, the riparian plot showed a 13% decrease from the Pre-Invasion to the Replacement scenario. The most marked declines occurred at the near stream section, were soil N availability decrease by 15% between the Pre-invasion and Replacement scenarios. Yet, there were no

statistically significant differences in simulated soil N availability between the Pre-invasion and the other two scenarios for any of the three riparian sections (ANOVA; $p > 0.05$) (Fig. 7.3, Table E.2).

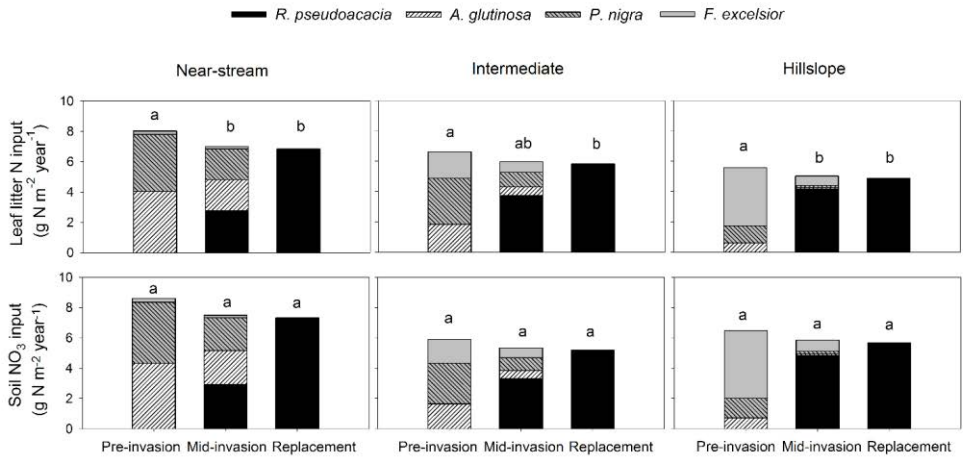

Figure 7.3 Contribution of each riparian tree species to annual leaf litter N input to the forest floor (top panels) and corresponding soil nitrate input (bottom panels) for the three scenarios considered: riparian plot free of R. pseudoacacia (Pre-invasion), present situation (Mid-invasion), and only presence of R. pseudoacacia after exclusion of all native species (Replacement). The simulations are shown separately for each riparian section. Letters indicate differences among scenarios within each riparian section (ANOVA, $p < 0.05$).

7.4. Discussion

This study aimed to investigate the influence of the N-fixing invasive species *R. pseudoacacia* on the soil N cycling and soil N availability in a mixed Mediterranean riparian forest. The study plot was within the Natural Park of the Montseny Mountains, and thus, had a relatively low human influence. Nevertheless, the fact that individuals of *R. pseudoacacia*, *A. glutinosa*, and *P. nigra* had the same age (~25 years old; Poblador, unpublished data) suggests that the introduction of *R. pseudoacacia* in the study plot was either intentionally or at least facilitated by the clear cutting of the riparian forest at the valley bottom of the catchment. After 25 years from its arrival, the presence of *R. pseudoacacia* was conspicuous across the study plot, and contributed to > 75% of the total basal area of riparian trees. Moreover, its leaf litter N content

was high (2.4%), especially compared to the two non-fixing native species (< 2.0%). Consequently, *R. pseudoacacia* was responsible for > 60% of the N entering to the riparian forest floor via leaf litter (39 kg N ha^{-1} $year^{-1}$). This value is similar to those reported for other riparian forests with similar *R. pseudoacacia* densities (15.3 - 47.86 kg N ha^{-1} $year^{-1}$; (Boring and Swank, 1984; Buzhdygan et al., 2016; Medina-Villar et al., 2015b), though far from the 200 kg N ha^{-1} $year^{-1}$ measured for other N-fixing species as *Alnus rubra* (Binkley et al., 1994).

Given the potential of *R. pseudoacacia* to fix N from the atmosphere, one would expect increases in leaf litter N inputs associated with the spread of this species. However, our model simulations suggested that the introduction and spread of *R. pseudoacacia* contributed to decrease leaf litter N inputs compared to the Pre-invasion conditions. This pattern could be a consequence of the low leaf mass area of *R. pseudoacacia* (6.2 mg cm^{-2}) compared to the other three native species (7.7 - 11.3 mg cm^{-2}). This difference could have caused an overall decrease in leaf litter mass inputs from the Pre-invasion to the Mid-invasion and Replacement scenarios, and the consequent decrease in N inputs. In the same way, Gonzalez-Muñoz et al. (2013) pinpointed the low leaf litter mass produced by *R. pseudoacacia* individuals compared to native species with similar basal area in another Mediterranean riparian forest in Spain. The same study reported lower N availability in riparian soils under the presence of *R. pseudoacacia*. Similarly, our simulations suggested decreases in soil N availability between the Pre-invasion and Replacement scenarios, though differences were small (~15%) and not statistically significant. The capacity of *R. pseudoacacia* to fix N is the highest during intermediate succession stages, while both N fixation and soil N stocks decrease as tree stands mature (Benesperi et al., 2012; Boring and Swank, 1984; Motta et al., 2009). Thus, it is likely that soil N availability in the study plot could decrease to a larger extend in the future if individuals of *R. pseudoacacia* get older and fix less atmospheric N.

We found that *R. pseudoacacia* was not equally distributed across the riparian plot; individuals tended to aggregate in the intermediate and hillslope sections,

while the basal area of this species was low at the near-stream edge. However, leaf litter inputs of *R. pseudoacacia* were evenly distributed throughout the plot, and thus, the contribution of this species to leaf litter N inputs to the forest floor was similar among the three sections. When considering all the species together, we observed that leaf litter N inputs increased from the hillslope to the near-stream section, likely because the later section included (i) *P. nigra*, the species with the highest production of leaf litter, and (ii) the two N-fixing species with the highest N content in leaf litter. The spatial pattern exhibited by leaf litter N inputs was not resembled by soil N processes. In fact, we found no differences in soil N mineralization and nitrification rates nor in soil inorganic N content among the three riparian sections despite the substantial differences in species composition. Concordantly, Castro-Díez et al. (2009, 2012) reported no differences in the potential N mineralization nor in the mineral N content of riparian soils below native and exotic N-fixing trees. In our case, similar soil N availability across the riparian plot could result from a generalized N enrichment of soils by root and nodule exudates at the intermediate and hillslope sections where *R. pseudoacacia* predominated (Janzen, 1990; Tateno et al., 2007; Uselman et al., 1999; Vítková et al., 2015). Yet, this explanation would contradict other studies suggesting that leaves of some *Acacia* N-fixing species slow down decomposition and mineralization because of high concentration of lignin or polyphenols (Castro-Díez et al., 2009; Knops et al., 2002; Yelenik et al., 2007). Alternatively, the lower than expected soil N content in the near-stream section could be attributed to higher denitrification rates (Poblador et al., 2017) or to hydrological N losses towards the stream (Berthold, 2005; Buzhdygan et al., 2016; Lupon et al., 2016a; Williard et al., 2005). Another factor that could contribute to hold down soil N at the near-stream section could be the slow decomposition exhibited by *P. nigra*, one of the species contributing the most to leaf litter in this section. Low decomposition rates could be related to the content of lignin, which is high in *P. nigra* (33- 47%) leaves compared to *R. pseudoacacia* (15-30%), *A. glutinosa* (4-19%) and *Fraxinus spss* (6-22%) (Alonso et al., 2010; Chauvet, 1987; Ferreira and Graça, 2016; Jacob et al., 2010; Medina-Villar et al., 2015a).

The consequences of invasive N-fixing species on the soil N cycle of invaded ecosystems remains elusive. In N poor ecosystems, previous studies usually show increases in soil N processes and the availability of mineral N forms with the establishment of invasive N-fixing species (Hellmann et al., 2011; Malcolm et al., 2008; Vítková et al., 2015). Yet, studies conducted in more N enriched ecosystems such as riparian soils have shown either increases (Akamatsu et al., 2011; Medina-Villar et al., 2015b) or no changes (Castro-Díez et al., 2009; González-Muñoz et al., 2013) in soil N availability. In our case, results suggested that the introduction of *R. pseudoacacia* contributed to homogenize soil N availability across the riparian plot by increasing soil N concentrations at the intermediate and hillslope sections. First, we found similar soil N mineralization and nitrification despite the three sections had different species composition and leaf litter inputs. Second, our results suggest that leaves of non-fixing native species were already enriched in N because leaves of *F. excelsior* exhibited higher N content (2.04%) in *Font del Regàs* than in non-invaded riparian forests (0.8 - 1.5 %) (Alonso et al., 2010; Langenbruch et al., 2012; Medina-Villar et al., 2015a) as well as in other individuals of the same species located upstream of the invaded plots (1.8 %, Table S1). Similarly, Hellmann et al. (2011) also reported an increase in foliar N content of native species when the N-fixing species *Acacia longifolia* was present. Our results suggest that 25 years was time enough for *R. pseudoacacia*, to enrich with atmospheric N riparian forest floor sections that were originally out of the influence of N-fixing species. Yet, further studies would be needed for assessing whether this invasive species will further expand in *Font del Regàs*, and the extent to which it will contribute to increase riparian soil N stocks. Some authors consider *R. pseudoacacia* as an intermediate successional species that would finally be substituted by autochthons species, while other studies show that *R. pseudoacacia* has been naturalized in many regions of climates across the globe (Vítková et al., 2015; Weber, 2003). Our study highlights that the impact of invasive tree species such as *R. pseudoacacia* on soil N biogeochemistry needs to be assessed from both a temporal and spatial perspective.

Acknowledgments

We are thankful to Alfons Casalé and Abdellah Bougmar for their invaluable assistance in the field. Special thanks to V. Ramon Vallejo for helpful comments on the final version of the manuscript. Financial support was provided by the Spanish Government through the projects MONTES-Consolider (CSD2008-00040-MONTES), MEDFORESTREAM (CGL2011-30590), NICUS (CGL-2014-55234-JIN), and MEDSOUL (CGL2014-59977-C3-2). Sílvia Poblador was supported by a FPI PhD fellowship from the Spanish Ministry of Economy and Competitiveness (BES-2012-054572). Anna Lupon was supported by a Kempe Foundation post-doctoral grant (Sweden). We also thank site cooperators, including Vichy Catalan and the Catalan Water Agency (ACA) for permission to sample at the *Font del Regàs* catchment. Sílvia Poblador, Anna Lupon, Santiago Sabaté, and Francesc Sabater are members of the research group FORESTREAM (AGAUR, Catalonia 2014SGR949).

CHAPTER 8

General Discussion

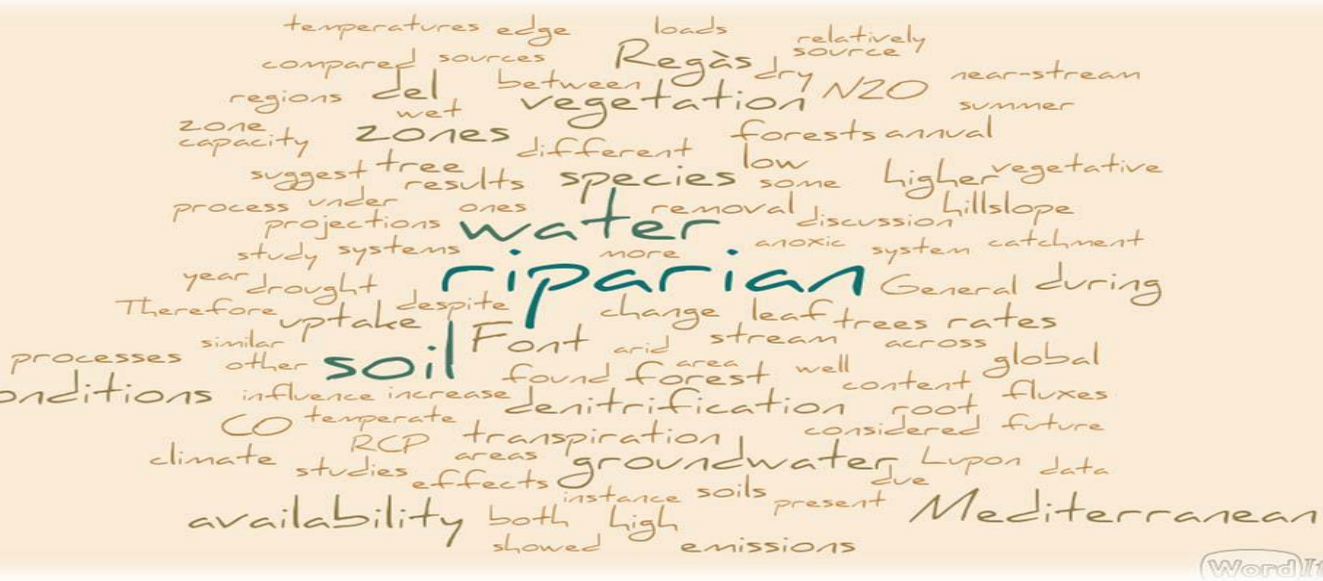

8.1.Introduction

It is well recognized that riparian zones are hotspots of N processes in catchments due to their role in reducing N loads arriving from uplands and adjacent agricultural fields, just before they could reach the stream. The role of riparian vegetation for N removal could become more important in regions where denitrification rates are particularly weak, as the Mediterranean one (Bernal et al., 2007). In this section we discuss the sensitivity of riparian trees to water availability and the implication of Mediterranean riparian forest in processing N. We also discuss how global change may influence the Mediterranean riparian processes. For that, we compared our results with a review of studies carried out in riparian zones across the globe determining water sources of riparian vegetation (Table F.1), soil denitrification rates (Table F.2), and soil CO2 and N2O emissions (Table F.3 and F.4, respectively).

There is increasing published information on climate effects on tree growth and performance, however too little focus has been addressed to the riparian vegetation case. Even though, it is well recognized its relevance on many aspects such as N removal, floods control, and stream biogeochemistry control (Clément et al., 2003; Lupon et al., 2016c; Schade et al., 2005). In this dissertation we have combined ecophysiology and soil biogeochemistry knowledge to achieve our goals. Moreover, we have applied empirical and modeling approaches in order to examine in detail how water availability modifies tree's performance and soil biogeochemistry. Furthermore, we inferred how climate change would affect riparian trees and soil compartments, and to what extend riparian soil might switch from a N sink to a source.

The results presented in this thesis show how water availability governs both compartments separately (vegetation and soil) and the interaction between them in Mediterranean riparian zones. In this general discussion three issues are evaluated: (i) riparian trees dependence on water availability, (ii) the influence of water availability on riparian soil N cycle and (iii) how the global change might affect the Mediterranean riparian forest.

8.2. Riparian trees dependence on water availability

To our best knowledge, until now research has been mainly focused on how tree species from uplands deal with water scarcity (Jump et al., 2006; Martínez-Sancho et al., 2018), but little is known about the effects of water availability on riparian tree species. However, we found some hints that suggest that riparian trees are already suffering from climate variations, and they are likely to experience difficulties to cope with future climate conditions.

We studied different riparian tree species from two riparian forests that where, in turn, experiencing different conditions of water availability. On one hand, the *Roureda de Tordera*, located at the depositional zone of the Tordera Basin, exhibits a flooding gradient that allows higher water availability in the area than other zones along the fluvial gradient. On the other hand, *Font del Regàs*, located at the transfer zone of the Tordera Basin, presents higher water availability at the near-stream edge than at the hillslope edge. Despite being in the Mediterranean region, both forests are submitted to sub-humid conditions that can counterbalance the inherent high temperatures and summer droughts of this region.

Our results demonstrate that tree species at Mediterranean riparian zones are extremely dependent on high water availability, and hence drought episodes affect their physiological activity. In particular, our results suggest that drought periods affect especially those riparian tree species with high water requirements either because they are usually established in wet regions (*Q. robur*) or in the wet areas of the riparian forest (*A. angustifolia* and *P. nigra*). Thus, these species do not present physiological trait adaptations to cope with water scarcity. For instance, *Q. robur* close stomata and reduces its growth rate to cope with the effects of increasing temperatures at the forest zones with relatively low water availability, demonstrating that this species is being affected by water scarcity at Mediterranean climate conditions. At the specific wet zone of the *Roureda de Tordera*, future projected drier conditions in the area would result in a substitution of *Q. robur* by *Q. canariensis*, which is now established at the adjacent dry zones. Likewise, riparian tree species at *Font del*

Regàs showed water limitations during the dry year in comparison with the wet one. All autochthonous tree species (*A. glutinosa*, *P. nigra*, and *F. excelsior*) reduced leaf biomass production during the dry year, although we barely detected other physiological responses to drier conditions on leaves morphological traits nor on wood production. Yet, *P. nigra* leaves showed higher iWUE during the dry year than during the wet one. In the case of F. excelsior this species constrains its transpiration when soil water content is too low (Nadal-Sala et al., 2017). This response concurs with the similar behavior found for *F. angustifolia* across forest zones at *Roureda de Tordera*. *Fraxinus spp* are well known riparian tree species usually observed at relative long distance from the river channel to avoid flooding condition (Magdaleno et al., 2014). Their shallow root system avoid to submerge its roots into the groundwater table (Singer et al., 2013) although it also affected by extremely low soil water content. The low response of *A. glutinosa* to drier conditions may reflect either its low response capacity to cope with water scarcity either its ability to uptake enough water in both situations. In fact, soil water content remains quite constant along the year at the near-stream zone, where this species grows. We hypothesized that, at the specific site of *Font del Regàs*, the low physiological response capacity under water stress shown by these autochthonous riparian tree species may lead to their replacement by the invasive *R. pseudoacacia* if dry conditions persist. This invasive N-fixing species is already present across all the riparian forest at this section of the catchment, and took advantage from autochthonous vegetation during the dry year producing higher leaf biomass. Moreover, this species exhibited different physiological responses that highlight its capacity to adapt to relatively dry conditions, such as higher iWUE, capacity to loss leaves during summer drought and to reabsorb nutrients before leaf litter fall.

It has been traditionally believed that riparian trees, and particularly, those considered of phreatophytic species, use always soil water when soil water availability is not scarce. Nevertheless, groundwater uptake becomes important during prolonged droughts, provided that their roots reach the saturated soil (Dawson and Pate 1996). Isotopic studies of sap and water

sources (Dawson and Ehleringer, 1991) have demonstrated how those species habiting at regions with a pronounced dry season are more dependent on groundwater availability. In these cases, groundwater source can represent up to 49% and almost 100% of transpired water in upland and riparian forests respectively (Barbeta and Peñuelas, 2017). However, water sources in *Font del Regàs* revealed that those trees located at the near-stream edge transpired higher amounts of water from groundwater during spring (~70 % of transpired water) while it was higher from soil during summer (>80%). This fact might be explained by trees with relatively short root systems, but reaching the capillarity fringe of the water table at the near-stream zone (Bleam et al., 2012; Devi et al., 2017). Thus they get to be disconnected from water table at small decreases of groundwater level. An inverse pattern, but less marked, was found for those tree individuals of *F. excelsior* and *R. pseudoacacia* located at the hillslope edge. In this case, they slightly increase the relative contribution of groundwater from the transpired water during spring (10-20%) compared to the relative contribution in summer (20-30%). In that case, the root systems of those trees living at the hillslope edge would be better adapted to drier periods, as well as to higher water availability variation range. Therefore, these trees may have developed deeper root systems to reach the water table under extremely dry conditions. In this sense, Snyder and Williams (2000) already suggested that the root system of some species would be adapted to water availability conditions of the specific site. They compared three riparian reaches within the same catchment under different stream water regimes: perennial, intermittent and ephemeral streams. They found that species at the ephemeral streams were more dependent on groundwater than those species living in the perennial ones probably due to deeper root systems.

We suggest that our different results about water sources of riparian transpiration may be attributable to the high annual precipitation in Font del Regàs (900 mm year-1) that would have prevented riparian trees of developing deep root systems to deal with water stress conditions. To our best knowledge, most of the studies reporting strong influence of groundwater during summer riparian trees' transpiration have been conducted in arid regions. This could

justify this pattern, rather comparable to upland forests. There are few studies that have carried out sap water isotopic analyses in wet riparian zones. The few present in the literature, together with those combining oxygen and deuterium isotopic analyses on tree-rings wood, suggest that riparian tree species growing in wet zones are already experiencing drought stress during dry years. For instance, Sargeant and Singer (2016) reported BAI difficulties for *P. nigra* within wet regions during dry years, highlighting its difficulty to uptake water from the saturated soil, despite its deep root system. In this context, we have compiled data from different studies performed in riparian areas all around the world. The study sites were plotted by aridity index continuum (i.e. AI=P/PET), which are covering Mediterranean, arid, and humid environmental conditions (Table F.1). In each site we obtained the % of water transpired from groundwater source, which is plotted in Figure 8.1. Here, *Font del Regàs* is located close to other temperate conditions, what justifies the seasonal pattern found on the water sources of our riparian forest.

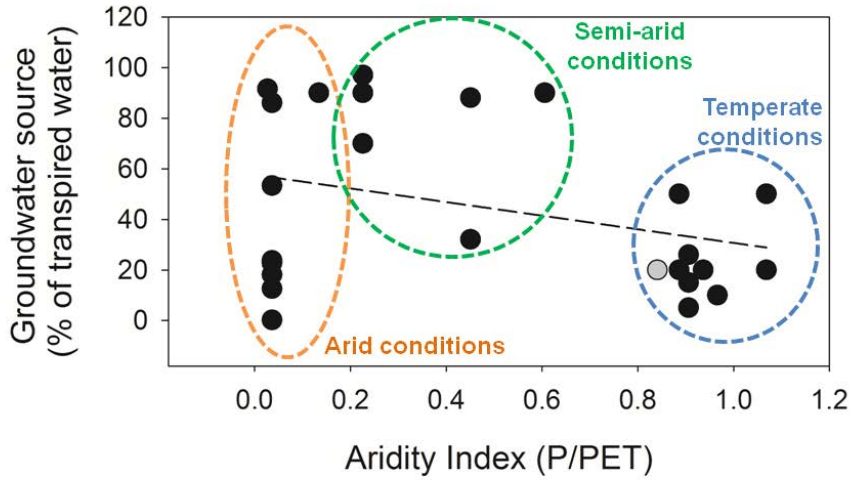

Figure 8.1 Relationship between the relative contribution of groundwater to riparian transpiration to annual and the aridity index (P / PET) for a set of riparian worldwide (n=16). The *Font del Regàs* forest (present study) is indicated with a gray circle. More information and references of the study sites are presented in Supplement (Table F.1).

These results imply that transpiration from groundwater and unsaturated soil layers by riparian vegetation may depend on the interaction between site conditions and species assemblage.

Based on the idea that root system reach until the capillarity fringe zone at *Font del Regàs*, we have developed a model for each riparian zone (near-stream, intermediate, and hillslope), to test both vegetation transpiration accounts from the total water fluxes of the forest, as well as the spatial heterogeneity within the riparian forest (Chapter 6). First, we corroborate the importance of transpiration on water balances from the riparian soil compartment, accounting for 25 - 35% of the fluxes. Second, we found that transpiration had a high impact during summer soil water content, decreasing it as it is the first water source for transpiration during this season. Third, climate change projections did not differed much among IPCC scenarios (RCP 2.6, RCP 4.5, and RCP 8.5) in terms soil water content, despite applying a decrease in plant transpiration as projected by some authors (Luo et al., 2008). Yet, groundwater level assumptions appeared to be the key for riparian forest survival. Strong decreases of groundwater table could drive to drier soil conditions. This would worsen the effects of increasing temperatures on riparian vegetation or even worse if disconnecting the groundwater table from the root systems. Thus, groundwater availability may be critical in transient and chronic drought, and it is important to increase our knowledge about the effects that climate change projections could have on groundwater tables to better infer the effects on riparian vegetation.

8.3. Soil N removal in Mediterranean riparian zones: The major role of vegetation N uptake

Riparian zones are considered hot spots of N removal processes within the catchment reducing N loads arriving from the uplands and before reaching the stream (McClain et al., 2003; Vidon et al., 2010). Denitrification is considered the main biological N-removal process occurring at the riparian areas when soil water content, anoxic conditions and organic carbon accumulation happen to meet, facilitating this anaerobic process (Hill et al., 2000; Pinay et al., 2015).

However, we found very low denitrification rates in the riparian soil at *Font del Regàs* (< 4 μg $N\text{-}N_2O$ kg $soil^{-1}$ d^{-1}) compared with those reported for humid-temperate zones (up to 2 mg $N\text{-}N_2O$ kg $soil^{-1}$ d^{-1}; Clément et al., 2002) but similar to the ones reported from other Mediterranean zones (0.7g $N\text{-}N_2O$ kg^{-1} day^{-1}; Pinay et al., 2015; Hefting et al., 2004) (Fig. 8.2). Some studies comparing denitrification rates at different latitudes have highlighted the importance of soil moisture (and thus the associated soil anoxia), on top of temperature and nitrate concentration, as the main variable controlling microbial denitrification in alluvial soils (Pinay et al., 2007). In *Font del Regàs*, riparian hydrology is also the main factor controlling microbial denitrification across the riparian area and along the year. The spatial variability of soil water content in *Font del Regàs* promoted higher denitrification rates at the near-stream zones than at the hillslope ones (30-40% and 10-25% of soil water content, respectively). These results contrast with non-water limited riparian forests, where higher substrate availability (C and N) at the hillslope edge enhanced denitrification activity (DeSimone et al., 2010; Dhondt et al., 2004). This would concurs with *Font del Regàs* if no anoxia limitation would happen, as our potential denitrification analyses showed higher denitrification rates at the intermediate and hillslope zones under similar anoxia conditions. We did not measure denitrification rates at the groundwater compartment, which us usually considered the main and faster path from uplands to the stream. However, we assumed that this process was negligible as dissolved organic carbon (DOC) was very low (DOC concentrations = 1.32 ± 1.43 mg C l^{-1}; groundwater depth = 0.6 - 3 m), and because of the barely anoxic conditions measured on the groundwater (D.O. = 4.52 ± 2.24 mg O_2 l^{-1}) (Mean values across the riparian zone for the period 2010-2013; unpublished data).

Although Mediterranean riparian soils may not act as hotspots of denitrification processes, riparian vegetation uptake plays a relevant role on annual soil N removal rates in arid and semi-arid zones (Ranalli and Macalady, 2010; Gerber and Brookshire, 2014). Indeed, in temperate riparian zones it is commonly accepted that vegetation N uptake is a dominant soil N removal process during summer (Haycock et al., 1993; Clément et al., 2003).

Our vegetation uptake simulations (Chapter 6) showed a remarkable decrease of soil N concentrations during vegetative periods and had special importance at the intermediate and hillslope zones.

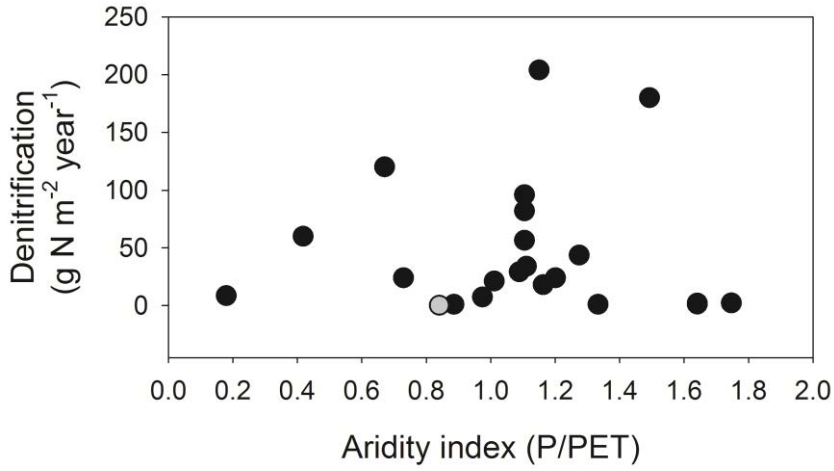

Figure 8.2 Relationship between denitrification rates and the aridity index (P / PET) for a set of riparian worldwide (n=20). The *Font del Regàs* forest (present study) is indicated with a gray circle. More information and references of the study sites are in the Supplement (Table F.2).

The exhaustive measurements of N fluxes over three vegetative periods (2010-2013) in *Font del Regàs* allow us to perform a N mass balance of this Mediterranean riparian forest (Fig. 8.3). Thus, we used the annual mass balance of *Font del Regàs* to infer the capacity of the Mediterranean riparian forests to reduce N loads reaching the stream. N-emissions to the atmosphere considered natural soil N_2O emissions and N_2 from soil denitrification (Chapter 5). Annual tree uptake and leaf litterfall input to the soil was estimated from annual leaf production related to specific leaf N concentration of fresh leaves (tree uptake) and senescent leaves (leaf litterfall) (Chapters 4 and 7). Groundwater N flux was calculated from daily groundwater N concentration data and the hydraulic conductivity on saturated soil (unpublished data). Annual dry and deposition N was obtain from Avila and

Rodà (2012) for the Montseny mountains, but was of similar magnitude of N precipitation analyses at the meteorological station nearby the studied forest. For subsurface leaching, we used data from inorganic N available in the soil captured by ion exchange resins (Lupon et al., 2016). Despite this measurement can subestimate leaching fluxes, it is comparable with the values found in others forests (Bernal et al., 2005). No differences were found between inorganic N available in the soil at the hillslope and at the near-stream edge, and thus the sub-surface leaching was considered a loss of the system. Altogether, our results suggest that on annual basis riparian vegetation do not retain enough N, and thus, together with the low denitrification rates, Mediterranean riparian forests may act as source of N to the stream instead of sinks.

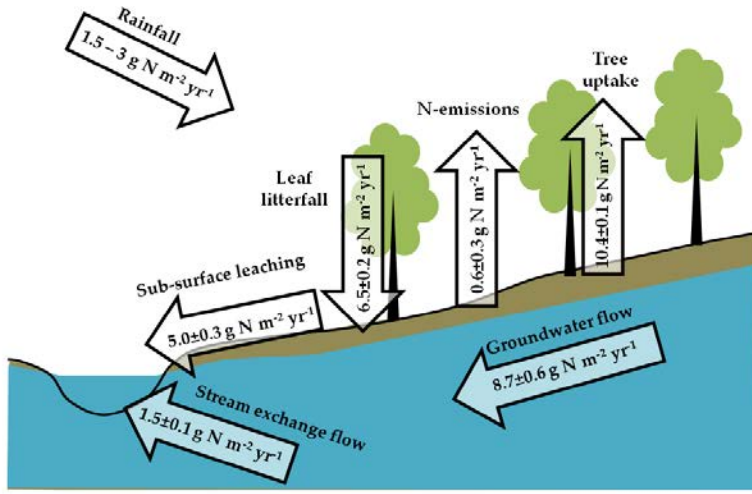

Figure 8.3 Estimated annual nitrogen (N) fluxes at the riparian forest of *Font del Regàs*. Rainfall, leaf litter inputs, tree uptake, surface leaching and groundwater fluxes are calculated as the mean annual values from 2011-2012. N2O emission flux is calculated from the field measurements carried out in 2013.

However, this annual N-source behavior of Mediterranean riparian zones can be different along the year. For instance, soil N processes are enhanced by high temperatures and water availability during early spring. Denitrification can rapidly increase once waterlogging conditions are set in riparian zones (Fig.

8.4a). These hot moments can be relevant on the global denitrification processes in these soils, but the rates are still low compared with the ones in wetter regions. Vegetation N uptake is the main removal process during spring and summer, but part of the N removed returns to the soil compartment at the end of the vegetative period via leaf litterfall (Fig. 8.4b). Both graphs of Fig. 4 showed that despite soil processes are highly influenced by temperature and vegetation by the vegetative period itself, water availability is extremely governing the temporal and annual capacity of soil N retention of the riparian forest. Studies at catchment scale in *Font del Regàs* have also questioned the paper of Mediterranean riparian zones as N buffers despite its capacity to provoke stream hydrological retention during the vegetative periods (Lupon et al 2016).

The idea of intensive sampling to better understand fluxes and processes at plot scale is of essential importance to obtain reliable modeled projections of global change effects on natural ecosystems. Our results in Chapter 6 suggest that projected climate conditions scenarios by IPCC (RCP 2.6, RCP 4.5, and RCP 8.5) could reduce the vegetative control of Mediterranean riparian forests, and, thus, increase soil N concentrations. These changes would be a consequence of (i) a reduction of transpiration rates to cope with drought conditions, and (ii) a possible disconnection between root systems and groundwater table, what would also restrict capillarity fluxes to recharge unsaturated soil profile. In the same way, Mayer et al. (2005) reported that relatively small riparian areas (such as *Font del Regàs*) are able to remove through plant uptake more than 75% of nitrate before it is exported to the stream, but this capacity is reduced when groundwater decrease to depths unreachable by root systems (Mayer et al., 2005; Hefting et al., 2004). Nevertheless, the soil N removal term when considering N uptake by deciduous vegetation is often questioned. The leaf litter fall at the end of the vegetative period reintroduce part of this previously uptaken N to the soil, which can be mineralized and leached into the groundwater and the stream (Hefting et al., 2005).

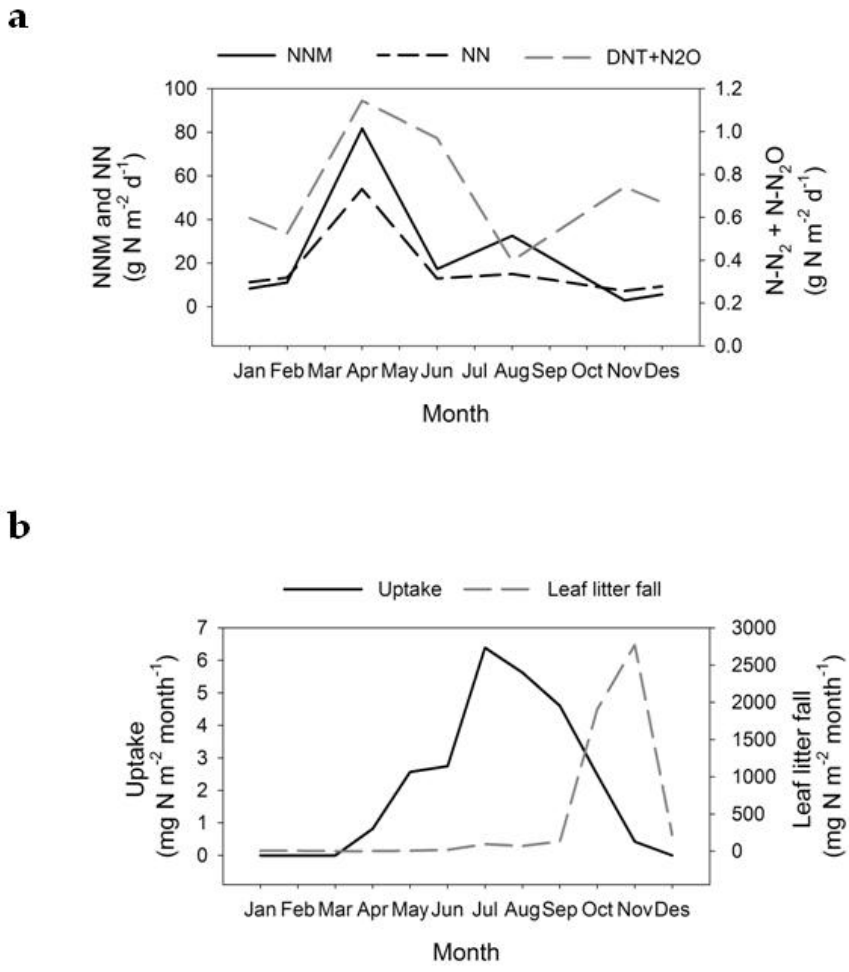

Figure 8.4 (a) Temporal patterns of soil nitrogen (N) processes: net mineralization (NNM), net nitrification (NN), and N gas emissions through denitrification and N2O natural emissions (DNT+N2O). (b) Temporal patterns of vegetation N fluxes: uptake and leaf litter fall.

8.4. Global change implications in Mediterranean riparian forests: final considerations

Both studied riparian forests have a remarkable spatial gradient of water availability across relatively small distance areas. This gradient of soil water availability and flooding conditions influences riparian tree species

distribution, tree species physiology and soil biogeochemistry processes. Therefore, we can affirm that space matters in semi-arid riparian zones being mainly driven by water availability. Thus, we should not consider these riparian areas as uniform zones, despite they have been traditionally assumed uniform for many temperate riparian systems. Moreover, our global change projections (Chapter 6) suggested that the possible disconnection between the vegetation uptake zone and the groundwater table alters vegetation transpiration and reduces the effective riparian soil N removal. Similarly, some authors also predict the contraction of mesic riparian vegetation corridors if water table declines under very low discharges, and as a consequence, soil moisture decreases at larger geomorphic surfaces (Rood et al., 2003; Auble et al., 2005).

8.4.1. Are Mediterranean riparian soils sources of greenhouse gases?

Riparian zones are the wettest areas in Mediterranean catchments, and thus, potential hotspots of soil microbial activity. Soil microbial processes can have gases as end-product, and some of them are considered greenhouse gases that contribute to climate warming (such as CO_2, N_2O, and CH_4). Soil respiration is predominantly an aerobic process that accounts by 20% of global CO_2 emissions. Yet, shallow groundwater tables and high soil water contents at riparian zones facilitate anaerobic microbial processes on top of aerobics ones. For instance, riparian zones can account by 70% of global N_2O emissions due to incomplete nitrification and denitrification processes under barely oxic conditions (Kim and Verma, 1990; Raich et al., 2002; Rastogi et al., 2002), and by 15-40% of the global CH_4 emissions, as a result of methanogenesis (Audet et al 2014; Segers 1998).

In contrast, the soil gas emissions measured in *Font del Regàs* showed large annual CO_2 emissions (1.2 – 10 g C m^{-2} d^{-1}) but very low annual N_2O emissions (0.001 – 0.2 mg N m^{-2} d^{-1}). We compared our results with studies reporting soil CO2 and N2O emissions (n=11 and n=20, respectively) across different biomes (Fig. 8.5). Mediterranean regions emitted higher amounts of CO_2 compared to arid and temperate regions, where they could be limited by low water availability and anoxic conditions, respectively (Fig. 8.5a). However, the wide

range of precipitation comprised within Mediterranean region bring about higher variability on soil CO_2 emission rates. Conversely, soil N_2O emissions were much higher at temperate zones than at arid and Mediterranean regions, due to extended soil anoxic conditions in this region (Fig. 8.5b). Similar to this latitudinal gradient of gas emissions, but at smaller scale, we found a spatio-temporal decoupling between N_2O and CO_2 following soil water availability variations in *Font del Regàs*. Large amounts of CO_2 were emitted from the hillslope and intermediate riparian zones, while N_2O soil emissions increased from the hillslope zone to the near-stream zone. Our results suggest that Mediterranean forest soils can act as a source of C to the atmosphere, but at the same time as a sink of N. This perception contrasts with the well-established idea that riparian soils are able to remove high amounts of N via denitrification, and produce N_2O when the process is incomplete (Mander et al., 2008; Vidon 2017). Thus, Mediterranean riparian zones act as upland forests producing high amounts of CO_2 due to soil respiration (Barba et al., 2014). Furthermore, warmer conditions expected by climate change can enhance CO_2 emissions at riparian zones whenever there would be a suitable soil water availability-although such emissions could be constricted under very low soil moisture (Chang et al., 2014).

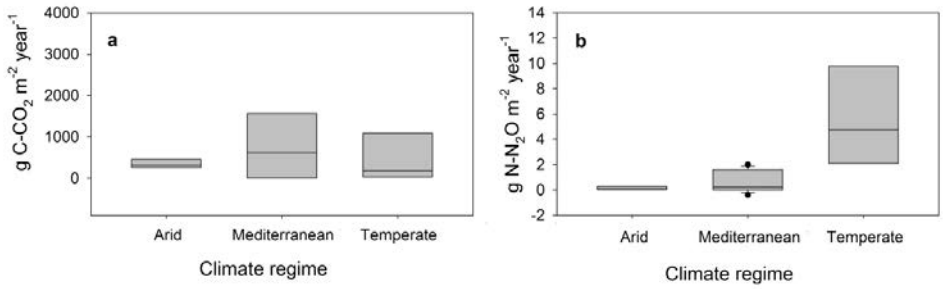

Figure 8.5 Greenhouse gas emissions from riparian forest soils worldwide: (a) CO_2 (n=11) and (b) N_2O (n=20). More information and references of the study sites are in the Supplement (Table F.3 and F.4).

8.4.2. Mediterranean riparian areas: sink or source of N in the future?

Riparian soils have been considered sinks of N due to both, the high concentrations that usually arrive from the catchment, and the high rate of N processes endorsed by the high water availability in riparian areas. Our results demonstrate that riparian soils in *Font del Regàs* are water limited (i.e. anoxic conditions limitation) for denitrification activity: Nevertheless, the highest mineralization and nitrification rates from the catchment soils had been measured in riparian soils (Lupon et al., 2016). Therefore, riparian zones are considered hot spots of net nitrification rates which can be strengthened by short-periods of elevated temperature and water availability, and lead to increase in stream N loads (Lupon et al., 2016; Lupon et al., 2017). Climate change projections show no changes in mineralization and nitrification rates in this area, as the benefits of higher temperatures would be negatively counterbalanced by lower soil water availability (Lupon et al., 2015).

Global change can promote changes of vegetation species, due to natural or human induced disturbances, promoting cascade effects on the ecosystem functioning. For instance, the presence of riparian vegetation with the ability to fix atmospheric N_2 through bacteria symbioses in *Font del Regàs* (*A. glutinosa* and *R. pseudoacacia*) can influence soil N availability. In some cases, disturbances caused by deforestation activities can facilitate the entrance and spread of invasive species which can substitute the native ones. Some studies have indicated that although new invader species could have clear drought sensitivity, better adaptations to drought of native species do not suppose any advantages for them (Werner et al., 2010; Castro-Diez et al., 2009). In *Font del Regàs*, the invasive N-fixing species *R. pseudoacacia* is spread across all the riparian area cohabiting with native tree species. Our results in chapter 7 demonstrated that its presence in *Font del Regàs* may have homogenized soil N availability across the whole riparian area. Yet, a complete invasion by *R. pseudoacacia* in *Font del Regàs*, would reduce total soil N stocks. Therefore, the substitution of non-fixing species by N-fixing ones, and vice versa, can also alter the capacity of riparian soils to retain or export N to streams.

The riparian vegetation acts as a source of soil N, through leaf litterfall, but it can also retain N via uptake. Indeed, high correlation between plant uptake and N concentration leached into the stream has been reported by some authors, highlighting the influence of vegetation on N retention (Schade et al., 2005). Our plant uptake simulations also support the role of riparian vegetation on soil N removal (Chapter 6). However, global change can cause water stress to riparian vegetation due to an increase of the evaporative demand and a reduction of water resources. As a consequence, riparian vegetation can decrease transpiration rates or even be substituted by other species, with less transpiration and N-uptake rates. Our simulations of reduced transpiration, and thus N uptake, under climate change conditions suggest that soil N would increase during subsequent years and the effective N removal areas could be restricted to zones adjacent to the stream channel. In addition, higher frequency and intensity of extreme rainfall and flooding events, also expected by climate change projections, might increase the arrival of N loads via surface (leaching) and subsurface (groundwater coming from the watershed). Low processing rates of Mediterranean riparian forests would not be able to reduce the export of N loads to the stream.

Overall, N retention in Mediterranean riparian soils would be mainly due to vegetation uptake. Yet, future climate projections may exacerbate water scarcity problems, inhibiting denitrification rates and reducing vegetation uptake. Therefore, these results suggest that Mediterranean riparian soils would become a potential source of N to adjacent aquatic systems in the future.

CHAPTER 9

General conclusions

Conclusions of this thesis are listed by chapters below:

CHAPTER 3

* *Q. canariensis*, at its northern distribution range, showed no effects of increasing temperature over the last decades on its growth. However, iWUE significantly increased over such period by stomatal control.

* In the southernmost limit of distribution range of *Q. robur*, this species is found from the wet to the extremely flooded zones in the studied area. The increasing temperature over the last decades only affected negatively individual's growth at the wet zone, confirming their high needs of water availability. Nevertheless, *Q. robur* increased its iWUE at the wet and mid-flooded zones by stomatal control.

* *F. angustifolia* is currently co-habiting with *Q. robur*. The increasing temperature over the last decades caused only a decreased of growth trends at the mid-flooded zone. Both, higher iWUE and stomatal control at the extremely-flooded zone indicate root anoxia symptoms in this zone.

* In Mediterranean regions, the presence of a mid-European species as *Q. robur* will be certainly endangered if climate conditions become drier than the present ones. These worsening conditions would be a combination of increasing temperature, less precipitation and groundwater availability decline.

CHAPTER 4

* The studied native riparian tree species (*A. glutinosa*, *P. nigra*, and *F. excelsior*) responded to the environmental conditions of the dry year through lower leaf biomass production in comparison to the wet one.

* Few physiological control mechanisms were found for native species to cope with drier conditions. Among them, *P. nigra* and *F. excelsior* released few amounts of leaves during low summer soil water content periods, and *P. nigra* increased its iWUE in the dry year. Despite *A. glutinosa* was affected by drier conditions, it did not show any physiological control mechanism.

* The invasive *R. pseudoacacia* produced higher leaf biomass than native species during the dry year, evidencing its higher competitive ability to cope with drought.

* *R. pseudoacacia* coped with drier annual conditions through its high plasticity, being able to release leaves during summer, better performing leaf N reabsorption before leaf fall, and showing higher iWUE when compared to natives' species.

* Riparian tree species are mainly uptaking water from the deep soil layer. Phreatophitic species, *A. glutinosa* and *P. nigra*, used mainly groundwater specially during spring. However, they depend on soil water during summer, when groundwater level decreases away from the roots. *R. pseudoacacia* is able to increase its use of groundwater at the hillslope zone during summer drought, likely supported by a deep root system that reaches the groundwater table. *F. excelsior* presented no differences on its water sources behavior among seasons.

CHAPTER 5

* Greenhouse gas emissions from the riparian soil occurred mostly as CO_2 across all the riparian zones. The highest CO_2 emissions occurred near the hillslope, since deep groundwater tables promoted large respiration rates in those relatively dry soils.

* Denitrification rates were very low and they mainly occurred in the wet zones located near the stream channel. Soil N_2O emissions were also negligible and occurred mainly at the near-stream zone.

* Mediterranean riparian zones are dynamic systems that show high spatio-temporal shifts of biogeochemical processes driven by changes in both soil water content and substrate availability. After spring rewetting events, both CO_2 and N_2O emissions peaked, supported by optimal conditions of soil water content, temperature, and N availability that promote microbial respiration, nitrification, and denitrification activities.

* Future variations of catchment hydrology due to climate change are expected to affect the riparian functionality in Mediterranean areas, as well as their contribution to regional and global C and N cycles.

CHAPTER 6

* Mediterranean riparian areas are ecosystems with high water availability and with high spatial heterogeneity of soil properties throughout short distances (~25 m wide), mainly due to large differences in soil granulometry and in groundwater level from near-stream to hillslope edges.

* Plant transpiration is the main water flux across the riparian zones (25 to 35% of water fluxes), forcing a clear decrease of soil water content during summer drought. Moreover, transpiration rates decreases from the near-stream to the hillslope edge, following soil water content availability.

* Plant-root N uptake plays the main role for N retention and turnover, in Mediterranean riparian systems particularly in zones where the groundwater level is deeper and dry conditions are leading to almost zero denitrification.

* Projected climate change scenarios, with increasing temperature and less precipitation can cause a strong groundwater availability depletion. This would constrain transpiration rates and plant-root N uptake. These effects would be stronger at the hillslope edge, reducing the effective riparian N removal area to shorter distances from the stream channel. This fact would increase soil N availability and N leaching risk from riparian areas into the stream.

CHAPTER 7

* Leaf litter N content of the invasive and N-fixing *R. pseudoacacia* species was higher than N leaf litter content of native non-fixing species, but similar to A. glutinosa.

* *R. pseudoacacia* contribution to annual leaf litter N inputs increased from the near-stream to the hillslope zones. Nevertheless, no differences were found on soil N processing rates nor on soil N availability among riparian zones.

* The spreading of *R. pseudoacacia* across the riparian forest contributed to homogenize soil N availability. Nevertheless, it would decrease the total soil N availability of the forest floor in case of a complete invasion scenario. The results obtained from these simulations highlighted the importance of an integrated spatio-temporal perception of the invasive process in order to assess its impact on soil N biogeochemistry.

References

2012, R. C. T.: Team RDC.R: A Language And Environment For Statistical Computing., n.d.

Aber, J. D., McDowell, W. H., Nadelhoffer, K., Magill, A., Berntson, G., Kamakea, M., McNulty, S. G., Currie, W. S., Rustad, L. E. and Fernandez, I.: Nitrogen saturation in temperate forest ecosystems, Bioscience, 48(11), 921–934, 1998.

Aguiar, F. C., Cerdeira, J. O., Martins, M. J. and Ferreira, M. T.: Riparian forests of Southwest Europe: Are functional trait and species composition assemblages constrained by environment?, J. Veg. Sci., 24(4), 628–638, doi:10.1111/jvs.12009, 2013.

Ajbilou, R., Marañón, T. and Arroyo, J.: Ecological and biogeographical analyses of Mediterranean forests of northern Morocco, Acta Oecologica, 29(1), 104–113, doi:10.1016/j.actao.2005.08.006, 2006.

Akamatsu, F., Ide, K., Shimano, K. and Toda, H.: Nitrogen stocks in a riparian area invaded by N-fixing black locust (Robinia pseudoacacia L.), Landsc. Ecol. Eng., 7(1), 109–115, doi:10.1007/s11355-010-0125-0, 2011.

Allen, R. G., Pereira, L. S., Raes, D., Smith, M. and Ab, W.: Crop evapotranspiration. Guidelines for computing crop water requirements., FAO Irrig. Drain. Pap., 56, doi:10.1016/j.eja.2010.12.001, 1998.

Allison, S. D., Wallenstein, M. D. and Bradford, M. A.: Soil-carbon response to warming dependent on microbial physiology, Nat. Geosci., 3(5), 336–340, doi:10.1038/ngeo846, 2010.

Alongi, D. M., Pfitzner, J., Trott, L. A., Tirendi, F., Dixon, P. and Klumpp, D. W.: Rapid sediment accumulation and microbial mineralization in forests of the mangrove Kandelia candel in the Jiulongjiang Estuary, China, Estuar. Coast. Shelf Sci., 63(4), 605–618, doi:10.1016/j.ecss.2005.01.004, 2005.

Alonso, A., González-Muñoz, N. and Castro-Díez, P.: Comparison of leaf decomposition and macroinvertebrate colonization between exotic and native trees in a freshwater ecosystem, Ecol. Res., 25(3), 647–653, doi:10.1007/s11284-010-0698-y, 2010.

Angstmann, J. L., Ewers, B. E., Barber, J. and Kwon, H.: Testing transpiration controls by quantifying spatial variability along a boreal black spruce forest drainage gradient, Ecohydrology, 6, 783–793, doi:10.1002/eco.1300, 2013.

Asaeda, T., Rashid, M. H. and Abu Bakar, R.: Dynamic modelling of soil nitrogen budget and vegetation colonitzation in sediment bars of a regulated river, River

Res. Appl., 31, 470–484, doi:10.1002/rra.2802 DYNAMIC, 2015.

Asensio, D., Peñuelas, J., Ogaya, R. and Llusià, J.: Seasonal soil and leaf CO2 exchange rates in a Mediterranean holm oak forest and their responses to drought conditions, Atmos. Environ., 41, 2447–2455, doi:10.1016/j.atmosenv.2006.05.008, 2007.

Audet, J., Hoffmann, C. C., Andersen, P. M., Baattrup-Pedersen, A., Johansen, J. R., Larsen, S. E., Kjaergaard, C. and Elsgaard, L.: Nitrous oxide fluxes in undisturbed riparian wetlands located in agricultural catchments: Emission, uptake and controlling factors, Soil Biol. Biochem., 68, 291–299, doi:10.1016/j.soilbio.2013.10.011, 2014.

Àvila, A. and Rodà, F.: Changes in atmospheric deposition and streamwater chemistry over 25 years in undisturbed catchments in a Mediterranean mountain environment, Sci. Total Environ., 434, 18–27, doi:10.1016/j.scitotenv.2011.11.062, 2012.

Baethgen, W. E. and Alley, M. M.: A manual colorimetric procedure for measuring ammonium nitrogen in soil and plant Kjeldahl digests, Commun. Soil Sci. Plant Anal., 20(9–10), 961–969, doi:10.1080/00103628909368129, 1989.

Baggs, E. M.: A review of stable isotope techniques for N2O source partitioning in soils: recent progress, remaining challenges and future considerations, Rapid Commun. Mass Spectrom., 22, 1664–1672, doi:10.1002/rcm, 2008.

Balboa-Murias, M. A., Rojo, A., Álvarez, J. G. and Merino, A.: Original article Carbon and nutrient stocks in mature Quercus robur L . stands in NW Spain, Ann. For. Sci., 63, 557–565, doi:10.1051/forest:2006038, 2006.

Barba, J., Curiel Yuste, J., Poyatos, R., Janssens, I. A. and Lloret, F.: Strong resilience of soil respiration components to drought-induced die-off resulting in forest secondary succession, Oecologia, 182(1), 27–41, doi:10.1007/s00442-016-3567-8, 2016.

Barbeta, A. and Peñuelas, J.: Relative contribution of groundwater to plant transpiration estimated with stable isotopes, Sci. Rep., 7(1), 1–10, doi:10.1038/s41598-017-09643-x, 2017.

Bardon, C., Piola, F., Bellvert, F., Haichar, F. el Z., Comte, G., Meiffren, G., Pommier, T., Puijalon, S., Tsafack, N. and Poly, F.: Evidence for biological denitrification inhibition (BDI) by plant secondary metabolites, New Phytol., 204(3), 620–630, doi:10.1111/nph.12944, 2014.

Barnard, H. ., Graham, C. B., Van Verseveld, W. J., Brooks, J. R., Bond, B. J. and McDonnell, J. .: Mechanistic assessment of hillslope transpiration controls of diel subsurface flow: a steady-state irrigation approach, Ecohydrology, 3, 133–142, doi:10.1002/eco.114 Mechanistic, 2010.

Batson, J., Noe, G. B., Hupp, C. R., Krauss, K. W., Rybicki, N. B. and Schenk, E. R.: Soil greenhouse gas emissions and carbon budgeting in a short-hydroperiod floodplain wetland, J. Geophys. Res. G Biogeosciences, 120(1), 77–95, doi:10.1002/2014JG002817, 2015.

Becker, M., Nieminen, T. M. and Geremia, F.: Short-term variations and long-term changes in oak productivity in northeastern France. The role of climate and atmospheric CO2, Ann. des Sci. For., 51(5), 477–492, doi:10.1051/forest:19940504, 1994.

Belnap, J., Welter, J. R., Grimm, N. B., Barger, N. and Ludwig, J. a: Linkages between Microbial and Hydrologic Processes in Arid and Semiarid Watersheds LINKAGES BETWEEN MICROBIAL AND HYDROLOGIC PROCESSES IN ARID AND SEMIARID WATERSHEDS, Ecol. Soc. Am., 86(2), 298–307, 2005.

Benesperi, R., Giuliani, C., Zanetti, S., Gennai, M., Mariotti Lippi, M., Guidi, T., Nascimbene, J. and Foggi, B.: Forest plant diversity is threatened by Robinia pseudoacacia (black-locust) invasion, Biodivers. Conserv., 21(14), 3555–3568, doi:10.1007/s10531-012-0380-5, 2012.

Benfield, E. F.: Comparison of litterfall input to streams., J.N.Am.Benthol. Soc., 16, 104–108, 1997.

Bernal, S., Butturini, A. and Sabater, F.: Variability of DOC and nitrate responses to storms in a small Mediterranean forested catchment, Hydrol. Earth Syst. Sci., 6(6), 1031–1041, doi:10.5194/hess-6-1031-2002, 2002.

Bernal, S., Butturini, A., Nin, E., Sabater, F. and Sabater, S.: Leaf litter dynamics and nitrous oxide emission in a Mediterranean riparian forest: implications for soil nitrogen dynamics., J. Environ. Qual., 32(1), 191–197 [online] Available from: http://www.ncbi.nlm.nih.gov/pubmed/12549558, 2003.

Bernal, S., Sabater, F., Butturini, A., Nin, E. and Sabater, S.: Factors limiting denitrification in a Mediterranean riparian forest, Soil Biol. Biochem., 39(10), 2685–2688, doi:10.1016/j.soilbio.2007.04.027, 2007.

Bernal, S., Hedin, L. O., Likens, G. E., Gerber, S. and Buso, D. C.: Complex response of the forest nitrogen cycle to climate change, Proc. Natl. Acad. Sci., 109(9), 3406–3411, doi:10.1073/pnas.1121448109, 2012.

Bernal, S., Lupon, A., Ribot, M., Sabater, F. and Martí, E.: Riparian and in-stream controls on nutrient concentrations and fluxes in a headwater forested stream, Biogeosciences, 12(6), 1941–1954, doi:10.5194/bg-12-1941-2015, 2015.

Berthold, D.: Soil chemical and biological changes through the N 2 fixation of black locust (Robinia pseudoacacia L .) - A contribution to the research of tree neophytes, Georg. Göttingen, 2005.

Bertrand, G., Masini, J., Goldscheider, N., Meeks, J., Lavastre, V., Celle-Jeanton, H., Gobat, J. M. and Hunkeler, D.: Determination of spatiotemporal variability of tree water uptake using stable isotopes (δ18O, δ2H) in an alluvial system supplied by a high-altitude watershed, Pfyn forest, Switzerland, Ecohydrology, 7(2), 319–333, doi:10.1002/eco.1347, 2014.

Binkley, D., Cromack, K. and Backer, D. D.: Nitrogen fixation by red alder: Biology, rates, and controls, Biol. Manag. Red Alder, (January 1994), 57–72, 1994.

Boada, M., Mayo, S. and Maneja, R., Eds.: Els sistemes socioecològics de la conca de La Tordera, Institució Catalana d'Història Natural, Barcelona., 2008.

Bolós, J. and Vigo, O.: Flora dels Països Catalans, Editorial Barcino., 1984.

Bond-Lamberty, B. and Thomson, A.: Temperature-associated increases in the global soil respiration record., Nature, 464(7288), 579–582, doi:10.1038/nature08930, 2010.

Boring, L. R. and Swank, W. T.: The role of black locust (Robinia pseudoacacia) in a forest succession, J. Ecol., 72, 749–766, 1984.

Bosch, D. D., Marshall, L. K. and Teskey, R.: Forest transpiration from sap flux density measurements in a Southeastern Coastal Plain riparian buffer system, Agric. For. Meteorol., 187, 72–82, doi:10.1016/j.agrformet.2013.12.002, 2014.

Boumghar, A.: Étude et évaluation du comportement de quatre espèces de forêts reveraines aux cours d'eau (Alnus glutinosa L., Robinia pseudoacacia L., Populus nigra L., et Fraxinus excelsior L.) quant aux conditions de stress hydrique, Univ. Barcelona, (Master Thesis), 2012.

Breda, N., Cochard, H., Dreyer, E. and Granier, a: Field Comparison of Transpiration, Stomatal Conductance and Vulnerability To Cavitation of Quercus-petraea and Quercus-robur Under Water-stress, Ann. Des Sci. For., 50(6), 571–582, doi:10.1051/forest:19930606, 1993.

Briones, M. J. I., Ostle, N. J., McNamara, N. P. and Poskitt, J.: Functional shifts of

grassland soil communities in response to soil warming, Soil Biol. Biochem., 41(2), 315–322, doi:10.1016/j.soilbio.2008.11.003, 2009.

Brooks, J. R., Barnard, H. R., Coulombe, R. and McDonnell, J. J.: Ecohydrologic separation of water between trees and streams in a Mediterranean climate, Nat. Geosci., 3, 100–104, doi:10.1038/ngeo722, 2010.

Bruland, G. L., Richardson, C. J. and Whalen, S. C.: Spatial variability of denitrification potential and related soil properties in created, restored, and paired natural wetlands, Wetlands, 26(4), 1042–1056, doi:10.1672/0277-5212(2006)26[1042:SVODPA]2.0.CO;2, 2006.

Burgin, A. J. and Groffman, P. M.: Soil O2 controls denitrification rates and N2O yield in a riparian wetland, J. Geophys. Res. Biogeosciences, 117(1), 1–10, doi:10.1029/2011JG001799, 2012.

Butturini, A., Bernal, S., Hellin, C., Nin, E., Rivero, L., Sabater, S. and Sabater, F.: Influences of the stream groundwater hydrology on nitrate concentration in unsaturated riparian area bounded by an intermittent Mediterranean stream, Water Resour. Res., 39(4), 1–13, doi:10.1029/2001WR001260, 2003a.

Butturini, A., Bernal, S., Hellin, C., Nin, E., Rivero, L., Sabater, S. and Sabater, F.: Influences of the stream groundwater hydrology on nitrate concentration in unsaturated riparian area bounded by an intermittent Mediterranean stream, Water Resour. Res., 39(4), doi:10.1029/2001WR001260, 2003b.

Butturini, A., Bernal, S. and Sabater, F.: Modeling storm events to investigate the influence of the stream-catchment interface zone on stream biogeochemistry, Water Resour. Res., 41(8), 1–12, doi:10.1029/2004WR003842, 2005.

Buzhdygan, O. Y., Rudenko, S. S., Kazanci, C. and Patten, B. C.: Effect of invasive black locust (Robinia pseudoacacia L.) on nitrogen cycle in floodplain ecosystem, Ecol. Modell., 319, 170–177, doi:10.1016/j.ecolmodel.2015.07.025, 2016.

Calder, I. R.: Water use by forests, limits and controls., Tree Physiol., 18(18), 625–631, doi:10.1093/treephys/18.8-9.625, 1998.

Casals, P., Lopez-Sangil, L., Carrara, A., Gimeno, C. and Nogués, S.: Autotrophic and heterotrophic contributions to short-term soil CO2 efflux following simulated summer precipitation pulses in a Mediterranean dehesa, Global Biogeochem. Cycles, 25(3), 1–12, doi:10.1029/2010GB003973, 2011.

Castro-Díez, P., González-Muñoz, N., Alonso, A., Gallardo, A. and Poorter, L.: Effects of exotic invasive trees on nitrogen cycling: A case study in Central Spain,

Biol. Invasions, 11(8), 1973–1986, doi:10.1007/s10530-008-9374-3, 2009.

Castro-Díez, P., Fierro-Brunnenmeister, N., González-Muñoz, N. and Gallardo, A.: Effects of exotic and native tree leaf litter on soil properties of two contrasting sites in the Iberian Peninsula, Plant Soil, 350(1–2), 179–191, doi:10.1007/s11104-011-0893-9, 2012.

Cermák, J. and Prax, A.: Water balance of a Southern Moravian floodplain forest under natural and modified soil water regimes and its ecological consequences, Ann. For. Sci., 58(1), 15–29, doi:10.1051/forest:2001100, 2001.

Chang, C. T., Sabaté, S., Sperlich, D., Poblador, S., Sabater, F. and Gracia, C.: Does soil moisture overrule temperature dependence of soil respiration in Mediterranean riparian forests?, Biogeosciences, 11(21), 6173–6185, doi:10.5194/bg-11-6173-2014, 2014.

Chauvet, E.: Changes in the chemical composition of alder, poplar and willow leaves during decomposition in a river, Hydrobiologia, 148(1), 35–44, doi:https://doi.org/10.1007/BF00018164, 1987.

Chen, C., Cleverly, J., Zhang, L., Yu, Q. and Eamus, D.: Modelling Seasonal and Inter-annual Variations in Carbon and Water Fluxes in an Arid-Zone Acacia Savanna Woodland, 1981–2012, Ecosystems, 19, 625–644, doi:10.1007/s10021-015-9956-8, 2016.

Clausnitzer, F., Köstner, B., Schwärzel, K. and Bernhofer, C.: Relationships between canopy transpiration, atmospheric conditions and soil water availability-Analyses of long-term sap-flow measurements in an old Norway spruce forest at the Ore Mountains/Germany, Agric. For. Meteorol., 151, 1023–1034, doi:10.1016/j.agrformet.2011.04.007, 2011.

Clément, J.-C., Pinay, G. and Marmonier, P.: Seasonal dynamics of denitrification along topohydrosequences in three different riparian wetlands, J. Environ. Qual., 31, 1025–1037, doi:10.2134/jeq2002.1025, 2002.

Clément, J. C., Holmes, R. M., Peterson, B. J. and Pinay, G.: Isotopic investigation of denitrification in a riparian ecosystem in western France, J. Appl. Ecol., 40, 1035–1048, doi:10.1111/j.1365-2664.2003.00854.x, 2003.

Coble, A. P. and Cavaleri, M. A.: Light acclimation optimizes leaf functional traits despite height-related constraints in a canopy shading experiment, Oecologia, 177(4), 1131–1143, doi:10.1007/s00442-015-3219-4, 2015.

Connor, S., Nelson, P. N., Armour, J. D. and Hénault, C.: Hydrology of a forested

riparian zone in an agricultural landscape of the humid tropics, Agric. Ecosyst. Environ., 180, 111–122, doi:10.1016/j.agee.2011.12.006, 2013.

Damesin, C., Rambal, S. and Joffre, R.: Between-tree variations in leaf δ13C of Quercus pubescens and Quercus ilex among mediterranean habitats with different water availability, Oecologia, 111(1), 26–35, doi:10.1007/s004420050204, 1997.

Davidson, E. A., Janssens, I. A. and Lou, Y.: On the variability of respiration in terrestrial ecosystems: Moving beyond Q10, Glob. Chang. Biol., 12(2), 154–164, doi:10.1111/j.1365-2486.2005.01065.x, 2006.

Dawson, T. E. and Ehleringer, J. R.: Streamside trees that do not use stream water, Nature, 350, 1991a.

Dawson, T. E. and Ehleringer, J. R.: Streamside trees that do not use stream water, Nature, 350(6316), 335–337, 1991b.

DeSimone, J., Macrae, M. L. and Bourbonniere, R. a.: Spatial variability in surface N2O fluxes across a riparian zone and relationships with soil environmental conditions and nutrient supply, Agric. Ecosyst. Environ., 138(1–2), 1–9, doi:10.1016/j.agee.2010.03.007, 2010.

Dhondt, K., Boeckx, P., Hofman, G. and Cleemput, O.: Temporal and spatial patterns of denitrification enzyme activity and nitrous oxide fluxes in three adjacent vegetated riparian buffer zones, Biol. Fertil. Soils, 40(4), 243–251, doi:10.1007/s00374-004-0773-z, 2004.

Doble, R. C. and Crosbie, R. S.: Review: Current and emerging methods for catchment-scale modelling of recharge and evapotranspiration from shallow groundwater, Hydrogeol. J., 25, 3–23, doi:10.1007/s10040-016-1470-3, 2017.

Doody, C. N. and O'Reilly, C.: Drying and soaking pretreatments affect germination in pedunculate oak, Ann. For. Sci., 65, doi:10.1051/forest:2008027, 2008.

Douda, J., Boublík, K., Slezák, M., Biurrun, I., Nociar, J., Havrdová, A., Doudová, J., Aćić, S., Brisse, H., Brunet, J., Chytrý, M., Claessens, H., Csiky, J., Didukh, Y., Dimopoulos, P., Dullinger, S., Fitzpatrick, Ú., Guisan, A., Horchler, P. J., Hrivnák, R., Jandt, U., Kacki, Z., Kevey, B., Landucci, F., Lecomte, H., Lenoir, J., Paal, J., Paternoster, D., Pauli, H., Pielech, R., Rodwell, J. S., Roelandt, B., Svenning, J. C., Šibík, J., Šilc, U., Škvorc, Ž., Tsiripidis, I., Tzonev, R. T., Wohlgemuth, T. and Zimmermann, N. E.: Vegetation classification and biogeography of European floodplain forests and alder carrs, Appl. Veg. Sci., 19(1), 147–163, doi:10.1111/avsc.12201, 2016.

Dyderski, M. K., Paź, S., Frelich, L. E. and Jagodziński, A. M.: How much does climate change threaten European forest tree species distributions?, Glob. Chang. Biol., 24(3), 1150–1163, doi:10.1111/gcb.13925, 2018.

Ellenberg, H.: Nitrogen as Soil Factor, Especially for Central European Plant Populations, Oecologia Plant., 12(1), 1–22, 1977.

Emmett, B. A., Beier, C., Estiarte, M., Tietema, A., Kristensen, H. L., Williams, D., Peñuelas, J., Schmidt, I. and Sowerby, A.: The response of soil processes to climate change: Results from manipulation studies of shrublands across an environmental gradient, Ecosystems, 7(6), 625–637, doi:10.1007/s10021-004-0220-x, 2004.

Eno, C. F.: Nitrate production in the field by incubating the soil in polyethylene bags, Soil Sci. Soc. Am. J., 24, 227–279, 1960a.

Eno, C. F.: Nitrate production in the field by incubating the soil in polyethylene bags, Soil Sicence Soc. Am., 24(4), 277–279, 1960b.

Eno, C. F.: Nitrate production in the field by incubating the soil in polyethylene bags., Soil Sci. Soc. Am. J., 24, 277–279, 1960c.

Eriksson, L.; Byrne, T.; Johansson, E.; Trygg, J.; Vikström, C.: Multi- and Megavariate Data Analysis. Basic principles and applications., 2006.

Evaristo, J., Jasechko, S. and McDonnell, J. J.: Global separation of plant transpiration from groundwater and streamflow, Nature, 525(7567), 91–94, doi:10.1038/nature14983, 2015.

Fang, Y., Koba, K., Makabe, A., Takahashi, C., Zhu, W., Hayashi, T., Hokari, A. A., Urakawa, R., Bai, E., Houlton, B. Z., Xi, D., Zhang, S., Matsushita, K., Tu, Y., Liu, D., Zhu, F., Wang, Z., Zhou, G., Chen, D., Makita, T., Toda, H., Liu, X., Chen, Q., Zhang, D., Li, Y. and Yoh, M.: Microbial denitrification dominates nitrate losses from forest ecosystems, Proc. Natl. Acad. Sci., 112(5), 1470–1474, doi:10.1073/pnas.1416776112, 2015.

Farquhar, G., O'Leary, M. and Berry, J.: On the Relationship Between Carbon Isotope Discrimination and the Intercellular Carbon Dioxide Concentration in Leaves, Aust. J. Plant Physiol., 9(2), 121, doi:10.1071/PP9820121, 1982.

Feddes, R. A., Bresler, E. and Neuman, S. P.: Field test of a modified numerical model for water uptake by root systems, Water Resour. Res., 10(6), 1199–1206, doi:10.1029/WR010i006p01199, 1974.

Fernandes, P., Antunes, C., Correia, O. and Máguas, C.: Do climatic and habitat

conditions affect the reproductive success of an invasive tree species? An assessment of the phenology of Acacia longifolia in Portugal, Plant Ecol., 216(2), 343–355, doi:10.1007/s11258-014-0441-9, 2014.

Ferreira, V. and Graça, M. A. S.: Effects of whole-stream nitrogen enrichment and litter species mixing on litter decomposition and associated fungi, Limnologica, 58, 69–77, doi:10.1016/j.limno.2016.03.002, 2016.

Follstad Shah, J. J. and Dahm, C. N.: Flood regime and leaf fall determine soil inorganic nitrogen dynamics in semiarid riparian forests, Ecol. Appl., 18(3), 771–788, doi:10.1890/07-0447.1, 2008.

Ford, C. R., Goranson, C. E., Mitchell, R. J., Will, R. E. and Teskey, R. O.: Modeling canopy transpiration using time series analysis: A case study illustrating the effect of soil moisture deficit on Pinus taeda, Agric. For. Meteorol., 130, 163–175, doi:10.1016/j.agrformet.2005.03.004, 2005.

Ford, C. R., Mitchell, R. J. and Teskey, R. O.: Water table depth affects productivity, water use, and the response to nitrogen addition in a savanna system, Can. J. For. Res., 38, 2118–2127, doi:10.1139/X08-061, 2008.

Francey, R. J., Allison, C. E., Etheridge, D. M., Trudinger, C. M., Enting, I. G., Leuenberger, M., Langenfelds, R. L., Michel, E. and Steele, L. P.: A 1000-year high precision record of $\delta^{13}C$ in atmospheric CO_2, Tellus B Chem. Phys. Meteorol., 51(2), 170–193, doi:10.3402/tellusb.v51i2.16269, 1999.

Frank, D. C., Poulter, B., Saurer, M., Esper, J., Huntingford, C., Helle, G., Treydte, K., Zimmermann, N. E., Schleser, G. H., Ahlström, A., Ciais, P., Friedlingstein, P., Levis, S., Lomas, M., Sitch, S., Viovy, N., Andreu-Hayles, L., Bednarz, Z., Berninger, F., Boettger, T., D'alessandro, C. M., Daux, V., Filot, M., Grabner, M., Gutierrez, E., Haupt, M., Hilasvuori, E., Jungner, H., Kalela-Brundin, M., Krapiec, M., Leuenberger, M., Loader, N. J., Marah, H., Masson-Delmotte, V., Pazdur, A., Pawelczyk, S., Pierre, M., Planells, O., Pukiene, R., Reynolds-Henne, C. E., Rinne, K. T., Saracino, A., Sonninen, E., Stievenard, M., Switsur, V. R., Szczepanek, M., Szychowska-Krapiec, E., Todaro, L., Waterhouse, J. S. and Weigl, M.: Water-use efficiency and transpiration across European forests during the Anthropocene, Nat. Clim. Chang., 5(6), 579–583, doi:10.1038/nclimate2614, 2015.

Fuentes, L., Duguy, B. and Nadal-Sala, D.: Short-term effects of spring prescribed burning on the understory vegetation of a Pinus halepensis forest in Northeastern Spain, Sci. Total Environ., 610–611, 720–731, doi:10.1016/j.scitotenv.2017.08.050, 2018.

García-Suárez, A. M., Butler, C. J. and Baillie, M. G. L.: Climate signal in tree-ring

chronologies in a temperate climate: A multi-species approach, Dendrochronologia, 27(3), 183–198, doi:10.1016/j.dendro.2009.05.003, 2009.

Gérard, P. R., Temunović, M., Sannier, J., Bertolino, P., Dufour, J., Frascaria-Lacoste, N. and Fernández-Manjarrés, J. F.: Chilled but not frosty: Understanding the role of climate in the hybridization between the Mediterranean Fraxinus angustifolia Vahl and the temperate Fraxinus excelsior L. (Oleaceae) ash trees, J. Biogeogr., 40(5), 835–846, doi:10.1111/jbi.12021, 2013.

Gerber, S. and Brookshire, E. N. J.: Scaling of Physical Constraints at the Root-Soil Interface to Macroscopic Patterns of Nutrient Retention in Ecosystems, Am. Nat., 183(3), 418–430, doi:10.1086/674907, 2014.

Ghazavi, R., Thomas, Z., Hamon, Y. and Merot, P.: Soil water movement under a bottomland hedgerow during contrasting meteorological conditions, Hydrol. Process., 25, 1431–1442, doi:10.1002/hyp.7909, 2011.

Giles, M., Morley, N., Baggs, E. M. and Daniell, T. J.: Soil nitrate reducing processes - Drivers, mechanisms for spatial variation, and significance for nitrous oxide production, Front. Microbiol., 3(DEC), 1–16, doi:10.3389/fmicb.2012.00407, 2012.

Gómez-Gener, L., Obrador, B., von Schiller, D., Marcé, R., Casas-Ruiz, J. P., Proia, L., Acuña, V., Catalán, N., Muñoz, I. and Koschorreck, M.: Hot spots for carbon emissions from Mediterranean fluvial networks during summer drought, Biogeochemistry, 125(3), 409–426, doi:10.1007/s10533-015-0139-7, 2015.

González-Muñoz, N., Castro-Díez, P. and Fierro-Brunnenmeister, N.: Establishment success of coexisting native and exotic trees under an experimental gradient of irradiance and soil moisture, Environ. Manage., 48(4), 764–773, doi:10.1007/s00267-011-9731-3, 2011.

González-Muñoz, N., Castro-Díez, P. and Parker, I. M.: Differences in nitrogen use strategies between native and exotic tree species: Predicting impacts on invaded ecosystems, Plant Soil, 363(1–2), 319–329, doi:10.1007/s11104-012-1329-x, 2013.

González-Muñoz, N., Linares, J. C., Castro-Díez, P. and Sass-Klaassen, U.: Contrasting secondary growth and water-use efficiency patterns in native and exotic trees co-occurring in inner Spain riparian forests, For. Syst., 24(1), 1–10, doi:10.5424/fs/2015241-06586, 2015.

González, E.: Seasonal patterns of litterfall in the floodplain forest of a large Mediterranean river, Limnetica, 31(1), 173–186, 2012.

Goulden, M. L., Miller, S. D., Da Rocha, H. R., Menton, M. C., De Freitas, H. C., De

Silva Figueira, A. M. and Dias de Sousa, C. A.: Diel and Seasonal Patterns of Tropical Forest CO2 Exchange, Ecol. Appl., 14(4), 42–54, doi:10.1890/02-6008, 2004.

Graça, M. A. S., Pozo, J., Canhoto, C. and Elosegi, A.: Effects of Eucalyptus Plantations on Detritus, Decomposers, and Detritivores in Streams, Sci. World J., 2(May), 1173–1185, doi:10.1100/tsw.2002.193, 2002.

Grace, J., Berninger, F. and Nagy, L.: Impacts of climate change on the tree line, Ann. Bot., 90(4), 537–544, doi:10.1093/aob/mcf222, 2002.

Grady, K. C., Ferrier, S. M., Kolb, T. E., Hart, S. C., Allan, G. J. and Whitham, T. G.: Genetic variation in productivity of foundation riparian species at the edge of their distribution: Implications for restoration and assisted migration in a warming climate, Glob. Chang. Biol., 17, 3724–3735, doi:10.1111/j.1365-2486.2011.02524.x, 2011.

Green, T. R., Taniguchi, M., Kooi, H., Gurdak, J. J., Allen, D. M., Hiscock, K. M., Treidel, H. and Aureli, A.: Beneath the surface of global change: Impacts of climate change on groundwater, J. Hydrol., 405(3–4), 532–560, doi:10.1016/j.jhydrol.2011.05.002, 2011.

Gribovszki, Z., Szillágyi, J. and Kalicz, P.: Diurnal fluctuations in shallow groundwater levels and streamflow rates and their interpretation - A review, J. Hydrol., 385, 371–383, doi:10.1016/j.jhydrol.2010.02.001, 2010.

Groffman, P. M., Gold, A. J. and Simmons, R. C.: Nitrate dynamics in riparian forests: Microbial studies, J. Environ. Qual., 21(4), 666–671, doi:10.2134/jeq1992.00472425002100040022x, 1992.

Groffman, P. M., Gold, A. J. and Jacinthe, P.-A. a: Nitrous oxide production in riparian zones and groundwater, Chemosph. - Glob. Chang. Sci., 2, 291–299, doi:10.1023/A:1009719923861, 2000.

Guckland, A., Corre, M. D. and Flessa, H.: Variability of soil N cycling and N2O emission in a mixed deciduous forest with different abundance of beech, Plant Soil, 336(1–2), 25–38, doi:10.1007/s11104-010-0437-8, 2010.

Guidolotti, G., Rey, A., D'Andrea, E., Matteuci, G. and De Angelis, P.: Effect of environmental variables and stand structure on ecosystem respiration components in a Mediterranean beech forest, Tree Physiol., 0, 1–13, doi:10.1093/treephys/tpt065, 2013.

Hagedorn, F.: Hot spots and hot moments for greenhouse gas emissions from soils, Swiss Fed. Inst. For. Snow Landsc. Res., (1), 2010.

Hao, X. M., Li, Y. and Deng, H. J.: Assessment of hydraulic redistribution on desert riparian forests in an extremely arid area, Environ. Monit. Assess., 185(12), 10027–10038, doi:10.1007/s10661-013-3310-4, 2013.

Harms, T. K. and Grimm, N. B.: Hot spots and hot moments of carbon and nitrogen dynamics in a semiarid riparian zone, J. Geophys. Res., 113(G1), 1–14, doi:10.1029/2007JG000588, 2008.

Harms, T. K. and Grimm, N. B.: Responses of trace gases to hydrologic pulses in desert floodplains, J. Geophys. Res. Biogeosciences, 117(1), 1–14, doi:10.1029/2011JG001775, 2012.

Harms, T. K., Wentz, E. A. and Grimm, N. B.: Spatial heterogeneity of denitrification in semi-arid floodplains, Ecosystems, 12(1), 129–143, doi:10.1007/s10021-008-9212-6, 2009.

Hassler, S. K., Weiler, M. and Blume, T.: Tree-, stand- and site-specific controls on landscape-scale patterns of transpiration, Hydrol. Earth Syst. Sci. Discuss., doi:10.5194/hess-2017-47, 2017.

Healy, R. W., Striegl, R. G., Russell, T. F., Hutchinson, G. L. and Livingston, G. P.: Numerical Evaluation of Static-Chamber Measurements of Soil - Atmosphere Gas Exchange : Identification of Physical Processes, Soil Sci. Soc. Am. J., 60(3), 740–747, doi:10.2136/sssaj1996.03615995006000030009x, 1996.

Hedin, L. O., Fischer, J. C. Von, Ostrom, N. E., Kennedy, B. P., Brown, M. G., Robertson, G. P., Ecology, S. and Mar, N.: Thermodynamic Constraints on Nitrogen Transformations and Other Biogeochemical Processes at Soil-Stream Interfaces, , 79(2), 684–703, 1998.

Hefting, M. M., Bobbink, R. and de Caluwe, H.: Nitrous oxide emission and denitrification in chronically nitrate-loaded riparian buffer zones., J. Environ. Qual., 32(4), 1194–203 [online] Available from: http://www.ncbi.nlm.nih.gov/pubmed/12931872, 2003.

Hefting, M. M., Clément, J.-C., Dowrick, D., Cosandey, A. C., Bernal, S., Cimpian, C., Tatur, A., Burt, T. P. and Pinay, G.: Water table elevations controls on soil nitrogen cycling in riparian wetlands along a European climatic gradient, Biogeochemistry, 67, 113–134, doi:10.1023/B:BIOG.0000015320.69868.33, 2004.

Hefting, M. M., Clement, J. C., Bienkowski, P., Dowrick, D., Guenat, C., Butturini, A., Topa, S., Pinay, G. and Verhoeven, J. T. A.: The role of vegetation and litter in the nitrogen dynamics of riparian buffer zones in Europe, Ecol. Eng., 24, 465–482, doi:10.1016/j.ecoleng.2005.01.003, 2005.

Hellmann, C., Sutter, R., Rascher, K. G., Máguas, C., Correia, O. and Werner, C.: Impact of an exotic N2-fixing Acacia on composition and N status of a native Mediterranean community, Acta Oecologica, 37(1), 43–50, doi:10.1016/j.actao.2010.11.005, 2011.

Hernandez-Santana, V., Asbjornsen, H., Sauer, T., Isenhart, T., Schilling, K. and Schultz, R.: Enhanced transpiration by riparian buffer trees in response to advection in a humid temperate agricultural landscape, For. Ecol. Manage., 261, 1415–1427, doi:10.1016/j.foreco.2011.01.027, 2011.

Hill, A. R.: Nitrate Removal in Stream Riparian Zones, J. Environ. Qual., 25, 743–755, doi:10.2134/jeq1996.00472425002500040014x, 1996.

Hill, A. R., Devito, K. J., Campagnolo, S. and Sanmugadas, K.: Subsurface denitrification in a forest riparianzone: Interactions between hydrology and supplies ofnitrate and organic carbon, Biogeochemistry, 51, 193–223, doi:10.1023/a:1006476514038, 2000.

Hirota, M., Senga, Y., Seike, Y., Nohara, S. and Kunii, H.: Fluxes of carbon dioxide, methane and nitrous oxide in two contrastive fringing zones of coastal lagoon, Lake Nakaumi, Japan, Chemosphere, 68(3), 597–603, doi:10.1016/j.chemosphere.2007.01.002, 2007.

Hobson, K. A. and Wassenaar, L. I.: Stable isotope ecology: An introduction, Oecologia, 120(3), 312–313, doi:10.1007/s004420050864, 1999.

Hoelscher, M. T., Nehls, T., Jänicke, B. and Wessolek, G.: Quantifying cooling effects of facade greening: Shading, transpiration and insulation, Energy Build., 114, 283–290, doi:10.1016/j.enbuild.2015.06.047, 2015.

Hoover, T. M., Pinto, X. and Richardson, J. S.: Riparian canopy type, management history, and successional stage control fluxes of plant litter to streams, Can. J. For. Res., 41(7), 1394–1404, doi:10.1139/x11-067, 2011.

Huang, W., Fonti, P., Larsen, J. B., Ræbild, A., Callesen, I., Pedersen, N. B. and Hansen, J. K.: Projecting tree-growth responses into future climate: A study case from a Danish-wide common garden, Agric. For. Meteorol., 247(October), 240–251, doi:10.1016/j.agrformet.2017.07.016, 2017.

Hultine, K. R., Burtch, K. G. and Ehleringer, J. R.: Gender specific patterns of carbon uptake and water use in a dominant riparian tree species exposed to a warming climate, Glob. Chang. Biol., 19, 3390–3405, doi:10.1111/gcb.12230, 2013.

Huxman, T. E., Wilcox, B. P., Breshears, D. D., Scott, R. L., Snyder, K. A., Small, E.

E., Hultine, K., Pockman, W. T. and Jackson, R. B.: Ecohydrological implications of woody plant encroachment, Ecology, 86(2), 308–319, 2005.

Inclán, R., Uribe, C., Sánchez, L., Sánchez, D. M., Clavero, Á., Fernández, A. M., Morante, R. and Blanco, A.: N2O and CH4 fluxes in undisturbed and burned holm oak, scots pine and pyrenean oak forests in central Spain, , (September), doi:10.1007/s10533-010-9520-8, 2014.

Jacinthe, P. a., Vidon, P., Fisher, K., Liu, X. and Baker, M. E.: Soil Methane and Carbon Dioxide Fluxes from Cropland and Riparian Buffers in Different Hydrogeomorphic Settings, J. Environ. Qual., 44(0), 1080–1090, doi:10.2134/jeq2015.01.0014, 2015.

Jacinthe, P. A. and Dick, W. A.: Soil management and nitrous oxide emissions from cultivated fields in southern Ohio, Soil Tillage Res., 41, 221–235, doi:10.1016/S0167-1987(96)01094-X, 1997.

Jack Brookshire, E. N., Gerber, S., Webster, J. R., Vose, J. M. and Swank, W. T.: Direct effects of temperature on forest nitrogen cycling revealed through analysis of long-term watershed records, Glob. Chang. Biol., 17, 297–308, doi:10.1111/j.1365-2486.2010.02245.x, 2011.

Jacob, M., Viedenz, K., Polle, A. and Thomas, F. M.: Leaf litter decomposition in temperate deciduous forest stands with a decreasing fraction of beech (Fagus sylvatica), Oecologia, 164(4), 1083–1094, doi:10.1007/s00442-010-1699-9, 2010.

Jaeger, C., Gessler, A., Biller, S., Rennenberg, H. and Kreuzwieser, J.: Differences in C metabolism of ash species and provenances as a consequence of root oxygen deprivation by waterlogging, J. Exp. Bot., 60(15), 4335–4345, doi:10.1093/jxb/erp268, 2009.

Janík, D., Adam, D., Hort, L., Král, K., Šamonil, P., Unar, P. and Vrška, T.: Patterns of Fraxinus angustifolia in an alluvial old-growth forest after declines in flooding events, Eur. J. For. Res., 135(2), 215–228, doi:10.1007/s10342-015-0925-8, 2016.

Janzen, H. H.: Deposition of nitrogen into the rhizosphere by wheat roots, Soil Biol. Biochem., 22(8), 1155–1160, doi:10.1016/0038-0717(90)90043-Y, 1990.

Johnson, S. E. and Abrams, M. D.: Age class, longevity and growth rate relationships: Protracted growth increases in old trees in the eastern United States, Tree Physiol., 29(11), 1317–1328, doi:10.1093/treephys/tpp068, 2009.

Jump, A. S., Hunt, J. M. and Peñuelas, J.: Rapid climate change-related growth decline at the southern range edge of Fagus sylvatica, Glob. Chang. Biol., 12(11),

2163–2174, doi:10.1111/j.1365-2486.2006.01250.x, 2006.

Jung, M., Reichstein, M., Ciais, P., Seneviratne, S. I., Sheffield, J., Goulden, M. L., Bonan, G., Cescatti, A., Chen, J., de Jeu, R., Dolman, A. J., Eugster, W., Gerten, D., Gianelle, D., Gobron, N., Heinke, J., Kimball, J., Law, B. E., Montagnani, L., Mu, Q., Mueller, B., Oleson, K., Papale, D., Richardson, A. D., Roupsard, O., Running, S., Tomelleri, E., Viovy, N., Weber, U., Williams, C., Wood, E., Zaehle, S. and Zhang, K.: Recent decline in the global land evapotranspiration trend due to limited moisture supply, Nature, 467, 951–954, doi:10.1038/nature09396, 2010.

Kazda, M., Salzer, J. and Reiter, I.: Photosynthetic capacity in relation to nitrogen in the canopy of a Quercus robur, Fraxinus angustifolia and Tilia cordata flood plain forest, Tree Physiol., 20(15), 1029–1037, doi:10.1093/treephys/20.15.1029, 2000.

Keeney, D. R.; Nelson, D. W.: Nitrogen-inorganic forms., in Agronomy Monography 9, ASA and SSSA., pp. 643–698, Madison., 1982.

Kesik, M., Ambus, P., Baritz, R., Brüggemann, N., Butterbach-Bahl, K., Damm, M., Guyzer, J., Horváth, L., Kiese, R., Kitzler, B., Leip, A., LI, C., Pihlatie, M. and Pilegaard, K.: Inventories of N 2 O and NO emissions from European forest soils, , 353–375, 2005.

Kim, J. and Verma, S. B.: Components of surface energy balance in a temperate grassland ecosystem, Boundary-Layer Meteorol., 51(4), 401–417, 1990.

Kløve, B., Ala-aho, P., Bertrand, G., Boukalova, Z., Ertürk, A., Goldscheider, N., Ilmonen, J., Karakaya, N., Kupfersberger, H., Kvœrner, J., Lundberg, A., Mileusnić, M., Moszczynska, A., Muotka, T., Preda, E., Rossi, P., Siergieiev, D., Šimek, J., Wachniew, P., Angheluta, V. and Widerlund, A.: Groundwater dependent ecosystems. Part I: Hydroecological status and trends, Environ. Sci. Policy, 14(7), 770–781, doi:10.1016/j.envsci.2011.04.002, 2011.

Kløve, B., Ala-Aho, P., Bertrand, G., Gurdak, J. J., Kupfersberger, H., Kværner, J., Muotka, T., Mykrä, H., Preda, E., Rossi, P., Uvo, C. B., Velasco, E. and Pulido-Velazquez, M.: Climate change impacts on groundwater and dependent ecosystems, J. Hydrol., 518(PB), 250–266, doi:10.1016/j.jhydrol.2013.06.037, 2014.

Knops, J. M. H., Bradley, K. L. and Wedin, D. A.: Mechanisms of plant species impacts on ecosystem nitrogen cycling, Ecol. Lett., 5(3), 454–466, doi:10.1046/j.1461-0248.2002.00332.x, 2002.

Kominoski, J. S., Shah, J. J. F., Canhoto, C., Fischer, D. G., Giling, D. P., González, E., Griffiths, N. A., Larrañaga, A., LeRoy, C. J., Mineau, M. M., McElarney, Y. R., Shirley, S. M., Swan, C. M. and Tiegs, S. D.: Forecasting functional implications of

global changes in riparian plant communities, Front. Ecol. Environ., 11(8), 423–432, doi:10.1890/120056, 2013.

de la Riva, E. G., Marañón, T., Violle, C., Villar, R. and Pérez-Ramos, I. M.: Biogeochemical and Ecomorphological Niche Segregation of Mediterranean Woody Species along a Local Gradient, Front. Plant Sci., 8(July), 1–9, doi:10.3389/fpls.2017.01242, 2017.

De La Riva, E. G., Olmo, M., Poorter, H., Ubera, J. L. and Villar, R.: Leaf mass per area (LMA) and its relationship with leaf structure and anatomy in 34 mediterranean woody species along a water availability gradient, PLoS One, 11(2), 1–18, doi:10.1371/journal.pone.0148788, 2016.

Lang, P., Ahlborn, J., Schäfer, P., Wommelsdorf, T., Jeschke, M., Zhang, X. and Thomas, F. M.: Growth and water use of Populus euphratica trees and stands with different water supply along the Tarim River, NW China, For. Ecol. Manage., 380, 139–148, doi:10.1016/j.foreco.2016.08.049, 2016.

Langenbruch, C., Helfrich, M. and Flessa, H.: Effects of beech (Fagus sylvatica), ash (Fraxinus excelsior) and lime (Tilia spec.) on soil chemical properties in a mixed deciduous forest, Plant Soil, 352(1–2), 389–403, doi:10.1007/s11104-011-1004-7, 2012.

Laudon, H., Kuglerová, L., Sponseller, R. A., Futter, M., Nordin, A., Bishop, K., Lundmark, T., Egnell, G. and Ågren, A. M.: The role of biogeochemical hotspots, landscape heterogeneity, and hydrological connectivity for minimizing forestry effects on water quality, Ambio, 45, 152–162, doi:10.1007/s13280-015-0751-8, 2016.

Legner, N., Fleck, S. and Leuschner, C.: Low light acclimation in five temperate broad-leaved tree species of different successional status: The significance of a shade canopy, Ann. For. Sci., 70(6), 557–570, doi:10.1007/s13595-013-0298-4, 2013.

Lemoine, D., Peltier, J.-P. and Marigo, G.: Comparative studies of the water relations and the hydraulic characteristics in Fraxinus excelsior, Acer pseudoplatanus and A. opalus trees under soil water contrasted conditions, Ann. For. Sci., 58(7), 723–731, doi:10.1051/forest:2001159, 2001.

Li, W., Yan, M., Qingfeng, Z. and Xingchang, Z.: Groundwater use by plants in a semi-arid coal-mining area at the Mu Us Desert frontier, Environ. Earth Sci., 69(3), 1015–1024, doi:10.1007/s12665-012-2023-2, 2013.

Linares, J. C. and Tíscar, P. A.: Climate change impacts and vulnerability of the southern populations of Pinus nigra subsp. salzmannii, Tree Physiol., 30(7), 795–806, doi:10.1093/treephys/tpq052, 2010.

Linn, D. M. and Doran, J. W.: Effect of Water-Filled Pore Space on Carbon Dioxide and Nitrous Oxide Production in Tilled and Nontilled Soils, Soil Sci. Soc. Am. J., 48(1961), 1267–1272, doi:10.2136/sssaj1984.03615995004800060013x, 1984.

Lite, S. J. and Stromberg, J. C.: Surface water and ground-water thresholds for maintaining Populus-Salix forests, San Pedro River, Arizona, Biol. Conserv., 125(2), 153–167, doi:10.1016/j.biocon.2005.01.020, 2005.

Liu, B., Guan, H., Zhao, W., Yang, Y. and Li, S.: Groundwater facilitated water-use efficiency along a gradient of groundwater depth in arid northwestern China, Agric. For. Meteorol., 233, 235–241, doi:10.1016/j.agrformet.2016.12.003, 2017.

Liu, S., Chen, Y., Chen, Y., Friedman, J. M., Hati, J. H. A. and Fang, G.: Use of 2H and 18O stable isotopes to investigate water sources for different ages of Populus euphratica along the lower Heihe River, Ecol. Res., 30(4), 581–587, doi:10.1007/s11284-015-1270-6, 2015.

Loader, N. J., Robertson, I. and McCarroll, D.: Comparison of stable carbon isotope ratios in the whole wood, cellulose and lignin of oak tree-rings, Palaeogeogr. Palaeoclimatol. Palaeoecol., 196(3–4), 395–407, doi:10.1016/S0031-0182(03)00466-8, 2003.

Luo, Y., Gerten, D., Le Maire, G., Parton, W. J., Weng, E., Zhou, X., Keough, C., Beier, C., Ciais, P., Cramer, W., Dukes, J. S., Emmett, B., Hanson, P. J., Knapp, A., Linder, S., Nepstad, D. and Rustad, L.: Modeled interactive effects of precipitation, temperature, and [CO2] on ecosystem carbon and water dynamics in different climatic zones, Glob. Chang. Biol., 14, 1986–1999, doi:10.1111/j.1365-2486.2008.01629.x, 2008.

Lupon, A., Gerber, S., Sabater, F. and Bernal, S.: Climate response of the soil nitrogen cycle in three forest types of a headwater Mediterranean catchment, J. Geophys. Res. Biogeosciences, 120, 859–875, doi:10.1002/2014JG002791.Received, 2015.

Lupon, A., Sabater, F., Miñarro, A. and Bernal, S.: Contribution of pulses of soil nitrogen mineralization and nitrification to soil nitrogen availability in three Mediterranean forests, Environ. J. Soil Sci., 67, 303–313, doi:10.1016/j.aqpro.2013.07.003, 2016a.

Lupon, A., Martí, E., Sabater, F. and Bernal, S.: Green light: Gross primary production influences seasonal stream N export by controlling fine-scale N dynamics, Ecology, 97(1), 133–144, doi:10.1890/14-2296.1, 2016b.

Lupon, A., Bernal, S., Poblador, S., Martí, E. and Sabater, F.: The influence of

riparian evapotranspiration on stream hydrology and nitrogen retention in a subhumid Mediterranean catchment, Hydrol. Earth Syst. Sci., 20, 3831–3842, doi:10.5194/hess-20-3831-2016, 2016c.

Magdaleno, F., Blanco-Garrido, F., Bonada, N. and Herrera-Grao, T.: How are riparian plants distributed along the riverbank topographic gradient in Mediterranean rivers? Application to minimally altered river stretches in Southern Spain, Limnetica, 33(1), 121–138, doi:10.1007/s10750-012-1304-9, 2014.

Malcolm, G. M., Bush, D. S. and Rice, S. K.: Soil nitrogen conditions approach preinvasion levels following restoration of nitrogen-fixing black locust (robinia pseudoacacia) stands in a pine-oak Ecosystem, Restor. Ecol., 16(1), 70–78, doi:10.1111/j.1526-100X.2007.00263.x, 2008.

Mander, Ü., Well, R., Weymann, D., Soosaar, K., Maddison, M., Kanal, A., Lõhmus, K., Truu, J., Augustin, J. and Tournebize, J.: Isotopologue Ratios of N 2 O and N 2 Measurements Underpin the Importance of Denitri fi cation in Di ff erently N - Loaded Riparian Alder Forests, Environ. Sci. Technol., 48, 11910–11918, doi:dx.doi.org/10.1021/es501727h, 2014.

Mander, Ü. ¨, Lõhmus, K., Teiter, S., Mauring, T., Nurk, K. and Augustin, J.: Gaseous fluxes in the nitrogen and carbon budgets of subsurface flow constructed wetlands, Sci. Total Environ., 404(2–3), 343–353, doi:10.1016/j.scitotenv.2008.03.014, 2008.

Mantovani, D., Veste, M. and Freese, D.: Black locust (Robinia pseudoacacia L.) ecophysiological and morphological adaptations to drought and their consequence on biomass production and water-use efficiency, New Zeal. J. For. Sci., 44(1), 1–11, doi:10.1186/s40490-014-0029-0, 2014.

Marañón, T. and Ojeda, J. F.: Ecology and history of a wooded landscape in suthern Spain, Ecol. Hist. Eur. For., 1998.

De Marco, A., Spaccini, R., Vittozzi, P., Esposito, F., Berg, B. and Virzo De Santo, A.: Decomposition of black locust and black pine leaf litter in two coeval forest stands on Mount Vesuvius and dynamics of organic components assessed through proximate analysis and NMR spectroscopy, Soil Biol. Biochem., 51, 1–15, doi:10.1016/j.soilbio.2012.03.025, 2012.

Martí, E., Schade, J. D. and Grimm, N. B.: Flood frequency and stream-riparian linkages in arid lands, in Stream and Ground Waters, edited by J. B. Jones and J. Mulholland, pp. 111–135., 2000.

Martínez-Sancho, E., Dorado-Liñán, I., Gutiérrez Merino, E., Matiu, M., Helle, G.,

Heinrich, I. and Menzel, A.: Increased water-use efficiency translates into contrasting growth patterns of Scots pine and sessile oak at their southern distribution limits, Glob. Chang. Biol., 24(3), 1012–1028, doi:10.1111/gcb.13937, 2018.

Martnez-Vilalta, J., Poyatos, R., Aguade, D., Retana, J. and Mencuccini, M.: A new look at water transport regulation in plants, New Phytol., 204(1), 105–115, doi:10.1111/nph.12912, 2014.

Mayer, P. M., Reynolds, S. K. and Canfield, T. J.: Riparian buffer width, vegetative cover, and nitrogen removal effectiveness: a review of current science and regulations., Epa/600/R-05/118, 1–40 [online] Available from: http://nepis.epa.gov/Exe/ZyPDF.cgi/2000O182.PDF?Dockey=2000O182.PDF, 2005.

McCarroll, D. and Loader, N. J.: Stable isotopes in tree rings, Quat. Sci. Rev., 23(7–8), 771–801, doi:10.1016/j.quascirev.2003.06.017, 2004.

McClain, M. E., Boyer, E. W., Dent, C. L., Gergel, S. E., Grimm, N. B., Groffman, P. M., Hart, S. C., Harvey, J. W., Johnston, C. a., Mayorga, E., McDowell, W. H. and Pinay, G.: Biogeochemical Hot Spots and Hot Moments at the Interface of Terrestrial and Aquatic Ecosystems, Ecosystems, 6(4), 301–312, doi:10.1007/s10021-003-0161-9, 2003.

McGlynn, B. L. and Seibert, J.: Distributed assessment of contributing area and riparian buffering along stream networks, Water Resour. Res., 39(4), 1–7, doi:10.1029/2002WR001521, 2003.

McLain, J. E. T. and Martens, D. A.: N2O production by heterotrophic N transformations in a semiarid soil, Appl. Soil Ecol., 32(2), 253–263, doi:10.1016/j.apsoil.2005.06.005, 2006.

Medici, C., Butturini, A., Bernal, S., Vázquez, E., Sabater, F., Vélez, J. I. and Francés, F.: Modelling the non-linear hydrological behaviour of a small Mediterranean forested catchment, Hydrol. Process., 22, 3814–3828, doi:10.1002/hyp, 2008.

Medina-Villar, S., Alonso, Á., Vázquez De Aldana, B. R., Pérez-Corona, E. and Castro-Díez, P.: Decomposition and biological colonization of native and exotic leaf litter in a Central Spain stream, Limnetica, 34(2), 293–310, 2015a.

Medina-Villar, S., Castro-Díez, P., Alonso, A., Cabra-Rivas, I., Parker, I. M. and Pérez-Corona, E.: Do the invasive trees, Ailanthus altissima and Robinia pseudoacacia, alter litterfall dynamics and soil properties of riparian ecosystems in Central Spain?, Plant Soil, 396(1–2), 311–324, doi:10.1007/s11104-015-2592-4, 2015b.

Meixner, T., Manning, A. H., Stonestrom, D. A., Allen, D. M., Ajami, H., Blasch, K. W., Brookfield, A. E., Castro, C. L., Clark, J. F., Gochis, D. J., Flint, A. L., Neff, K. L., Niraula, R., Rodell, M., Scanlon, B. R., Singha, K. and Walvoord, M. A.: Implications of projected climate change for groundwater recharge in the western United States, J. Hydrol., 534, 124–138, doi:10.1016/j.jhydrol.2015.12.027, 2016.

Menzel, A.: Phenology: Its Importance To the Global Change Community, Clim. Change, (54), 379–385, doi:10.1023/A:1016125215496, 2002.

Messaoudène, M. and Tessier, L.: Relations cerne-climat dans des peuplements de Quercus afares willd et Quercus canariensis Pomel en Algerie, Ann. des Sci. For., 54(4), 347–358, 1997.

Michelot, A., Eglin, T., Dufrêne, E., Lelarge-Trouverie, C. and Damesin, C.: Comparison of seasonal variations in water-use efficiency calculated from the carbon isotope composition of tree rings and flux data in a temperate forest, Plant, Cell Environ., 34(2), 230–244, doi:10.1111/j.1365-3040.2010.02238.x, 2011.

Mitsch, W. J. . and Gosselink, J. G.: Wetlands, 4th editio., edited by I. J. Wiley & Sons., 2007.

Moore, G. W. and Heilman, J. L.: Ecohydrology Bearing - Invited Commentary Transformation ecosystem change and ecohydology: ushering in a new era for watershed management, Ecohydrology, 4, 351–358, doi:10.1002/eco.232, 2011.

Morse, J. L. ., Ardon, M. and Benhartdt, E. S.: Greenhouse gas fluxes in southeastern U.S. coastal plain wetlands under contrasting land uses, Ecol. Appl., 22(1), 264–280, doi:10.1890/11-0527.1, 2012.

Motta, R., Nola, P. and Berretti, R.: The rise and fall of the black locust (Robinia pseudoacacia L.) in the "Siro Negri" Forest Reserve (Lombardy, Italy): lessons learned and future uncertainties, Ann. For. Sci., 66(4), 410–410, doi:10.1051/forest/2009012, 2009.

Muller, D., Warneke, T., Rixen, T., Muller, M., Jamahari, S., Denis, N., Mujahid, A. and Notholt, J.: Lateral carbon fluxes and CO2 outgassing from a tropical peat-draining river, Biogeosciences, 12, 5967–5979, doi:10.5194/bg-12-5967-2015, 2015.

Myers, N., Mittermeier, R. A., Mittermeier, C. G., da Fonseca, G. A. B. and Kent, J.: Biodiversity hotspots for conservation priorities, Nature, 403(6772), 853–858, doi:10.1038/35002501, 2000.

Nadal-Sala, D., Sabaté, S., Sánchez-Costa, E., Poblador, S., Sabater, F. and Gracia, C.: Growth and water use performance of four co-occurring riparian tree species in

a Mediterranean riparian forest, For. Ecol. Manage., 396, 132–142, doi:10.1016/j.foreco.2017.04.021, 2017.

Naiman, R. J., Décamps, H. and McClain, M. E.: Riparia — Ecology, Conservation and Management of Streamside Communities, in Aquatic Conservation: Marine and Freshwater Ecosystems, vol. 17, edited by E. A. Press, pp. 657–657, London., 2005.

Nakagawa, S. and Schielzeth, H.: A general and simple method for obtaining R2 from generalized linear mixed-effects models, Methods Ecol. Evol., 4(2), 133–142, doi:10.1111/j.2041-210x.2012.00261.x, 2013.

Nardini, A. and Tyree, M. T.: Root and shoot hydraulic conductance of seven Quercus species, Ann. For. Sci., 56(5), 371–377, doi:10.1051/forest:19990502, 1999.

Nechita, C., Popa, I. and Eggertsson, Ó.: Climate response of oak (Quercus spp.), an evidence of a bioclimatic boundary induced by the Carpathians, Sci. Total Environ., 599–600, 1598–1607, doi:10.1016/j.scitotenv.2017.05.118, 2017.

Niinemets, Ü.: Global-scale climatic controls of leaf dry mass per area, density and thickness in trees and shrubs, Ecology, 82(2), 453–469, 2001.

O'Grady, A. P., Eamus, D., Cook, P. G. and Lamontagne, S.: Groundwater use by riparian vegetation in the wet-dry tropics of northern Australia, Aust. J. Bot., 54(2), 145–154, doi:10.1071/BT04164, 2006.

O'Neill, G. A., Hamann, A. and Wang, T.: Accounting for population variation improves estimates of the impact of climate change on species' growth and distribution, J. Appl. Ecol., 45, 1040–1049, doi:10.1111/j.1365-2664.2008.01472.x, 2008.

Ocampo, C. J., Sivapalan, M. and Oldham, C.: Hydrological connectivity of upland-riparian zones in agricultural catchments: Implications for runoff generation and nitrate transport, J. Hydrol., 331, 643–658, doi:10.1016/j.jhydrol.2006.06.010, 2006.

Oertel, C., Matschullat, J., Zurba, K., Zimmermann, F. and Erasmi, S.: Greenhouse gas emissions from soils - A review, Chemie der Erde - Geochemistry, 76, 327–352, doi:10.1016/j.chemer.2016.04.002, 2016.

Ogaya, R. and Peñuelas, J.: Contrasting foliar responses to drought in Quercus ilex and Phillyrea latifolia, Biol. Plant., 50(3), 373–382, doi:10.1007/s10535-006-0052-y, 2006.

Ogaya, R. and Peñuelas, J.: Leaf mass per area ratio in Quercus ilex leaves under a

wide range of climatic conditions. The importance of low temperatures, Acta Oecologica, 31(2), 168–173, doi:10.1016/j.actao.2006.07.004, 2007.

Oliveira, P. J. C., Davin, E. L., Levis, S. and Seneviratne, S. I.: Vegetation-mediated impacts of trends in global radiation on land hydrology: A global sensitivity study, Glob. Chang. Biol., 17, 3453–3467, doi:10.1111/j.1365-2486.2011.02506.x, 2011.

Olson, J. S.: Energy Storage and the Balance of Producers and Decomposers in Ecological Systems, Ecology, 44(2), 322–331, doi:10.2307/1932179, 1963.

Osborne, L. L. and Kovacic, D. A.: Riparian vegetated buffer strips in water-quality restoration and stream management, Freshw. Biol., 29(2), 243–258, doi:10.1111/j.1365-2427.1993.tb00761.x, 1993.

Oshun, J., Dietrich, W. E., Dawson, T. E. and Fung, I.: Dynamic, structured heterogeneity of water isotopes inside hillslopes, Water Resour. Res., 52(1), 164–189, doi:10.1002/2015WR017485, 2016.

Pacific, V. J., McGlynn, B. L., Riveros-Iregui, D. A., Welsch, D. L. and Epstein, H. E.: Variability in soil respiration across riparian-hillslope transitions, Biogeochemistry, 91(1), 51–70, doi:10.1007/s10533-008-9258-8, 2008.

Page, A. L., Miller, R. H. and Keeney, D. R.: Methods of Soil Analysis. Part 2: Chemical and Microbiological Properties., edited by I. SSSA and ASA and W. Madison., 1982.

Paredes, D., Cayuela, L., Gurr, G. M. and Campos, M.: Is ground cover vegetation an effective biological control enhancement strategy against Olive Pests?, PLoS One, 10(2), 1–13, doi:10.1371/journal.pone.0117265, 2015.

Pastor, A., Riera, J. L., Peipoch, M., Cañas, L., Ribot, M., Gacia, E., Martí, E. and Sabater, F.: Temporal variability of nitrogen stable isotopes in primary uptake xompartments in four streams differing in human impacts, Environ. Sci. Technol., 48, 6612–6619, 2014.

Pedersen, B. S.: The role of stress in the mortality of Midwestern oaks as indicated by growth prior to death, Ecology, 79(1), 79–93, doi:10.2307/176866, 1998.

Peñuelas, J. and Boada, M.: A global change-induced biome shift in the Montseny mountains (NE Spain), Glob. Chang. Biol., 9, 131–140, doi:10.1046/j.1365-2486.2003.00566.x, 2003.

Peñuelas, J., Hunt, J. M., Ogaya, R. and Jump, A. S.: Twentieth century changes of tree-ring δ13C at the southern range-edge of Fagus sylvatica: Increasing water-use

efficiency does not avoid the growth decline induced by warming at low altitudes, Glob. Chang. Biol., 14(5), 1076–1088, doi:10.1111/j.1365-2486.2008.01563.x, 2008.

Pérez-Ramos, I. M., Aponte, C., García, L. V., Padilla-Díaz, C. M., Marañón, T. and Delzon, S.: Why Is seed production so variable among individuals? A ten-year study with oaks reveals the importance of soil environment, PLoS One, 9(12), 1–19, doi:10.1371/journal.pone.0115371, 2014.

Perry, L. G., Andersen, D. C., Reynolds, L. V., Nelson, S. M. and Shafroth, P. B.: Vulnerability of riparian ecosystems to elevated CO2 and climate change in arid and semiarid western North America, Glob. Chang. Biol., 18(3), 821–842, doi:10.1111/j.1365-2486.2011.02588.x, 2012.

Pert, P. L., Butler, J. R. A., Brodie, J. E., Bruce, C., Honzák, M., Metcalfe, D., Mitchell, D. and Wong, G.: A catchment-based approach to mapping hydrological ecosystem services using riparian habitat: A case study from the Wet Tropics, Australia, Ecol. Complex., 7(3), 378–388, doi:10.1016/j.ecocom.2010.05.002, 2010.

Pezeshki, S. R. and Delaune, R. D.: Effects of Soil Hypoxia and Salinity on Gas-Exchange and Growth of Spartina-Patens, Mar. Ecol. Ser., 96(1), 75–81, doi:10.3354/meps096075, 1993.

Phipps, R. L. and Whiton, J. C.: Decline in long-term growth trends of white oak., Can. J. For. Res., 18, 24–32, 1988.

Pielech, R., Anioł-Kwiatkowska, J. and Szcześniak, E.: Landscape-scale factors driving plant species composition in mountain streamside and spring riparian forests, For. Ecol. Manage., 347, 217–227, doi:10.1016/j.foreco.2015.03.038, 2015.

Pinay, G., Gumiero, B., Tabacchi, E., Gimenez, O., Tabacchi-Planty, a. M., Hefting, M. M., Burt, T. P., Black, V. a., Nilsson, C., Iordache, V., Bureau, F., Vought, L., Petts, G. E. and Décamps, H.: Patterns of denitrification rates in European alluvial soils under various hydrological regimes, Freshw. Biol., 52(2), 252–266, doi:10.1111/j.1365-2427.2006.01680.x, 2007a.

Pinay, G., Gumiero, B., Tabacchi, E., Gimenez, O., Tabacchi-Planty, A. M., Hefting, M. M., Burt, T. P., Black, V. A., Nilsson, C., Iordache, V., Bureau, F., Vought, L., Petts, G. E. and Décamps, H.: Patterns of denitrification rates in European alluvial soils under various hydrological regimes, Freshw. Biol., 52, 252–266, doi:10.1111/j.1365-2427.2006.01680.x, 2007b.

Pinay, G., Peiffer, S., De Dreuzy, J.-R., Krause, S., Hannah, D. M., Fleckenstein, J. H., Sebilo, M., Bishop, K. and Hubert-moy, L.: Upscaling Nitrogen Removal Capacity from Local Hotspots to Low Stream Orders ' Drainage Basins,

Ecosystems, 18, 1101–1120, doi:10.1007/s10021-015-9878-5, 2015.

Poblador, S., Lupon, A., Sabaté, S. and Sabater, F.: Soil water content drives spatiotemporal patterns of CO2 and N2O emissions from a Mediterranean riparian forest soil, Biogeosciences, 14(18), 4195–4208, doi:10.5194/bg-14-4195-2017, 2017.

Poblador, S., Sperlich, D., Nadal-Sala, D., Sabater, F. and Sabaté, S.: Riparian tree species responses to water availability limitations in a Mediterranean riparian forest, n.d.

Poorter, H., Niinemets, Ü., Poorter, L., Wright, I. J., Villar, R., Niinemets, U., Poorter, L., Wright, I. J. and Villar, R.: Causes and consequences of variation in leaf mass per area (LMA):a meta-analysis, New Phytol., 182(3), 565–588, doi:10.1111/j.1469-8137.2009.02830.x, 2009.

Qualls, R. G. and Haines, B. L.: Biodegradability of Dissolved Organic Matter in Forest Throughfall, Soil Solution, and Stream Water, Soil Sci. Soc. Am. J., 56(2), 578, doi:10.2136/sssaj1992.03615995005600020038x, 1992.

Quero, J. L., Villar, R., Marañón, T. and Zamora, R.: Interactions of drought and shade effects on seedlings of four Quercus species: physiological and structural leaf responses., New Phytol., 170(4), 819–33, doi:10.1111/j.1469-8137.2006.01713.x, 2006.

Quero, J. L., Villar, R., Marañón, T., Murillo, A. and Zamora, R.: Respuesta plástica a la luz y al agua en cuatro especies mediterráneas del género Quercus (Fagaceae), Rev. Chil. Hist. Nat., 81(3), 373–385, doi:10.4067/S0716-078X2008000300006, 2008.

Radtke, A., Ambraß, S., Zerbe, S., Tonon, G., Fontana, V. and Ammer, C.: Traditional coppice forest management drives the invasion of Ailanthus altissima and Robinia pseudoacacia into deciduous forests, For. Ecol. Manage., 291, 308–317, doi:10.1016/j.foreco.2012.11.022, 2013.

Raich, J. W., Potter, C. S. and Bhagawati, D.: Interannual variability in global soil respiration , 1980 - 94, Glob. Chang. Biol., 8, 800–812, 2002.

Ranalli, A. J. and Macalady, D. L.: The importance of the riparian zone and in-stream processes in nitrate attenuation in undisturbed and agricultural watersheds - A review of the scientific literature, J. Hydrol., 389, 406–415, doi:10.1016/j.jhydrol.2010.05.045, 2010.

Rascher, K. G., Hellmann, C., Máguas, C. and Werner, C.: Community scale 15N isoscapes: Tracing the spatial impact of an exotic N 2-fixing invader, Ecol. Lett., 15(5), 484–491, doi:10.1111/j.1461-0248.2012.01761.x, 2012.

Rastogi, M., Singh, S. and Pathak, H.: Emission of carbon dioxide from soil, Curr. Sci., 82(5), 510–517, 2002.

Rennenberg, H., Dannenmann, M., Gessler, A., Kreuzwieser, J., Simon, J. and Papen, H.: Nitrogen balance in forest soils: Nutritional limitation of plants under climate change stresses, Plant Biol., 11(SUPPL.1), 4–23, doi:10.1111/j.1438-8677.2009.00241.x, 2009.

Rice, S. K., Westerman, B. and Federici, R.: Impacts of the exotic, nitrogen-fixing black locust (Robinia pseudoacacia) on nitrogen-cycling in a pine-oak ecosystem, Plant Ecol., 174(1), 97–107, doi:10.1023/B:VEGE.0000046049.21900.5a, 2004.

Richards, L. A.: Capillary conduction of liquids through porous mediums, Physics (College. Park. Md)., 1(5), 318–333, doi:doi:10.1063/1.1745010.., 1934.

Rieger, I., Kowarik, I., Cherubini, P. and Cierjacks, A.: A novel dendrochronological approach reveals drivers of carbon sequestration in tree species of riparian forests across spatiotemporal scales, Sci. Total Environ., 574, 1261–1275, doi:10.1016/j.scitotenv.2016.07.174, 2017.

Roberts, J.: Forest transpiration: A conservative hydrological process?, J. Hydrol., 66, 133–141, doi:10.1016/0022-1694(83)90181-6, 1983.

Robertson, I., Waterhouse, J. S., Barker, A. C., Carter, A. H. C. and Switsur, V. R.: Oxygen isotope ratios of oak in east England: Implications for reconstructing the isotopic composition of precipitation, Earth Planet. Sci. Lett., 191(1–2), 21–31, doi:10.1016/S0012-821X(01)00399-5, 2001.

Rodríguez-González, P. M., Stella, J. C., Campelo, F., Ferreira, M. T. and Albuquerque, A.: Subsidy or stress? Tree structure and growth in wetland forests along a hydrological gradient in Southern Europe, For. Ecol. Manage., 259(10), 2015–2025, doi:10.1016/j.foreco.2010.02.012, 2010.

Rodríguez-González, P. M., Albuquerque, A., Martínez-Almarza, M. and Díaz-Delgado, R.: Long-term monitoring for conservation management: Lessons from a case study integrating remote sensing and field approaches in floodplain forests, J. Environ. Manage., 202, 392–402, doi:10.1016/j.jenvman.2017.01.067, 2017.

Rozas, V.: Dendrochronology of pedunculate oak (Quercus robur L.) in an old-growth pollarded woodland in northern Spain: establishment patterns and the management history, Annu. For. Sci., 62, 13–22, doi:10.1051/forest, 2005.

Rubino, D. L. and McCarthy, B. C.: Dendroclimatological Analysis of White Oak (Quercus alba L., Fagaceae) from an Old-Growth Forest of Southeastern Ohio,

USA, J. Torrey Bot. Soc., 127(3), 240–250, 2000.

Sabater, F. and Bernal, S.: Keeping healthy riparian and aquatic ecosystems in the Mediterranean: challenges and solutions through riparian forest management, in Water for forests and people in the Mediterrane, edited by M. Boirot, Y. Gracia, and C. Palahí, pp. 151–155., 2011.

Sala, O. E., Chapin, F. S., Armesto, J. J., Berlow, E., Bloomfield, J., Dirzo, R., Huber-Sanwald, E., Huenneke, L. F., Jackson, R. B., Kinzig, A., Leemans, R., Lodge, D. M., Mooney, H. A., Oesterheld, M., LeRoy Poff, N., Sykes, M. T., Walker, B. H., Walker, M. and Wall, D. H.: Global biodiversity scenarios for the year 2100, Science (80-.)., 287, 1770–1774, 2000a.

Sala, O. E., Chapin, F. S., Armesto, J. J., Berlow, E., Bloomfield, J., Dirzo, R., Huber-Sanwald, E., Huenneke, L. F., Jackson, R. B., Kinzig, A., Leemans, R., Lodge, D. M., Mooney, H. A., Oesterheld, M., LeRoy Poff, N., Sykes, M. T., Walker, B. H., Walker, M. and Wall: Global biodiversity scenarios for the year 2100, Sciences (New. York)., 287, 1770–1774, 2000b.

Sánchez-Pérez, J. M., Lucot, E., Bariac, T. and Trémolières, M.: Water uptake by trees in a riparian hardwood forest (Rhine floodplain , France), Hydrol. Process., 22, 366–375, doi:10.1002/hyp.6604, 2008.

Sanpera-Calbet, I., Acuña, V., Butturini, A., Marcé, R. and Muñoz, I.: El Niño southern oscillation and seasonal drought drive riparian input dynamics in a Mediterranean stream, Limnol. Oceanogr., 61(1), 214–226, doi:10.1002/lno.10211, 2016.

Santini, A., Bottacci, A. and Gellini, R.: Preliminary dendroecological survey on pedunculate oak (Quercus robur L.) stands in Tuscany (Italy), Ann. des Sci. For., 51(1), 1–10, doi:10.1051/forest:19940101, 1994.

Sanz Elorza, M., Dana Sánchez, E. and Sobrino Vesperinas, E.: El Atlas de Plantas Invasoras de España, Dir. Gen. para la Biodiversidad. Minist. Medio Ambient. Madrid, (Ma 643037) [online] Available from: http://www.magrama.gob.es/es/biodiversidad/temas/inventarios-nacionales/c2_atlas_tcm7-21522.pdf, 2004.

Sargeant, C. I. and Singer, M. B.: Sub-annual variability in historical water source use by Mediterranean riparian trees, Ecohydrology, 9(7), 1328–1345, doi:10.1002/eco.1730, 2016.

Saurer, M., Siegwolf, R. T. W. and Schweingruber, F. H.: Carbon isotope discrimination indicates improving water-use efficiency of trees in northern

Eurasia over the last 100 years, Glob. Chang. Biol., 10(12), 2109–2120, doi:10.1111/j.1365-2486.2004.00869.x, 2004.

Saurer, M., Spahni, R., Frank, D. C., Joos, F., Leuenberger, M., Loader, N. J., Mccarroll, D., Gagen, M., Poulter, B., Siegwolf, R. T. W., Andreu-Hayles, L., Boettger, T., Dorado Liñán, I., Fairchild, I. J., Friedrich, M., Gutierrez, E., Haupt, M., Hilasvuori, E., Heinrich, I., Helle, G., Grudd, H., Jalkanen, R., Levanič, T., Linderholm, H. W., Robertson, I., Sonninen, E., Treydte, K., Waterhouse, J. S., Woodley, E. J., Wynn, P. M. and Young, G. H. F.: Spatial variability and temporal trends in water-use efficiency of European forests, Glob. Chang. Biol., 20(12), 3700–3712, doi:10.1111/gcb.12717, 2014.

Schaap, M. G., Leij, F. J. and Van Gencuhten, M. T.: A computer program for estimating soil hydraulic parameters with hierarchical pedotransfer functions, J. Hydrol., 251, 163–176, 2002.

Schade, J. D., Welter, J. R., Martí, E. and Grimm, N. B.: Hydrologic exchange and N uptake by riparian vegetation in an arid-land stream, J.N.Am.Benthol. Soc., 24(1), 19–28, 2005.

Von Schiller, D., Martí, E., Riera, J. L., Ribot, M., Marks, J. C. and Sabater, F.: Influence of land use on stream ecosystem function in a Mediterranean catchment, Freshw. Biol., 53(12), 2600–2612, doi:10.1111/j.1365-2427.2008.02059.x, 2008.

Schmidt, M. W. I., Torn, M. S., Abiven, S., Dittmar, T., Guggenberger, G., Janssens, I. a., Kleber, M., Kögel-Knabner, I., Lehmann, J., Manning, D. a. C., Nannipieri, P., Rasse, D. P., Weiner, S. and Trumbore, S. E.: Persistence of soil organic matter as an ecosystem property, Nature, 478(7367), 49–56, doi:10.1038/nature10386, 2011.

Schume, H., Jost, G. and Hager, H.: Soil water depletion and recharge patterns in mixed and pure forest stands of European beech and Norway spruce, J. Hydrol., 289, 258–274, doi:10.1016/j.jhydrol.2003.11.036, 2004.

Scott, R. L., Cable, W. L., Huxman, T. E., Nagler, P. L., Hernandez, M. and Goodrich, D. C.: Multiyear riparian evapotranspiration and groundwater use for a semiarid watershed, J. Arid Environ., 72, 1232–1246, doi:10.1016/j.jaridenv.2008.01.001, 2008.

Segers, R.: Methane production and methane consumption : a review of processes underlying wetland methane fluxes, Biogeochemistry, 41, 23–51, 1998.

Si, J., Feng, Q., Cao, S., Yu, T. and Zhao, C.: Water use sources of desert riparian Populus euphratica forests, Environ. Monit. Assess., 186(9), 5469–5477, doi:10.1007/s10661-014-3796-4, 2014.

Silva, L. C. R., Anand, M. and Leithead, M. D.: Recent widespread tree growth decline despite increasing atmospheric CO2, PLoS One, 5(7), doi:10.1371/journal.pone.0011543, 2010.

Silvester, W. B.: Ecological and economic significance of the non-legume symbioses, in Proceedings of the 1st International Symposium of Nitrogen Fixation., edited by E. Newton and C. J. Nyman, pp. 489–506, Washington State University Press, Pullman., 1976.

Simunek, J., Jacques, D., van Guenchten, M. T. and Mallants, D.: Multicomponent geochemical transport using HYDRUS-1D and HP1, J. Am. Water Resour. Assoc., 1537–1547, 2006.

Šimůnek, J., van Genunchten, M. T. and Šejna, M.: Modeling Subsurface Water Flow and Solute Transport with HYDRUS and Related Numerical Software Packages, Numer. Model. Hydrodyn. Water Resour., 95–115, 2008.

Singer, M. B., Stella, J. C., Dufour, S., Pi??gay, H., Wilson, R. J. S. and Johnstone, L.: Contrasting water-uptake and growth responses to drought in co-occurring riparian tree species, Ecohydrology, 6(3), 402–412, doi:10.1002/eco.1283, 2013.

Singer, M. B., Sargeant, C. I., Piégay, H., Riquier, J., Wilson, R. J. S. and Evans, C. M.: Floodplain ecohydrology: Climatic, anthropogenic, and local physical controls on partitioning of water sources to riparian trees, Water Resour. Res., 50(5), 4490–4513, doi:10.1002/2014WR015581, 2014.

Smith, M. S. and Tiedje, J. M.: Phases of desnitrification following oxygen depletion in soil, Soil Biol. Biochem., 11(3), 261–267, doi:10.1016/0038-0717(79)90071-3, 1979.

Smith, S. D., Wellington, a B., Nachlinger, J. L., Fox, C. a, Applications, E., Feb, N., Smith, D. and Fox, a: Functional Responses of Riparian Vegetation to Streamflow Diversion in the Eastern Sierra Nevada FUNCTIONAL RESPONSES OF RIPARIAN VEGETATION TO STREAMFLOW DIVERSION IN THE EASTERN SIERRA NEVADA ', , 1(1), 89–97, 1991.

Snyder, K. A. and Williams, D. G.: Water sources used by riparian trees varies among stream types on the San Pedro River, Arizona, Agric. For. Meteorol., 105, 227–240, doi:10.1016/S0168-1923(00)00193-3, 2000.

Soylu, M. E., Istanbulluoglu, E., Lenters, J. D. and Wang, T.: Quantifying the impact of groundwater depth on evapotranspiration in a semi-arid grassland region, Hydrol. Earth Syst. Sci., 15, 787–806, doi:10.5194/hess-15-787-2011, 2011.

Sperry, J. S., Hacke, U. G., Oren, R. and Comstock, J. P.: Water deficits and

hydraulic limits to leaf water supply, Plant, Cell Environ., 25(2), 251–263, doi:10.1046/j.0016-8025.2001.00799.x, 2002.

Stark, J. M. and Firestone, M. K.: Mechanisms for soil moisture effects on activity of nitrifying bacteria, Appl. Environ. Microbiol., 61(1), 218–221 [online] Available from: papers2://publication/uuid/0BBA43AD-EACB-4300-A741-A11EA89C2422, 1995.

Staska, B., Essl, F. and Samimi, C.: Density and age of invasive Robinia pseudoacacia modulate its impact on floodplain forests, Basic Appl. Ecol., 15(6), 551–558, doi:10.1016/j.baae.2014.07.010, 2014.

Stern, S. N.: The Stern Review on the Economic Effects of climate change, Popul. Dev. Rev., 32(December), 793–798, doi:10.2307/20058936, 2006.

Stocke, V. B. et al: IPCC (2013), Summary for policymakers, in Climate Change 2013: The Physical Science Basis, 2013.

Sürmen, B., Güray, H., Kiliç, D. D. and Sürmen, M.: Foliar resorption in nitrogen-fixing and non-fixing species in a swamp forest in northern Turkey, Rev. Écol (Terre Vie), 69, 318–327, 2014.

Suseela, V., Conant, R. T., Wallenstein, M. D. and Dukes, J. S.: Effects of soil moisture on the temperature sensitivity of heterotrophic respiration vary seasonally in an old-field climate change experiment, Glob. Chang. Biol., 18(1), 336–348, doi:10.1111/j.1365-2486.2011.02516.x, 2012.

Tateno, R., Tokuchi, N., Yamanaka, N., Du, S., Otsuki, K., Shimamura, T., Xue, Z., Wang, S. and Hou, Q.: Comparison of litterfall production and leaf litter decomposition between an exotic black locust plantation and an indigenous oak forest near Yan'an on the Loess Plateau, China, For. Ecol. Manage., 241(1–3), 84–90, doi:10.1016/j.foreco.2006.12.026, 2007.

Teiter, S. and Mander, Ü.: Emission of N2O, N2, CH4, and CO2 from constructed wetlands for wastewater treatment and from riparian buffer zones, Ecol. Eng., 25(5), 528–541, doi:10.1016/j.ecoleng.2005.07.011, 2005.

Tessier, L., Nola, P. and Serre-Bachet, F.: Deciduous Quercus in the Mediterranean region: tree-ring / climate relationships., New Phytol., 126(November 1992), 355–367, 1994.

TESSIER, L., NOLA, P. and SERRE-BACHET, F.: Deciduous Quercus in the Mediterranean region: tree-ring/climate relationships, New Phytol., 126(2), 355–367, doi:10.1111/j.1469-8137.1994.tb03955.x, 1994.

Thomas, Z., Ghazavi, R., Merot, P. and Granier, A.: Modelling and observation of hedgerow transpiration effect on water balance components at the hillslope scale in Brittany, Hydrol. Process., 26, 4001–4014, doi:10.1002/hyp.9198, 2012.

Tockner, K. and Stanford, J. A.: Riverine flood plains: present state and future trends, Environ. Conserv., 29(3), 308–330, 2002.

Traiser, C., Klotz, S., Uhl, D. and Mosbrugger, V.: Environmental signals from leaves--a physiognomic analysis of European vegetation., New Phytol., 166(2), 465–484, doi:10.1111/j.1469-8137.2005.01316.x, 2005.

Tromp-van Meerveld, H. J. and McDonnell, J. J.: On the interrelations between topography, soil depth, soil moisture, transpiration rates and species distribution at the hillslope scale, Adv. Water Resour., 29, 293–310, doi:10.1016/j.advwatres.2005.02.016, 2006.

Tsai, C. W., Young, T., Warren, P. H. and Maltby, L.: Phenological responses of ash (Fraxinus excelsior) and sycamore (Acer pseudoplatanus) to riparian thermal conditions, Urban For. Urban Green., 16, 95–102, doi:10.1016/j.ufug.2016.02.001, 2016.

Tylianakis, J. M., Didham, R. K., Bascompte, J. and Wardle, D. A.: Global change and species interactions in terrestrial ecosystems, Ecol. Lett., 11, 1351–1363, doi:10.1111/j.1461-0248.2008.01250.x, 2008.

Urbieta, I. R., Pérez-Ramos, I. M., Zavala, M. A., Marañón, T. and Kobe, R. K.: Soil water content and emergence time control seedling establishment in three co-occurring Mediterranean oak species, Can. J. For. Res., 38(9), 2382–2393, doi:10.1139/X08-089, 2008.

Uselman, S. M., Qualls, R. G. and Thomas, R. B.: A test of a potential short cut in the nitrogen cycle: The role of exudation of symbiotically fixed nitrogen from the roots of a N-fixing tree and the effects of increased atmospheric CO2 and temperature, Plant Soil, 210(1), 21–32, doi:10.1023/A:1004619509878, 1999.

Vidon, P., Allan, C., Burns, D., Duval, T. P., Gurwick, N., Inamdar, S., Lowrance, R., Okay, J., Scott, D. and Sebestyen, S.: Hot spots and hot moments in riparian zones: Potential for improved water quality management, J. Am. Water Resour. Assoc., 46(2), 278–298, doi:10.1111/j.1752-1688.2010.00420.x, 2010.

Vidon, P., Marchese, S., Welsh, M. and McMillan, S.: Impact of Precipitation Intensity and Riparian Geomorphic Characteristics on Greenhouse Gas Emissions at the Soil-Atmosphere Interface in a Water-Limited Riparian Zone, Water. Air. Soil Pollut., 227(8), doi:10.1007/s11270-015-2717-7, 2016.

Vidon, P. G.: Not all riparian zones are wetlands: Understanding the limitation of the "wetland bias" problem, Hydrol. Process., 31, 2125–2127, doi:10.1002/hyp.11153, 2017.

Vidon, P. G. and Hill, A. R.: A landscape-based approach to estimate riparian hydrological and nitrate removal functions, J. Am. Water Resour. Assoc., 3, 1099–1112, 2006.

Vila-Viçosa, C., Vázquez, F. M., Mendes, P., Del Rio, S., Musarella, C., Cano-Ortiz, A. and Meireles, C.: Syntaxonomic update on the relict groves of Mirbeck's oak (Quercus canariensis Willd. and Q. marianica C. Vicioso) in southern Iberia, Plant Biosyst., 149(3), 512–526, doi:10.1080/11263504.2015.1040484, 2015.

Vilà, M., Espinar, J. L., Hejda, M., Hulme, P. E., Jarošík, V., Maron, J. L., Pergl, J., Schaffner, U., Sun, Y. and Pyšek, P.: Ecological impacts of invasive alien plants: A meta-analysis of their effects on species, communities and ecosystems, Ecol. Lett., 14(7), 702–708, doi:10.1111/j.1461-0248.2011.01628.x, 2011.

Vitasse, Y., Delzon, S., Dufrêne, E., Pontailler, J. Y., Louvet, J. M., Kremer, A. and Michalet, R.: Leaf phenology sensitivity to temperature in European trees: Do within-species populations exhibit similar responses?, Agric. For. Meteorol., 149(5), 735–744, doi:10.1016/j.agrformet.2008.10.019, 2009.

Vítková, M., Tonika, J. and Müllerová, J.: Black locust-Successful invader of a wide range of soil conditions, Sci. Total Environ., 505, 315–328, doi:10.1016/j.scitotenv.2014.09.104, 2015.

Vitousek, P. M.: Litterfall, Nutrient Cycling, and Nutrient Limitation in Tropical Forests, Ecology, 65(1), 285–298, 1984.

Walentowski, H., Falk, W., Mette, T., Kunz, J., Bräuning, A., Meinardus, C., Zang, C., Sutcliffe, L. M. E. and Leuschner, C.: Assessing future suitability of tree species under climate change by multiple methods: A case study in southern Germany, Ann. For. Res., 60(1), 101–126, doi:10.15287/afr.2016.789, 2017.

Walker, J. T., Geron, C. D., Vose, J. M. and Swank, W. T.: Nitrogen trace gas emissions from a riparian ecosystem in southern Appalachia, Chemosphere, 49(10), 1389–1398, doi:10.1016/S0045-6535(02)00320-X, 2002.

Wazen, N. and Fady, B.: Geographic distribution of 24 major tree species in the Mediterranean and their genetic resources, FAO., 2015.

Webb, M., Reid, M., Capon, S. J., Thoms, M., Rayburg, S. and James, C.: Are flood plain–wetland plant communities determined by seed bank composition or

inundation periods?, Sediment Dyn. Hydromorphology Fluv. Syst., (July), 241–248, 2006.

Weber, E.: Invasive plant species of the world: a reference guide to environmental weeds., Wallingford: CABI Publishing., 2003.

Weiler, M. and McDonnell, J.: Virtual experiments: A new approach for improving process conceptualization in hillslope hydrology, J. Hydrol., 285, 3–18, doi:10.1016/S0022-1694(03)00271-3, 2004.

Welti, N., Bondar-Kunze, E., Singer, G., Tritthart, M., Zechmeister-Boltenstern, S., Hein, T. and Pinay, G.: Large-scale controls on potential respiration and denitrification in riverine floodplains, Ecol. Eng., 42, 73–84, doi:10.1016/j.ecoleng.2012.02.005, 2012.

Werner, C., Reiser, K., Dannenmann, M., Hutley, L. B., Jacobeit, J. and Butterbach-Bahl, K.: N2O, NO, N2and CO2 emissions from tropical savanna and grassland of northern Australia: An incubation experiment with intact soil cores, Biogeosciences, 11, 6047–6065, doi:10.5194/bg-11-6047-2014, 2014.

West, J. B., Bowen, G. J., Cerling, T. E. and Ehleringer, J. R.: Stable isotopes as one of nature's ecological recorders, Trends Ecol. Evol., 21(7), 408–414, doi:10.1016/j.tree.2006.04.002, 2006.

Wickland, K. P. ;, Neff, J. C. . and Harden, J. W.: The role of soil drainage class in carbon dioxide exchange and decomposition in boreal black spruce (Picea mariana) forest stands, Can. J. For. Res., 40(11), 2123–2134, 2010.

Williams, C. J., Shingara, E. A. and Yavitt, J. B.: Phenol oxidase activity in peatlands in New York State: Response to summer drought and peat type, Wetlands, 20(2), 416–421, doi:10.1672/0277-5212(2000)020[0416:POAIPI]2.0.CO;2, 2000.

Williams, D. G. and Scott, R. L.: Vegetation-hydrology interactions: dynamics of riparian plant water use., in Ecology and Conservation of the San Pedro River, edited by T. B. Stromberg JC, University of Arizona Press: Tucson., 2009.

Williard, K. W. J., Dewalle, D. R. and Edwards, P. J.: Influence of bedrock geology and tree species compositions on stream nitrate concentrations in mid-appalachian forested watersheds, Water, Air, Soil Pollut., 160, 55–76, 2005.

Wolfe, B. E. and Klironomos, J. N.: Breaking new ground: soil communities and exotic plant invasion, Bioscience, 55(6), 477–487, doi:10.1641/0006-3568(2005)055[0477:BNGSCA]2.0.CO;2, 2005.

Wright, I. J., Reich, P. B., Westoby, M., Ackerly, D. D., Baruch, Z., Bongers, F., Cavender-Bares, J., Chapin, T., Cornellssen, J. H. C., Diemer, M., Flexas, J., Garnier, E., Groom, P. K., Gulias, J., Hikosaka, K., Lamont, B. B., Lee, T., Lee, W., Lusk, C., Midgley, J. J., Navas, M. L., Niinemets, Ü., Oleksyn, J., Osada, H., Poorter, H., Pool, P., Prior, L., Pyankov, V. I., Roumet, C., Thomas, S. C., Tjoelker, M. G., Veneklaas, E. J. and Villar, R.: The worldwide leaf economics spectrum, Nature, 428(6985), 821–827, doi:10.1038/nature02403, 2004.

Wright, I. J., Dong, N., Maire, V., Prentice, I. C., Westoby, M., Díaz, S., Gallagher, R. V., Jacobs, B. F., Kooyman, R., Law, E. A., Leishman, M. R., Niinemets, Ü., Reich, P. B., Sack, L., Villar, R., Wang, H. and Wilf, P.: SI: Global climatic drivers of leaf size, Science (80-.)., 357(6354), 917–921, doi:10.1126/science.aal4760, 2017.

Yavitt, J. B., Williams, C. J. and Wieder, R. K.: Production of methane and carbon dioxide in peatland ecosystems across North America: Effects of temperature, aeration, and organic chemistry of peat, Geomicrobiol. J., 14(4), 299–316, 1997.

Yelenik, S. G., Stock, W. D. and Richardson, D. M.: Functional group identity does not predict invader impacts: differential effects of nitrogen-fixing exotic plants on ecosystem function, Biol. Invasions, 9(2), 117–125, doi:10.1007/s10530-006-0008-3, 2007.

Yepez, E. A., Williams, D. G., Scott, R. L. and Lin, G.: Partitioning overstory and understory evapotranspiration in a semiarid savanna woodland from the isotopic composition of water vapor, Agric. For. Meteorol., 119, 53–68, doi:10.1016/S0168-1923(03)00116-3, 2003.

Yu, K. and Rinklebe, J.: Soil Redox Potential and pH Controllers, Methods Biochem. Wetl., (10), 107–116, doi:10.2136/sssabookser10.c7, 2013.

Zar, J. H.: Biostatistical Analysis, Prentice-H., 2010.

Zhang, L., Dawes, W. R. and Walker, G. R.: Response of mean annual evapotranspiration to vegetationchanges at catchment scale, Water Resour. Res., 37(3), 701–708, 2001.

Zhang, Y., Munkhtsetseg, E., Kadota, T. and Ohata, T.: An observational study of ecohydrology of a sparse grassland at the edge of the Eurasian cryosphere in Mongolia, J. Geophys. Res., 110, 1–14, doi:10.1029/2004JD005474, 2005.

Supporting information

This section comprises supporting information for Chapters 3 to 8

APPENDIX A. Supplementary information of Chapter 3: Living at the edge of the species distribution: Effects of temperature increase and flooding conditions on growth and iWUE of *Quercus robur* and *Q. canariensis*.

APPENDIX B. Supplementary information of Chapter 4: Linking foliar dynamics and traits to water availability. The idiosincratic tree species responses in a Mediterranean riparian forest.

APPENDIX C. Supplementary information of Chapter 5: Soil water content drives spatiotemporal patterns of CO_2 and N_2O emissions from a Mediterranean riparian forest soil.

APPENDIX D. Supplementary information of Chapter 6: Riparian forest transpiration under the current and projected Mediterranean climate: effects on soil water and nitrate uptake.

APPENDIX E. Supplementary information of Chapter 7: The influence of the invasive nitrogen-fixing *Robinia pseudoacacia* on soil nitrogen availability in a mixed Mediterranean riparian forest.

APPENDIX F. Supplementary information of Chapter 8: General discussion.

APPENDIX A

Supplementary information of Chapter 3: Living at the edge of the species distribution: Effects of temperature increase and flooding conditions on growth and iWUE of *Quercus robur* and *Q. canariensis*

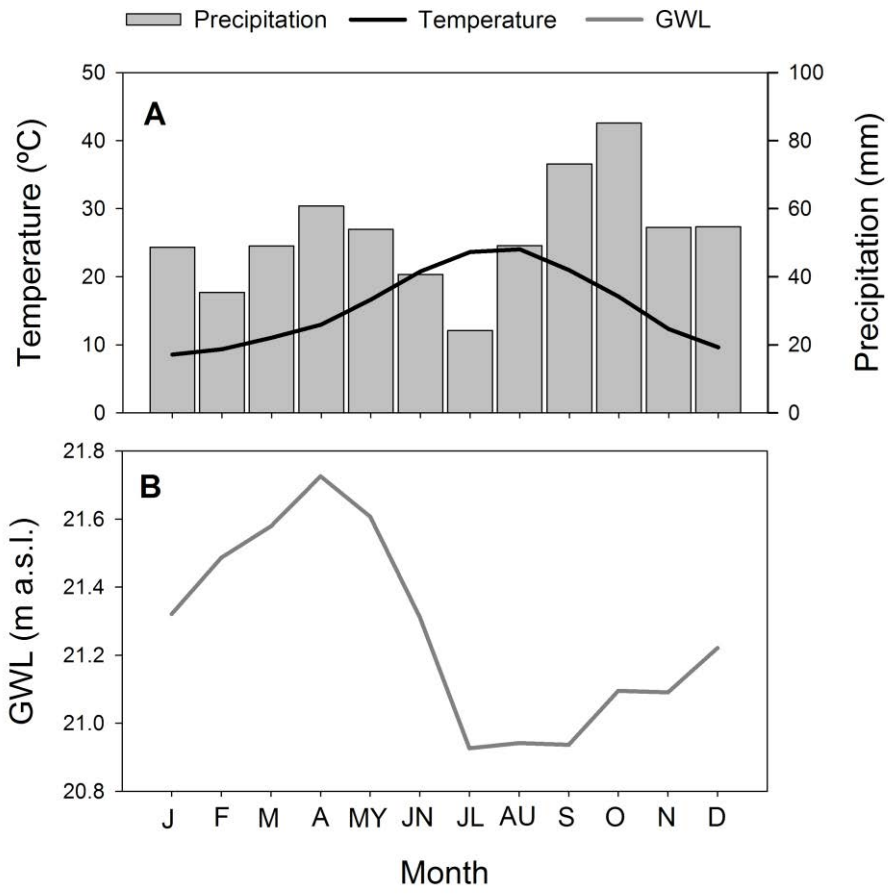

Figure A.1 A) Ombrothermic diagram at c.a. 10km from Tordera (Blanes 1968-2008, Arxiu Municipal de l'Ajuntament de Blanes). Mean monthly temperature (ºC) and mean monthly total precipitation (mm). B) Mean monthly groundwater level (GWL) in m above see level (a.s.l.) (Data obtained from Agència Catalana de l'Aigua: piezometer G-1 Tordera/Maresme, UTMX 476854 UTMY 4617581).

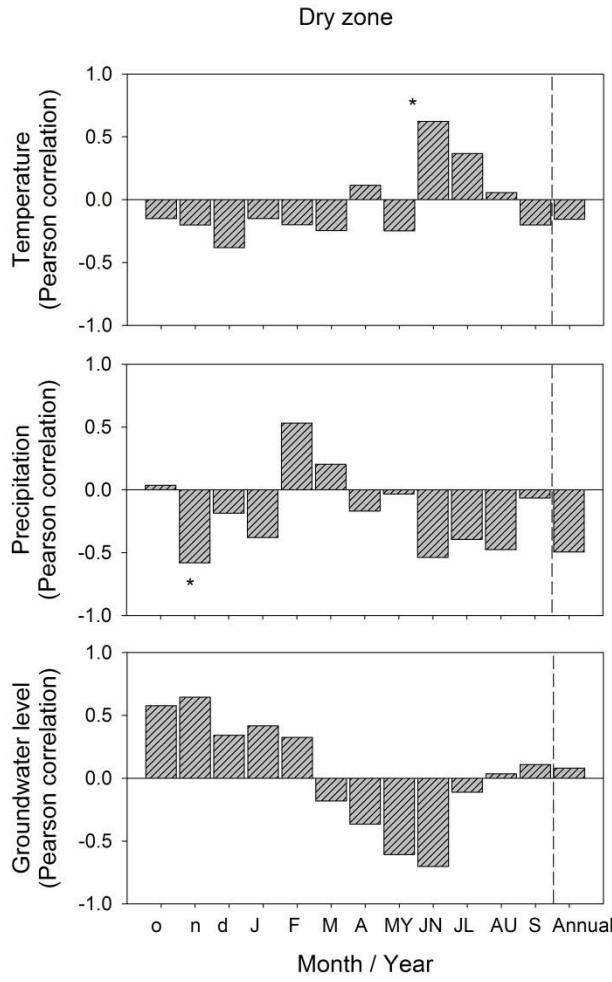

Figure A.2 Pearson correlation values for iWUE of mature *Q. canariensis* and monthly and annual environmental conditions (temperature, precipitation, and groundwater level). Data shown from october of previous year to september of current year. Significant correlations are indicated by asterisks: ***, $p < 0.001$; **, $p < 0.01$; *, $p < 0.05$).

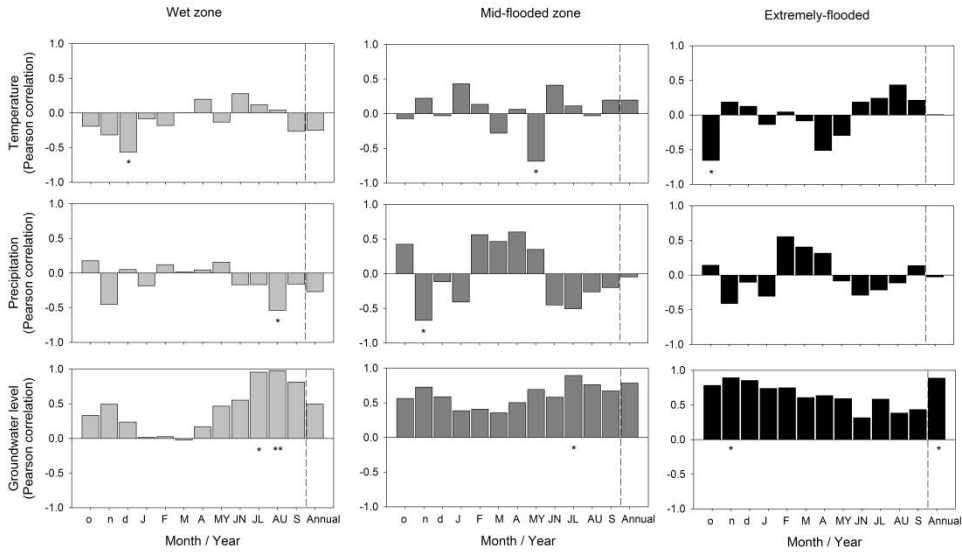

Figure A.3 Pearson correlation values for iWUE of mature *Q. robur* and monthly and annual environmental conditions (temperature, precipitation, and groundwater level). Data shown from october of previous year to september of current year. Significant correlations are indicated by asterisks: ***, $p < 0.001$; **, $p < 0.01$; *, $p < 0.05$).

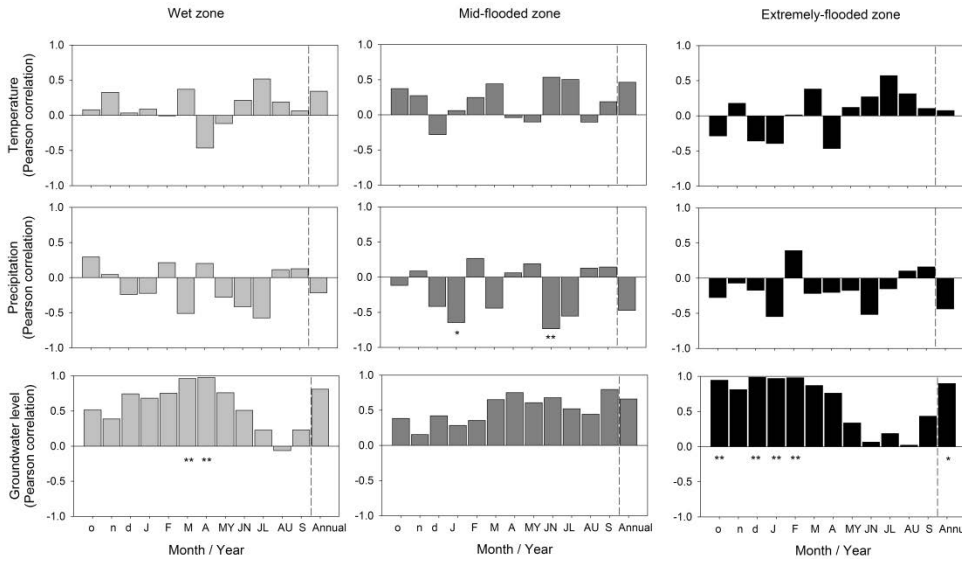

Figure A.4 Pearson correlation values for iWUE of mature *F. angustifolia* and monthly and annual environmental conditions (temperature, precipitation, and groundwater level). Data shown from october of previous year to september of current year. Significant correlations are indicated by asterisks: ***, $p < 0.001$; **, $p < 0.01$; *, $p < 0.05$).

APPENDIX B

Supplementary information of Chapter 4: Linking foliar dynamics and traits to water availability. The idiosincratic tree species responses in a Mediterranean riparian forest.

Table B.1 Litter fall (g DW m^{-2}) for all riparian tree species of both studied years. *R.* pseudoacacia is shown by riparian sections.

	Fruits	Branches	Other sps
2011			
Physiology	35.77	41.38	160.25
Phenology	101.49	79.65	43.43
Annual	**137.25**	**121.03**	**203.68**
2012			
Physiology	55.39	103.16	174.67
Phenology	17.55	52.36	36.87
Annual	**72.94**	**155.51**	**211.54**

Table B.2 Spearman correlations of environmental variables influencing litter fall from riparian tree species during non phenological fall period. Litter fall is considered as relative annual contribution. Meteorlogical data is calculated as mean value between sampling dates. All correlations (r^2) are shown for all sampling dates, year 2011, and year 2012 ($p<0.05$; n = 19, 11, and 8, respectfully).

Litter	Varible	r2		
		All	2011	2012
Fruits	WindSeep	0.505	-	-
	WindMax	0.494	-	-
Branches	WindSeep	0.585	-	-
	Tº ac	0.517	-	-
Other sps	VPD	-	-0.733	-
	WindMax	-	0.721	-
	Precip	0.582	-	-
	SWC	0.643	-	-
	GWL	-	-0.214	-
	Tº ac	0.633	-	-

Table B.3 Leaf morphological traits of four riparian tree species for the years 2011 and 2012. Values are means ± standard error. Bold values indicate significant differences between years (P-value < 0.05).

	A. glutinosa		***P. nigra***		***F. excelsior***		***R. pseudoacacia***	
	2011	**2012**	**2011**	**2012**	**2011**	**2012**	**2011**	**2012**
Fresh weight	0.50 ± 0.04	0.57 ± 0.08	0.72 ± 0.1	0.89 ± 0.07	0.19 ± 0.02	0.18 ± 0.03	0.08 ± 0.01	0.10 ± 0.01
Dry weight	0.18 ± 0.02	0.22 ± 0.02	**0.22 ± 0.03**	**0.29 ± 0.03**	0.07 ± 0.01	0.07 ± 0.01	0.03 ± 0.002	0.03 ± 0.002
Leaf Area	26.11 ± 2.49	32.20 ± 2.49	24.89 ± 2.94	30.67 ± 2.94	8.29 ± 0.71	10.13 ± 0.71	6.98 ± 0.66	6.73 ± 0.66
LT	21.10 ± 1.22	26.60 ± 1.22	27.68 ± 0.45	22.52 ± 0.45	18.23 ± 2.64	25.53 ± 2.64	16.49 ± 0.86	15.90 ± 0.86
LMA	6.93 ± 0.55	6.84 ± 0.55	8.79 ± 0.38	9.50 ± 0.38	8.10 ± 0.55	7.31 ± 0.55	4.10 ± 0.56	4.78 ± 0.56
LDMC	2.83 ± 0.14	2.56 ± 0.14	3.30 ± 0.03	3.38 ± 0.03	2.89 ± 0.10	2.22 ± 0.10	2.77 ± 0.25	3.01 ± 0.25
D	0.31 ± 0.01	0.26 ± 0.01	0.32 ± 0.02	0.42 ± 0.02	0.46 ± 0.06	0.36 ± 0.06	0.25 ± 0.02	0.33 ± 0.02
S	12.53 ± 0.68	10.64 ± 0.68	20.23 ± 0.75	22.23 ± 0.75	15.17 ± 0.46	8.88 ± 0.46	7.73 ± 1.80	9.57 ± 1.80
WC	64.45 ± 1.64	60.88 ± 1.64	69.72 ± 0.31	67.77 ± 0.31	65.31 ± 1.15	54.76 ± 1.15	67.28 ± 1.42	64.47 ± 1.42
CN	14.90 ± 1.06	16.06 ± 1.06	**21.27 ± 2.13**	**16.69 ± 2.13**	15.38 ± 0.60	15.69 ± 0.60	11.60 ± 0.29	13.80 ± 0.29
N%	3.31 ± 0.28	3.02 ± 0.28	2.13 ± 0.40	2.67 ± 0.40	3.03 ± 0.11	2.90 ± 0.11	4.16 ± 0.14	3.64 ± 0.14
N AREA	2.31 ± 0.30	2.05 ± 0.30	1.87 ± 0.37	2.54 ± 0.37	2.43 ± 0.09	2.12 ± 0.10	1.69 ± 0.22	1.73 ± 0.22
15/14N	-1.79 ± 0.25	-1.53 ± 0.25	**-0.68 ± 0.58**	**-2.02 ± 0.58**	-0.38 ± 0.30	0.70 ± 0.30	0.10 ± 0.09	-0.42 ± 0.09
C%	48.52 ± 1.24	48.06 ± 1.24	43.52 ± 4.00	44.45 ± 4.00	46.40 ± 0.62	45.44 ± 0.62	48.01 ± 1.15	49.62 ± 1.15
C AREA	33.59 ± 2.68	32.89 ± 2.68	38.16 ± 3.56	42.19 ± 3.56	37.58 ± 2.61	33.23 ± 2.61	19.69 ± 2.73	23.67 ± 2.73
13/12C	-30.72 ± 0.44	-29.13 ± 0.44	**-30.08 ± 0.42**	**-28.35 ± 0.42**	-29.45 ± 0.54	-28.77 ± 0.54	**-28.47 ± 0.33**	**-27.25 ± 0.33**
WUE	48.87 ± 4.70	66.28 ± 4.70	**55.67 ± 4.46**	**74.67 ± 4.46**	62.34 ± 5.68	70.19 ± 5.68	**72.73 ± 3.50**	**86.30 ± 3.50**

Table B.4 Linear model statistical results for each morphological trait. For each species and year estimate value is given, p-value <0.05 indicate differences between years and letters indicate differences among riparian tree species.

Traits	*A. glutinosa*				*P. nigra*				*F. excelsior*				*R. pseudoacacia*			
	2011	2012	p-value		2011	2012	p-value		2011	2012	p-value		2011	2012	p-value	
Fresh weight	0.504	0.063	0.983	A	0.219	0.108	0.199	B	-0.311	-0.072	1	C	-0.422	-0.05	1	D
Dry weght	0.181	0.041	0.514	A	0.038	0.031	**0.023**	B	-0.113	-0.035	1	C	-0.155	-0.033	0.999	D
Leaf Area	1.926	-0.005	0.433	A	0.246	0.084	0.364	A	0.158	-0.091	0.968	B	-0.573	0.202	1	B
LT	0.023	0.005	0.455	A	0.006	-0.1	0.264	A	-0.004	0.003	0.108	A	-0.006	-0.005	1	B
LMA	6.93	-0.087	1	A	1.86	0.8	0.978	B	1.167	-0.702	0.985	AB	-2.83	0.766	0.838	C
LDMC	2.832	-0.275	1	A	0.471	0.351	1	A	0.06	-0.395	0.979	A	-0.066	0.516	0.998	A
D	0.314	-0.055	0.936	A	0.004	0.161	0.31	B	0.15	-0.047	0.557	B	-0.068	0.142	0.086	A
S	12.526	-1.89	1	A	7.707	3.886	1	B	2.645	-4.403	0.884	A	-4.8	3.735	0.996	A
WC	64.453	-3.575	0.991	A	5.271	1.622	1	A	0.856	-6.975	0.427	A	2.831	0.757	0.962	A
CN	14.902	1.159	0.983	A	6.37	-5.742	**0.015**	B	0.483	-0.85	1	A	-3.301	1.044	0.123	C
N%	3.313	-0.297	0.981	A	-1.186	0.843	0.634	B	-0.284	0.165	1	AB	0.845	-0.219	0.175	C
N AREA	2.308	-0.256	0.993	AB	-0.441	0.926	0.4	A	0.127	-0.059	0.988	A	-0.615	0.291	1	B
15/14N	-0.1786	0.257	0.998	A	1.105	-1.589	**0.027**	A	1.407	0.825	0.281	B	1.882	-0.774	0.418	B
C%	48.518	-0.461	1	A	-4.998	1.393	1	B	-2.115	-0.508	1	AB	-0.505	2.066	0.888	A
C AREA	33.588	-0.702	1	A	4.575	4.734	0.957	B	3.996	-3.655	0.974	A	-13.9	4.685	0.702	C
13/12C	-30.724	1.59	0.101	A	0.641	0.147	**0.04**	A	1.27	-0.902	0.949	A	2.25	-0.369	**0.017**	B
WUE	48.872	17.407	0.083	A	6.799	1.59	**0.031**	A	13.468	-9.559	0.926	A	23.857	-3.835	**0.011**	B

Table B.5 Linear model statistical results for each morphological trait. For each species and year estimate value is given. Capital letters indicate differences among riparian tree species within the season. Asterisks indicate significant differences between seasons for each riparian tree species (ANOVA, $p < 0.05$).

Water sources	*A. glutinosa*	*P. nigra*	*F. excelsior*	*R. pseudoacacia*		
				Near-stream	Intermediate	Hillslope
Shallow Soil Water						
Spring	0.083^{A}	-0.014^{A}	0.072^{AB}	0.193^{AB} *	0.271^{BC} *	0.314^{C} *
Summer	-0.025^{AB}	-0.007^{A}	0.152^{B}	-0.202^{AB} *	-0.233^{AB} *	-0.225^{AB} *
Deep soil water						
Spring	0.19^{A} *	0.105^{A} *	0.611^{B}	0.01^{A} *	0.232^{A}	0.2^{A}
Summer	0.598^{AB} *	0.005^{A} *	-0.794^{AB}	-0.079^{AB} *	-0.364^{AB}	-0.503^{B}
Groundwater						
Spring	0.727^{A} *	-0.091^{A} *	-0.683^{B}	-0.293^{AC}	-0.503^{BC}	-0.533^{BC}
Summer	-0.573^{A} *	0.001^{A} *	0.642^{A}	0.281^{A}	0.596^{A}	0.728^{A}

APPENDIX C

Supplementary information of Chapter 5: Soil water content drives spatiotemporal patterns of CO_2 and N_2O emissions from a Mediterranean riparian forest soil

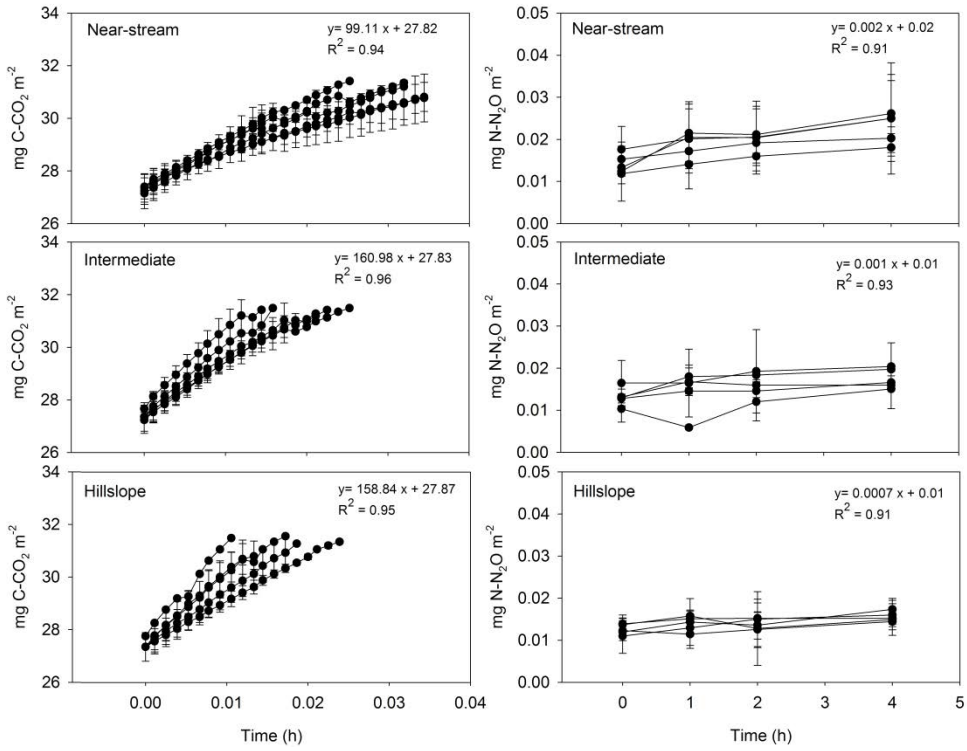

Figure C.1 Concentrations of carbon dioxide (left column) and nitrous oxide (right column) during the incubation time for the sampling campaign of June 2013. Data is shown for the near-stream, intermediate and hillslope zones separately. For each plot, data is shown as mean ± SD (n = 5) for all sampling days of June. The best fit linear model used to calculate gas emissions is shown for each plot.

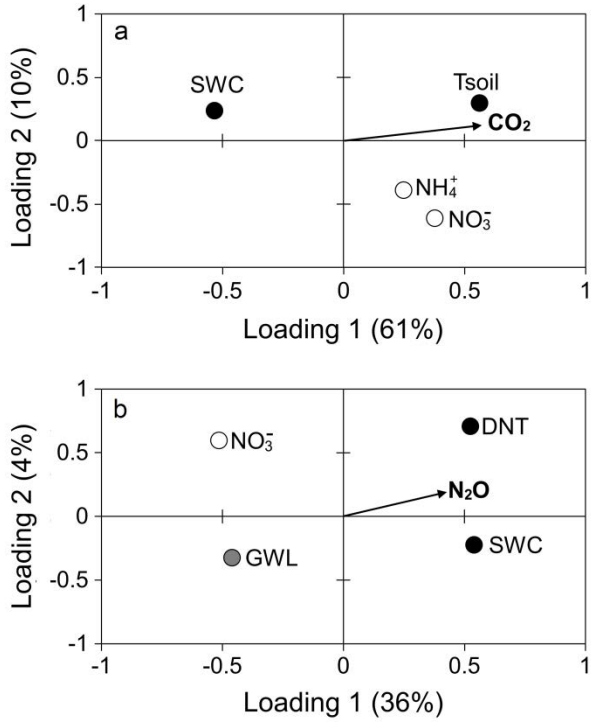

Figure C.2 Loading plot of the (a) CO2 and (b) N2O partial least squares models (PLS) for the 75 measurements. The graph depicts the correlation structures between the X variables (circles) and gas emissions (vectors). Variables situated along the same directional axis correlate with each other. Different color in X variables indicates their influence on gas emissions based on the "variable importance in the projection (VIP)" scores for each model. In each case, white has VIP scores < 0.8, grey has VIP scores < 1.0 and black has VIP scores > 1.0.

APPENDIX D

Supplementary information of Chapter 6: Riparian forest transpiration under the current and projected Mediterranean climate: effects on soil water and nitrate uptake

Table D.1 Summary of HYDRUS-1D model predictions of transpiration for near-stream, intermediate, and hillslope riparian zones as a function of the percentage of potential evapotranspiration that is transpiration. Field data is referred to Nadal-Sala et al. (2017). For each model and studied year (2012, 2013, and 2014), the table shows potential (introduced in the model) and actual (simulated by the model) transpiration values (mm) and the difference between them (all in mm). RMSE = root mean squared error. Nash = Nash-Sutcliffe model efficiency.

				2012			2013			2014		
Zone	**Transpiration**	**RMSE**	**Nash**	***Potential***	***Actual***	***Difference***	***Potential***	***Actual***	***Difference***	***Potential***	***Actual***	***Difference***
Near-stream	Field data	0.008	0.511	168	168	0						
	20%	0.008	0.511	182	182	0	172	172	0	147	147	0
	50%	0.008	0.516	456	456	0	430	429	1	368	368	0
	60%	0.008	0.517	547	547	0	516	515	1	441	441	0
	70%	0.008	0.517	638	638	0	602	601	1	515	515	0
	80%	0.008	0.518	729	729	0	688	686	1	589	589	0
Intermediate	Field data	0.036	0.166	168	168	0						
	20%	0.036	0.170	182	182	0	172	172	0	147	147	0
	50%	0.022	0.686	456	452	4	430	430	0	368	368	0
	60%	0.018	0.801	547	524	23	516	512	4	441	441	0
	70%	0.017	0.823	638	591	47	602	588	13	515	515	0
	80%	0.017	0.807	729	656	74	688	665	23	589	589	0
Hillslope	Field data	0.034	0.432	168	168	0						
	20%	0.033	0.445	182	182	0	172	172	0	147	147	0
	50%	0.030	0.551	456	371	85	430	372	57	368	333	35
	60%	0.029	0.568	547	416	131	516	424	91	441	380	62
	70%	0.031	0.533	638	468	170	602	477	125	515	426	89
	80%	0.033	0.439	729	520	210	688	535	153	589	483	106

APPENDIX E

Supplementary information of Chapter 7: The influence of the invasive nitrogen-fixing Robinia pseudoacacia on soil nitrogen availability in a mixed Mediterranean riparian forest

Table E.1 Values of the parameters used in the model scenarios: specific LMA, leaf N and LAI. Specific LMA is calculated as mean leaf specific weight (n = 10) for mean leave specific area (n = 30). For leaf N content n = 17, 13, 17 and 19 for R. pseudoacacia, A. glutinosa, P. nigra and F. excelsior, respectively. LAI was calculated from annual leaf litter inputs to the forest floor using LMA values (see Eq. 3).

	R. pseudoacacia	*A. glutinosa*	*P. nigra*	*F. excelsior*
Pre-invasion scenario				
Leaf *k* (year^{-1})	---	0.56 ± 0.21	0.25 ± 0.17	0.69 ± 0.18
LMAi (mg cm^{-2})	---	7.75	11.35	9.45
Leaf N (%)	---	2.56 ± 0.23	1.36 ± 0.21	1.80 ± 0.18
f(t) (g DW m^{-2})				
Near-stream	---	151.1	260.9	9.62
Intermediate	---	58.73	215.31	77.58
Hillslope	---	25.99	76.21	188.36
L (g DW m^{-2})				
Near-stream	---	271.77	1028.49	14
Intermediate	---	105.63	848.76	112.9
Hillslope	---	46.75	300.43	274.12
LAI (m^2 m^{-2})				
Near-stream	---	1.95	2.3	0.1
Intermediate	---	0.76	1.9	0.82
Hillslope	---	0.34	0.67	1.99
NN/NNM				
Near-stream	---	1.07	1.07	1.07
Intermediate	---	0.89	0.89	0.89
Hillslope	---	1.16	1.16	1.16
Mid-invasion scenario				
Leaf *k* (year^{-1})	0.29 ± 0.03	0.56 ± 0.21	0.25 ± 0.17	0.69 ± 0.18
LMAi (mg cm^{-2})	6.21	7.75	11.35	9.45
Leaf N (%)	2.39 ± 0.24	2.20 ± 0.39	1.22 ± 0.33	2.04 ± 0.17
f(t) (g DW m^{-2})				
Near-stream	114.32	87.2	150.55	5.55
Intermediate	148.5	18.35	67.27	24.24
Hillslope	161.97	3.41	10.01	24.74
L (g DW m^{-2})				
Near-stream	399.86	156.83	593.5	8.08
Intermediate	519.44	33	265.17	35.27
Hillslope	566.54	6.14	39.46	36.01
LAI (m^2 m^{-2})				
Near-stream	1.84	1.13	1.33	0.06

Intermediate	2.39	0.24	0.59	0.26
Hillslope	2.61	0.04	0.09	0.26
NN/NNM				
Near-stream	1.07	1.07	1.07	1.07
Intermediate	0.89	0.89	0.89	0.89
Hillslope	1.16	1.16	1.16	1.16
Replacement scenario				
Leaf *k* (year^{-1})	0.29 ± 0.03	---	---	---
LMAi (mg cm^{-2})	6.21	---	---	---
Leaf N (%)	2.39 ± 0.24	---	---	---
f(t) (g DW m^{-2})				
Near-stream	270.29	---	---	---
Intermediate	215.98	---	---	---
Hillslope	186.46	---	---	---
L (g DW m^{-2})				
Near-stream	945.44	---	---	---
Intermediate	755.45	---	---	---
Hillslope	652.22	---	---	---
LAI (m^2 m^{-2})				
Near-stream	4.35	---	---	---
Intermediate	3.48	---	---	---
Hillslope	3	---	---	---
NN/NNM				
Near-stream	1.07	---	---	---
Intermediate	0.89	---	---	---
Hillslope	1.16	---	---	---

Table E.2 Model results of leaf litter N inputs and soil N availability for Pre-invasion, Mid-invasion and Replacement scenarios. Results are shown for all the plot as well as for each individual section separately.

	Leaf litter N (g N m^{-2} $year^{-1}$)				Soil NO_3^- (g N m^{-2} $year^{-1}$)			
	R. pseudoacacia	*A. glutinosa*	*P. nigra*	*F. excelsior*	*R. pseudoacacia*	*A. glutinosa*	*P. nigra*	*F. excelsior*
Near-stream								
Pre-invasion	0	4.04 ± 0.36	3.76 ± 0.53	0.23 ±0.06	0	4.33 ± 2.62	4.02 ± 2.49	0.24 ± 0.16
Mid-invasion	2.76 ± 0.23	2.07 ± 0.35	2.01 ± 0.49	0.15 ± 0.04	2.95 ± 1.78	2.22 ± 1.39	2.15 ± 1.42	0.16 ± 0.11
Replacement	6.84 ±0.70	0	0	0	7.32 ± 4.45	0	0	0
Intermediate								
Pre-invasion	0	1.84 ± 0.38	3.02 ± 0.41	1.75 ± 0.39	0	1.64 ± 0.73	2.70 ± 1.11	1.56 ± 0.71
Mid-invasion	3.73 ± 0.37	0.57 ± 0.19	0.96 ± 0.27	0.72 ± 0.23	3.33 ± 1.33	0.51 ± 0.27	0.86 ± 0.42	0.64 ± 0.33
Replacement	5.81 ± 0.83	0	0	0	5.18 ± 2.15	0	0	0
Hillslope								
Pre-invasion	0	0.63 ± 0.06	1.11 ± 0.16	3.84 ± 0.56	0	0.73 ± 0.31	1.29 ± 0.58	4.45 ± 2.00
Mid-invasion	4.18 ± 0.48	0.08 ± 0.01	0.14 ± 0.04	0.63 ± 0.14	4.85 ± 2.12	0.09 ± 0.04	0.17 ± 0.09	0.73 ± 0.35
Replacement	4.89 ± 0.61	0	0	0	5.68 ± 2.50	0	0	0

APPENDIX F

Supplementary information of Chapter 8: General discussion

Table F.1 Precipitation (P), Potential Evapotranspiration (PET), Aridity index (AI), proportion of groundwater used for transpiration (GW use), and riparian species studied for different riparian forests located worldwide.

Climate	P (mm yr^{-1})	PET (mm yr^{-1})	AI	GW use (%)	Species	Source
Arid	35	1305	0.03	91.5	*Poplus*	Hao et al., 2013
Arid	42	1157	0.04	0.2	*Populus euphratica, Tamarix*	Si et al., 2014
Arid	42	1157	0.04	53.3	*Populus euphratica , Tamarix*	Si et al., 2014
Arid	42	1157	0.04	18.1	*Populus euphratica, Tamarix*	Si et al., 2014
Arid	42	1157	0.04	23.7	*Populus euphratica, Tamarix*	Si et al., 2014
Arid	42	1157	0.04	12.6	*Populus euphratica*	Liu et al., 2015
Arid	42	1157	0.04	86	*Populus euphratica*	Liu et al., 2015
Arid	42	1157	0.04	22.8	*Populus euphratica*	Liu et al., 2015
Arid	132.33	987	0.134	90	*Populus*	Smith et al., 1991
Semi-arid	350	1549	0.23	90	*Populus, Salix*	Snyder and Williams, 2000
Semi-arid	350	1549	0.23	97	*Populus, Salix*	Sydner and Williams, 2000
Semi-arid	350	1549	0.23	70	*Populus, Salix*	Sydner and Williams, 2000
Semi-arid	450	998	0.45	88	*Populus euphratica*	Li et al., 2013
Semi-arid	450	998	0.45	32	*Salix*	Li et al., 2013
Semi-arid	1200	1981	0.61	90		O'Grady et al., 2006
Humid	925	1100	0.84	20		Font del Regàs
Humid	576	650	0.89	50	*Populus*	Sánchez-Pérez et al., 2008
Humid	576	650	0.89	20	*Ash*	SánchezPérez et al., 2008
Humid	589	650	0.91	26	*Alnus, Populus*	Bernard et al., 2014
Humid	589	650	0.91	15	*Alnus, Populus*	Bernard et al., 2014
Humid	589	650	0.91	5	*Alnus, Populus*	Bernard et al., 2014
Humid	1200	1281	0.94	20	*Betula*	White and Smith, 1991
Humid	952	985	0.97	10	*Acer*	Bouling et al., 2017
Humid	700	655	1.07	50	*Populus*	Sargeant and Singer, 2016
Humid	700	655	1.07	20	*Ash*	Sargeant and Ssinger, 2016

Table F.2 Precipitation (P), Potential Evapotranspiration (PET), Aridity index (AI), and soil denitrification rates (DNT) for different riparian forests located worldwide.

Climate	P (mm yr-1)	PET (mm yr-1)	AI	DNT (g N m^{-2} yr^{-1})	Source
Arid	300	1670	0.18	8.44	Harms et al., 2009
Arid	408	976	0.42	60.00	Pinay et al., 2007
Arid	585	503	1.16	18.00	Pinay et al., 2007
Semi-arid	600	677	0.89	0.97	Hefting et al., 2004
Semi-arid	664	910	0.73	24.00	Pinay et al., 2007
Semi-arid	671	1000	0.67	120.00	Pinay et al., 2007
Semi-arid	698	581	1.20	24.00	Pinay et al., 2007
Semi-arid	761	699	1.09	29.20	Hefting et al., 2004
Semi-arid	766	666	1.15	204.00	Pinay et al., 2007
Semi-arid	800	600	1.33	0.97	Hefting et al., 2004
Semi-arid	875	792	1.10	96.00	Clement et al., 2002
Semi-arid	875	792	1.10	56.50	Clement et al., 2002
Semi-arid	875	792	1.10	81.90	Clement et al., 2002
Semi-arid	880	792	1.11	33.98	Hefting et al., 2004
Semi-arid	885	908	0.97	7.28	Hefting et al., 2004
Semi-arid	925	1100	0.84	0.19	Font del Regàs
Humid	1100	863	1.27	43.69	Hefting et al., 2004
Humid	1169	783	1.49	180.00	Pinay et al., 2007
Humid	1284	1270	1.01	21.24	Alongi et al., 2005
Humid	1743	1062	1.64	1.21	Fang et al., 2015
Humid	1743	1062	1.64	1.97	Fang et al., 2015
Humid	1780	1019	1.75	2.23	Fang et al., 2015

Table F.3 Precipitation (P), Potential Evapotranspiration (PET), Aridity index (AI), soil respiration (CO_2 emissions) for different riparian forests located worldwide.

Climate	P (mm yr^{-1})	PET (mm yr^{-1})	AI	CO_2 (g C m^{-2} yr^{-1})	Source
Arid	300	1670	0.18	583.33	Harms and Grimm, 2012
Arid	350	1521	0.23	329.81	McLain and Martens, 2006
Arid	350	1521	0.23	313.93	McLain and Marens, 2006
Arid	350	1521	0.23	302.22	McLain and Martens, 2006
Semi-arid	555	571	0.97	219	Mander et al., 2008
Semi-arid	711	571	1.25	620.5	Mander et al., 2008
Semi-arid	750	1670	0.45	672.59	Harms and Grimm, 2012
Semi-arid	880	915	0.96	1.19	Pacific et al., 2008
Semi-arid	880	915	0.96	3.58	Pacific et al., 2008
Semi-arid	925	1100	0.84	438	Font del Regàs
Semi-arid	925	1100	0.84	3650	Font del Regàs
Semi-arid	988	1036	0.95	1569.5	Vidon et al., 2015
Humid	1084	1097	0.99	1091	Batson et al., 2014
Humid	1864	996	1.87	33.45	Hirota et al., 2007
Humid	1864	996	1.87	179.18	Hirota et al., 2007

Table F.4 Precipitation (P), Potential Evapotranspiration (PET), Aridity index (AI), and soil natural emissions of N_2O (N_2O) for different riparian forests located worldwide.

Climate	P (mm yr^{-1})	PET (mm yr^{-1})	AI	N_2O (gN m^{-2} yr^{-1})	Source
Arid	300	1670	0.18	0.01	Harms and Grimm, 2012
Arid	350	1521	0.23	0.10	McLain and Martens, 2006
Arid	350	1521	0.23	0.05	McLain and Martens, 2006
Arid	350	1521	0.23	0.03	McLain and Martens, 2006
Semi-arid	555	571	0.97	0.47	Mander et al., 2008
Semi-arid	711	571	1.25	0.51	Mander et al., 2008
Semi-arid	750	1670	0.45	0.02	Harms and Grimm, 2012
Semi-arid	760	578	1.31	-0.39	Audet et al., 2014
Semi-arid	760	578	1.31	1.07	Audet et al., 2014
Semi-arid	761	699	1.09	0.30	Hefting et al., 2003
Semi-arid	761	699	1.09	2.00	Hefting et al., 2003
Semi-arid	875	792	1.10	1.65	Clement et al., 2002
Semi-arid	875	792	1.10	1.80	Clement et al., 2002
Semi-arid	875	792	1.10	1.60	Clement et al., 2002
Semi-arid	885	908	0.97	0.01	Bernal et al., 2007
Semi-arid	885	908	0.97	0.15	Bernal et al., 2007
Semi-arid	925	1100	0.84	0.00	Font del Regàs
Semi-arid	925	1100	0.84	0.07	Font del Regàs
Semi-arid	988	1036	0.95	-0.03	Vidon et al., 2015
Humid	1082	900	1.20	0.00	Burgin and Groffman, 2012
Humid	1082	900	1.20	7.01	Burgin et al., 2012
Humid	1084	1097	0.99	3.88	Batson et al., 2014
Humid	1146	1471	0.78	10.69	Allen et al., 2007
Humid	1284	1270	1.01	13.30	Alongi et al., 2005
Humid	1755	1106	1.59	2.45	Walker et al., 2002
Humid	1864	996	1.87	5.60	Hirota et al., 2007
Humid	2163	1663	1.30	1.97	Melling et al., 2005

Biogeosciences, 14, 4195–4208, 2017
https://doi.org/10.5194/bg-14-4195-2017

Biogeosciences
Open Access
EGU

Soil water content drives spatiotemporal patterns of CO_2 and N_2O emissions from a Mediterranean riparian forest soil

Sílvia Poblador[1,*], **Anna Lupon**[1,2,*], **Santiago Sabaté**[1,3], **and Francesc Sabater**[1,3]

[1]Departament de Biologia Evolutiva, Ecologia i Ciències Ambientals (BEECA), Universitat de Barcelona, Av. Diagonal 643, 08028, Barcelona, Spain
[2]Department of Forest Ecology and Management, Swedish University of Agricultural Sciences (SLU), Skogsmarksgränd 17S, 90183, Umeå, Sweden
[3]CREAF, Campus de Bellaterra Edifici C, 08193, Cerdanyola del Vallès, Spain
[*]These authors contributed equally to this work.

Correspondence to: Sílvia Poblador (spoblador@ub.edu)

Received: 16 January 2017 – Discussion started: 10 March 2017
Revised: 25 July 2017 – Accepted: 7 August 2017 – Published: 21 September 2017

Abstract. Riparian zones play a fundamental role in regulating the amount of carbon (C) and nitrogen (N) that is exported from catchments. However, C and N removal via soil gaseous pathways can influence local budgets of greenhouse gas (GHG) emissions and contribute to climate change. Over a year, we quantified soil effluxes of carbon dioxide (CO_2) and nitrous oxide (N_2O) from a Mediterranean riparian forest in order to understand the role of these ecosystems on catchment GHG emissions. In addition, we evaluated the main soil microbial processes that produce GHG (mineralization, nitrification, and denitrification) and how changes in soil properties can modify the GHG production over time and space. Riparian soils emitted larger amounts of CO_2 (1.2–10 $g C m^{-2} d^{-1}$) than N_2O (0.001–0.2 $mg N m^{-2} d^{-1}$) to the atmosphere attributed to high respiration and low denitrification rates. Both CO_2 and N_2O emissions showed a marked (but antagonistic) spatial gradient as a result of variations in soil water content across the riparian zone. Deep groundwater tables fueled large soil CO_2 effluxes near the hillslope, while N_2O emissions were higher in the wet zones adjacent to the stream channel. However, both CO_2 and N_2O emissions peaked after spring rewetting events, when optimal conditions of soil water content, temperature, and N availability favor microbial respiration, nitrification, and denitrification. Overall, our results highlight the role of water availability on riparian soil biogeochemistry and GHG emissions and suggest that climate change alterations in hydrologic regimes can affect the microbial processes that produce GHG as well as the contribution of these systems to regional and global biogeochemical cycles.

1 Introduction

Riparian zones are hotspots of nitrogen (N) transformations across the landscape, providing a natural filter for nitrate (NO_3^-) transported from surrounding lands via runoff and subsurface flow paths (Hill, 1996; Vidon et al., 2010). Although interest in riparian zones has primarily been motivated by the benefits of these ecotones as effective N sinks, enhanced microbial activity in riparian landscapes can play a key role in atmospheric pollution. For instance, riparian zones can account by 70 % of global (natural processes and human activities) terrestrial emissions of nitrous oxide (N_2O) to the atmosphere, a powerful greenhouse gas (GHG) with 298 times the global warming potential of carbon dioxide (CO_2) (Audet et al., 2014; Groffman et al., 2000; Hefting et al., 2003). Moreover, riparian soils can significantly contribute to global CO_2 emissions because they can hold high rates of heterotrophic and autotrophic respiration (Chang et al., 2014). Soil respiration is the main natural carbon (C) efflux to the atmosphere, contributing to 20 % of the global emission of CO_2 (Kim and Verma, 1990; Raich et al., 2002; Rastogi et al., 2002). Finally, riparian zones can support large methane (CH_4) fluxes that account for the 15–40 % of global emissions (Audet et al., 2014; Segers, 1998). However, there

are still many uncertainties regarding the magnitude and spatiotemporal variability of soil GHG emissions in riparian zones, reaching contradictory results concerning the potential role of riparian zones as sinks or sources of C and N (Bruland et al., 2006; Groffman et al., 1992; Harms et al., 2009; Walker et al., 2002).

Understanding the processes regulating GHG emissions from riparian soils is essential to quantify the role of riparian zones in the global C and N cycles. Multiple environmental variables, such as soil temperature, soil water content, and both C and N availability, have been identified as key factors influencing the rate and variability of soil microbial activities that produce GHG (Chang et al., 2014; Hefting et al., 2003; Mander et al., 2008; McGlynn and Seibert, 2003). Among them, riparian hydrology seems to play a fundamental role on GHG production because it controls the substrate subsides and, most importantly, the redox conditions of riparian soils (Jacinthe et al., 2015; Vidon, 2017). Under saturated conditions, anaerobic processes such as methanogenesis (i.e., the transformation of CO_2 to CH_4) and denitrification (i.e., the transformation of NO_3^- to N gas (N_2) or N_2O) are the primary processes involved in the C and N cycles (Clément et al., 2002). Conversely, in dry soils, aerobic transformations involved in the oxidation of the organic matter (i.e., respiration, mineralization, nitrification, methane oxidation) dominate the riparian biogeochemistry (Harms and Grimm, 2008). From such observations, one would expect that there is a strong correlation between soil wetness and the relative importance of CO_2, N_2O, and CH_4 riparian soil emissions to the total GHG fluxes. However, there are still relatively few studies that analyze the direct influence of soil water content on several GHG effluxes simultaneously (but see Harms and Grimm, 2008; Jacinthe et al., 2015), and even less that combine such analyses with other environmental factors and soil processes. Thus, it is still unclear under which circumstances soil water content (rather than temperature or substrate availability) is the primary control factor of the riparian functionality.

Mediterranean systems are a unique natural laboratory to understand the close link between spatiotemporal variations in hydrology and riparian biogeochemistry because they are characterized by a marked spatial gradient of soil water content, that can range from $< 10\,\%$ in the hillslope edge to $> 80\,\%$ close to the stream (Chang et al., 2014; Lupon et al., 2016). Moreover, Mediterranean regions are subjected to seasonal alterations of precipitation and temperature regimes that might affect riparian hydrology as well as microbial activity in the riparian soils (Bernal et al., 2007; Bruland et al., 2006; Harms and Grimm, 2008; Harms et al., 2009). Increments in GHG emissions in riparian zones might occur following storms or flood events because sharp increments in soil water content enhance nitrification, denitrification, respiration, and methanogenesis rates (Casals et al., 2011; Jacinthe et al., 2015; Werner et al., 2014). However, recent studies have shown that high temperatures can sustain large respiration and N mineralization rates in riparian soils (Chang et al., 2014; Lupon et al. 2016), and, hence, the contribution of rewetting microbial pulses to annual CO_2 and N_2O production in Mediterranean riparian soils is still under debate. Moreover, improved understanding of interactions among hydrology, microbial processes, and gas emissions within Mediterranean riparian zones is not only fundamental to understand the temporal pattern of riparian biogeochemistry but also necessary to estimate the contribution of these ecosystems to atmospheric GHG budgets at local and global scale.

In this study, soil properties, soil N processes, and CO_2 and N_2O soil emissions were measured over a year across a Mediterranean riparian forest that exhibited a strong gradient in soil water content (Fig. 1a). We did not measure CH_4 emissions because previous studies reported extremely low values in dry systems (-0.06–$0.42\,\mathrm{mg\,C\,m^{-2}\,d^{-1}}$; Batson et al., 2015; Gómez-Gener et al., 2015). Specifically, we aimed (i) to evaluate the spatiotemporal patterns of CO_2 and N_2O emissions in Mediterranean riparian soils, (ii) to analyze under which conditions soil water content rules microbial processes and GHG over other physicochemical variables, and (iii) to provide some reliable estimates of GHG emissions from Mediterranean riparian soils. We hypothesized that the magnitude and the relative contribution of N_2O and CO_2 to total GHG emission strongly depend on soil water content conditions rather than other variables during all year long (see conceptual approach in Fig. 1b). In the near-stream zone, we expected that saturated anoxic soils would enhance denitrification but constrain both respiration and nitrification. Thus, we predicted higher N_2O than CO_2 emissions in this zone. In the intermediate zone, we expected that wet (but not saturated) soils would enhance aerobic processes such as respiration, N mineralization or nitrification, and thus we predicted high CO_2 emissions compared to N_2O. Finally, we expect that dry soils would deplete (or even inhibit) the soil microbial activity near the hillslope edge, and therefore we predicted low GHG emissions in this zone. Because Mediterranean regions are subjected to strong intra-annual variations in soil water content, we expected that this general behavior would be maximized in summer, when only near-stream soils would keep wet. Conversely, we expected that all microbial processes would be enhanced shortly after rainfall events, and thus simultaneous pulses of CO_2 and N_2O emissions would occur in spring and fall.

2 Materials and methods

2.1 Study site

The research was conducted in a riparian forest of Font del Regàs, a forested headwater catchment ($14.2\,\mathrm{km^2}$, 500–1500 m a.s.l. (above sea level), located in the Montseny Natural Park, NE Spain (41°50′ N, 2°30′ E) (Fig. 1a). The climate

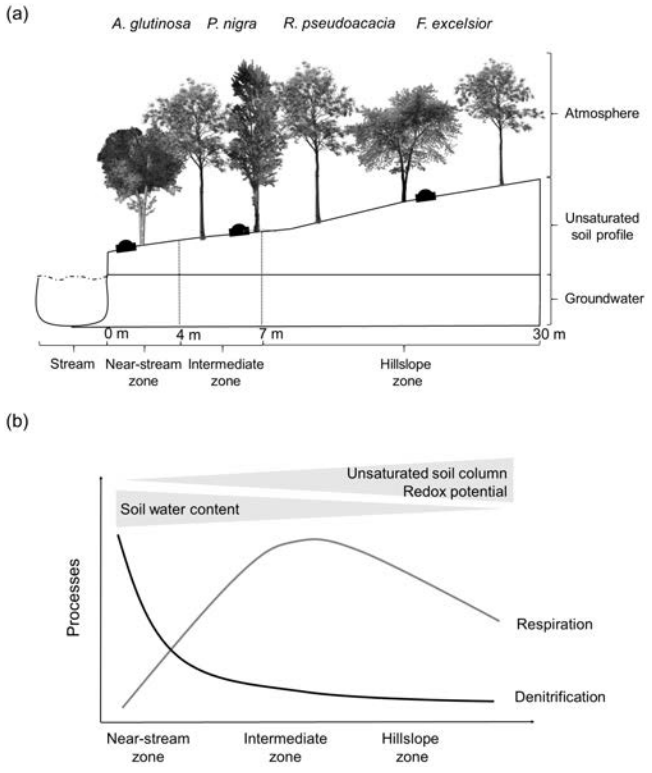

Figure 1. (a) Plot layout for the studied Mediterranean riparian forest showing the three riparian zones and the location of the chambers ($n = 5$ for each riparian zone). **(b)** Conceptual approach of the influence of riparian hydrology on soil microbial processes across a Mediterranean riparian zone. Soil water content decreases from the near-stream to the hillslope zone due to changes in groundwater table, increasing unsaturated soil column and oxic conditions. Anaerobic processes (denitrification) occur under anoxic conditions while aerobic processes (respiration) are optimized under a moderate range of soil water content.

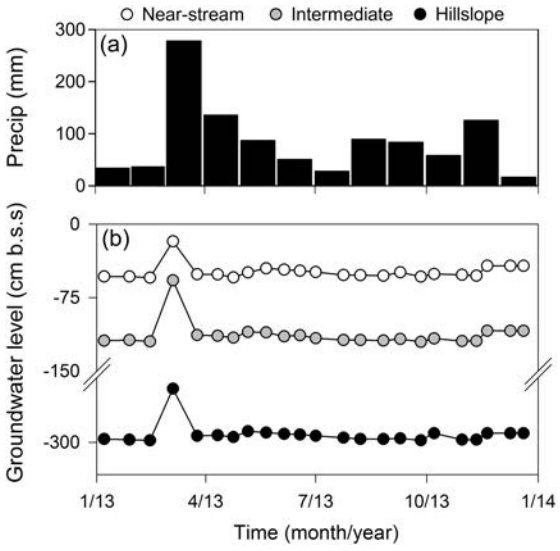

Figure 2. Temporal pattern of **(a)** mean monthly precipitation and **(b)** biweekly groundwater level at the studied riparian site during the year 2013. Circles are mean values of groundwater level at the near-stream (white), intermediate (grey), and hillslope (black) zones. Precipitation data were obtained from a meteorological station located at ca. 300 m from the studied riparian site. At each riparian zone, groundwater level was measured in three PVC piezometers (32 mm diameter, 1–3 m long) with a water level sensor (Eijkelkamp 11.03.30).

is sub-humid Mediterranean, with mean temperature ranging from 5 °C in February to 25 °C in August. In 2013, annual precipitation (1020 mm) was higher than long-term average (925 ± 151 mm), with most of rain falling in spring (500 mm) (Fig. 2a). Total inorganic N deposition oscillates between 15 and 30 kg N ha^{-1} yr^{-1} (period 1983–2007; Àvila and Rodà, 2012).

We selected a riparian site ($\sim 600\,m^2$, ~ 30 m wide) that flanked a third-order stream close to the catchment outlet (536 m a.s.l., 5.3 km from headwaters). The riparian site was divided into three zones characterized by different species compositions (Fig. 1a). The near-stream zone was located adjacent to the stream (0–4 m from the stream edge) and was composed of *Alnus glutinosa* (45 % of basal area) and *Populus nigra* (33 % of basal area). The intermediate zone (4–7 m from the stream edge) was composed by *P. nigra* and *Robinia pseudoacacia* (29 and 71 % of basal area, respectively). Finally, the hillslope zone (7–30 m from the stream edge) bordered upland forests and was composed by *R. pseudoacacia* (93 % of basal area) and *Fraxinus excelsior* (7 % of basal area). The three riparian zones had sandy-loam soils (bulk density = 0.9–1.1 g cm^{-3}), with a 5 cm deep organic layer followed by a 30 cm deep A horizon. The top soil layer (0–10 cm depth) was mainly composed by sands (~ 90 %) and silts (~ 7 %) at the near-stream zone, whereas gravels (~ 16 %) and sands (~ 80 %) were the dominant particle sizes at the intermediate and hillslope zones. During the study period, groundwater level averaged -54 ± 14 cm b.s.s. (below the soil surface) at the near-stream zone, and decreased to -125 ± 4 and -358 ± 26 cm b.s.s. at the intermediate and hillslope zones, respectively (Figs. 1a and 2b).

2.2 Field sampling

We delimited five plots (1×1 m) within each riparian zone (near-stream, intermediate, and hillslope) (Fig. 1a). During the year 2013, soil physicochemical properties, soil N processes, and gas emissions were measured in each plot every 2–3 months in order to cover a wide range of soil water content and temperature conditions. On each sampling month, one soil sample (0–10 cm depth, including O and A horizons) was collected randomly from each plot to analyze soil physicochemical properties. Soil samples were taken with a 5 cm diameter core sampler and placed gently into plastic bags after carefully removing the litter layer. Close to each soil sample, we performed in situ soil incubations to mea-

sure soil net N mineralization and net nitrification rates (Eno, 1960). For this purpose, a second soil core (0–10 cm depth) was taken, placed in a polyethylene bag, and buried at the same depth. Soil incubations were buried for 4 days and then removed from the soil.

Gas emissions and denitrification rates were measured simultaneously and during four consecutive days (i.e., during the entire soil incubation period) in order to facilitate the direct comparison between microbial rates and gas fluxes. Soil CO_2 effluxes were measured with a SRC-1 soil chamber attached to an EGM-4 portable infrared gas analyzer (IRGA) (PP Systems, Amesbury, MA). The EGM-4 has a measurement range of 0–2000 ppm ($\mu mol\,mol^{-1}$), with an accuracy of 1 % and a linearity of 1 % throughout the range. Every field day, CO_2 measurements started at 12:00 and were conducted consecutively at the 15 plots starting for the near stream zone. At each plot, the SCR-1 soil chamber was placed over the top soil for a 120 s incubation. Before each measurement, we carefully removed the litter layer to ensure no leaks. Furthermore, we aerated the SCR-1 between samples to ensure the accuracy of the instrument as well as to avoid contamination between samples. For each plot, CO_2 emissions rates were calculated from the best-fit linear regression of the CO_2 accumulated in the headspace with incubation time (Fig. S1 in the Supplement). CO_2 fluxes on an areal basis (F_{CO_2}, in $\mu mol\,m^{-2}\,h^{-1}$) were calculated following Healy et al. (1996):

$$F_g = \frac{dg}{dt} \times \frac{V P_0}{S R T_0}, \quad (1)$$

where dg/dt is the rate of change in gas concentration (in $\mu mol\,mol^{-1}\,h^{-1}$) in the chamber, V is chamber volume (in m^3), P_0 is initial pressure (in Pa), S is the soil surface area (in m^2), R is the gas constant ($8.314\,Pa\,m^3\,K^{-1}\,mol^{-1}$), and T_0 is the initial chamber temperature (in K). For budgeting, moles of CO_2 and N_2O were converted to grams of C and N, respectively.

In situ denitrification rates and N_2O emissions were measured using closed cylinder (0.37 L) and open cylinder (0.314 m^2) chambers, respectively. For denitrification analyses, an intact soil core (0–10 cm depth) was introduced in the chamber, closed with a rubber serum stopper, amended with acetone-free acetylene to inhibit the transformation of N_2O to N_2 (10 % v/v atmosphere), and placed at the same depth. For N_2O analysis, chambers were placed directly on the soil and no special treatment was carried out. Gas samples for both denitrification and N_2O chambers were taken at the same time (0, 1, 2, and 4 h of incubation) with a 20 mL syringe and stored in evacuated tubes. All soil and gas samples were kept at $< 4\,°C$ until laboratory analysis (< 24 h after collection).

Soil physical properties were measured within each plot simultaneously to gas emissions. Volumetric soil water content (%) (five replicates per plot) and soil temperature (°C) (one replicate per plot) were measured at 10 cm depth by using a time-domain reflectometer sensor (HH2 moisture meter, Delta-T Devices) and a temperature sensor (CRISON 25), respectively. Soil pH and reduction potential (Eh, mV) (1 replicate per plot) were measured at 0–10 cm depth by water extraction (1 : 2.5 v/v) using a Thermo Scientific ORION sensor (STAR 9107BNMD). Although Eh measures performed by water extraction may not be as accurate as other field techniques, these values have been previously used as a good proxy of the soil redox potential (Yu and Rinklebe, 2013).

2.3 Laboratory analyses

Pre-incubation soil samples were oven dried at 60 °C, sieved, and the fraction < 2 mm was used for measuring soil chemical properties. The relative soil organic matter content (%) was measured by loss on ignition (450 °C, 4 h). Total soil C and N contents were determined on a gas chromatograph coupled to a thermal conductivity detector after combustion at 1000 °C at the Scientific Technical Service of the University of Barcelona.

To estimate microbial N processes, we extracted 5 g of pre- and post-incubation field-moist soil samples with 50 mL of 2 M KCl (1 g : 10 mL, ww : v; 1 h shacking at 110 rpm and 20 °C). The supernatant was filtered (Whatman GF/F 0.7 µm pore diameter) and analyzed for ammonium (NH_4^+) and nitrate (NO_3^-). NH_4^+ was analyzed by the salicylate–nitroprusside method (Baethgen and Alley, 1989) using a spectrophotometer (PharmaSpec UV-1700, Shimadzu). NO_3^- was analyzed by the cadmium reduction method (Keeney and Nelson, 1982) using a Technicon autoanalyzer (Technicon, 1987). For each pair of samples, net N mineralization and net nitrification were calculated as the differences between pre- and post-incubations values of inorganic N (NH_4^+ and NO_3^-) and NO_3^-, respectively (Eno, 1960). Pre-incubation NH_4^+ and NO_3^- concentrations were further used to calculate the availability of dissolved inorganic nitrogen in riparian soils.

To estimate denitrification and natural N_2O emissions, we analyzed the N_2O of all gas samples using a gas chromatograph (Agilent Technologies, 7820A GC) that was calibrated using certified standards (4.66 ppm N_2O; Air Liquide). Both denitrification and N_2O emissions rates were calculated similarly to CO_2 fluxes (Fig. S1). In addition, we measured the denitrification enzyme activity (DEA) for three soil cores of each riparian zone to determine the factors limiting denitrification. For each soil core, four sub-samples (20 g of fresh soil) were placed into 125 mL glass jars containing different treatments. The first jar (DEA_{MQ}) contained Milli-Q water (20 mL) to test anaerobiosis limitation. The second jar (DEA_C) was amended with glucose solution ($4\,g\,glucose\,kg\,soil^{-1}$) to test C limitation. The third jar (DEA_{NO_3}) was amended with nitrate solution ($72.22\,mg\,KNO_3\,kg\,soil^{-1}$) to test N limitation. Finally, the fourth jar (DEA_{C+NO_3}) was amended with

both nitrate and glucose solutions (4 g glucose kg soil^{-1} and 72.22 mg KNO_3 kg soil^{-1}) to test simultaneously C and N limitation. All jars were capped with rubber serum stoppers, made anaerobic by flushing N_2, and amended with acetone-free acetylene (10 % v/v) (Smith and Tiedje, 1979). Gas samples were collected after 4 and 8 h of incubation and analyzed following the same procedure of field DNT samples. DEA rates were calculated similarly to denitrification rates.

2.4 Statistical analysis

Statistical analyses were carried out using the package *lmer* and *pls* of R 2.15.1 statistical software (R Development Core Team, 2012). We performed linear mixed-model analysis of variance (ANOVA) to test differences in soil properties, microbial N processes, and gas emissions across riparian zones and seasons. We used riparian zone and season as fixed effects and plot (nested within riparian zones) as a random effect. When multiple samples were taken within a plot (soil physical properties, denitrification, and gas emissions), the ANOVA was performed on plot means, with $n =$ 75 (5 plots $\times$ 3 zones $\times$ 5 dates). For each model, post hoc Tukey contrasts were used to test which zones or seasons differed from each other. In all cases, residuals were tested for normality using a Shapiro–Wilk test and homogeneity of variance was examined visually by plotting the predicted and residual values. In those cases that the normality assumption was unmet, data were log transformed. In all analyses, differences were considered significant when $p < 0.05$.

We used partial least squares regression (PLS) to explore how soil properties, C and N availability, groundwater level, and soil N processes predict variation in CO_2 and N_2O emissions. PLS identifies the relationship between independent (X) and dependent (Y) data matrices through a linear, multivariate model and produces latent variables (PLS components) representing the combination of X variables that best describe the distribution of observations in "Y space" (Eriksson et al., 2006). We determined the goodness of fit (R^2Y) and the predictive ability (Q^2Y) of the model by comparing modeled and actual Y observations through a cross-validation process. Each model was refined by iteratively removing variables that had non-significant coefficients in order to minimize the model overfitting (i.e., low Q^2Y values) as well as the multicollinearity of the explanatory variables (i.e., variance inflation factor (VIF) < 5). Furthermore, we identified the importance of each X variable by using variable importance on the projection (VIP) scores, calculated as the sum of square of the PLS weights across all components. VIP values > 1 indicate variables that are most important to the overall model (Eriksson et al., 2006). In all PLS models, data were ranked and centered prior to analysis.

3 Results

3.1 Spatial pattern of soil properties, microbial rates, and gas emissions

During the study period, all riparian zones had similar mean soil temperature (11–12 °C), pH (6–7), and redox potential (170–185 mV) (Table 1). However, soil water content exhibited strong differences across riparian zones (Table 2), with the near-stream zone holding wetter soils than the intermediate and the hillslope zones (Table 1). There were significant differences in most of soil chemical properties (Tables 1 and 2). Both organic matter and soil C and N content were 2-fold lower in the near-stream zone than in the intermediate and hillslope zones, though all zones exhibited similar C : N ratios (C : N = 14). Moreover, inorganic N concentrations (NH_4^+ and NO_3^-) were from 2- to 5-fold lower for the near-stream zone than for the other two zones.

On annual basis, net N mineralization averaged 0.14 ± 0.40, 0.39 ± 1.23, and 0.22 ± 1.03 mg N kg^{-1} d^{-1} at the near-stream, intermediate, and hillslope zones, respectively. Mean annual net nitrification rates were close to net N mineralization, averaging 0.17 ± 0.38, 0.25 ± 0.69, and 0.28 ± 0.73 mg N kg^{-1} d^{-1} at the near-stream, intermediate, and hillslope zones, respectively. There were no significant differences in mean annual net N mineralization and net nitrification rates among riparian zones (in both cases: mixed-model ANOVA test, $F > F_{0.05}$, $p > 0.05$). Mean annual denitrification was higher at the near-stream zone (2.69 ± 5.30 µg N Kg^{-1} d^{-1}) than at the intermediate (0.72 ± 1.85 µg N Kg^{-1} d^{-1}) and hillslope (0.76 ± 1.59 µg N Kg^{-1} d^{-1}) zones (mixed-model ANOVA test, $F = 4.33$, $p = 0.038$). However, potential denitrification rates were lower in the near-stream zone (0.3–0.6 mg N kg^{-1} d^{-1}) compared to intermediate (1.0–2.4 mg N kg^{-1} d^{-1}) and hillslope (1.3–3.8 mg N kg^{-1} d^{-1}) zones (Table 3).

Natural CO_2 and N_2O emissions differed among riparian zones, yet they showed opposite spatial patterns. Near-stream zone exhibited lower CO_2 emissions (318 ± 195 mg C m^{-2} h^{-1}) compared to the intermediate (472 ± 298 mg C m^{-2} h^{-1}) and hillslope (458 ± 308 mg C m^{-2} h^{-1}) zones (mixed-model ANOVA test, $F = 7.08$, $p = 0.009$). Conversely, near-stream zone showed higher N_2O emissions (0.035 ± 0.022 mg N m^{-2} h^{-1}) than the other two zones (intermediate = 0.032 ± 0.025 mg N m^{-2} h^{-1}; hillslope = 0.022 ± 0.012 mg N m^{-2} h^{-1}) (mixed-model ANOVA test, $F = 7.31$, $p = 0.008$).

3.2 Temporal pattern of soil properties, microbial rates, and gas emissions

During the study period, there was a marked seasonality in most of soil physical properties, except for pH and Eh, which did not show any temporal pattern (Table 2). Soil water content exhibited a marked seasonality, though it differed among

Table 1. Mean annual values (±SD) of soil water content (volumetric), soil temperature, soil pH, soil redox capacity (Eh), soil organic matter, soil molar C : N ratio, soil carbon (C) and nitrogen (N) content, and soil ammonium (NH_4^+) and nitrate (NO_3^-) concentrations for the three riparian zones. For each variable, different letters indicate statistical significant differences between riparian zones (post hoc Tukey HSD test, $p < 0.05$).

	Near-stream	Intermediate	Hillslope
Soil water content (%)	29.58 ± 7.55^{A}	19.36 ± 6.00^{B}	19.81 ± 6.24^{B}
Temperature (°C)	11.37 ± 5.39^{A}	11.82 ± 5.90^{A}	12.01 ± 6.34^{A}
Eh	170 ± 111^{A}	184 ± 103^{A}	184 ± 95^{A}
pH	6.66 ± 0.42^{A}	6.31 ± 0.50^{A}	6.68 ± 0.53^{A}
Organic matter (%)	4.41 ± 0.71^{A}	7.98 ± 2.88^{B}	9.53 ± 1.99^{C}
C : N ratio	14.25 ± 3.64^{A}	14.09 ± 1.78^{A}	13.63 ± 1.18^{A}
C ($mg\,kg^{-1}$)	2004 ± 1038^{A}	4007 ± 1785^{B}	4923 ± 1428^{B}
N ($mg\,kg^{-1}$)	160 ± 44^{A}	330 ± 135^{B}	418 ± 107^{C}
NH_4^+ ($mg\,N\,kg^{-1}$)	1.88 ± 1.21^{A}	5.58 ± 3.48^{B}	3.90 ± 2.07^{B}
NO_3^- ($mg\,N\,kg^{-1}$)	0.75 ± 0.58^{A}	4.66 ± 4.25^{B}	5.30 ± 4.20^{B}

Table 2. Results from the mixed-model analysis of variance (ANOVA) showing the effects of riparian zones and seasons on soil water content, soil temperature, soil pH, soil redox capacity (Eh), soil organic matter, soil molar C : N ratio, soil carbon (C) and nitrogen (N) content, and soil ammonium (NH_4^+) and nitrate (NO_3^-) concentrations. Plot was treated as a random effect in the model, whereas riparian zones, seasons, and their interactions were considered fixed effects. Values are F values and the p values are shown in brackets. P values < 0.05 are shown in bold.

	Riparian zone	Seasons	Zone × season
Soil water content	**18.6 [< 0.001]**	**100 [< 0.001]**	**13.6 [< 0.001]**
Temperature	0.33 [0.721]	**2117 [< 0.001]**	0.42 [0.906]
pH	1.97 [0.182]	2.43 [0.060]	2.73 [0.052]
Eh	1.34 [0.247]	3.53 [0.062]	1.88 [0.084]
Organic matter	**27.8 [< 0.001]**	2.77 [0.053]	1.62 [0.144]
C : N ratio	0.99 [0.400]	**10.9 [< 0.001]**	1.72 [1.118]
C	**27.1 [< 0.001]**	1.86 [0.132]	0.77 [0.630]
N	**39.7 [< 0.001]**	1.22 [0.311]	0.63 [0.746]
NH_4^+	**12.4 [0.001]**	2.71 [0.051]	1.52 [0.176]
NO_3^-	**22.4 [< 0.001]**	**5.63 [< 0.001]**	**4.09 [< 0.001]**

Zone: near-stream, intermediate, hillslope.
Season: Feb, Apr, Jun, Aug, and Nov.

riparian zones (Table 2, "zone × season"). In the intermediate and hillslope zones, soil water content was maxima in November and minima in August, while the near-stream soils were wetter during both spring (April–June) and fall (November) (Fig. 3a). Conversely, soil temperature showed similar seasonality but opposite values in all riparian zones (Table 2), with a maxima in summer (August) and minima in winter (February) (Fig. 3b). Soil chemical properties (soil organic matter and both soil C and N content) did not show any seasonal trend, but all riparian zones exhibited lower C : N ratios in February compared to the other seasons (Fig. 3c). There was no seasonality in soil NH_4^+ concentrations at any riparian zone (Table 2). However, soil NO_3^- concentrations showed a marked temporal pattern, yet it differed among riparian zones (Table 2, "zone × season"). The highest soil NO_3^- concentrations occurred in February at both the near-stream and hillslope zones, but in June–August at the intermediate zone (Fig. 3d).

Soil N processes showed similar seasonal patterns in all riparian zones (in all cases: $F_{date} < F_{0.05}$, $F_{interaction} > F_{0.05}$). Both net N mineralization and net nitrification rates were higher in April than February, June, and November (Fig. 4a and b), while denitrification rates were higher in April and June compared to the rest of the year (Fig. 4c). In April, both net N mineralization and net nitrification rates differed across riparian zone, with higher rates in the intermediate zone than in the near-stream one. Net N mineralization rates also differed in August, when the intermediate zone exhibited 2-fold higher rates than the other two zones. Finally, denitrification was higher at the near-stream than at the other two zones in both June and August.

Natural gas emissions showed a clear seasonal pattern (in both cases: mixed-model ANOVA test, $F_{date} < F_{0.05}$, $p <$

Table 3. Mean values (± SD) of potential denitrification rates (in mg N kg^{-1} d^{-1}) after anoxia (DEA_{MQ}), carbon addition (DEA_C), nitrogen addition (DEA_{NO_3}), and carbon and nitrogen addition (DEA_{C+NO_3}) treatments for the three riparian zones during the study period. For each zone, different letters indicate statistical significant differences between treatments (post hoc Tukey HSD test, $n = 15$, $p < 0.01$).

	Potential denitrification rates (mg N kg^{-1} d^{-1})			
	DEA_{MQ}	DEA_C	DEA_{NO_3}	DEA_{C+NO_3}
Near-stream	0.31 ± 0.41^{A}	0.26 ± 0.27^{A}	0.42 ± 0.42^{A}	0.63 ± 0.85^{A}
Intermediate	1.01 ± 1.12^{A}	1.88 ± 1.59^{A}	2.28 ± 3.57^{A}	2.40 ± 2.45^{A}
Hillslope	1.34 ± 1.33^{A}	2.35 ± 1.97^{AB}	1.73 ± 1.43^{AB}	3.82 ± 2.78^{B}

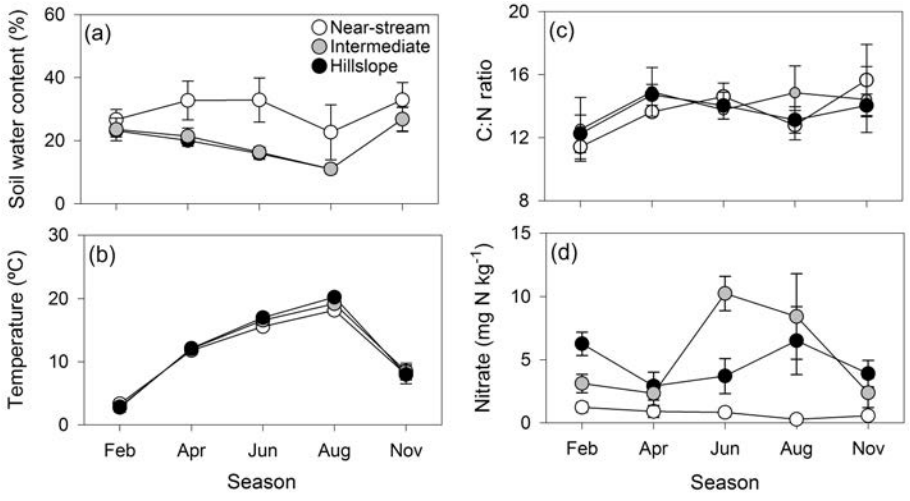

Figure 3. Temporal pattern of **(a)** soil water content, **(b)** soil temperature, **(c)** soil C : N molar ratio, and **(d)** soil nitrate concentration at 10 cm depth. Data are shown for the near-stream (white), intermediate (grey), and hillslope (black) zones during the study period. Circles are mean values and error bars are standard deviations.

0.001), yet it differed between CO_2 and N_2O emissions. In all zones, CO_2 emissions were maxima in June and minima in February (Fig. 5a), while highest N_2O emission rates occurred in April and lowest in both February and August (Fig. 5b). In spring (April and June), CO_2 emissions were higher at the intermediate and hillslope zones compared to the near-stream one (Fig. 5a). Moreover, the near-stream zone showed higher N_2O emissions than the hillslope zone in February, April, and June (Fig. 5b).

3.3 Relationship between soil properties, microbial processes, and gas emissions

PLS models extracted two components that explained the 71 % and the 40 % of the variance in CO_2 and N_2O emissions, respectively (Table 4). The model predictability was high for CO_2 ($Q^2Y = 0.66$), but weak for N_2O ($Q^2Y = 0.34$). Moreover, PLS models identified few variables as key predictors of GHG emissions (VIF < 2, VIP > 0.8), yet these variables differed between CO_2 and N_2O emissions (Table 4). Soil temperature (PLS coefficient [coef] = +0.60), and soil water content (coef = −0.24) explained most of the variation in CO_2 emissions (Table 4, Fig. S2a). Conversely, variations in N_2O emissions were primarily related to changes in denitrification rates (coef = +0.45), soil water content (coef = +0.21) and, to a lesser extent, groundwater level (coef = −0.16) (Table 4, Fig. S2b).

4 Discussion

This study emphasized the role of soil water content as a main driver of riparian biogeochemistry and GHG emissions. By analyzing soil microbial processes and GHG emissions over a year in a Mediterranean riparian forest, we clearly demonstrate that soil water content has a major role in driving soil microbial processes, the spatiotemporal patters of CO_2 and N_2O emissions and the overall role of Mediterranean riparian soils in the global C and N cycles.

4.1 Microbial processes regulating GHG emissions

Mean daily emissions of CO_2 found in the present study (1.2–10 g C m^{-2} d^{-1}) were generally high, especially during spring and summer months. These soil CO_2 emissions were higher than those reported for temperate riparian regions (0.2–4.8 g C m^{-2} d^{-1}; Batson et al., 2015; Bond-Lamberty

Table 4. Summary of the partial least squares (PLS) models produced for CO_2 and N_2O emissions at the riparian site ($n = 75$). Values are the coefficients from PLS models which describe the relationship (direction and relative strength) between explanatory variables and gas emissions. The variance inflation factor (VIF) of each explanatory variable, indicative of collinearity, is shown in brackets. Bold values indicate the most influencing variables (variable importance in the projection (VIP) > 1.0).

	X variable	Abbreviation	CO_2	N_2O
Soil properties	Soil water content	SWC	**−0.235 [1.72]**	**0.205 [1.32]**
	Groundwater level	GWL	–	−0.157 [1.24]
	Temperature	Tsoil	**0.599 [1.45]**	–
	pH	pH	–	–
	Redox potential	Eh	–	–
	Bulk density	BD	–	–
	Coarse texture	% Sand	–	–
	Organic matter	SOM	–	–
	Total carbon	C	–	–
	Total nitrogen	N	–	–
	Molar C : N ratio	C : N ratio	–	–
	Ammonium	NH_4^+	0.167 [1.61]	–
	Nitrate	NO_3^-	0.066 [1.80]	−0.060 [1.47]
Soil N processes	Net N mineralization	NNM	–	–
	Net nitrification	NN	–	–
	Denitrification	DNT	–	**0.449 [1.09]**
R^2Y			**0.71**	**0.40**
Q^2Y			**0.66**	**0.34**

All abbreviations are used in Fig. S2 for PLS loading plots.

and Thomson, 2010; Mander et al., 2008), although similar values have been reported in some dry forested wetlands of Europe and North America (Harms and Grimm, 2008; Oertel et al., 2016). These substantially high CO_2 emissions observed in Font del Regàs may be attributed to high microbial respiration rates associated with relatively moist and organic-matter-enriched soils (Mitsch and Gosselink, 2007; Pacific et al., 2008; Stern, 2006). In agreement, previous studies have reported that microbial heterotrophic respiration can be an important contributor (> 60 %) to CO_2 soil effluxes in water-limited riparian zones (Harms and Grimm, 2012; McLain and Martens, 2006). However, the absence of a relationship between soil N processes and CO_2 emissions suggests that soil C and N cycles are decoupled in Mediterranean riparian forests, and thus soil N mineralization may be not a good descriptor of bulk organic matter mineralization. Moreover, plant root respiration and methane oxidation can increase the CO_2 emissions in riparian soils with deep groundwater tables such as in Font del Regàs (Chang et al., 2014).

Conversely, N_2O emissions of our riparian site (0.001–0.2 $mg\,N\,m^{-2}\,d^{-1}$) were relatively low during the whole year. Similar N_2O emissions were reported in other water-limited riparian forests that are rarely flooded (−0.9–0.39 $mg\,m^{-2}\,d^{-1}$; Bernal et al., 2003; Harms and Grimm, 2012; Vidon et al., 2016), yet these values were, on average, much lower than those found in temperate riparian regions (0–54 $mg\,N\,m^{-2}\,d^{-1}$; Burgin and Groffman, 2012; Hefting et al., 2003; Mander et al., 2008). In Font del Regàs, most N_2O was produced by denitrification, as we found an intimate link between this microbial process and N_2O emissions. Additionally, other processes such as nitrification or nitrate ammonification can contribute to N_2O emissions (Baggs, 2008; Hefting et al., 2003). However, it seems unlikely that nitrification could account for the observed N_2O emissions because no relationship was found between net nitrification rates and N_2O emissions. Likewise relatively oxic conditions (Eh > 100) and low C : N ratios (C : N < 20) in Font del Regàs suggest low nitrate ammonification in riparian soils (Schmidt et al., 2011). Currently, the influence of soil denitrification on N_2O emissions in riparian zones is still under debate (Giles et al., 2012). Nonetheless, our results suggest that performing simultaneous measurements of different soil N can contribute to disentangling the mechanisms underlying net N_2O emissions in riparian areas.

4.2 Effects of soil water content on soil CO_2 effluxes

As expected, we found higher soil CO_2 effluxes at the intermediate and hillslope zones than at the near-stream zone. This spatial pattern was negative and strongly related to soil water content (Table 4), suggesting that, as soils become less moist and more aerated, oxidizing aerobic respiration increases, ultimately stimulating CO_2 production in the top soil layer (Müller et al., 2015). In agreement, other aerobic processes, such as N mineralization, were also higher in the

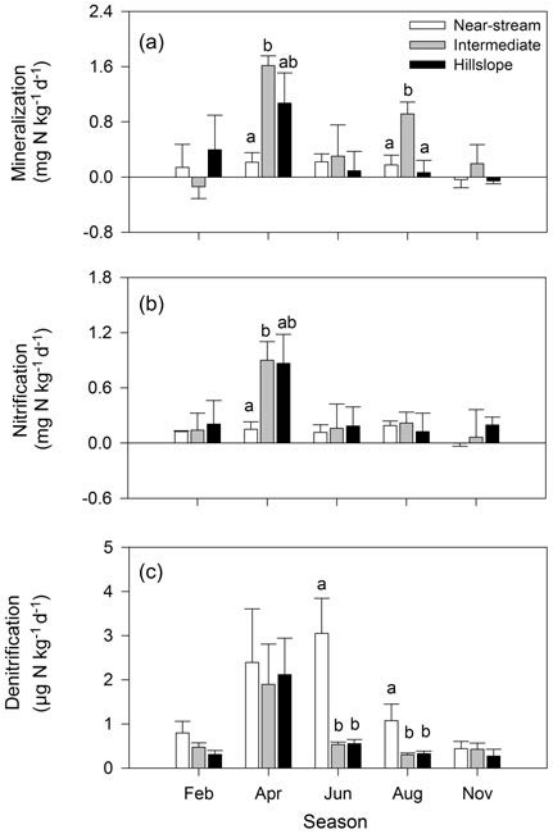

Figure 4. Temporal pattern of **(a)** soil net N mineralization, **(b)** net nitrification, and **(c)** denitrification rates at the near-stream (white), intermediate (grey), and hillslope (black) zones during the study period. Bars are mean values for each section and error bars are standard errors. For each season, different letters indicate significant differences among sections (mixed-model ANOVA, $p < 0.05$).

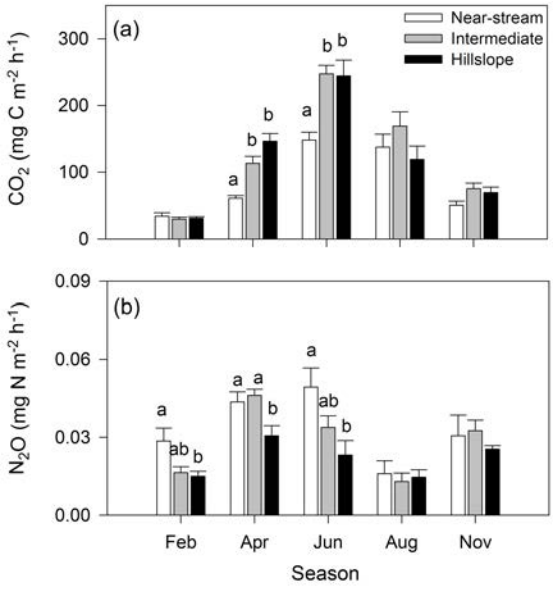

Figure 5. Temporal pattern of soil **(a)** CO_2 and **(b)** N_2O emissions at the near-stream (white), intermediate (grey), and hillslope (black) zones during the study period. Bars are mean values for each section and error bars are standard errors. For each season, different letters indicate significant differences among sections (mixed-model ANOVA, $p < 0.05$).

intermediate and hillslope zones. Moreover, deep groundwater tables in the hillslope zone can increase the volume of aerated soil, which can increase the area-specific soil CO_2 emissions near the hillslope edge (Chang et al., 2014). Increasing CO_2 emissions from wet to dry zones has been reported in other wetlands and riparian forests (Batson et al., 2015; Morse et al., 2012; Welti et al., 2012), showing a close linkage between riparian hydrology and spatial variations in microbial respiration rates.

Nonetheless, the intra-annual variations of soil CO_2 emissions were strongly dependent on soil temperature (Table 4). Probably, cold temperatures ($< 4\,°C$) limited soil respiration during winter, while warmer conditions ($> 15\,°C$) stimulated this process in June and August (Emmett et al., 2004; Suseela et al., 2012; Teiter and Mander, 2005). However, lower CO_2 emissions than expected for temperature dynamics were reported in summer at the intermediate and hillslope zones, likely because extreme soil dryness (soil water content $< 20\,\%$) limited respiration rates during such period (Chang et al., 2014; Goulden et al., 2004; Wickland et al., 2010). Although the mechanisms by which soil dryness may affect microbial C demand are still poorly understood, suppressed microbial respiration in summer can be attributed to a disconnection between microbes and resources (Belnap et al., 2005; Davidson et al., 2006), decreases in photosynthetic and exo-enzymatic activities (Stark and Firestone, 1995; Williams et al., 2000), or a relocation of the invested energy on growth (Allison et al., 2010). Altogether, these results suggest that soil water content may be as important as soil temperature to understand soil CO_2 effluxes, and therefore future warmer conditions may not fuel higher CO_2 emissions, at least in those regions experiencing severe water limitation.

4.3 Effects of soil water content on soil N_2O effluxes

As occurred for CO_2 emissions, N_2O fluxes showed a clear spatial pattern associated with changes in soil water content across the riparian zone. In the near-stream zone, relatively wet conditions (SWC = 30–40 %) likely promoted denitrification rates, while dry soils (SWC = 10–25 %) could limit both nitrification and denitrification in the intermediate and hillslope zones (Linn and Doran, 1984; Pinay et al., 2007). Such spatial pattern differed from those found in non-water-limited riparian forests, where higher N_2O emissions occurred in the hillslope edge as a result of high resource supply (DeSimone et al., 2010; Dhondt et al., 2004; Hedin et al., 1998). These results suggest that riparian hydrology is

the primary mechanisms controlling denitrification but, once water is unlimited, substrate availability controls the magnitude of denitrification rates. This former idea is supported by our potential denitrification results, which showed that, after adding water, denitrification rates at the intermediate and hillslope zones were 3–4 times the rate at the near-stream zone. Moreover, $N_2 : N_2O$ ratios estimated from acetylene method suggest that there was a spatial pattern in denitrification efficiency as well. During the study period, $N_2 : N_2O$ ratios were always higher at the near-stream (21.50 ± 40.32) than at the intermediate and hillslope zones (5.90 ± 16.02 and 4.23 ± 8.31, respectively), yet all values were much lower than those reported for temperate riparian forests (184–844; Mander et al., 2014). All together, these results support the idea that saturated soils favored the complete denitrification process to N_2 and can potentially emit less N_2O compared to less saturated soils (Giles et al., 2012).

Intra-annual variation in N_2O emission was also related to riparian hydrology because high rates of N_2O effluxes occurred in April, when large precipitation events (400 mm) raised the groundwater level and increased soil water content at the whole riparian plot. Such pulses of N_2O emissions short-after rewetting events can reflect the microbial use of the NO_3^- that has been accumulated during dry antecedent periods (Chang et al., 2014; Hefting et al., 2004; Pinay et al., 2007). In agreement, the PLS model showed a negative relation between soil water content and NO_3^- concentrations. Moreover, our results further suggest that rewetting events promote a fast N cycle because all microbial N processes were maxima in April. Nevertheless, we also expected a fast N cycle as well as large N_2O emissions following rains in November because, similarly to spring, environmental conditions (i.e., high soil water content and increments in soil NO_3^- concentrations during the antecedent dry summer) should enhance microbial activity. Likely, low rates of N transformations during fall may be attributed to an increase in microbial N demand following large C inputs from litterfall (Guckland et al., 2010). Moreover, leaf litter from *R. pseudoacacia*, the main tree species in our study site, holds a high lignin content (Castro-Díez et al., 2009; Yavitt et al., 1997), which might enrich the riparian soil with phenolic compounds and ultimately limit the use of N by microbes (Bardon et al., 2014). These results suggest that the response of N cycling to changes in water availability is more complex and less predictable than C cycling, likely because N processes depend on the interplay of additional ecosystem factors not included in this study.

4.4 Riparian soils as hotspots of GHG effluxes

There are several studies that attempt to upscale riparian GHG emissions at catchment scale, yet there are still fundamental uncertainties regarding the magnitude and sources of GHG emissions (Hagedorn, 2010; Pinay et al., 2015; Vidon and Hill, 2006). When accounting for all GHG ($CO_2 + N_2O$), our study suggest that our riparian soils can emit between 438 and 3650 $g\,C\,m^{-2}\,yr^{-1}$. Assuming that GHG emissions ($CO_2 + N_2O$) from upland evergreen oak and beech soils (54 and 38 % of the catchment, respectively) are similar to other Mediterranean regions (oak: 19–1240 $g\,C\,m^{-2}\,yr^{-1}$; Asensio et al., 2007; Barba et al., 2016; Inclán et al., 2014; beech: 214–1182 $g\,C\,m^{-2}\,yr^{-1}$; Guidolotti et al., 2013; Kesik et al., 2005), then riparian soils (6 % of the catchment area) can contribute between 16 and 22 % to the total catchment soil GHG emissions. Although these estimates are rough (i.e., we assumed that riparian soils emit the same rate of GHG that our study site), our results clearly pinpoint that riparian soils can be potential hotspots of GHG emissions within Mediterranean catchments. These findings contrast with the common knowledge that water-limited soils are powerless GHG sources to the atmosphere (Bernal et al., 2007; Vidon et al., 2016) and stress the importance of simultaneously consider several GHG emissions (i.e., CO_2, N_2O, CH_4) to get a whole picture of the role of riparian soils in climate change.

5 Conclusions

Mediterranean riparian zones are dynamic systems that undergo spatial and temporal shifts in biogeochemical processes due to changes in both soil water content and substrate availability. In a first attempt to simultaneously quantify CO_2 and N_2O emissions from Mediterranean riparian soils, we show that most of GHG emissions occur in the form of CO_2, even in the wet soils located near the stream. In addition, our results clearly illustrate a strong linkage between riparian hydrology and the microbial processes that produce GHG. Deep groundwater tables fueled large respiration rates in the relatively dry soils near the hillslope, while denitrification mostly occurred in the wet zones located near the stream channel. As occurred at spatial scale, riparian soil water content was a primarily control of the temporal patterns of CO_2 and N_2O emissions. Soil dryness diminished respiration rates during summer, while a fast soil N cycling promoted high N_2O emissions after a rewetting event in spring. Overall, our study shows that future variations in catchment hydrology due to climate change can potentially affect the riparian functionality in Mediterranean zones, as well as their contribution to regional and global C and N cycles.

Data availability. The data sets used in this paper can be obtained from the authors upon request.

The Supplement related to this article is available online at https://doi.org/10.5194/bg-14-4195-2017-supplement.

Author contributions. SP, SS, and FS designed the experiments. SP and AL carried them out. SP performed all laboratory analysis. AL and SP analyzed the data set and prepared the manuscript, with contributions from SS and FS.

Competing interests. The authors declare that they have no conflict of interest.

Acknowledgements. We are thankful to Ada Pastor and Lídia Cañas for their invaluable assistance in the field. Special thanks are extended to Núria Catalán for helpful comments on an earlier version of the manuscript. Financial support was provided by the Spanish Government through the projects MONTES-Consolider (CSD2008-00040-MONTES), MEDFORESTREAM (CGL2011-30590), and MEDSOUL (CGL2014-59977-C3-2). Sílvia Poblador was supported by a FPI PhD fellowship from the Spanish Ministry of Economy and Competitiveness (BES-2012-054572). Anna Lupon was supported by a Kempe Foundation post-doctoral grant (Sweden) and the MEDSOUL project. We also thank site cooperators, including Vichy Catalan and the Catalan Water Agency (ACA), for permission to sample at the Font del Regàs catchment. Sílvia Poblador, Anna Lupon, Santiago Sabaté, and Francesc Sabater are members of the research group FORESTREAM (AGAUR, Catalonia 2014SGR949).

Edited by: Akihiko Ito
Reviewed by: three anonymous referees

References

Allison, S. D., Wallenstein, M. D., and Bradford, M. A.: Soil-carbon response to warming dependent on microbial physiology, Nat. Geosci., 3, 336–340, https://doi.org/10.1038/ngeo846, 2010.

Asensio, D., Peñuelas, J., Ogaya, R., and Llusià, J.: Seasonal soil and leaf CO_2 exchange rates in a Mediterranean holm oak forest and their responses to drought conditions, Atmos. Environ., 41, 2447–2455, https://doi.org/10.1016/j.atmosenv.2006.05.008, 2007.

Audet, J., Hoffmann, C. C., Andersen, P. M., Baattrup-Pedersen, A., Johansen, J. R., Larsen, S. E., Kjaergaard, C., and Elsgaard, L.: Nitrous oxide fluxes in undisturbed riparian wetlands located in agricultural catchments: emission, uptake and controlling factors, Soil Biol. Biochem., 68, 291–299, https://doi.org/10.1016/j.soilbio.2013.10.011, 2014.

Àvila, A. and Rodà, F.: Changes in atmospheric deposition and streamwater chemistry over 25 years in undisturbed catchments in a Mediterranean mountain environment, Sci. Total Environ., 434, 18–27, https://doi.org/10.1016/j.scitotenv.2011.11.062, 2012.

Baethgen, W. E. and Alley, M. M.: A manual colorimetric procedure for measuring ammonium nitrogen in soil and plant Kjeldahl digests, Commun. Soil Sci. Plan., 20, 961–969, https://doi.org/10.1080/00103628909368129, 1989.

Baggs, E. M.: A review of stable isotope techniques for N_2O source partitioning in soils: recent progress, remaining challenges and future considerations, Rapid Commun. Mass Sp., 22, 1664–1672, https://doi.org/10.1002/rcm.3456, 2008.

Barba, J., Curiel Yuste, J., Poyatos, R., Janssens, I. A., and Lloret, F.: Strong resilience of soil respiration components to drought-induced die-off resulting in forest secondary succession, Oecologia, 182, 27–41, https://doi.org/10.1007/s00442-016-3567-8, 2016.

Bardon, C., Piola, F., Bellvert, F., Haichar, F. el Z., Comte, G., Meiffren, G., Pommier, T., Puijalon, S., Tsafack, N., and Poly, F.: Evidence for biological denitrification inhibition (BDI) by plant secondary metabolites, New Phytol., 204, 620–630, https://doi.org/10.1111/nph.12944, 2014.

Batson, J., Noe, G. B., Hupp, C. R., Krauss, K. W., Rybicki, N. B., and Schenk, E. R.: Soil greenhouse gas emissions and carbon budgeting in a short-hydroperiod floodplain wetland, J. Geophys. Res.-Biogeo., 120, 77–95, https://doi.org/10.1002/2014JG002817, 2015.

Belnap, J., Welter, J. R., Grimm, N. B., Barger, N., and Ludwig, J. A: Linkages between Microbial and Hydrologic Processes in Arid and Semiarid Watersheds, Ecology, 86, 298–307, https://doi.org/10.1890/04-0631, 2005.

Bernal, S., Butturini, A., Nin, E., Sabater, F., and Sabater, S.: Leaf litter dynamics and nitrous oxide emission in a Mediterranean riparian forest: implications for soil nitrogen dynamics, J. Environ. Qual., 32, 191–197, available at: http://www.ncbi.nlm.nih.gov/pubmed/12549558, 2003.

Bernal, S., Sabater, F., Butturini, A., Nin, E., and Sabater, S.: Factors limiting denitrification in a Mediterranean riparian forest, Soil Biol. Biochem., 39, 2685–2688, https://doi.org/10.1016/j.soilbio.2007.04.027, 2007.

Bond-Lamberty, B. and Thomson, A.: Temperature-associated increases in the global soil respiration record, Nature, 464, 579–582, https://doi.org/10.1038/nature08930, 2010.

Bruland, G. L., Richardson, C. J., and Whalen, S. C.: Spatial variability of denitrification potential and related soil properties in created, restored, and paired natural wetlands, Wetlands, 26, 1042–1056, https://doi.org/10.1672/0277-5212(2006)26[1042:SVODPA]2.0.CO;2, 2006.

Burgin, A. J. and Groffman, P. M.: Soil O_2 controls denitrification rates and N2O yield in a riparian wetland, J. Geophys. Res.-Biogeo., 117, 1–10, https://doi.org/10.1029/2011JG001799, 2012.

Casals, P., Lopez-Sangil, L., Carrara, A., Gimeno, C., and Nogués, S.: Autotrophic and heterotrophic contributions to short-term soil CO_2 efflux following simulated summer precipitation pulses in a Mediterranean dehesa, Global Biogeochem. Cy., 25, 1–12, https://doi.org/10.1029/2010GB003973, 2011.

Castro-Díez, P., González-Muñoz, N., Alonso, A., Gallardo, A., and Poorter, L.: Effects of exotic invasive trees on nitrogen cycling: A case study in Central Spain, Biol. Invasions, 11, 1973–1986, https://doi.org/10.1007/s10530-008-9374-3, 2009.

Chang, C. T., Sabaté, S., Sperlich, D., Poblador, S., Sabater, F., and Gracia, C.: Does soil moisture overrule temperature dependence of soil respiration in Mediterranean riparian forests?, Biogeosciences, 11, 6173–6185, https://doi.org/10.5194/bg-11-6173-2014, 2014.

Clément, J.-C., Pinay, G., and Marmonier, P.: Seasonal dynamics of denitrification along topohydrosequences in three dif-

ferent riparian wetlands, J. Environ. Qual., 31, 1025–1037, https://doi.org/10.2134/jeq2002.1025, 2002.

Davidson, E. A., Janssens, I. A., and Lou, Y.: On the variability of respiration in terrestrial ecosystems: Moving beyond Q10, Glob. Change Biol., 12, 154–164, https://doi.org/10.1111/j.1365-2486.2005.01065.x, 2006.

DeSimone, J., Macrae, M. L., and Bourbonniere, R. A.: Spatial variability in surface N_2O fluxes across a riparian zone and relationships with soil environmental conditions and nutrient supply, Agr. Ecosyst. Environ., 138, 1–9, https://doi.org/10.1016/j.agee.2010.03.007, 2010.

Dhondt, K., Boeckx, P., Hofman, G., and Cleemput, O.: Temporal and spatial patterns of denitrification enzyme activity and nitrous oxide fluxes in three adjacent vegetated riparian buffer zones, Biol. Fert. Soils, 40, 243–251, https://doi.org/10.1007/s00374-004-0773-z, 2004.

Emmett, B. A., Beier, C., Estiarte, M., Tietema, A., Kristensen, H. L., Williams, D., Peñuelas, J., Schmidt, I., and Sowerby, A.: The response of soil processes to climate change: Results from manipulation studies of shrublands across an environmental gradient, Ecosystems, 7, 625–637, https://doi.org/10.1007/s10021-004-0220-x, 2004.

Eno, C. F.: Nitrate production in the field by incubating the soil in polyethylene bags, Soil Sci. Soc. Am. J., 24, 227–279, 1960.

Eriksson, L., Byrne, T., Johansson, E., Trygg, J., and Vikström, C.: Multi- and Megavariate Data Analysis, Basic Principles and Applications, 2006.

Giles, M., Morley, N., Baggs, E. M., and Daniell, T. J.: Soil nitrate reducing processes – drivers, mechanisms for spatial variation, and significance for nitrous oxide production, Front. Microbiol., 3, 1–16, https://doi.org/10.3389/fmicb.2012.00407, 2012.

Gómez-Gener, L., Obrador, B., von Schiller, D., Marcé, R., Casas-Ruiz, J. P., Proia, L., Acuña, V., Catalán, N., Muñoz, I., and Koschorreck, M.: Hot spots for carbon emissions from Mediterranean fluvial networks during summer drought, Biogeochemistry, 125, 409–426, https://doi.org/10.1007/s10533-015-0139-7, 2015.

Goulden, M. L., Miller, S. D., Da Rocha, H. R., Menton, M. C., De Freitas, H. C., De Silva Figueira, A. M., and Dias de Sousa, C. A.: Diel and seasonal patterns of tropical forest CO_2 exchange, Ecol. Appl., 14, 42–54, https://doi.org/10.1890/02-6008, 2004.

Groffman, P. M., Gold, A. J., and Simmons, R. C.: Nitrate dynamics in riparian forests: Microbial studies, J. Environ. Qual., 21, 666–671, https://doi.org/10.2134/jeq1992.00472425002100040022x, 1992.

Groffman, P. M., Gold, A. J., and Jacinthe, P.-A. A: Nitrous oxide production in riparian zones and groundwater, Chemosph.-Glob. Chang. Sci., 2, 291–299, https://doi.org/10.1023/A:1009719923861, 2000.

Guckland, A., Corre, M. D., and Flessa, H.: Variability of soil N cycling and N_2O emission in a mixed deciduous forest with different abundance of beech, Plant Soil, 336, 25–38, https://doi.org/10.1007/s11104-010-0437-8, 2010.

Guidolotti, G., Rey, A., D'Andrea, E., Matteuci, G., and De Angelis, P.: Effect of environmental variables and stand structure on ecosystem respiration components in a Mediterranean beech forest, Tree Physiol., 33, 1–13, https://doi.org/10.1093/treephys/tpt065, 2013.

Hagedorn, F.: Hot spots and hot moments for greenhouse gas emissions from soils, Swiss Fed. Inst. For. Snow Landsc. Res., 1, 9–14, 2010.

Harms, T. K. and Grimm, N. B.: Hot spots and hot moments of carbon and nitrogen dynamics in a semiarid riparian zone, J. Geophys. Res., 113, 1–14, https://doi.org/10.1029/2007JG000588, 2008.

Harms, T. K. and Grimm, N. B.: Responses of trace gases to hydrologic pulses in desert floodplains, J. Geophys. Res.-Biogeo., 117, 1–14, https://doi.org/10.1029/2011JG001775, 2012.

Harms, T. K., Wentz, E. A., and Grimm, N. B.: Spatial heterogeneity of denitrification in semi-arid floodplains, Ecosystems, 12, 129–143, https://doi.org/10.1007/s10021-008-9212-6, 2009.

Healy, R. W., Striegl, R. G., Russell, T. F., Hutchinson, G. L., and Livingston, G. P.: Numerical evaluation of static-chamber measurements of soil – atmosphere gas exchange?: identification of physical processes, Soil Sci. Soc. Am. J., 60, 740–747, https://doi.org/10.2136/sssaj1996.03615995006000030009x, 1996.

Hedin, L. O., Fischer, J. C. von, Ostrom, N. E., Kennedy, B. P., Brown, M. G., Robertson, G. P., Ecology, S., and Mar, N.: Thermodynamic constraints on nitrogen transformations and other biogeochemical processes at soil-stream interfaces, 79, 684–703, 1998.

Hefting, M. M., Bobbink, R., and de Caluwe, H.: Nitrous oxide emission and denitrification in chronically nitrate-loaded riparian buffer zones., J. Environ. Qual., 32, 1194–203, https://doi.org/10.2134/jeq2003.1194, 2003.

Hefting, M. M., Clément, J.-C., Dowrick, D., Cosandey, A. C., Bernal, S., Cimpian, C., Tatur, A., Burt, T. P., and Pinay, G.: Water table elevations controls on soil nitrogen cycling in riparian wetlands along a European climatic gradient, Biogeochemistry, 67, 113–134, https://doi.org/10.1023/B:BIOG.0000015320.69868.33, 2004.

Hill, A. R.: Nitrate removal in stream riparian zones, J. Environ. Qual., 25, 743–755, https://doi.org/10.2134/jeq1996.00472425002500040014x, 1996.

Inclán, R., Uribe, C., Sánchez, L., Sánchez, D. M., Clavero, Á., Fernández, A. M., Morante, R., and Blanco, A.: N_2O and CH_4 fluxes in undisturbed and burned holm oak, scots pine and pyrenean oak forests in central Spain, Biogeochemistry, 107, 19–41, https://doi.org/10.1007/s10533-010-9520-8, 2014.

Jacinthe, P. A., Vidon, P., Fisher, K., Liu, X., and Baker, M. E.: Soil methane and carbon dioxide fluxes from cropland and riparian buffers in different hydrogeomorphic settings, J. Environ. Qual., 44, 1080–1090, https://doi.org/10.2134/jeq2015.01.0014, 2015.

Keeney, D. R. and Nelson, D. W.: Nitrogen-Inorganic Forms, in Agronomy Monography 9, ASA and SSSA, Madison, 643–698, 1982.

Kesik, M., Ambus, P., Baritz, R., Brüggemann, N., Butterbach-Bahl, K., Damm, M., Duyzer, J., Horváth, L., Kiese, R., Kitzler, B., Leip, A., Li, C., Pihlatie, M., Pilegaard, K., Seufert, S., Simpson, D., Skiba, U., Smiatek, G., Vesala, T., and Zechmeister-Boltenstern, S.: Inventories of N_2O and NO emissions from European forest soils, Biogeosciences, 2, 353–375, https://doi.org/10.5194/bg-2-353-2005, 2005.

Kim, J. and Verma, S. B.: Components of surface energy balance in a temperate grassland ecosystem, Bound.-Lay. Meteorol., 51, 401–417, 1990.

Linn, D. M. and Doran, J. W.: Effect of water-filled pore space on carbon dioxide and nitrous oxide production in tilled and nontilled soils, Soil Sci. Soc. Am. J., 48, 1267–1272, https://doi.org/10.2136/sssaj1984.03615995004800060013x, 1984.

Lupon, A., Sabater, F., Miñarro, A., and Bernal, S.: Contribution of pulses of soil nitrogen mineralization and nitrification to soil nitrogen availability in three Mediterranean forests, Environ. J. Soil Sci., 67, 303–313, https://doi.org/10.1016/j.aqpro.2013.07.003, 2016.

Mander, Ü., Lõhmus, K., Teiter, S., Mauring, T., Nurk, K., and Augustin, J.: Gaseous fluxes in the nitrogen and carbon budgets of subsurface flow constructed wetlands, Sci. Total Environ., 404, 343–353, https://doi.org/10.1016/j.scitotenv.2008.03.014, 2008.

Mander, Ü., Well, R., Weymann, D., Soosaar, K., Maddison, M., Kanal, A., Lõhmus, K., Truu, J., Augustin, J., and Tournebize, J.: Isotopologue ratios of N_2O and N_2 measurements underpin the importance of denitrification in differently n – loaded riparian alder forests, Environ. Sci. Technol., 48, 11910–11918, https://doi.org/dx.doi.org/10.1021/es501727h, 2014.

McGlynn, B. L. and Seibert, J.: Distributed assessment of contributing area and riparian buffering along stream networks, Water Resour. Res., 39, 1–7, https://doi.org/10.1029/2002WR001521, 2003.

McLain, J. E. T. and Martens, D. A.: N_2O production by heterotrophic N transformations in a semiarid soil, Appl. Soil Ecol., 32, 253–263, https://doi.org/10.1016/j.apsoil.2005.06.005, 2006.

Mitsch, W. J.. and Gosselink, J. G.: Wetlands, 4th edn., Wiley & Sons, Hoboken, NJ, 2007.

Morse, J. L., Ardon, M., and Benhartdt, E. S.: Greenhouse gas fluxes in southeastern U.S. coastal plain wetlands under contrasting land uses, Ecol. Appl., 22, 264–280, https://doi.org/10.1890/11-0527.1, 2012.

Müller, D., Warneke, T., Rixen, T., Müller, M., Jamahari, S., Denis, N., Mujahid, A., and Notholt, J.: Lateral carbon fluxes and CO_2 outgassing from a tropical peat-draining river, Biogeosciences, 12, 5967–5979, https://doi.org/10.5194/bg-12-5967-2015, 2015.

Oertel, C., Matschullat, J., Zurba, K., Zimmermann, F., and Erasmi, S.: Greenhouse gas emissions from soils – a review, Chem. Erde-Geochem., 76, 327–352, https://doi.org/10.1016/j.chemer.2016.04.002, 2016.

Pacific, V. J., McGlynn, B. L., Riveros-Iregui, D. A., Welsch, D. L., and Epstein, H. E.: Variability in soil respiration across riparian-hillslope transitions, Biogeochemistry, 91, 51–70, https://doi.org/10.1007/s10533-008-9258-8, 2008.

Pinay, G., Gumiero, B., Tabacchi, E., Gimenez, O., Tabacchi-Planty, a. M., Hefting, M. M., Burt, T. P., Black, V. a., Nilsson, C., Iordache, V., Bureau, F., Vought, L., Petts, G. E., and Décamps, H.: Patterns of denitrification rates in European alluvial soils under various hydrological regimes, Freshwater Biol., 52, 252–266, https://doi.org/10.1111/j.1365-2427.2006.01680.x, 2007.

Pinay, G., Peiffer, S., De Dreuzy, J.-R., Krause, S., Hannah, D. M., Fleckenstein, J. H., Sebilo, M., Bishop, K., and Hubert-Moy, L.: Upscaling nitrogen removal capacity from local hotspots to low stream orders' drainage basins, Ecosystems, 18, 1101–1120, https://doi.org/10.1007/s10021-015-9878-5, 2015.

R Development Core Team: R: A Language and Environment For Statistical Computing, Vienna, Austria, 2012.

Raich, J. W., Potter, C. S., and Bhagawati, D.: Interannual variability in global soil respiration, 1980–94, Global Change Biol., 8, 800–812, 2002.

Rastogi, M., Singh, S., and Pathak, H.: Emission of carbon dioxide from soil, Curr. Sci. India, 82, 510–517, 2002.

Schmidt, M. W. I., Torn, M. S., Abiven, S., Dittmar, T., Guggenberger, G., Janssens, I. A., Kleber, M., Kögel-Knabner, I., Lehmann, J., Manning, D. A. C., Nannipieri, P., Rasse, D. P., Weiner, S., and Trumbore, S. E.: Persistence of soil organic matter as an ecosystem property, Nature, 478, 49–56, https://doi.org/10.1038/nature10386, 2011.

Segers, R.: Methane production and methane consumption?: a review of processes underlying wetland methane fluxes, Biogeochemistry, 41, 23–51, 1998.

Smith, M. S. and Tiedje, J. M.: Phases of desnitrification following oxygen depletion in soil, Soil Biol. Biochem., 11, 261–267, https://doi.org/10.1016/0038-0717(79)90071-3, 1979.

Stark, J. M. and Firestone, M. K.: Mechanisms for soil moisture effects on activity of nitrifying bacteria, Appl. Environ. Microbiol., 61, 218–221, 1995.

Stern, S. N.: The stern review on the economic effects of climate change, Popul. Dev. Rev., 32, 793–798, https://doi.org/10.1111/j.1728-4457.2006.00153.x, 2006.

Suseela, V., Conant, R. T., Wallenstein, M. D., and Dukes, J. S.: Effects of soil moisture on the temperature sensitivity of heterotrophic respiration vary seasonally in an old-field climate change experiment, Global Change Biol., 18, 336–348, https://doi.org/10.1111/j.1365-2486.2011.02516.x, 2012.

Teiter, S. and Mander, Ü.: Emission of N_2O, N_2, CH_4, and CO_2 from constructed wetlands for wastewater treatment and from riparian buffer zones, Ecol. Eng., 25, 528–541, https://doi.org/10.1016/j.ecoleng.2005.07.011, 2005.

Vidon, P. G.: Not all riparian zones are wetlands: Understanding the limitation of the "wetland bias" problem, Hydrol. Process., 31, 2125–2127, https://doi.org/10.1002/hyp.11153, 2017.

Vidon, P. G. and Hill, A. R.: A landscape-based approach to estimate riparian hydrological and nitrate removal functions, J. Am. Water Resour. As., 3, 1099–1112, 2006.

Vidon, P., Allan, C., Burns, D., Duval, T. P., Gurwick, N., Inamdar, S., Lowrance, R., Okay, J., Scott, D., and Sebestyen, S.: Hot spots and hot moments in riparian zones: Potential for improved water quality management, J. Am. Water Resour. As., 46, 278–298, https://doi.org/10.1111/j.1752-1688.2010.00420.x, 2010.

Vidon, P., Marchese, S., Welsh, M., and McMillan, S.: Impact of precipitation intensity and riparian geomorphic characteristics on greenhouse gas emissions at the soil–atmosphere interface in a water-limited riparian zone, Water. Air. Soil Poll., 227, https://doi.org/10.1007/s11270-015-2717-7, 2016.

Walker, J. T., Geron, C. D., Vose, J. M., and Swank, W. T.: Nitrogen trace gas emissions from a riparian ecosystem in southern Appalachia, Chemosphere, 49, 1389–1398, https://doi.org/10.1016/S0045-6535(02)00320-X, 2002.

Welti, N., Bondar-Kunze, E., Singer, G., Tritthart, M., Zechmeister-Boltenstern, S., Hein, T., and Pinay, G.: Large-scale controls on potential respiration and denitrification in riverine floodplains, Ecol. Eng., 42, 73–84, https://doi.org/10.1016/j.ecoleng.2012.02.005, 2012.

Werner, C., Reiser, K., Dannenmann, M., Hutley, L. B., Jacobeit, J., and Butterbach-Bahl, K.: N_2O, NO, N_2 and CO_2 emissions from tropical savanna and grassland of northern Australia: an incubation experiment with intact soil cores, Biogeosciences, 11, 6047–6065, https://doi.org/10.5194/bg-11-6047-2014, 2014.

Wickland, K. P., Neff, J. C.., and Harden, J. W.: The role of soil drainage class in carbon dioxide exchange and decomposition in boreal black spruce (Picea mariana) forest stands, Can. J. Forest Res., 40, 2123–2134, 2010. Williams, C. J., Shingara, E. A., and Yavitt, J. B.: Phenol oxidase activity in peatlands in New York State: response to summer drought and peat type, Wetlands, 20, 416–421, https://doi.org/10.1672/0277-5212(2000)020[0416:POAIPI]2.0.CO;2, 2000.

Yavitt, J. B., Williams, C. J., and Wieder, R. K.: Production of methane and carbon dioxide in peatland ecosystems across North America: Effects of temperature, aeration, and organic chemistry of peat, Geomicrobiol. J., 14, 299–316, 1997.

Yu, K. and Rinklebe, J.: Soil redox potential and pH controllers, in: Methods in Biogeochemistry of Wetlands, 107–116, https://doi.org/10.2136/sssabookser10.c7, 2013.

Supplement of Biogeosciences, 14, 4195–4208, 2017
https://doi.org/10.5194/bg-14-4195-2017-supplement

Biogeosciences Open Access EGU

Supplement of

Soil water content drives spatiotemporal patterns of CO_2 and N_2O emissions from a Mediterranean riparian forest soil

Sílvia Poblador et al.

Correspondence to: Sílvia Poblador (spoblador@ub.edu)

Supplementary material

Figure S1: Concentrations of carbon dioxide (left column) and nitrous oxide (right column) during the incubation time for the sampling campaign of June 2013. Data is shown for the near-stream, intermediate and hillslope zones separately. For each plot, data is shown as mean ± SD (n = 5) for all sampling days of June. The best fit linear model used to calculate gas emissions is shown for each plot.

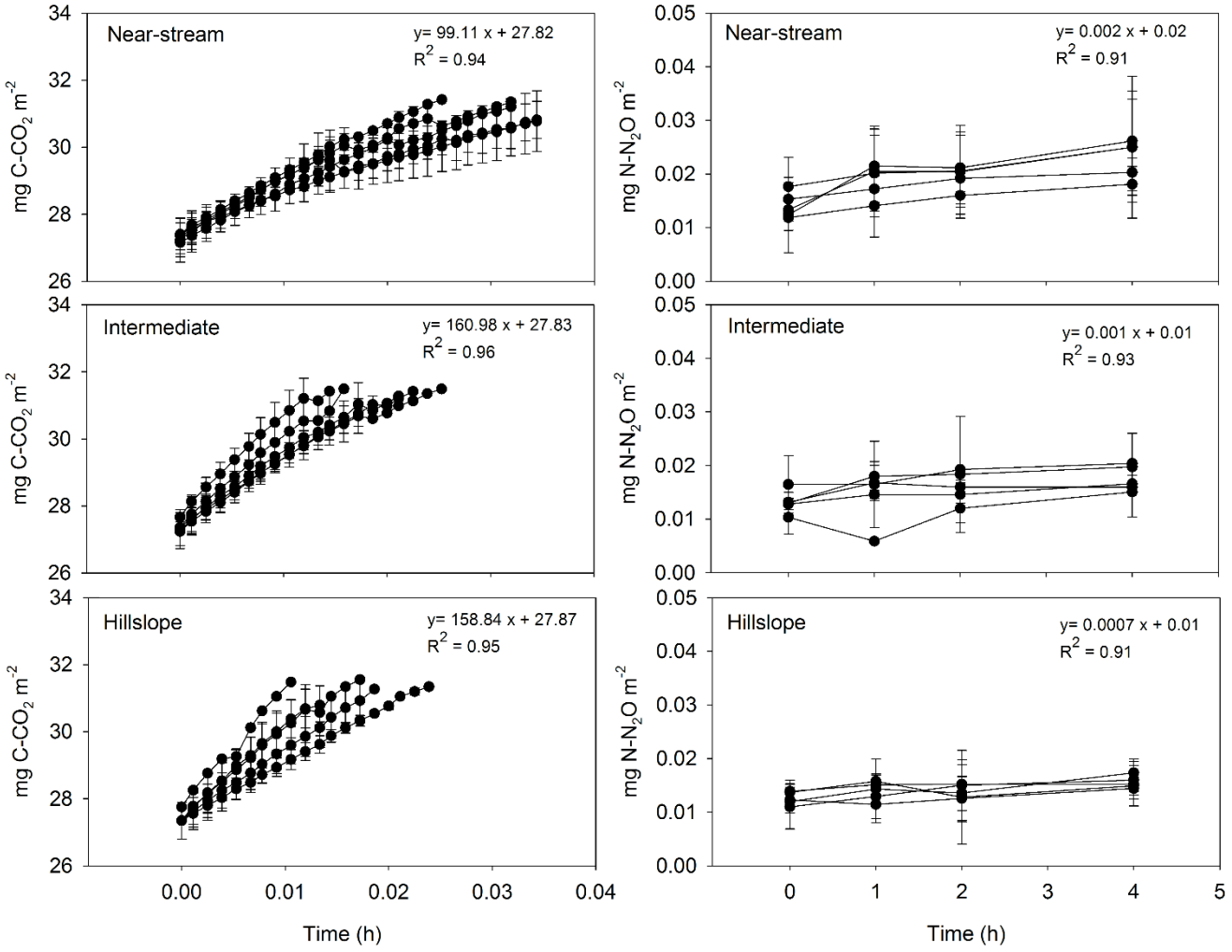

Figure S2. Loading plot of the (a) CO_2 and (b) N_2O partial least squares models (PLS) for the 75 measurements. The graph depicts the correlation structures between the X variables (circles) and gas emissions (vectors). Variables situated along the same directional axis correlate with each other. Different color in X variables indicates their influence on gas emissions based on the "variable importance in the projection (VIP)" scores for each model. In each case, white has VIP scores < 0.8, grey has VIP scores < 1.0 and black has VIP scores > 1.0.